1-1-2012

Investigation of Load Distribution Factors for Simply-Supported Composite Multiple Box Girder Bridges

Siham Kadhim Jawad
Ryerson University

INVESTIGATION OF LOAD DISTRIBUTION FACTORS FOR SIMPLY-SUPPORTED COMPOSITE MULTIPLE BOX GIRDER BRIDGES

BY

Siham Kadhim Jawad

B.Sc., Baghdad, Iraq, 1980

A Thesis

Presented to Ryerson University

In Partial Fulfillment of the

Requirement for the Degree of

Master of Applied Science

In the Program of

Civil Engineering

Toronto, Ontario, Canada, 2012

AUTHOR'S DECLARATION

I hereby declare that I am the sole author of this thesis. This is a true copy of the thesis, including any required final revisions, as accepted by my examiners.

I authorize Ryerson University to lend this thesis to other institutions or individuals for the purpose of scholarly research

I further authorize Ryerson University to reproduce this thesis by photocopying or by other means, in total or in part, at the request of other institutions or individuals for the purpose of scholarly research.

I understand that my thesis may be made electronically available to the public

Siham Kadhim Jawad

INVESTIGATION OF LOAD DISTRIBUTION FACTORS FOR SIMPLY-SUPPORTED COMPOSITE MULTIPLE BOX GIRDER BRIDGES

By
Siham Kadhim Jawad
Master of Applied Science in Civil Engineering
Department of Civil Engineering
Ryerson University
Toronto, Ontario, Canada, 2012

ABSTRACT

Composite box-girder bridges are recently used in modern highway urban system because of their profitable and structural aptitude advantages. North Americans Codes of Practice specify empirical equations for girder moment and shear forces in such bridges in the form of live load distribution factors. These factors were proven to be conservative in some cases and underestimate the response in other cases. Therefore, an extensive parametric study, using the finite-element modeling, was conducted to examine the key parameters that influence the load distribution factors of such bridges. A total of 276 prototype bridges were analyzed to evaluate girder bending moment, shear force and deflection distribution factors for simply-supported composite multiple box-girder bridges when subjected to CHBDC truck loading. Design parameters considered in this study were bridges span length, numbers of design lanes, number of box girders and girder spacing. Based on the data generated from parametric study, sets of simple empirical expressions were developed for bending moment; shear force and deflection distribution factors for such bridges. A correlation between the finite-element results with CHBDC and AASHTO-LRFD empirical expressions showed the former are more reliable in structural design of composite box-girder bridges.

ACKNOWLEDGEMENTS

I would like to thank God, the merciful and passionate, for providing me the opportunity to step in excellent world of science.

I would like to express my gratitude to my supervisor Dr. Khaled Sennah, whose expertise, understanding, and patient, added considerably to my graduate experience

I wish to thank everyone who gave me support in making this completion a magnificent experience. Special thank to my family for the support they provided me through my entire life and in particular, I must acknowledge my family without their love, encouragement and editing assistance, I would not have finished this thesis.

TO MY FAMILY

TABLE OF CONTENTS

LIST OF TABLES

LIST OF FIGURES

APPENDICES

NOTATIONS

A	= Bridge width
B	= Box girder width
D_X	=Total bending stiffness divided by the width of the bridge as per CHBDC
D_{XY}	=Total torsional stiffness of the cross section divided by the width of the bridge as per CHBDC
E	=Modulus of elasticity
F	=Total depth of composite bridge and width dimension that characterizes load distribution factor as per CHBDC
F_m	= Amplification factor to account for the transverse variation in maximum longitudinal moment intensity as per CHBDC
Fv	= Amplification factor to account for the transverse variation in maximum longitudinal vertical shear intensity as per CHBDC
C_f	=Correction factor as per CHBDC
I	=Moment of inertia
[K]	=The global stiffness matrix
L	=Centre line span of simply supported bridge
M_g	=Bending moment in box girder as per CHBDC
$M_{g\ avg}$	=Average moment per box girder as per CHBDC
M_T	= The Simply-supported mid span girder moment due to single CHBDC Truck loading
n	=Number of design lane as per CHBDC

N	=Number of steel box girder as per CHBDC
N_B	=Number of box girder as per Johanston and Mattock
N_L	=Number of Lanes as per Johanston and Mattock
[P]	= The nodal load vector
[U]	=The nodal displacement vector
R	=Radius of curvature of centre span as per CHBDC recommendations to consider bridge straight or a curvature bridge type
R_L	=Multilane factor based on the number of design lanes as per CHBDC
S	=Centre-to-centre steel box girder spacing
Fm	=Moment distribution factor
t_1	=Thickness of bottom flange of steel box girder
t_2	=Thickness of steel web of steel box girder
t_3	=Thickness of concrete deck slab
V	=Maximum shear force at the girder section close to the support of a straight simply-supported idealized girder
V_g	=Longitudinal vertical shear per box girder as per CHBDC
$V_{g\ avg}$	=Average shear per box girder as per CHBDC
V_{max}	=Maximum shear force at the girder section close to the support obtained from the finite element analysis
Vt	=Maximum shear force per lane at point of the span under consideration as per CHBDC

$(V_{FEA.\,ext})_{PL}$ = Maximum vertical reaction or shear force at support from the partial Loading case as obtained from finite element analysis

W_c =Bridge width as per CHBDC, Roadway width between curbs in ft as per Johanston and Mattock (1967)

W_e = Width of design lane in meter as per CHBDC

W_L = Live load distribution factor for each straight box girder as per Johanston and Mattock(1967)

υ =Poisson's ratio

Y_b = Distance from the natural axis of the selected modeled to the bottom fiber or flange

CHAPTER I

INTRODUCTION

1.1 General

Many engineers around the world attempted to develop modern and appropriate structural highways design to make destination accessible. The construction of recent highways systems generally impress designers to utilize reliable geometry, appropriate boundary condition and superlative type of connection between different materials used consequently since it can securely and efficiently transmit the loads imposed on it. Highway bridge designs should be designed based on applicable Standards such as the Canadian Highway Bridge Design Code (CHBDC, 2010) and AASHTO-LRFD Bridge Design Specifications (AASHTO, 2010). The research focused on the structural analysis of simply-supported composite Concrete slab-over-steel box-girder bridges. Box-girder bridges can be constructed using (i) reinforced concrete box-girders, (ii) steel box-girders with concrete deck slab or orthotope steel deck, or (iii) presetressed concrete box-girders. These bridge cross-section types are shown in Figure 1.1, while Figure 1.2 shows the basic cross-section configuration and symbols for the bridge under consideraition in this study. Box-girder bridges are considered better than steel I-girder bridges because of their light dead load, large flexural and torsional stiffness. In addition, steel boxes can carry the required utilities to give a better architectural view. Moreover, box-girder bridges are Proven of having better lateral load distribution among girder when compared to steel I-girder bridges of similar bridge span and width (Zhang and Lou, 2012). Box-girder cross-section shows a superior performance in Resistant torsion with insignificant torsional warping effects as compared to I-girder bridges (El-Tawil and Okeil, 2002). Figures 1.3 and 1.4 show views of two box-girder bridge and five box-girder bridge, respectively.

1.2 The Problem

The Canadian Highway Bridge Design Code (CHBDC, 2010) and AASHTO-LRFD Bridge Design Specifications (AASHTO, 2010) specify load distribution factor equations for the design of selected bridge configurations and recommend few analytical methods (such as grillage analogy, semi-continuum analysis method, folded plate and finite-element method) for analysis

of other bridge configurations not covered by the similfied design method of analysis. The literature review shows that AASHTO-LRFD load distribution factors are conservative for specific design parameters and geometries and underestimate the response in other cases (El-Tawil and Okeil, 2002; Yousif and Hindi, 2006). Other investigation indicated that AASHTO-LRFD significantly overestimate the load distribution factors compared to finite-elements analysis (Yousif and Hindi, 2007). Other studies showed that CHBDC showed scattered correlation with the results from the the finite-element modeling of composite multiple steel box girder bridges (Sennah et al, 2003). As a results, more precise expressions for load distribution factors among box-girders in composite bridge construction is needed (Suksawang, 2007).

1.3 The Objectives.

The objectives of the research are to:

1. Investigate the parameters that influence the behavior of straight simply-supported composite multiple box-girder bridges subjected to CHBDC truck loading and correlate the results with available CHBDC and AASHTO-LRFD specified values to examine their accuracy in structural design.
2. Determined the moment, shear and deflection distribution factors of such bridge using the three-dimensional finite-element modeling to develop more reliable expressions for structural design.

1.4 The Scopes of the research

The scope of the research includes:

1. Conduct a literature review of previous research and the code of practice related to the behavior of straight simply-supported composite bridges and related load distribution factors.

2. Develope of the three-dimensional finite-element (FEA) models of straight composite bridges made of concrete slab supported over steel box girders and subjtected to different CHBDC truck loading conditions.

3. Conduct a parametric study on different key parameters that ruled the moment, shear and deflection distribution factors such as number of lanes, number of box girders, bridge span length and girder spacing.

4. Correlate the FEA results with the results obtained from CHBDC and AASHTO-LRFD equations to examine the level of accurancy of the code design values.

5. Develop more reliable emperical expressions for the moment and shear distribution factors for such bridges in lieu of code equations.

1.5 Contents and Arrangements of This Study.

Chapter 2 reviews the previous work on concrete slab over-steel box-girder bridges as well as the load distribution factor equations available in CHBDC and AASHTO-LRFD Specifications. Chapter 3 illustrates the finite-element method as well as SAP2000 software used in modeling different bridge configurations with various CHBDC truck conditions. Chapter 4 summarizes the FEA results and their correlation with CHBDC and AASHTO-LRFD load distribution factor values. Correlations between the developed equations and the FEA results are also presented. Chapter 5 includes summary of the results and recommendations for future research.

CHAPTER II

LITERATURE REVIEW

2.1 General

The design of bridges in North America is conducted using North American Bridge Design Codes such as CHBDC (2010), AASHTO-LRFD Specification (2010). All these design codes and specifications consider the longitudinal and transverse effect of wheel load as uncoupled phenomena by simlyifing the design of a two-dimensional bridges to a beam subjected to truck loading. Then, the resulting bending moment and shear force are modified by multiplying them by a moment and shear distribution factors, respectively, to take into account the two-dimensional effect of bridge superstructure in distribution the truck loading among girders. Simplifying the design is such manner is complex and necessitates a challenge to determine the level of conservativeness. Some of these girder bridges include the single concrete box girder bridge shown in Fig. 2.1, the concrete multi-box girder bridge shown in Fig. 2.2, the composite concrete slab-over steel I-girders shown in Fig. 2.3, the steel box-girder bridge with orthotropic steel deck shown in Fig. 2.4 and the composite concrete slab-over multiple spine steel girder bridge shown in Fig. 2.5. The following subsections presented the literature related to these bridges including the slab-type bridges.

2.1.1 Slab Bridges

The concrete bridge is considered the simplest type of bridges. It is considered more economical and easier to erect although it may require more concrete materials and reinforcement for longer spans. This type of bridges is considered economical for simply-supported spans up to 9 m and a spans up to 12 m for continuous slabs. Composite slabs were used by many researchers. In 2004, Sudou and Sugihara developed composite slab called a “Hit Slab”. It contains a bulb plate with studs. In 2009, Kim and Jeong conducted experiments to study the steel-concrete composite bridges deck with profiled sheeting shear connectors and compared the experimental Findings with reinforced concrete slab. Results showed that the ultimate load-carrying capacity for the

proposed deck system is greater than that for the reinforced concrete slabs by about 220%, with composite slab weight of 23% less than that for the reinforced concrete slab.

2.1.2 Steel-Concrete Composite I-Girder Bridges

These types of bridges are usually used in straight and curved alignments. However, it may not be economical for sharp curved alignment because of its low torsional stiffness and stability when compared to box-girder type. In general , this type of bridges is desirable because of its simplicity in fabrication and erection. In 1992, Tarhini and Frederick used I-girder bridges to evaluate the AASHTO wheel load distribution factors. They then developed more reliable expressions for the wheel load distribution among girders which were similar in format to those in AASHTO Specifications. In 2010, Khalafalla and Sennah, investigated the behaviour of curved reinforced concrete slab on I-girder under the dead load condition to determine the major internal forces in selected bridge configurations to examine the code provisions for curvature limitations to treat a curved bridge as a straight bridge in structural design. Results showed that CHBDC and AASHTO-LRFD curvature limitations are unsafe in many bridge cases. They developed more reliable expressions for curvature limitation as a function of brige type, span, width and radius of curvature.

2.1.3 Steel-Concrete Composite Box girder Bridges

Generally, there are two types of composite bridges; one with concrete deck slab and the other one with orthotropic steel deck supported over steel box girders. This type of bridges exhibits high torsional stiffness as well as flexural stiffness as compared to the I-girder bridge type. CHBDC and AASHTO-LRFD specifies load distribution factors for shear and moment. However, Hassan (2005) showed that these factors conservative in some cases and underestimate the girder moment and shear in other cases.

2.2 Methods of Analysis Used in Bridge Design and Analysis

The following sub-sections present a summary of the structural analysis methods specified by CHBDC and AASHTO-LRFD Specifications for straight box-girder bridges. These methods can be used to analyze bridges if the conditions to use the code load distribution factors are not met.

2.2.1 Grillage Analogy Method

In 1975, Hambly and Pennells applied the grillage analogy method to cellular deck bridges which modeled as a grid assembly to evaluated the stiffness parameters for grillage analysis. In 1982, Cheng et al. used the finite-element to established the authority of grillage analogy method and the orthotropic plate method to calculate the longitudinal moment and transverse shear in multi-spine box girder. Results show that accuracy can be achieved if the numbers of spines is not less than three. In 1984, Evans et al. established a new technique to model the torsional stiffness of closed cells by means of an equivalent I-beam torsion stiffness which later established by Evans and Shanmugam. In 1997, Razqpur et al, used this method to analyze straight and curved bridges by modelling each segment with three nodal and six degree of freedom each.

2.2.2 Orthotropic Plate Theory Method

Canadian Highway Bridges Design Code has recommended this method in the analysis of straight box-girder bridges of multi-spine cross-section. In this method, the flexural and torsional stiffness and the stiffness of the diaphragm over the girders length were lumped into equivalent stiffness orthotropic plate with equivalent section properties. In 1969, Cheung recommended this method for curved bridges of high torsion rigidity such as multiple-spine girders. In 1982, Cheung et al. used three-dimensional analysis for multi-spine box girders to establish the capability of orthotropic and grillage methods and compare the results to stand on their level of accuracy.

2.2.3 Folded Plate Method

This method is suitable for linear elastic analysis of box-girder bridges by means of the elastic theory and by modeling the multiple-spine box-girder bridge as a folded system by considering both ends simply-supported by infinite stiff diaphragms in their planes and unified the longitudinal plate element along their longitudinal edge at joints. The folded plate method is suitable for simply-supported box-girder bridges with no intermediate diaphragm. In 1964, DeFries and Scordelis applied this method for general plate structures. In 1966, Scordelis and Gerasimenko, studied the behaviour of two reinforced-concrete folded plate models for a

structure under load used by Evans and Rockey. Later this method has been applied to analyze box girders by using an ordinary folded plate analysis. In 1994, Sitaram et al. compared the results obtained from the folded plate method and the finite-element modelling using quadratic shell elements. In 1984, Scordelis developed a Berkeley Computer Program, incorporating the folded-plate method, for simply-supported straight or curved and single-span or continuous bridges with single or multi cell box girder. In 1984, Batla et al, applied this method to straight folded plate type structures. The folded plate method was restricted to be used for bridges with line-support condition as specified in the Canadian Highway Bridge Design Code.

2.2.4 Finite Strip Method

The finite-strip method is a shift method between the folded-plate and finite-element methods. This method were used in the analysis of circularly and orthotropic curved plate elements for which direct application of the theory of elasticity becomes excessively concerned and considered as a prevailing technique. The methodology is to divide the bridge into narrow longitudinal number of strips in circumferential direction to the other end. it considers the bending, warping and membrane distortional effect in the finite strip. The finite-strip and finite-element methods are different in the assumption of displacement interpolation functions. In finite-strip method, the displacement functions for the resulting finite-strip are assumed as changeable mixture for longitudinally and are polynomials in the transverse direction. In 1970, Cheung et al used the finite-strip method to analyze simply-supported slab and girder bridges. In 1978, Cheung and Chan adopted this method to analyze straight multi-spine and multi-cell box girder bridges to define the effective width of the compression flanges. In 1985, Cheung introduced the finite-strip method to analyze box girders with deep or inclined girders and slab bridges with or without concentric beams.

In 1985, Arzumi et al. studied the behaviour of curved composite box girders with different cross-section geometry. In 1989, Cheung and Li applied the finite-strip method by using strips with curvilinear coordinate system and variable width to analyze the behaviour of the webs of continuous box-girder bridges. In 1990, Cheung et al. used the finite-strip method to investigate the improvement of two types of longitudinal shape functions for better accuracy. In 1990, Abdullah and Abdul-Razzak applied the finite-strip method to prestressed box-girder bridges. In

1994, Cheung et al. used a combination of the boundary element method and finite-strip method to analyze composite slab-on-girder and slab-on-box girder bridges and the results was very accurate in local bending moment results due to moving load. In 1999, Zureick and Naqib adopted the finite-strip method in bridge analysis too. Canadian Highway Bridges Design Code restricts the use of this method to single and multi-span bridges having interior supports equivalent to line supports.

2.2.5 Finite-Element Method

This numerical method present solutions to a problem that is not easy to be resolved. As such, this method has extensive applications in structural, fluid and thermal analyses. It have few advantages including being (i) powerful to multiple loading condition; (ii) aptitude to use many different materials distinguished in geometry and elasticity; (iii) able to determine accuracy prediction which makes the solution more acceptable; and (iv) applicable for irregular shape structure with different material charateristics. These methods became conventional techniques for the box-girder bridge analysis over the last decade. In this method, the structural is divided into elements connected together through nodal points. In 1941, Hrennikoff, was the first in history to use the finite-element method in analysis. In 1966, Roll and Aneja tested two types of bridge models made of simply supported box beam, both straight and curved in plan, to examine the accuracy of the finite-element modelling. In 1970, Sargious used the finite-element method to calculate the principal stresses and to obtain the stresses of two equal-span continues prestressed concrete beams.

In 1972, Sisodiya et al. used shell elements and new displacement function to derive the in-plane stiffness for variable depth of box-girder bridges. In1973, Yuki et al. used the method to Analyze suspension bridges for better accuracy. In 1974, Bazant et al. used it to analyse straight or curved single-cell girders with or without the presence of initial stress. In 1975, Fam and Turkstra used it in the analysis of box-girder bridges with orthogonal boundaries and arbitrary combination of straight and curved sections. In 1975, Moffat and Dowling suggested methods of simplifying the codes practice by the rules of shear lag. In 1979, Sargious et al. developed the monographs to determine the consequential forces and critical stresses due to external loads and prestressed forces at different locations of box-girder bridges. In 1981, Ghali et al. used the

finite-element method to analyze box-girder bridges and compared the results used in design of these types of bridges by the classical beam theories. In 1982, Owens et al. described new techniques for the fabrication of small-scale models of welded steel. In 1984, Kostem suggested how the final stresses and deformation check the designs for beam-slab type superstructures by the finite-element method. In 1984, Hays Jr developed a description of load distribution factor program application to find maximum distribution factors by the finite-element method across bridge cross-section. In 1985, Ishac et al. examined the the transverse moment in single-span and single-cell concrete box girder in simple bridge design. In 1990, Chan et al. analysed a three composite box girder over one or two year period by calculating the thermal stresses using the finite-element technique. In 1995, Tarhini et al. used the finite-element method to analyse box-girder bridges and compared results with the published wheel load distribution formula. In1995, Gulta and Cheung formulated a combination of the finite-element and boundary element methods (BEM-FEM) and explained its effective application to box girder bridge analysis.

In 2001, Sennah and Kennedy discussed the design of straight and curved box-girder bridges, the current design, bracing effects, load distribution and construction issues. In 2003, Samaan et al. investigated the simply-supported straight and curved multiple-spine box-girder bridges, using finite-element methods. They inviestigated the effect of key parameters in the structural response of such bridges, including span length, number of box girder, number of lanes and presence of internal and external bracing between box girders. In 2003, Zhang et al. determined the dynamic impact factors for straight composite concrete-steel celluar bridges under AASHTO loading conditions. In 2006, Razapur et al. used the finite-element method to evaluate 50 composite I-girder bridge configurations for moment distribution factors. In 2008, Vasseghi et al. developed the design concept for continuous link slabs as a jointless bridge and investigated the bridge response using the finite-element method for straight and skew bridge. Investigators and designers consider the finite-element method as attractive because of its numerical effectiveness and flexibility in solving linear and non-linear static and dynamic problems. This method was recommended by the Canadian Highway Bridge Design Code for the analysis of box-girder bridges.

2.2.6 Finite-Difference Method

This method was used in analyzing structures but it is not as familiar as the finite-element method. (Tene et al., 1975). This methods is restricted to the anlaysis of plates or bridges as a plate of equivalent section properties.

2.2.7 Thin walled Beam Theory

Initially, the thin-walled beam method was established and applied on open-section under flexure. In 1949, Valsov was the first to apply this method on airplane wings structures. In 1966, Richmond verified the used of the thin-walled theory to box girder analysis using the exact treatment for the two-dimensional elasticity. In 1974, Bazant et al. used this method to analyze different examples of arch girders and straight girder bridges as well as in curved alignment. In 1980, Mikkola and Paavola developed a computer program using Valsov's method and the finite-element method taking into account the cross-section distortion, deformations and, stresses to determine the longitudinal, transverse and flexural straining actions for straight single-box girder. In 1984, Boswell and Zhang used it to solve straight and curved box beams for distortion that happened in thin-walled structural members. In 1985, Maisel used Valsov's method to analyze straight thin-walled box beams and measured the shear lag affects on thin-walled box beam in uniform sections of single-cell and multi-cell shapes. In 1989, Mavaddat and Mirza applied the thin-walled theory into a computer program to analyze straight single-, two- or three-cell concrete box beams. In 1993, Kermani and Waldron developed a method of elastic analysis based on the stiffness approach which is economical and easier in investigating the response of continuous straight single-cell box girders under general loading conditions. In 2008, Zhang et al. derived the equation for continuous thin-walled straight box girders with segregated slabs. There are so many applications of thin-walled methods but most of them were applied on curved box girder bridges more than the straight ones.

2.2.8 Artificial Neural Networks

Artificial neural networks can be formed by placing many nodes of highly organized processing units together to form the neural network and the models of connecting those nodes called Architecture of Neural Networks. This type of Architecture Neural Network is divided into three

main types. The first type is called Feed-Forward on which only signals are transmitted from inputs to outputs in one direction and the standard types of this type consists of disjointed layers of nodes which are connected with succeeding layer in the same time. The second type is called Recurrent Networks, while the third type is called Cellular Neural Network. Neural networks were first used in 1980. This network is a non-linear system applied first to gather and determine the weight values and the connected pattern is then determined and neural networks is trained for possible interporation of data. Hassan (2005) using this technique to model the available data base he obtained for the load distribution factors for selected composite box grider bridges so that the load distribution factors of similar bridge configurations of different span length, bridge width and number of design lanes can be obtained by interpolation of data.

2.2.8.1 Artificial Neural Network Application in Structural Analysis

In 1980's, Artificial Neural Network was applied to structural engineering analysis by considering the available data as a non-linear system with a large interconnected processing numbers of units. In 1993, Jenkins used an objective function for the engineering design which was usually considered constrained. In 1995, Jenkins used neural network-based methods in structural design. In 1996, Jenkins used the same application of neural network and showed the alternatives of re-analysis by the Back-Propagation steps. In 1996, Li et al. used the Neural Network to analyse bridge conditions using five subnets designed to create the current bridge evaluation process. In 1998, Kaveh and Iranmanesh presented two Artificial Neural Network examples to design and analyze large-scale space structures using Counter-propagation Neural Net as well as the Back-propagation Neural Net. In 1999, Furuya and Lu used the Neural Network procedure to investigate how to achieve modeling between the design variables by Application Neural Network-global models and how the response of the structures can be by training a series of pattern on global design space. In 1999, Iranmanesh and Kaves used Counter-propagation Neural Network with parameters like the gradient computation or the weight matrices in the neural networks to express their approaches. In 1999, Rafiq et al. presented areas with defined policy and improved the powerful of using the Artificial Neural Network. They discussed how to use this method in solving engineering problems by using the Artificial Intelligent (AI). In 2006, Srinivas and Ramanjaneyulu trained Artificial Neural Network for many bridge deck with different configurations so that this application can be used for the

prediction of response of similar bridges. In 2006, Jenkins used an ordinary procedure of training but mutated the variables to calculate the values of trigonometric function in the analysis of reinforced concrete deep beams and to calculate buckling loads of steel hollow rectangular sections. Then they compared the results with the 'exact' results and with conventional Back-propagation Training Method of Neural Network.

2.2.9 Experimental Studies

There were few experimental and theoretical studies conducted in the past to examine the structural response of composite bridges. In 1995, Ebeido et al. investigated the shear distribution factors by building and testing six simply-supported skew composite bridges subjected to simulated truck loading. In 1995, Helba and Kennedy investigated the ultimate limit state design for concrete slab-on I-girder bridges using laboratory-scale models and the finite-element modeling. The experimental findings led to the development of the ultimate loading carrying capacity of such bridge using the yield-line theory. In 1997, Sennah et al. used finite-element method to analyzed 120 simply-supported multi-cell bridges considering parameters such as span-to-depth ratio, number of lanes, bridge aspect ratio. They verified the theoretical results by by correlating them with the experimental findings obtained from testing few 1/12 linear-scale simply-supported bridge models. In 1998, Miller et al. examined experimentally the effects of the sequence of construction the deck slab on the response of laboratory-scale bridge model.

In 2002, Samaan et al. investigated the orientation of bridge bearing in composite box-girder bridges after vertifying the three-dimensional finite element model using experimental findings obtained from testing few laboratory scale composite concrete slab-over steel box-girder bridges. In 2003, Androus utilized the finite-element ABAQUS software to investigate the structural behaviour of straight and curved composite box-girder bridges under CHBDC truck loading conditions. He built and tested to-collapse four twin-box girder bridge models to verify the finite element results. In 2007, Samman et al. experimentally conducted a study on two-span continuous curved composite bridge models to evaluate their frequencies and correlate the results with those obtained from the finite-element modeling. In 2007, Suksawang and Nassif proposed new load distribution factors based on experimental testing of actual box girders of differnet

types, including steel spread box girders and prestressed bridges and the results from the finite-element modelling

2.3 AASHTO Standard Methods

In bridge design, AASHTO introduced simplified method of analysis that is more convenient than analytical and numerical methods to define the truck load distribution across bridge cross-section. In this case, the bending moment and shear force in a girder is calculated for a single girder loaded by a line of AASHTO wheel loading. Then, the obtained values are to multiplied by a moment or shear distribution factor that take into account the increase in girder moment or shear due to loaded eccentricity in bridge cross-section. In the superseded AASHTO Standard for the Design of Highway Bridges (1996), the live load was considered as the HS20 truck or a line load, while AASHTO-LRFD Specifications (2010) considers the live load as the HS20 truck in conjunction with the lane load. In 1996, AASHTO Standard specifications used the AASHTO simplified formula for distribution factors based on a research done by Newmark in 1940's (1948). This formula was used to obtained the maximum bending moment in individual girders under wheel loads of truck or lane loading of HS20, then multiplying them by (S/2) or (S/D) where S is the girders spacing in feet and D is a constant depends on the types of girders. This formula was proven to be successful and accurate for short girders spacing of 1.8 m and short span of 18 m in straight (non skewed) bridges. However, it proved to be not precise for medium and long span bridges.

In 1960, Scordelis et al. proved that the design of concrete celluar bridges is govered by the girder bending as well as the transverse distribution between the girders that affects the design of the deck slab. In 1967, Guilford and Vanhorn developed lateral distribution factors for vehicle load on slab-beam bridges. In 1975, Heins and Kuo established reasonable lateral load distribution factors in combination with AASHTO load design Method to developed equations which involved solutions for inelastic actions by introducing modifications to the elastic response. In 1977, Culham and Ghali developed a formula for the wheel load distribution in simply-supported concrete bridge in the form T or I shapes and interconnected by cross girders. In 1987, Imbsen et al. defined different strength and live loading formula similar to the load

distribution factor method in AASHTO Standard. In 1996, AASHTO specified load distribution factors for girder ements in straight reinforced concrete box girder bridges of different design.

2.4 AASHTO-LRFD Method

Jahanston and Mattock (1967) and Fountain and Mattock (1968) analyzed a folded plate structure using a computers program to study the distribution of lateral loads in simply-supported composite multi-spine box-girder bridges with no transverse diaphragm. In developing empirical expressions for load distribution, the effect of the internal and external bracing was not taken into consideration. In addition, the ratio of the number of lanes to the number of boxes in bridge cross-section was taken between 0.5 and 1.5. Moreover, the study is limited to bridge having number of spines equal to number of lanes. This expression is as follows:

$$W_L = 0.1+1.7\frac{N_L}{N_B} + \frac{0.85}{N_L} \qquad (2.1)$$

Where:

W_L = live load distribution factor for each straight box girder

N_B = number of box girder

N_L = number of Lanes

AASHTO was first adopted this empirical expression in 1994 and later ASSHTO-LRFD adopted it in 1998. In 1997, Foinquinos et al. calculated the effects of live load distribution factors as affected by the presence of the intermediate diaphragms in straight multiple-spine steel box-girder bridges. Results showed that composite bridges with three steel box girders and two intermediate diaphragms, a redistribution of stresses in the range of 18% occurred and that insignificant increase in stresses was observed with increase in the number of intermediate diaphragm beyond 2. In 1997. Mabsout et al analyzed 120 models of simply-supported composite steel-girder bridges to study the effects of few parameters on the structural response, including presence of sidewalk, span length, girder spacing and railing. The finite-element

results showed an increase of 30% in load-carrying capacity in case of the presence of the sidewalk and railing.

In 1998 and 1999, Mabsout et al. analyzed two-equal-span straight composite steel girder bridge to study the effect of continuity on bridge response under truck loading. They observed that a reduction of 15% can be made in case of using AASHTO empirical formula for continuous bridges. In 2001, Shahawy and huang investigated the AASHTO-LRFD load distribution factors. Their results for bridge girder spacing 2.4 m and overhung of 0.9 m shows an error as low as 10% for the interior girder and 30% for the exterior one. In 2004, Phuvoravan et al developed new simplified equations for load distribution factors using the finite-element modelling. In 2004, Samaan et al. investigated continuous curved composite multiple-spine box-girder bridges with bracing spacing less than 10 m to examine the AASHTO-LRFD and CHBDC load distribution factors and impact factor using the finite-element ABAQUS software. The results showed that the most effective parameters influencing the load distribution factors were the span length, number of design lanes, and number of box girders and the span-to-radius of curvature ratio. Expressions for the load distribution factors were proposed. In 2005, Puckett et al. investigated the load distribution factors using Henry method and Lever Arm method to evaluate the shear and moment distribution factors. Results were more accurate than current AASHTO-LRFD equations but the study was limited to straight bridges.

2.5 Canadian Highway Bridges Design Code

In 2000, CHBDC specified simplified method for longitudinal bending moment and shear force in concrete slab-over multiple-spine steel box-girder bridges. Figures 2.6 through 2.8 show the CHBDC truck loading configuration used to design such bridges. CHBDC specifies that girder longitudinal bending moment in multiple-spine box-girder bridges can be written as:

$$M_g = F_m M_{g\,avg} \tag{2.2}$$

$$M_{g\,avg} = \frac{n\, M_T\, R_L}{N} \tag{2.3}$$

$$F_m = \frac{S.N}{F\left(1+\frac{\mu C_f}{100}\right)} \geq 1.05 \quad (2.4)$$

$$\mu = \frac{W_{e-3.3}}{0.6} \leq 1.0 \quad (2.5)$$

$$We = \frac{WC}{n} \quad (2.6)$$

$\left(1+\frac{\mu C_f}{100}\right)$ = the lane correction factor (2.7)

$$\beta = \pi \left(\frac{A}{L}\right)\left(\frac{D_x}{D_{XY}}\right)^{0.5} \quad (2.8)$$

Where:

M_g = Longitudinal moment per girder

$M_{g\ avg}$ =The avarage moment per box-girder determined by sharing equally the total moment on the bridge cross-section equally among all girders

F_m = An amplication factor for the transverse variation in maximum longitudal moment intensity

M_T = Maximum moment per design lane.

n = Number of design lanes as determine in Table 2.4

R_L = Modification factors for multilane loading from Table 2.1

N = Number of longitudinal girders

F_m = Amplification factors for the transverse variation in maximum longitudinal moment intensity factors

S = Centre-to-Centre girder spacing in meter

F = Width dimension that characterizes the load distribution for the bridges obtained from Table 2.3

W_e = Width of the design lanes in meter

W_c = Bridge deck width in meter

C_f = Correction factor obtained from CHBDC Table 2.3

B = width of the bridges for ULS and FLS, but not greater than three times the spacing in case of FLS in meter

L = bridges span length in meter

D_x = total bending stiffness, EI, of the bridges cross-section divided by the width of the bridges

D_{xy} = total torsion stiffness, GJ, of the cross-section divided by the width of bridges

For bridges having design lanes more than four-lanes, F values shall be calculated as follow:

$$F = F_4 \frac{nR_L}{2.80} \quad (2.9)$$

Where:

F_4 = value of F for four-lanes obtained from Table 2.4 in case of Fatigue Limit State the longitudinal bending moment per girder

Longitudinal vertical shear force per girder, V_g, for Ultimate, Serviceability Limit State and Fatigue Limit State as follow:

$$V_g = F_v V_{g\ avg} \quad (2.10)$$

$$V_{g\,avg} = \frac{nV_T R_L}{N} \quad (2.11)$$

$$F_V = \frac{S.N}{F} \quad (2.12)$$

Where:

$V_{g\,avg}$ = average shear per box girder

F_v = amplification factor for the transverse variation in maximum longitudinal vertical Shear intensity

V_T = maximum vertical shear per design lane

N = number of design lanes

R_L = modification factor for multi-lane loading

N = number of longitudinal box girders

S = center-to-center girder spacing in meter

W_e = width of the design lane in meter

F = width dimension that characterizes the load distribution for the bridge and can be obtained from Table 2.2

F_v = amplification factor for the transverse variation in maximum longitudinal vertical shear intensity

In case of Fatigue Limit State the longitudinal bending moment per girder the shear calculated as follow:

$$V_{g\,avg} = \frac{V_T}{N} \quad (2.13)$$

Where:

$V_{g\ avg}$ = average shear per box girder.

V_T = maximum vertical shear per design lane.

N = number of longitudinal box girders.

F = width dimension that characterizes the load distribution for the bridge and can be obtained from Table 2.2

$$F_V = \frac{S.N}{F} \tag{2.14}$$

F_v = amplification factor for the transverse variation in maximum longitudinal vertical shear intensity

S = center-to-center girder spacing in meter.

N = number of longitudinal box girders.

F = width dimension that characterizes the load distribution for the bridge and can be obtained from Table 2.2 for Fatigue Limit State

The general equation for deflection distribution factor taking the following form:

$$F_\Delta = \frac{S.N}{F\left(1+\frac{\mu C_f}{100}\right)} \tag{2.15}$$

$$\mu = \frac{W_{e-3.3}}{0.6} \leq 1.0 \tag{2.16}$$

$$F = \frac{\Delta_T}{N} \tag{2.17}$$

Where:

F_Δ = deflection distribution factor

S = center-to-center girder spacing in meter.

N = number of longitudinal box girders.

F = width dimension that characterizes the load distribution for the bridge

W_e = width of the design lane in meter

Δ_T = deflection distribution factor per design lanes.

N = number of longitudinal box girders.

CHAPTER III

FINITE-ELEMENT ANALYSIS

3.1 General

The results from the literature review showed that the finite-element method is best approach to model composite concrete slab deck-on-steel box girder bridges to investigate their load distribution factors for moment, shear, and deflection. In the finite-element modeling, the structure is divided into discrete elements connected together by nodal points. A typical finite element has a stiffness matrix relating the nodal vector displacement to nodal applied forces and can be expressed as functions of properties and shapes or geometries of elements. There are few types of functions shapes, namely: (i) one dimensional functions shape; (ii) two-dimensional function shape; and (iii) three-dimensional function shape. The one-or two-dimensional function shape can easily be solved without using computers. In a three-dimensional funation shape, the procedure would be more complicated and difficult to be solved because of many complicated equations that cannot be solved easily and if it does, it would have error which are not acceptable.

SAP2000 software is one of few available computer software that is user-friendly. In SAP2000 software, it is easy to model any structural shape and to generate element meshing. Also, it is easy to edit or view any data using spread sheets and it has automatic sections and section properties. Few researcher used SAP2000 software in their research. In 2008, Abdel-Mohti and Pekcan used SAP2000 software to investigate the seismic response of skew reinforced-concrete box-girder bridges. The results for nonlinear static pushover analysis, and linear and nonlinear time history analysis were conducted with great accuracy. In 2010, Jan et al. characterized two-lane box-girder bridges with different geometries subjected to truck loading using SAP2000 software. In 2010, Zhang et al. developed finite-element program BGAS for shear lag analysis using FORTRAN languages which showed good correlation between the FEA modeling and the experimental findings. In the current study, SAP2000 was used to analyse composite concrete slab-on steel box-girder bridges.

3.2 Finite-element Approach

The finite-element method is used in the field of structural engineering and in mathematical physics to solved problems. The methodology in this numerical method of analysis starts in discretization a model by dividing it into an equivalent system of smaller bodies or units called "elements" to decrease the error. The smaller mesh sizes will be, the more accurate results will be determined for the load prescribed and for the structural response to loads resulted in at the "nodes". The elements were interconnected at nodes common to two or more and an equation is then formulated combining all the elements to obtain solutions for one whole body. The stiffness matrix of each element is derived by using displacement formulations, and the global stiffness matrix of the entire structure can be formulated by the direct stiffness method. This global stiffness matrix, along with the given displacement boundary conditions and applied loads are then solved. The finite-element method is really a very extensive tools that has improved for engineering design standards and for successful methodology in most design application process before any design processed or manufactured. It is considered as most accurate and a faster design method that decrease error and increase productivity.

The formula in matrix equations expressed as follow:

$$[P] = [K] [U] \tag{3.1}$$

Where:

[P] = nodal load vector

[K] = global stiffness matrix

[U] = nodal displacement vector

In the finite-element modeling, problems can be solved either it is linear or non-linear. The global stiffness matrix is appropriate to many problem types but it is important to index the displacement and the stiffness in appropriate places for the particular modeled elements.

3.3 SAP2000 Software

SAP2000 software is one of finite-element popular programs used internationally to estimate structural responses due to different imposed loads. It is very powerful to Analyze and solve determinates and indeterminate structural analysis problems of complicated structures. It can solve static or dynamic problems, linear or non-linear types of structures utilizing both geometric and material properties. There are many types of dimension elements in SAP2000 software, namely: two-dimensional solid elements, three-dimensional solid elements, two-dimensional plane elements, three-dimensional frame element, and three-dimensional shell elements. In this particular shell element, the elements can be either three or four nodes depending on the modeled members. Shell elements are modeled by dividing the structure into an equivalent system of smaller elements which interconnected at nodes. The membrane performance of such elements includes a transformational in-plane stiffness components and rotational stiffness component in the direction standards to the plane of the elements.

SAP2000 software is extensive in analyzing the structures in both two dimensional and three-demensional format. It has the adventage of drawing windows of different planes and navigates for live multiple models and for complex modes. It's very simple in controlling complex geometries and easy to describe the concrete or steel shapes or fix modulus of elasticity for any materials particularly for composite construction. In 2002, El-Tawil and Okeil Investigated the behaviour of composite box-girder bridges using the finite-element method to analyse box girder bridges. Figure 3.1 shows view of the finite-element modelling and the mesh size used to attain more accurate results for the load prescribed.

3.4 Finite-element Modeling of Composed Multiple Box girder Bridges

Back in 1941, Hrennikoff was first used finite-elements to investigate membrane and plate bending of structures but with limited applications to only rectangular regular shapes rather than irregular shapes until 1971. With the development of shell elements and other sophisticated elements, computer software were developed and continued to grow in capabilities to solve engineering problems. In this research, SAP2000 software was used to mode the composite multiple-spine box-girder bridges. Shell elements were used to model simply-supported

composite concrete deck-on multiple-spine steel box-girder bridges to determine their load distribution characteristics under CHBDC truck loading. Thirty-six composite concrete slab deck-on-steel box girder bridges were modeled a three-dimensional form by considering the concrete deck slab, steel box girder, cross steel bracing and the restraint at each end of the bridges. In 2000, Nour used finite-element modeling, using ABAQUS software, to investigate the load distribution factors for similar bridges but under AASHTO Standard truck.

3.4.1 Material Modeling

In SAP2000 software, it is fundamental that material properties are defined so that the final results would be more accurate and acceptable. Material properties input includes modulus of elasticity and Poisson's ratio of the material. In this study, it was assumed that steel and concrete materials were homogenous and elastic. Concrete slab modulus of elasticity, Ec, was taken 27,000 MPa, with Poisson's ratio of 0.2. Steel modulus of elasticity, Es, was taken 200,000 MPa, with Poisson's ratio of 0.3. The concrete deck slab was 225 mm thick and has full shear interaction with the steel box girders.

3.4.2 Geometric Modeling

In this study the geometry of bridge superstructure is achieved by the proper selection of the number of elements representation the deck slab, webs, bottom flange, top flange, cross bracings and end diaphrams. Also, geomtetic nonlinearity was not considered in this study.

3.4.3 Modeling of Composite Bridges

3.4.3.1 Sensitive Sample Modeling for Composite Bridges

Sensitivity study was conducted to investigate the accuracy of the FEA modeling using SAP2000. A sample bridge configuration shown in Table 3.1 was analyzed as a beam under central load and other time using SAP2000 three-dimensional finite-element modeling. Table 3.1 shows similar trend in the values of mid-span flexural stresses, and deflection as well as the shear force at the support line.

3.4.3.2 Modeling of Composite Concrete Slab-on-steel Box girder Bridges

To model the studies bridges, the three-dimensional shell element in SAP2000 software was used to model the bottom flange, webs, and deck slabs. It has four corner nodes with six degree of freedom each, three displacements (U_1, U_2, U3) and three rotation (φ_1, φ_2, φ_3). Two-node frame elements were used to model the bracing members. The top flange of the steel box was informed in this study.As such, the web is assumed continuoud to the centreline of the top deck slab.

3.5 Aspect Ratio

Shell element aspect ratio is very important in representing the actual structural behavior. It is the ratio of the longest to shortest dimensions of the quadrilateral elements. In 2002, Logan mentioned that it is important that the aspect ratio is maintained below 4. In this parametric study, the aspect ratio was kept below 2.5 in each element division to obtain accurate results. This was achieved by using 50 elements in the longitudinal direction for 20-meter length composite bridge, 100 elements in the longitudinal direction for 40-meter length, 150 elements in the longitudinal direction for 60-meter length and 200 elements in the longitudinal direction for 80-meter length. Considering dividing the bottom flange width and the concrete slab between webs into four element, the aspect ratio was maintained less than 2.5 for all studied bridges.

3.6 Boundary Conditions

To achieve the boundary conditions at the support lines, one side of the bridges was assumed roller while the other side of the bridge is assumed hinged.The lower points of the web at the support lines were used to enforce this boundary condition. Figures 3.2 and 3.3 shows views of the FEA models extracted from SAP2000.

3.7 Applied Loads

In this study, composite bridge were modeled with different span lengths and different bridge widths and subjected to different loading conditions. CHBDC truck and lane loading. Chapter 4 summarizes the applied loading cases per CHBDC. SAP2000 accepts loading the structures at the nodes with concentrated load or on the shell element as uniform loading. In addition, the

software can consider the truck as a moving load over the top slab to get the maximum effect for flexural stresses at the mid-span location and the maximum shear force at the support line.

3.8 Calculation of Distribution Factors

3.8.1 Calculation of Moment Distribution Factors

Moment distribution factors for composite concrete slab deck-on-multiple steel box girders was determined from the finite-element SAP2000 software as the ratio between the flexural stress obtained from the FEA modeling (σ_{FEA}) and that from simple-beam analysis. ($\sigma_{straight}$). The calculation of (σ straight) moment due to single CHBDC truck is determined by the flexural formula:

$$(\sigma_{Straight})_{Truck} = \frac{(M_T . Y_b)}{I_t} \qquad (3.2)$$

Where:

M_T = mid-span girder moment due to single CHBDC truck loading

Y_b =distance from natural axis of the girder cross-section to to the bottom fiber or flange

I_t = moment of inertia of the girder

After obtaining the flexural stress at the mid-span location from the FEA modellig, the moment distribution factors were calculated using the equations listed below at exterior girder and interior girder locations for each truck loading case:

For Exterior girder:

$$(F_m)_{PL,\ ext} = \frac{(\sigma_{FEA,\ ext})_{PL} \cdot R'_L}{\frac{(\sigma_{straight})_{Truck,\ n.\ R_L}}{N}} \qquad (3.3)$$

$$(F_m)_{FL,\ ext} = \frac{(\sigma_{FEA,\ ext})_{FL}}{\frac{(\sigma_{straight})_{Truck,\ n,}}{N}} \qquad (3.4)$$

$$(F_m)_{FAT,\ ext} = \frac{(\sigma_{FEA,ext})_{FAT}}{\frac{(\sigma_{straight})_{Truck}}{N}} \quad (3.5)$$

For Middle girders:

$$(F_m)_{PL,Mid} = \frac{(\sigma_{FEA,\ Mid})_{PL} \cdot R'_L}{\frac{(\sigma_{straight})_{Truck,\ n,\ R_L}}{N}} \quad (3.6)$$

$$(F_m)_{FL,\ Mid} = \frac{(\sigma_{FEA,\ Mid})_{FL}}{\frac{(\sigma_{straight})_{Truck,\ n,}}{N}} \quad (3.7)$$

$$(F_m)_{FAT,\ Mid} = \frac{(\sigma_{FEA,Mid})_{FAT}}{\frac{(\sigma_{straight})_{Truck}}{N}} \quad (3.8)$$

Where:

$(F_m)_{PL}$ = moment distribution factor for partially-loaded lanes

$(F_m)_{FL}$ = moment distribution factor fully-loaded lanes

$(F_m)_{FAT}$ = moment distribution factor for fatigue limit state (i.e. a truck located at the centre of a travelling lane)

$(\sigma_{FEA,\ ext})_{PL}$ = maximum longitudinal stress for partially-loaded lanes obtained from the finite-element modelling

$(\sigma_{FEA,\ ext})_{FL}$ = maximum longitudinal stress for fully-loaded lanes obtained from the finite-element modelling

$(\sigma_{FEA,\ ext})_{FAT}$ = maximum longitudinalstress for fatigue-loaded lane obtained from the finite-element modelling

$(\sigma_{straight})_{Truck}$ = maximum calculated mid span moment, due to single CHBDC truck loaded

N = number of steel box girders

n = number of lanes, see Table 2.4

R'_L = multi-lane factor based on the number of loaded lanes, see Table 2.1

R_L = multi-lane factor based on the number of design lanes, see Table 2.1

3.8.2 Calculation of Shear Distribution Factors

Shear distribution factor F_v was considered as the ratio between the girder support reaction obtained from the finite-element modelling and the maximum support reaction of a simple beams of span length similar to the bridge span and loaded with CHBDC truck loading. These shear distribution factors are presented using the following equations:

For Exterior girder:

$$(F_V)_{PL,\ ext} = \frac{(V_{FEA,\ ext})_{PL} \cdot R'_L}{\frac{(V_{straight})_{Truck\ n.\ R_L}}{N}} \quad (3.9)$$

$$(F_V)_{FL,\ ext} = \frac{(V_{FEA,\ ext})_{FL}}{\frac{(V_{straight})_{Truck\ n,}}{N}} \quad (3.10)$$

$$(F_V)_{FAT,\ ext} = \frac{(V_{FEA,\ ext})_{FAT}}{\frac{(V_{straight})_{Truck}}{N}} \quad (3.11)$$

For Middle girders:

$$(F_V)_{PL,Mid} = \frac{(V_{FEA,\ Mid})_{PL} \cdot R'_L}{\frac{(V_{straight})_{Truck\ n.\ R_L}}{N}} \quad (3.12)$$

$$(F_V)_{FL,\ Mid} = \frac{(V_{FEA,\ Mid})_{FL}}{\frac{(V_{straight})_{Truck\ n,}}{N}} \quad (3.13)$$

$$(F_V)_{FAT,\ Mid} = \frac{(V_{FEA,\ Mid})_{FAT}}{\frac{(V_{straight})_{Truck}}{N}} \quad (3.14)$$

Where:

$(F_v)_{PL}$ = reaction or shear distribution factor for partially-loaded lanes

$(F_v)_{FL}$ = reaction or shear distribution factor for fully- loaded lanes

$(F_v)_{FAT}$ = reaction or shear distribution factor for fatigue-loaded lane

$(V_{FEA.\ ext})_{PL}$ = maximum vertical reaction or shear force at exterior support obtained from the finite elment modelling for partically-loaded lanes

$(V_{FEA.\ ext})_{FL}$ = maximum vertical reaction or shear force at exterior support obtained from the finite elment modelling for fully-loaded lanes

$(V_{FEA.\ ext)\ FAT}$ = maximum vertical reaction or shear force at exterior support obtained from the finite elment modelling for fatigue-loaded lane

$(V_{straight})_{Truck}$ = maximum calculated reaction or shear force of a beam due to single CHBDC truck load

N = number of steel box girders

n = number of lanes, see Table 2.4

R'_L = multi-lane factor based on the number of loaded lanes, see Table 2.1

R_L = multi-lane factor based on the number of design lanes, see Table 2.1

3.8.3 Calculation of Deflection Distribution Factors

The deflection distributed factor, F_Δ, for concrete slab-on-steel multi-box girder bridges was determined for each Fatigue loading case where the truck loading is located at the centre of each travelling lane. It was calculated from the following equations as the ratio between the maximum live load deflection under single truck load from the finite-element modelling to the live load deflection from the beam of a span equal to the bridge span and loaded with CHBDC truck loading including the dynamic load allowance.

$$(F_{\Delta})_{FAT,\ ext} = \frac{(\Delta_{FEA,ext})_{FAT}}{\frac{(\Delta_{straight})_{Truck}}{N}} \quad (3.15)$$

$$(F_{\Delta})_{FAT,\ Mid} = \frac{(\Delta_{FEA,Mid})_{FAT}}{\frac{(\Delta_{straight})_{Truck}}{N}} \quad (3.16)$$

Where:

$(\Delta_{FEA,\ ext})_{FAT}$ = maximum deflections at bottom flanges resulting from the finite-element modelling for bridges subjected to travelling single truck at the centre of travelling lane. It should be noted that the case of fatigue load condition in the exterior lane would provide the corresponding live load deflection Fatigue for exterior loaded lanes

$(\Delta_{FEA.\ Mid})_{FAT}$ = maximum deflections at bottom flange obtained from the finite element modelling for central travelling lane loaded with single truck at its mid-width

$(\Delta_{straight})_{Truck}$ = maximum calculated deflection of beam due to single CHBDC truck including dynamic load allowance

CHAPTER IV

RESULTS FROM THE PARAMATIC STUDY

4.1 General

The structural response of the composite concrete slab deck-on-steel multiple-spine box-girder bridges was evaluated using the finite-element modelling. A practical-design-oriented parametric study was conducted to determine the moment, shear and deflection distribution factors of such bridges. Thirty-six simply-supported straight bridges were modelled using SAP2000 software. Two live load conditions were considered in this study, namely: (i) CHBDC truck loading including the dynamic load allowance, and (ii) the lane loading, including a combination of 9 kN/m uniform load to be distributed over a 3 m width and 80% of the truck loading without dynamic load allowance. Figure 4.1 shows a schematic diagram of the finite element modelling of bridge cross-secion. While Figures 4.2, 4.3 and 4.3 shows schematic diagrams of number of boxes considered for two-, three- and four- lane bridge cross-section, respectively. In case of two-lane bridges, 2, 3 and 4 boxes were considered to form bridge cross-section of the same width. In case of three-lane bridges, number of boxes per same bridge width was taken as 3, 4 and 5, while the number of boxes for four-lane bridge cross-section was taken 4, 5 and 6. Both internal and external bracing between boxes were considered in this study. External bracings were also considered between boxes at the support in addition to solid steel diaphragm inside boxes at the support lines.

Bridge spans considered in this study were 20, 40, 60 and 80 m. While deck width was taken 9, 12.5, and 16 m. Considering barrier wall width of 0.5 m, the total bridge widths considered in this study were 10, 13.5 and 17 m. The number of design lanes was taken 2, 3 and 4. The span-to-depth ratio of the steel boxes was taken 25. Thicknesses of steel webs and bottom flanges were taken 16 mm, while the thickness of the concrete slab was taken 225 mm. The number of boxes within bridge cross-section was distributed evenly so that the length of the slab cantilever is half the width of the box. Table 4.1 summarizes the geometric configurations of bridges considered in the parametric study. Table 4.2 summarizes the material properties of steel and concrete used in the finite-element modelling.

Different truck loading conditions were considered in this study to maximum the effects on the box girders. Figure 4.5 shows schematic diagrams of the truck loading conditions for ultimate limit state, fatigue limit state and serviceability limit state design for two-lane bridges. Figures 4.6 and 4.7 showed similar loading conditions but for three-lane bridges. Figures 4.8, 4.9 and 4.10 show similar loading cases for four-lane bridges. The parametric study was conducted to examine the efftec of the following key parameters in the load distribution factors:

1. Bridge span length, L;
2. Bridge width, B;
3. Number of design lanes;
4. Number of box girders, N; and
5. Box girder spacing, S.

.

4.2 Moment Distribution Factors

In analyzing the bridges using the finite-element modelling, the moment distribution factor was calculated for each box girder for each loading case. Then, the greatest one of all girders for loadings cases used to ultimiate limit state (ULS) design was selected. Similar procedure was followed for calculating the moment distribution factor for fatigue limit state (FLS) design. Appendix A summarises the moment distribution factors for ULS and FLS designs along with the loading case from which the maximum values were obtained. In addition, these tables present correlations of the FEA results with CHBDC and proposed equation values. The following subsections present discussions on the effect of each parameter on the moment distrution factors.

4.2.1 Effect of Bridge Span Length on Moment Distribution Factors

Figures 4.11 and 4.16 depict the effect of the span length on the moment distribution factor of four-lane bridge at ultimate limit state and fatigue limit state, respectively. It can be observed that there is no specific trend in the change of the moment distribution factor with increase in span length when the number of design lanes is involved. For example, for two-lane bridge, it can be observed that the moment distribution factor slightly increases with increase of span length from 20 to 60 m. No increase was observed for span length beyond 80 m. This trend is altered for three-lane bridges where there is insignificant increase change in the moment

distribution factors for spans ranging from 20 to 60 m. However, the moment distribution factor increases for spans greater than 60 m. In case of four-lane bridges, the moment distribution factor at ULS decreases with increase in bridge spans from 20 to 40 m, while there is insignificant change in the moment distribution factor for spans greater that 40 m. Similar trend can be observed in Figures 4.16 for moment distribution factors at the FLS. Therefore, it is expected that there would be an empirical expression for the moment distribution factor in the simplified moment of analysis for each number of design lanes, which is the current case with CHBDC load distribution factors.

4.2.2 Effect of Number of Steel Box Girder on Moment Distribution Factors

The Effect of number of steel box girders on the behaviour of the composite concrete slab-on-steel box-girder bridges was studies. Figure 4.12 depcits the moment distribution factor at ULS for 20-m span bridges having different number of box girders for the same bridge width. It can be observed that the moment distribution factor decreases with increase in number of box girders, irrespective of the change in the number of design lanes. Figure 4.13 shows the change in moment distribution factor at ULS with the change in the number of box girders for different bridge span lengths of a three-lane bridge. It can be observed that the trend of increase in moment distribution factor with increase in number of box girders is not altered with change in span length. As such, one may expect that the the developed equation for moment distribution factor should include the change in number of box girders for the same bridge width of number of design lanes. Since the increase in number of boxes within the same bridge width increases both the flexural and torsional stiffness of the bridge, thus enhancing the load distribution characteristics of the girders, it would be appropriate to include the flexural and torsional stiffness values in the moment distribution factor equations, which is the case with CHBDC simplified method for box griders. Similar trend was observed for the three-lane bridges with different span lengths as depicted in Figs. 4.17 and 4.18 for moment distribution factors at FLS.

4.2.3 Effect of the Spacing of the Box Girders on Moment Distribution Factors

One may consider the effect of number of boxes within the same bridge width in a different sense through the change in the girder spacing. Within increase in number of boxes for the same bridge width, girder spacing decreases. Figures 4.15 and 4.20 depict the change of the moment

distributon at ULS and FLS, respectively, for 20-m span bridge with the change in girder spacing. It can be obserbed that there is a slight increase in moment distribution factor with increase in girder spacing. Still, one may consider the change in girder spacing in lieu of number of boxes in developed moment distribution factor's equations.

4.2.4 Effect of Numbers of Design Lanes on Moment Distribution Factors

The effect of numbers of design lanes is investigated for ultimate and fatigue limit state designs. Figures 4.14 and 4.19 depict the change in moment distribution factors with the change in number of design lanes as well as the span length at ULS and FLS, respectively. In case of FLS, the change is obvious as the moment distribution factor increases with increase in number of design lanes, irrespective of the change in span length. However, at ULS , the moment distribution factor slightly decrease with increase in number of design lanes for 40- and 60-m Span bridges.

4.2.5 Comparison between CHBDC Moment Distribution Equations and the Finite-Element Results

Canadian Highway Bridge design Code recommends using specified empirical equations to calculate moment distribution factors for different types of bridges. Appendix A lists the CHBDC moment distribution factors for the studies bridges along with values obtained from the finite-element analysis, while Figures. 4.44 and 4.45 show correlation between them at ULS and FLS, respectively. It can be observed that CHBDC generally specifies moment distribution factors at ULS and FLS greater than those obtained from the FEA analysis. In some cases, it reaches about 70% greater that FEA results in some cases. As such, the following sections will introduce more reliable expressions for economical design of such bridges.

4.2.6 Comparison between AASHTO-LRFD Live Load Distribution Equation and Moment Distribution Factors Obtained from Finite-element Analysis

The AASHTO-LRFD Bridge Design Sepecifications specify the following equation for live load distribution factors for multiple-spine steel bridges. More information about this equation can be found in Chapter 2.

$$WL = 0.1+1.7\frac{N_L}{N_B}+\frac{0.85}{N_L} \quad (4.1)$$

Figures 4.46 and 4.47 show correlation between the AASHTO-LRFD moment distribution factors and FEA results for the studies bridges at ULS and FLS, respectively. It can be observed that AASHTO-LRFD overestimates the moment distribution factors at ULS by a significant magin. However, it overestimate the response in some bridges with a significant margin and underestimate the response in few cases. For example FEA moment distribution factor for two-lane bridges with three box girders and 20 m span length was 0.93 but AASHTO-LRFD reading was 1.65, A 43% overestimation in the response.

4.3 Effect of Parameters on Shear Distribution Factors

In analysing the bridges using the finite-element modelling, the shear distribution factor was calculated for each box girder for each loading case. Then, the greatest one of all girders for loadings cases used to ultimiate limit state (ULS) design was selected. Similar procedure was followed for calculating the shear distribution factor for fatigue limit state (FLS) design. Appendix B summarises the shear distribution factors for ULS and FLS designs along with the loading case from which the maximum values were obtained. In addition, these tables present correlations of the FEA results with CHBDC and proposed equation values. The following subsections present discussions on the effect of each parameter on the shear distrution factors.

4.3.1 Effect of Bridge Span Length on Shear Distribution Factors

Figures 4.21 and 4.22 depicts the effect of the span length on the shear distribution factor of four-lane bridge at ultimate limit state and fatigue limit state, respectively. It can be observed that the shear distribution factor generally increases with increase of span length. This trend is altered for three-lane bridges where there is insignificant increase change in the moment distribution factors for spans ranging from 20 to 40 m. Figures 27 and 28 depict t he change in shear distribution factors at ULS and FLS, respectively, with the change in span length of four-lane bridges, in combination with increase in grider spacing or number of design lanes. Again, general trend was observed but from a different angle.

4.3.2 Effect of Numbers of Steel Box Girder on Shear Distribution Factors

The Effect of number of steel box girders on the behaviour of the composite concrete slab-on-steel box-girder bridges was studies. Figure 4.23 depcits the shear distribution factor at ULS for 20-m span bridges having different number of box girders for the same bridge width. It can be observed that the shear distribution factor increases with increase in number of box girders, irrespective of the change in the number of design lanes. Figure 4.24 shows the change in shear distribution factor at ULS with the change in the number of box girders for different bridge span lengths of a four-lane bridge. It can be observed that the trend of increase in shear distribution factor with increase in number of box girders is not altered with change in span length. As such, one may expect that the the developed equation for shear distribution factor should include the change in number of box girders for the same bridge width of number of design lanes. Similar trend was generally observed for the four-lane bridges with different span lengths as depicted in Figures. 4.30 and 4.31 for shear distribution factors at FLS.

4.3.3 Effect of Steel Box Girder Spacing on Shear Distribution Factors

One may consider the effect of number of boxes within the same bridge width in a different sense through the change in the girder spacing. Within increase in number of boxes for the same bridge width, girder spacing decreases. Figures 4.26 and 4.27 depict the change of the shear distributon factors at ULS and FLS, respectively, for 20-m span bridge with the change in girder spacing. It can be obserbed that there is an increase in shear distribution factor with increase in girder spacing. Still, one may consider the change in girder spacing in lieu of number of boxes in developed moment distribution factor's equations. Figures 4.33 and 4.34 show similar trend at FLS.

4.3.4 Effect of Number of Design Lanes on Shear Distribution Factors

The effect of numbers of design lanes is investigated for ultimate and fatigue limit state designs. Figures 4.25 and 4.32 depict the change in shear distribution factors with the change in number of design lanes as well as the span length at ULS and FLS, respectively. In case of FLS, the change is obvious as the shear distribution factor increases with increase in number of design

lanes, irrespective of the change in span length. However, at ULS , there is a slight change in the shear distribution factor for two- and three-lane bridges. However, it increases with increase in number of design lanes from 3 to 4. For example, for 40-m span bridge, the shear distribution increased linearly from 1.37 to 1.5 with increase in number of design lanes from 2 to 4. Also, it increases from 1.53 to 2.88 with increase of number of design lanes from 2 to 4 for 60-m span bridge at FLS.

4.3.5 Comparison between CHBDC Shear Distribution Equations and Those Obtained from Finite-element Analysis

Canadian Highway Bridge design Code recommends using specified empirical equations to calculate shear distribution factors for different types of bridges. Appendix B lists the CHBDC shear distribution factors for the studies bridges along with values obtained from the finite-element analysis, while Figs. 4.54 and 4.55 show correlation between them at ULS and FLS, respectively. It can be observed that CHBDC generally specifies shear distribution factors at ULS lower than those obtained using the FEA analysis. However, CHBDC always overestimates the shear distribution factor at FLS with a big margin in many bridge configurations considered in this study. As such, the following sections will introduce more reliable expressions for economical design of such bridges.

4.3.6 Comparison between AASHTO-LRFD Live load Distribution Equation and Shear Distribution Factors Obtained from the Finite-element Analysis

The AASHTO-LRFD Bridge Design Sepecifications specify equation 4.1 live load shear distribution factors for multiple-spine steel bridges. Figures 4.56 and 4.57 show correlation between the AASHTO-LRFD shear distribution factors and FEA results for the studies bridges at ULS and FLS, respectively. It can be observed that AASHTO-LRFD overestimates the shear distribution factors at ULS and FLS by a significant magin for many bridge configurations considered in this study. However, it underestimates the response in few bridge cases as depicted in Figs. 4.56 and 4.57. As an example, for 80-m span bridge with two design lanes and two box girders, the AASHTO-LRFD shear distribution factor was 2.23 while the FEA analysis showed that it is 1.5 for FLS.

4.4 Effect of Parameters on Deflection Distribution Factors

CHBDC specifies the deflection distribution factor as the moment distribution factor at ULS. This study showed that both the moment and shear distribution factors should be treated differently. In analysing the bridges using the finite-element modelling, the deflection distribution factor was calculated for each box girder for each loading case. Then, the greatest one of all girders for loadings cases used to serviceability limit state (SLS) design was selected. Appendix C summarises the deflection distribution factors at SLS design. In addition, these tables present correlations of the FEA results with CHBDC and proposed equation values. The following subsections present discussions on the effect of each parameter on the deflection distrution factors.

4.4.1 Effect of Bridges Span Length on Deflection Distribution Factors

Figures 4.35 and 4.36 depict the effect of the span length on the deflection distribution factor of four-lane bridge at SLS with the change in number of lanes and number of box girders, respectively. It can be observed that there is no specific trend in the change of the deflection distribution factor with increase in span length.One may observe that the deflection distribution factor decreases with increase in bridge span from 20 to 40 m, then it generally increase with increase in bridge spans from 40 to 80 m.

4.4.2 Effect of Number of Box Girders on Deflection Distribution Factors

The Effect of number of steel box girders on the behaviour of the composite concrete slab-on-steel box-girder bridges was studies. Figure 4.37 depcits the deflection distribution factor at SLS for 20-m span bridges having different number of box girders for the same bridge width. It can be observed that the deflection distribution factor slightly increases with increase in number of box girders, irrespective of the change in the number of design lanes. Figure 4.38 shows the change in deflection distribution factor at SLS with the change in the number of box girders for different bridge span lengths of a two-lane bridge. It can be observed that insignificant change was observed in the shear distribution factor with increase in number of box girders.

4.4.3 Effect of Box Girder Spacing on Deflection Distribution Factors

One may consider the effect of number of boxes within the same bridge width in a different sense through the change in the girder spacing. Within increase in number of boxes for the same bridge width, girder spacing decreases. Figures 4.41, 4.42 and 4.43 depict the change of the deflection distributon factors at SLS with the change in girder spacing. It can be obserbed that there is slight change in deflection distribution factor with increase in girder spacing.

4.4.4 Effect of Number of Design Lanes on Deflection Distribution Factors

The effect of numbers of design lanes is investigated for SLS design. Figure 4.40 depicts the change in deflection distribution factors with the change in number of design lanes as well as the span length. It can be observed that the deflection distribution factor significantly increases with increase in number of design lanes.

4.4.5 Comparison between CHBDC Deflection Distribution Equation and Those Obtained from the Finite-Element Analysis

Canadian Highway Bridge design Code recommends using specified empirical equations to calculate deflection distribution factors for different types of bridges. Appendix C lists the CHBDC deflection distribution factors for the studies bridges along with values obtained from the finite-element analysis, while Fig. 4.76 shows correlation between them. It can be observed that CHBDC generally specifies deflection distribution factors at SLS greater than those obtained from the FEA analysis. As such, the following sections will introduce more reliable expressions for economical design of such bridges.

4.4.6 Comparison between AASHTO-LRFD Live Load Distribution Equation and Deflection Distribution Factors Obtained from Finite-Element Analysis

The AASHTO-LRFD Bridge Design Sepecifications specify equation 4.1 live load deflection distribution factors for multiple-spine steel bridges. Figure 4.77 shows correlation between the AASHTO-LRFD deflection distribution factors and FEA results for the studies bridges at SLS. It can be observed that AASHTO-LRFD overestimates the deflection distribution factors by a

significant magin for many bridge configurations considered in this study. However, it underestimates the response in few bridge cases as depicted in Fig. 4.77.

4.5 Development of Empirical Equations for More Reliable Load Distribution Factors

Based on the data generated from the parametric study, more reliable and economical expressions for the moment, shear and deflection distribution factors were deduced using a statistical package for curve fit. The following subsections introduce these equations along with their correlations with the FEA results to gain confidence in their use in practice.

4.5.1 Proposed Moment Distribution Factors

CHBDC specifies the following equation for the moment distribution factors at ULS and FLS. More information in this equation can be found in Chapter 2.

$$F_m = \frac{S.N}{F\left(1+\frac{\mu C_f}{100}\right)} \geq 1.05 \qquad (4.2)$$

The parameters F and C_f in the equation were developed as follows as a function of the parameter β given in equation 2.8, and the number of boxes.

$$F = (a + b.\mathcal{B})\, N^c \qquad (4.3)$$

$$C_f = (d + e\,\mathcal{B})^m \qquad (4.4)$$

Where a, b, c, d, e and m are constants obtained using the least square technique incorporated in Microsoft Excel.

Expressions of F and C_f were derived for moment distribution factor as listed in Table 4.3 for ULS design and Table 4.4 for FLS design. Appendix A summarizes the corresponding moment distribution factors obtained using these equation. Figures 4.48 through 4.53 show excellent correlation between the moment distribution factors obtained from the developed equations and those obtained from the FEA analysis.

4.5.2 Proposed Shear Distribution Factors

CHBDC specifies the following equation for the shear distribution factors at ULS and FLS. More information in this equation can be found in Chapter 2.

$$F_v = \frac{S.N}{F} \quad (4.5)$$

The parameter F in the equation was developed as follows as a function of the span length and number of boxes.

$$F = (a + b.L). N^c \quad (4.6)$$

Where a, b and c are constants obtained using the least square technique incorporated in Microsoft Excel.

Expressions of F derived for shear distribution factor as listed in Table 4.5 for ULS design and Table 4.6 for FLS design. Appendix B summarizes the corresponding shear distribution factors obtained using these equation. Figures 4.54 through 4.63 show excellent correlation between the shear distribution factors obtained from the developed equations and those obtained from the FEA analysis.

To provide alternatives to the above-mentioned F_v values, the parameter F in the equation was developed as follows as a function of the parameter β given in equation 2.8, and the number of boxes.

$$F = (a + b. \mathcal{B}). N^c \quad (4.8)$$

Where a, b and c are constants obtained using the least square technique incorporated in Microsoft Excel.

Expressions of F were derived for shear distribution factor as listed in Table 4.7 for ULS design and Table 4.8 for FLS design. Appendix B summarizes the corresponding shear distribution factors obtained using these equation. Figures 4.64 through 4.69 show excellent correlation between the shear distribution factors obtained from the developed equations and those obtained from the FEA analysis.

Other set of equations for F to determine the shear distribution factor was derived as a fundtion of the of the parameter β given in equation 2.8, and box-girder spacing as follows.

$$F = (a + b .\mathcal{B}) .S^{c} \quad (4.9)$$

Where a, b and c are constants obtained using the least square technique incorporated in Microsoft Excel.

Expressions of F were derived for shear distribution factor as listed in Table 4.9 for ULS design and Table 4.10 for FLS design. Appendix B summarizes the corresponding shear distribution factors obtained using these equation. Figures 4.70 through 4.75 show excellent correlation between the shear distribution factors obtained from the developed equations and those obtained from the FEA analysis.

4.5.3 Proposed Deflection Distribution Factors

CHBDC specifies equation 4.2 for the deflection distribution factors at SLS. the parameters F and C_f in the equation were developed as a function of the parameter β given in equation 2.8, and the number of boxes.Expressions of F and C_f were derived for delfection distribution factors as listed in Table 4.11. Appendix C summarizes the corresponding deflection distribution factors obtained using these equation. Figures 4.76 through 4.80 show good correlation between the deflection distribution factors obtained from the developed equations and those obtained from the FEA analysis.

CHAPTER V

SUMMARY, CONCLUSIONS AND RECOMMENDATIONS FOR FUTURE RESEARCH

5.1 Summary

Composite box-girder bridges are recently used in modern highway urban system because of their profitable and structural aptitude advantages. North Americans Codes of Practice specify empirical equations for girder moment and shear forces in such bridges in the form of live load distribution factors. These factors were proven to be conservative in some cases and underestimate the response in other cases. Therefore, an extensive parametric study, using the finite-element modeling, was conducted to examine the key parameters that influence the load distribution factors of such bridges. A total of 276 prototype bridges were analyzed to evaluate girder bending moment, shear force and deflection distribution factors for simply-supported composite multiple box-girder bridges when subjected to CHBDC truck loading. Design parameters considered in this study were bridges span length, numbers of design lanes, number of box girders and girder spacing. The following sections summarize the research findings and recommendations for further research.

5.2 Conclusions

Bases on the data generated from the parametric study, the following conclusions are drawing:

1. The most important parameters that affecting the structural behaviour of simply-supported bridge are bridge span length, number of design lanes, number of box girders, flexural-to-torsional stiffness of girders and truck loading condition.
2. CHBDC equations for moment, shear and deflection distribution factors significantly overestimate the structural response in many bridge configurations and underestimate the response in few bridge cases. Similar conclusion is reached for the AASHTO-LRFD load distribution factor equations.

3. Bases on the data generated from the parametric study, sets of empirical expression for moment, shear and deflection distribution factors were developed for simply-supported composite bridge with multiple steel box girders. Excellent correlation between the developed equations and the FEA results was observed. Thus, engineers can use the developed expressions in designing new bridges and evaluate existing bridges with more confidence.

5.3 Recommendations for Future Research

1. Extend the developed equations to cover number of design lanes more that 4.
2. Study the effect of skew on the load distribution factors of box girder bridges.
3. Extend the study to cover the design of multiple-spine box girders made of precast concrete box beams or precast U shapes with cast-in-place deck slab.
4. Field testing to correlate the developed load distribution factors with those recorded during the test.

Table 2.1 Modification factors for multi-lane loading as determined by CHBDC (2006)

Number of loaded design lanes	Modification factor
1	1.00
2	0.90
3	0.80
4	0.70
5	0.6
6 or more	0.55

Table 2.2 F Expressions for longitudinal vertical shear in multi-spine bridges as determined by CHBDC (2006)

Limit state	Number of design lanes	F, m
ULS or SLS	2	7.2
	3	9.6
	4	11.2
FLS	2 or more	4.25

Table 2.3 F and C_f expressions for longitude moment in multi-spine bridge as determined by CHBDC (2006)

Limit state	Number of design lanes	F, M	C_f
ULS or SLS	2	8.5-0.3$\mathcal{B}$	16-2 $\mathcal{B}$
	3	11.5-0.5$\mathcal{B}$	16-2 $\mathcal{B}$
	4	14.5-0.7$\mathcal{B}$	16-2 $\mathcal{B}$
FLS	2 or more	8.5-0.9$\mathcal{B}$	16-2 $\mathcal{B}$

Table 2.4 Number of design lanes as determined by CHBDC (2006)

WC	n
6.0 mr or less	1
Over 6.0 mr to 10.0 mr incl	2
Over 10.0 mr to 13.5 mr incl	2 or 3
Over 13.5 mr to 17 mr incl	4
Over 17 mr to 20.5 mr incl	5
Over 20.5mr to 24.5 mr incl	6
Over 24.5 mr to 27.5 mr incl	7
Over 27.5 mr	8

Table 3.1 Comparison between FEA results and manual calculations for sensitive study

Results from	Stress, MPa	Shear, kN	Deflection, mm
FEA results	22.6	200	-5.4
Calculation results	22.6	200	-5.4

Table 4.1 Geometric of the prototype bridge used in the parametric study

Bridge Type`	Span length L (m)	No of design Lanes	Number of Box Girder (N)	Deck width (m)	Cross-section dimensions (mm)						
					A	B	C	F	t_1	t_2	t_3
2L-2B-20	20	2	2	9	10	2.500	800	1025	16	16	225
2L-3B-20			3	9	10	1.667	800	1025	16	16	225
2L-4B-20			4	9	10	1.250	800	1025	16	16	225
3L-3B-20		3	3	12.5	13.5	2.250	800	1025	16	16	225
3L-4B-20			4	12.5	13.5	1.687	800	1025	16	16	225
3L-5B-20			5	12.5	13.5	1.350	800	1025	16	16	225
4L-4B-20		4	4	16	17	2.125	800	1025	16	16	225
4L-5B-20			5	16	17	1.700	800	1025	16	16	225
4L-6B-20			6	16	17	1.417	800	1025	16	16	225
2L-2B-40	40	2	2	9	10	2.500	1600	1825	16	16	225
2L-3B-40			3	9	10	1.667	1600	1825	16	16	225
2L-4B-40			4	9	10	1.250	1600	1825	16	16	225
3L-3B-40		3	3	12.5	13.5	2.250	1600	1825	16	16	225
3L-4B-40			4	12.5	13.5	1.687	1600	1825	16	16	225
3L-5B-40			5	12.5	13.5	1.350	1600	1825	16	16	225
4L-4B-40		4	4	16	17	2.125	1600	1825	16	16	225
4L-5B-40			5	16	17	1.700	1600	1825	16	16	225
4L-6B-40			6	16	17	1.417	1600	1825	16	16	225
2L-2B-60	60	2	2	9	10	2.500	2400	2625	16	16	225
2L-3B-60			3	9	10	1.667	2400	2625	16	16	225
2L-4B-60			4	9	10	1.25	2400	2625	16	16	225
3L-3B-60		3	3	12.5	13.5	2.250	2400	2625	16	16	225
3L-4B-60			4	12.5	13.5	1.687	2400	2625	16	16	225
3L-5B-60			5	12.5	13.5	1.350	2400	2625	16	16	225
4L-4B-60		4	4	16	17	2.125	2400	2625	16	16	225
4L-5B-60			5	16	17	1.700	2400	2625	16	16	225
4L-6B-60			6	16	17	1.417	2400	2625	16	16	225
2L-2B-80	80	2	2	9	10	2.500	3200	3425	16	16	225
2L-3B-80			3	9	10	1.667	3200	3425	16	16	225
2L-4B-80			4	9	10	1.25	3200	3425	16	16	225
3L-3B-80		3	3	12.5	13.5	2.250	3200	3425	16	16	225
3L-4B-80			4	12.5	13.5	1.687	3200	3425	16	16	225
3L-5B-80			5	12.5	13.5	1.350	3200	3425	16	16	225
4L-4B-80		4	4	16	17	2.125	3200	3425	16	16	225
4L-5B-80			5	16	17	1.700	3200	3425	16	16	225
4L-6B-80			6	16	17	1.417	3200	3425	16	16	225

Table 4.2 Material properties for concrete and steel used in the parametric study

Material properties	Concrete	Steel
Modulus of Elasticity, E, MPa	27,000	200,000
Poisson's Ratio, υ	0.20	0.30

Table 4.3 Empirical equations for moment distribution factors at Ultimate Limit State

Number of Design Lanes	F	C_f	Parameters	
			c	m
2	$(9 + 0.45 \mathcal{B}) N^c$	$(14.0 -1.5 \mathcal{B}^m)$	-0.04	0.1
3	$(12.36 - 0.38 \mathcal{B}) N^c$	$(15.38 -1.6 \mathcal{B}^m)$	0.02	-0.1
4	$(14.72 - 0.7 \mathcal{B}) N^c$	$(4.0 - 8.0 \mathcal{B}^m)$	0.13	0.1

Table 4.4 Empirical equations for moment distribution factors at Fatigue Limit State

Number of Design Lanes	F	C_f	Parameters	
			c	m
2	$(8.53 - 0.69 \mathcal{B}) N^c$	$(9.51 - \mathcal{B})^m$	0.1	1.23
3	$(6.8 - 0.45 \mathcal{B}) N^c$	$(21.7 - 2.9 \mathcal{B})^m$	0.35	0.9
4	$(10 - \mathcal{B}) N^c$	$(18.8 - 2.4 \mathcal{B})^m$	0.11	0.95

Table 4.5 Empirical equations of shear distribution factors for composite bridges on which F is a function of span length L at Ultimate Limit State

Number of Design Lanes	F	**c** Parameter
2	(7.8 - 0.011 L) N^c	-0.11
3	(10.3 - 0.01 L) N^c	0.01
4	(21.2 + 0.09 L) N^c	-0.51

Table 4.6 Empirical equations of shear distribution factors for composite bridges on which F is a function of span length L at Fatigue Limit State

Number of Design Lanes	F	**c** Parameter
2	(7.0 - 0.01 L) N^c	-0.14
3	(6.12 - 0.02 L) N^c	0.05
4	(5.7 - 0.01 L) N^c	0.01

Table 4.7 Empirical equations of shear distribution factors for composite bridges on which F is a function of $\mathcal{B}$ at Ultimate Limit State

Number of Design Lanes	**F**	**c** Parameter
2	(7.0 - 0.15 $\mathcal{B}$) N^c	-0.13
3	(13.0 - 0.7 $\mathcal{B}$) N^c	-0.1
4	(15.3 + 0.17 $\mathcal{B}$) N^c	-0.2

Table 4.8 Empirical equations of shear distribution factors for composite bridges on which F is a Function of $\mathcal{B}$ at Fatigue Limit State

Number of Design Lanes	**F**	**c** Parameter
2	(6.9 - 0.11 $\mathcal{B}$) N^c	-0.1
3	(5.2 + 1.31 $\mathcal{B}$) N^c	-0.22
4	(7.5 - 0.01 $\mathcal{B}$) N^c	-0.22

Table 4.9 Empirical equation of shear distribution factors for composite bridges on which F is a function of S at Ultimate Limit State

Number of Design Lanes	**F**	**Parameter-c**
2	(5.45 - 0.07 $\mathcal{B}$) S^c	0.2
3	(8.0 - 0.05 $\mathcal{B}$) S^c	0.19
4	(9.43 - 0.01 $\mathcal{B}$) S^c	0.2

Table 4.10 Empirical equation of shear distribution factors for composite bridges on which F is a function of S at Fatigue Limit State

Number of Design Lanes	**F**	**C** Parameter
2	(7.3-0.035 S) N^c	-0.22
3	(3.8+0.6 S) N^c	-0.03
4	(12- 0.5 S) N^c	-0.42

Table 4.11 Empirical equation for deflection distribution factors at Fatigue Limit State

Number of Design Lanes	**F**	**C_f**	**Parameters**	
			c	**m**
2	$(10.2 - 0.7\,\mathscr{B})\,N^c$	$(9.5 - \mathscr{B})^m$	-0.1	1.23
3	$(10 + 0.81\,\mathscr{B})\,N^c$	$(21.7 - 2.8\,\mathscr{B})^m$	-0.1	0.9
4	$(13 - 0.19\,\mathscr{B})\,N^c$	$(18.8 - 2.4\,\mathscr{B})^m$	-0.14	0.95

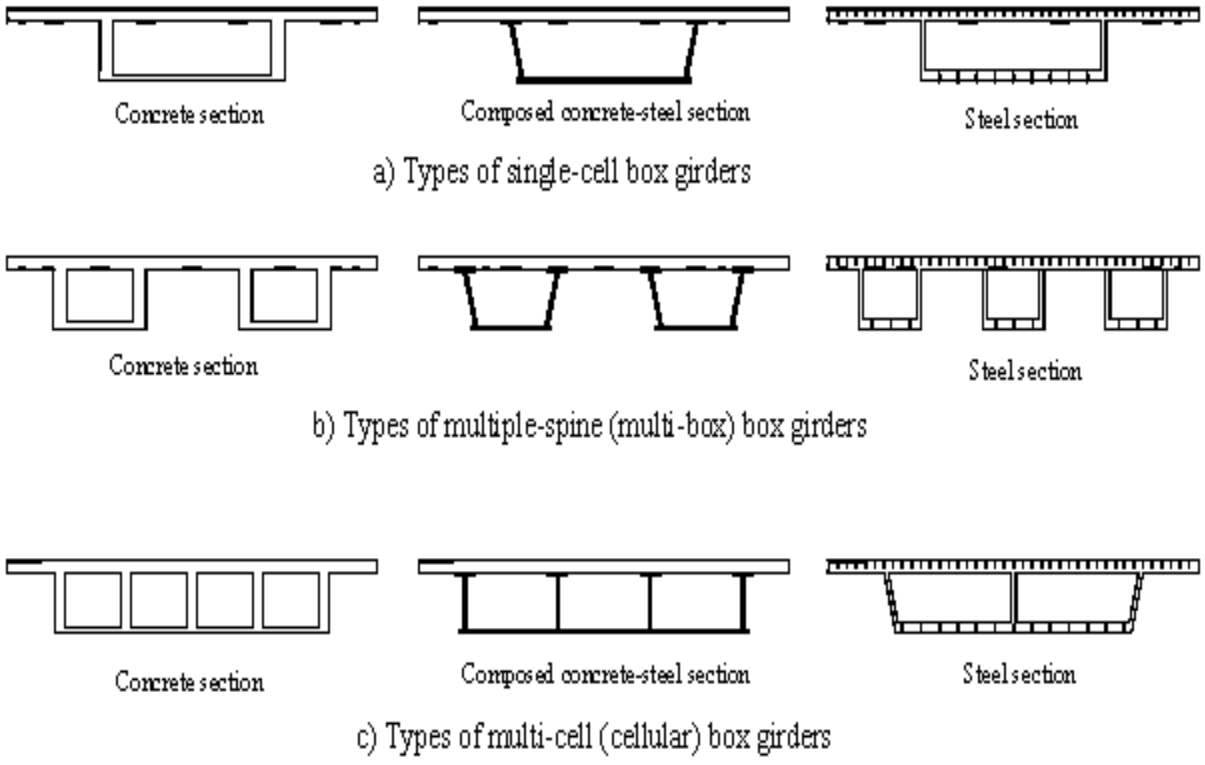

Figure 1.1 Box girders cross-sections

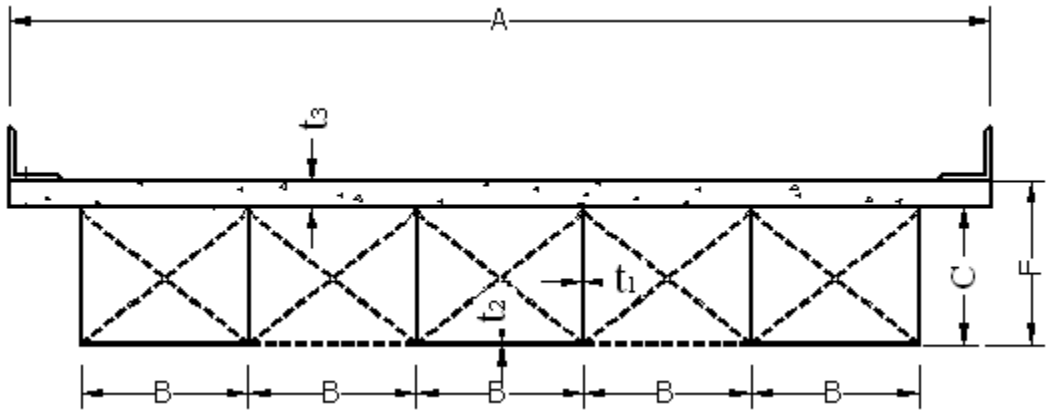

Figure 1.2 Basic box girder cross-section and symbols

Figure 1.3 View of two box girder bridges (El-Tawil and Okeil, 2002)

Figure 1.4 View of five box girder bridges

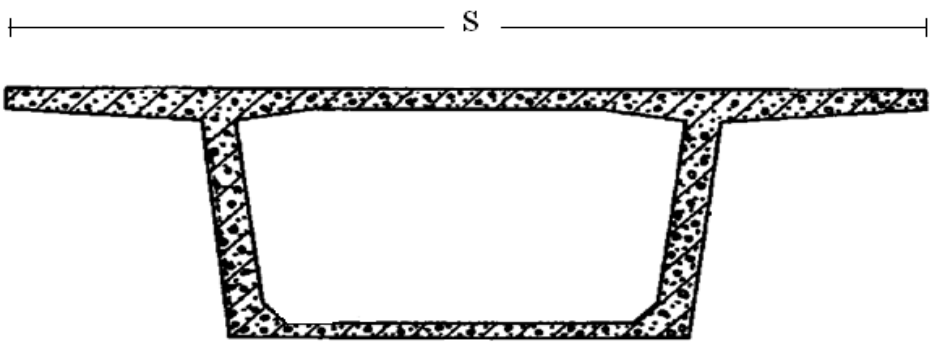

Figure 2.1 Single concrete box girders

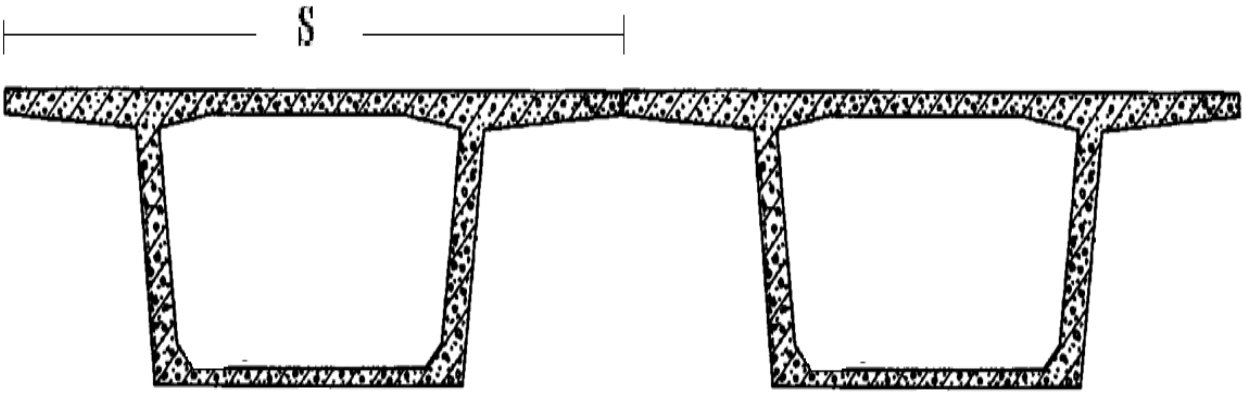

Figure 2.2 Concrete multi-box girder bridges

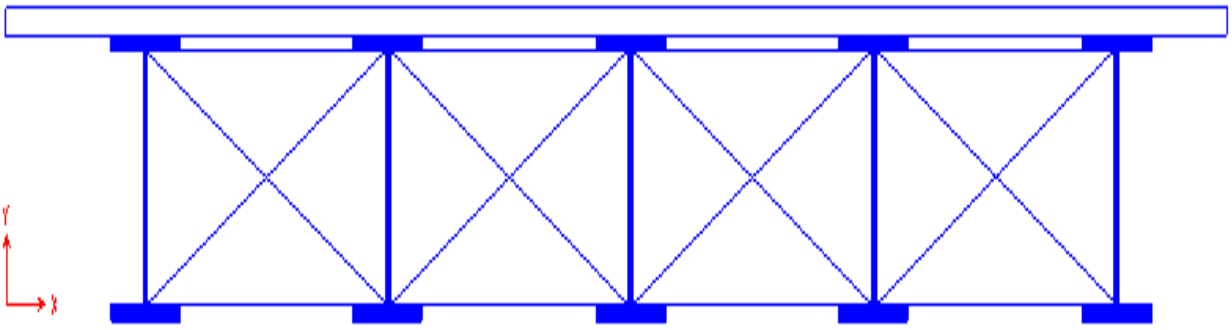

Figure 2.3 Composite bridge-concrete slabs over multi-steel I-girder bridges

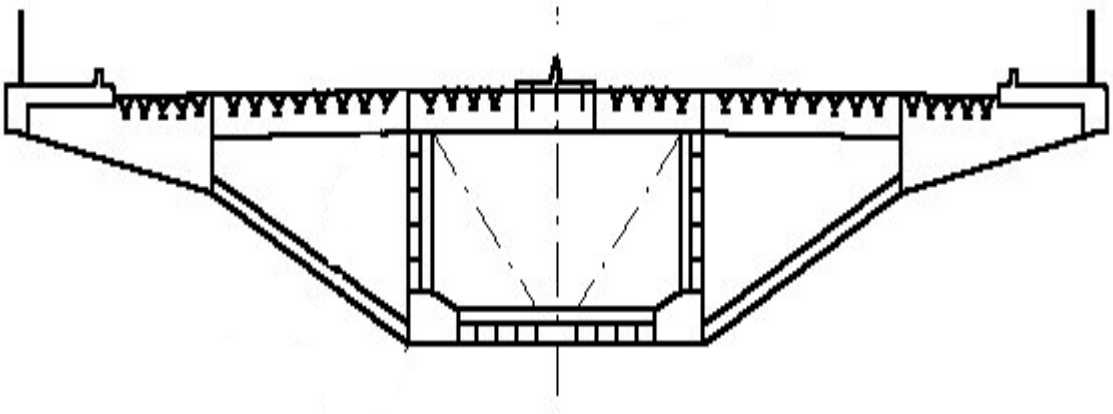

Figure 2.4 Orthotropic steel deck over single steel box girder bridges

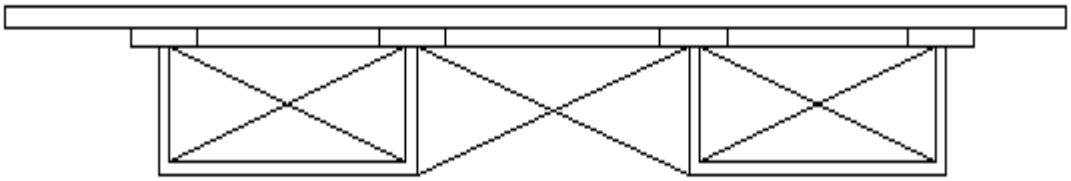

Figure 2.5 Concrete slabs over multi-steel box girder bridges

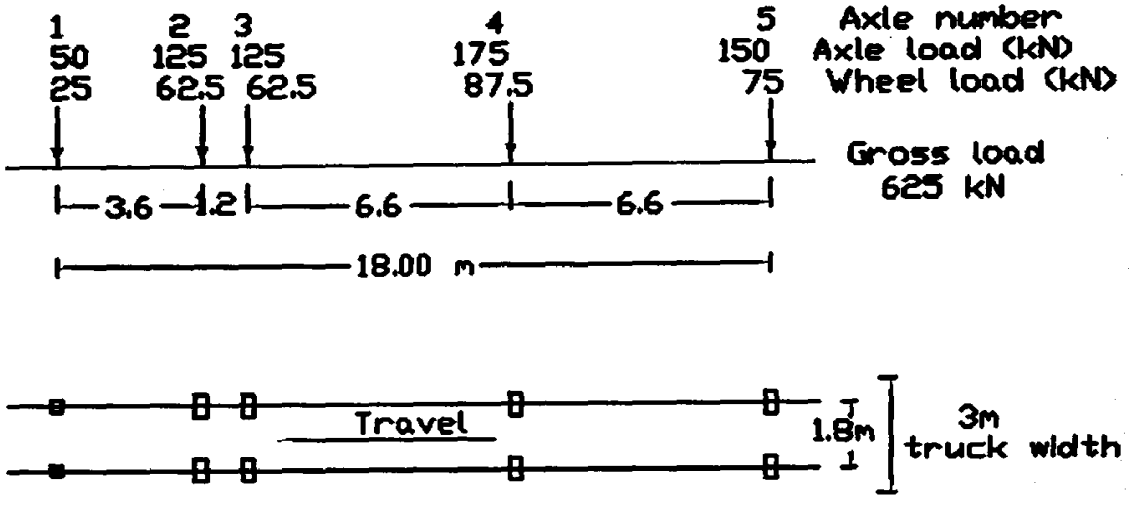

Figure 2.6 CHBDC truck loading

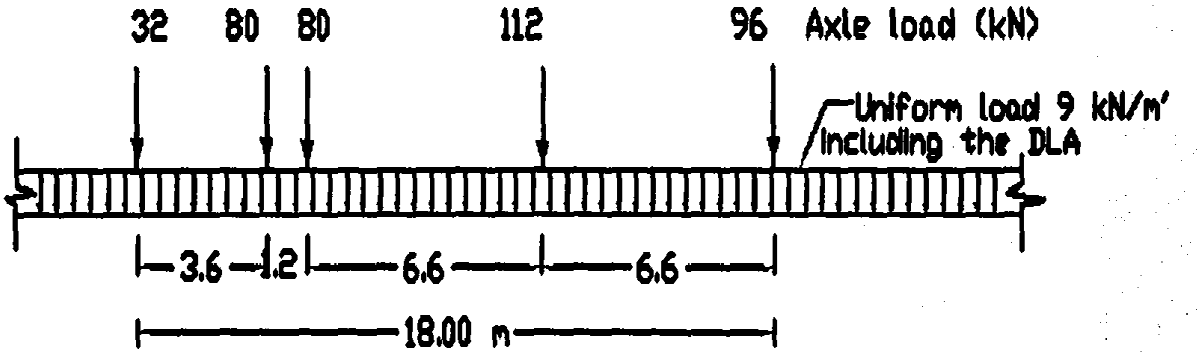

Figure 2.7 CHBDC lanes loading

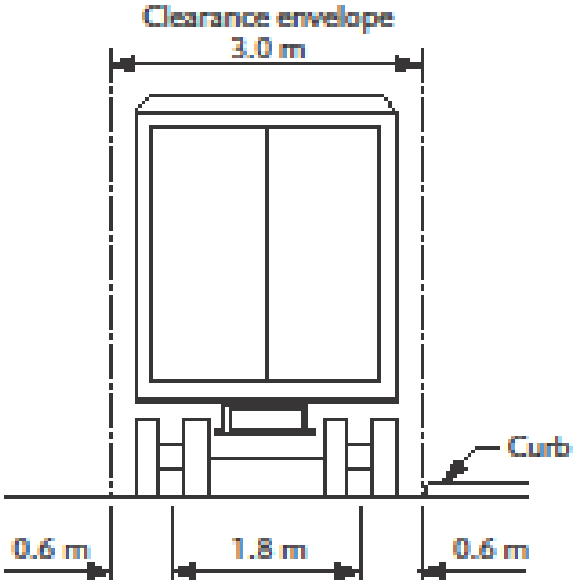

Figure 2.8 CL-W truck loading

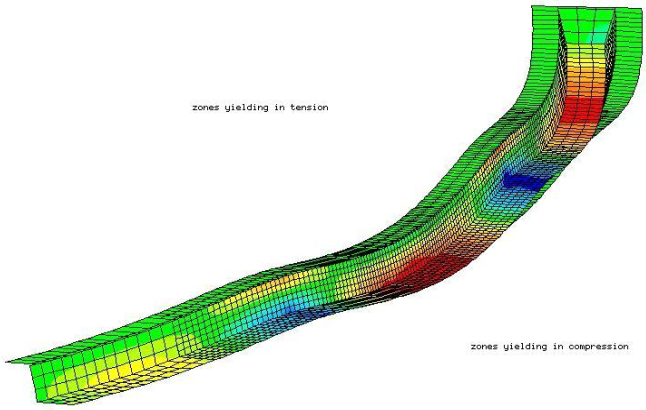

Figure 3.1 Finite-element models (El-Tawil and Okeil, 2002)

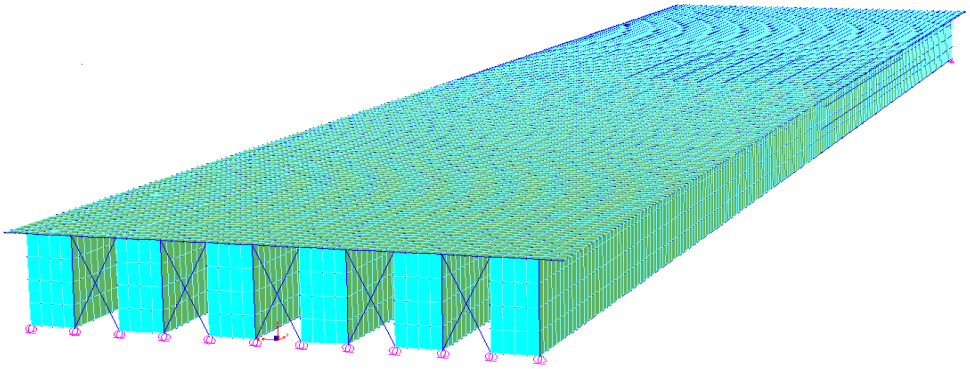

Figure 3.2 SAP2000 model view for composite multi-box girder bridges

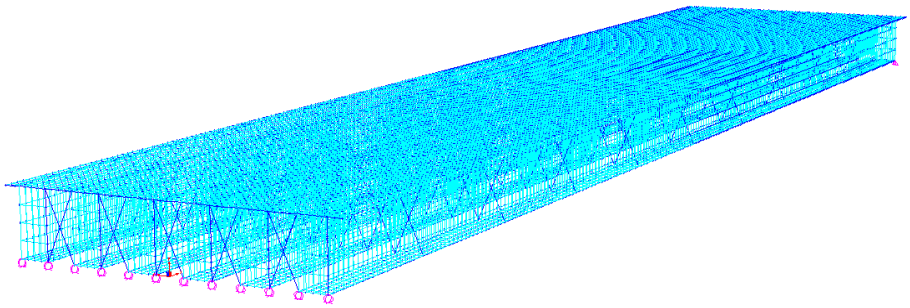

Figure 3.3 SAP2000 model view for composite multi-box girder X-bracing

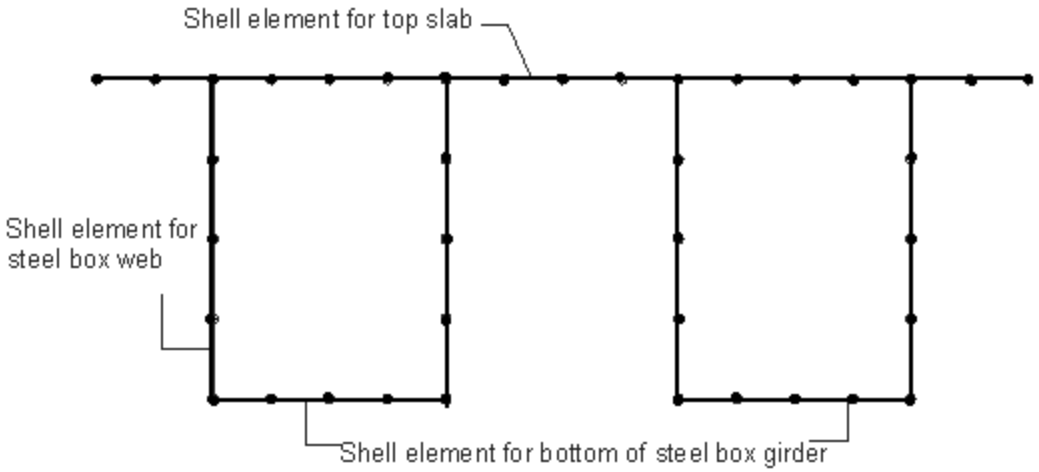

Figure 4.1 Finite-element representations for composite bridge cross-section

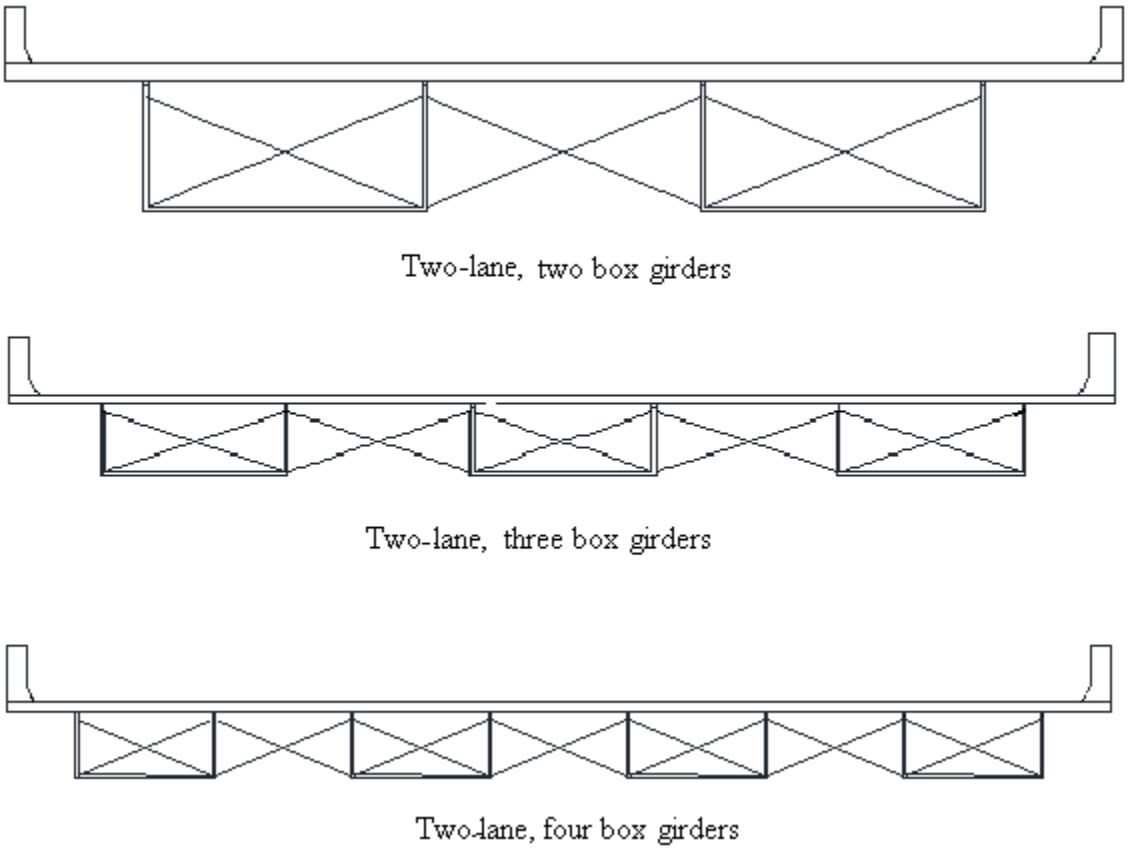

Figure 4.2 Cross-section configurations used in the parametric study for two-lane bridges

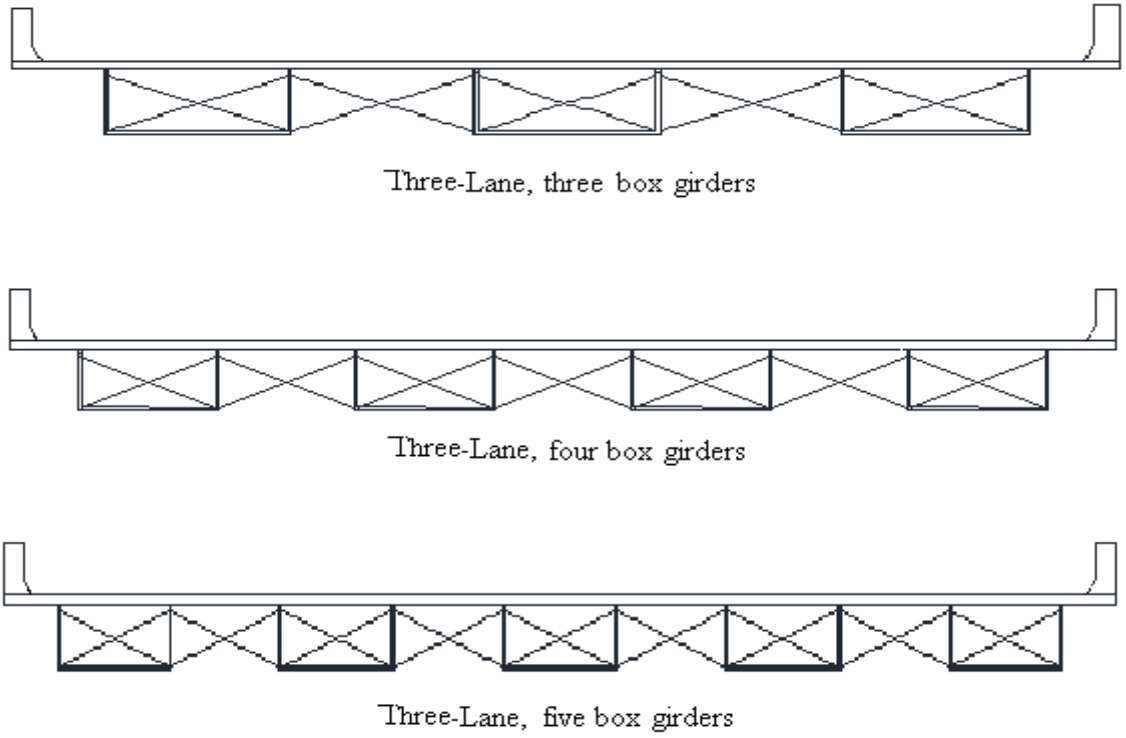

Figure 4.3 Cross-section configurations used in the parametric study for three-lane bridges

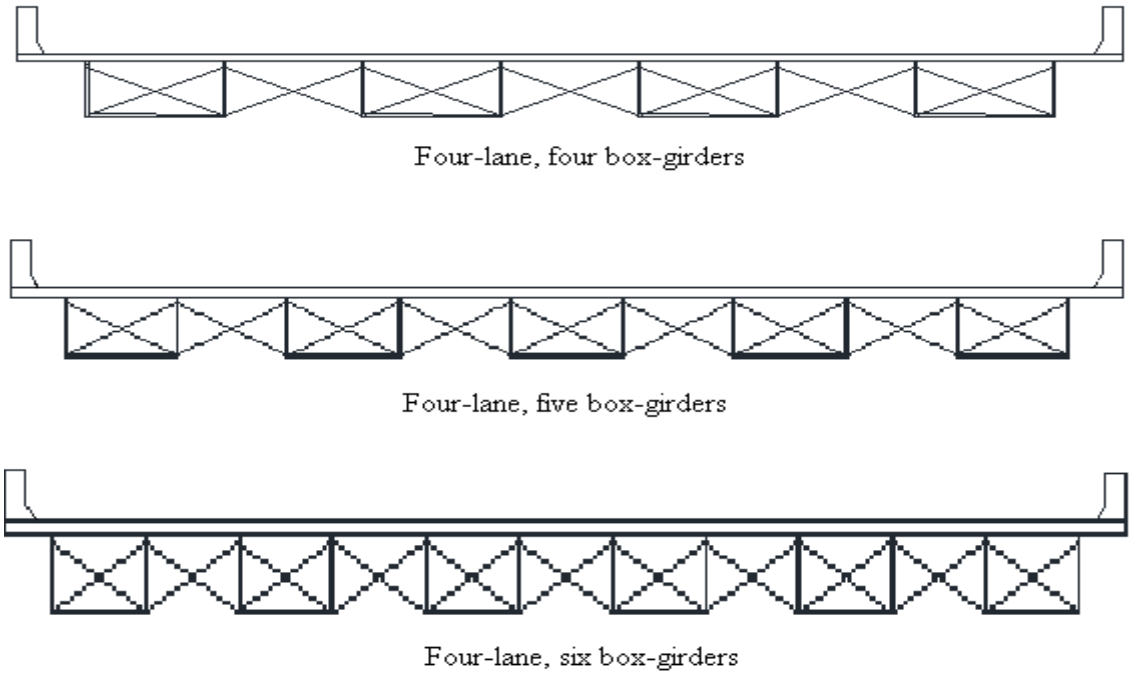

Figure 4.4 Cross-section configurations used in the parametric study for four-lane bridges

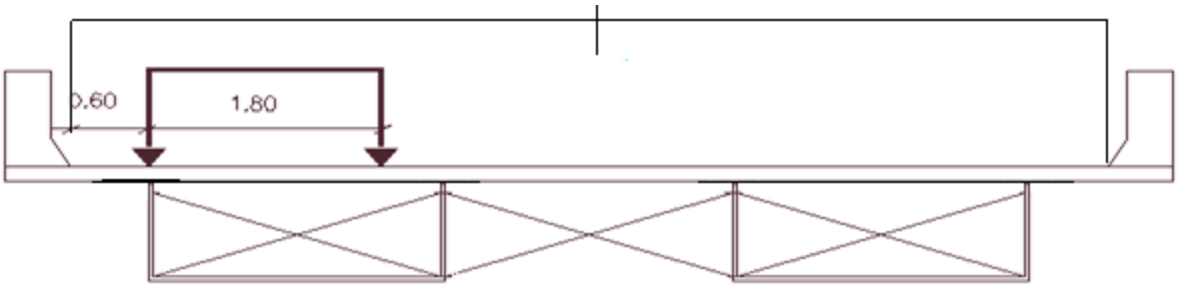

Case (1): Exterior girder-partial load

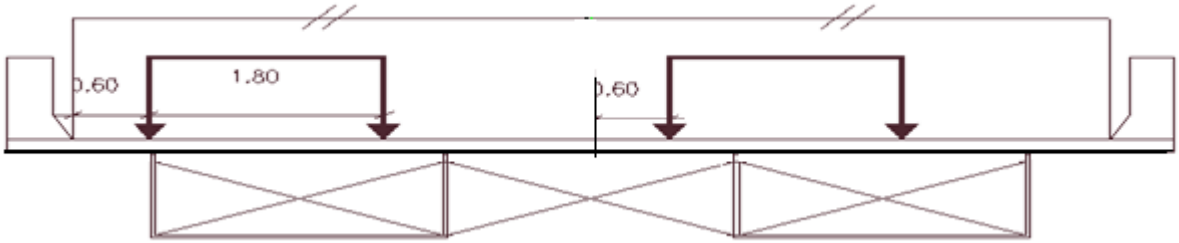

Case (2): Exterior girder-full load

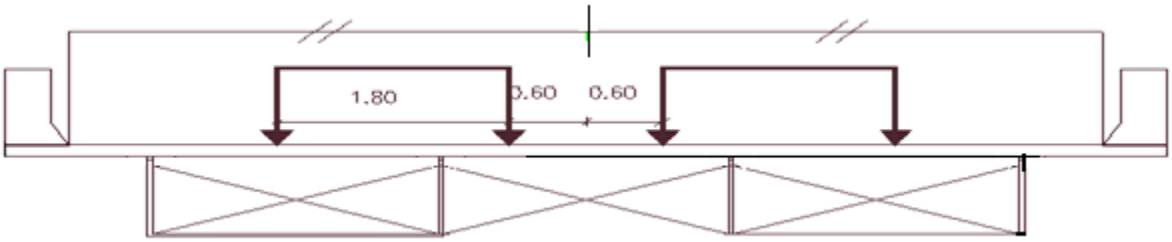

Case (3): Middle girder-full load

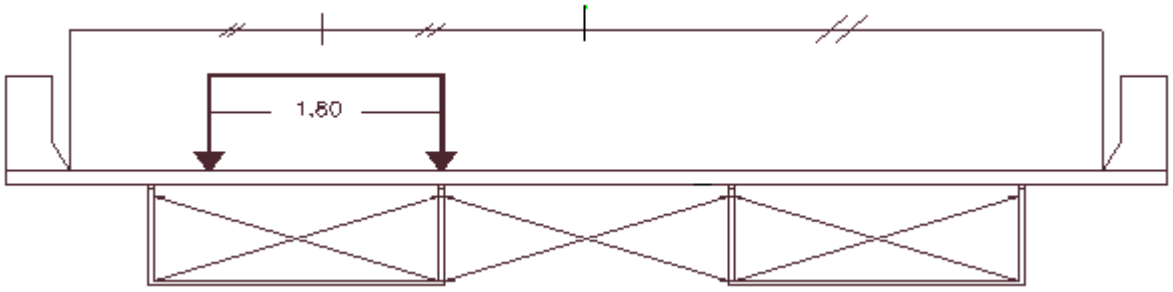

Case (4): Exterior girder-Fatigue case

Figure 4.5 Live loading cases for two-lane, two box girder bridges

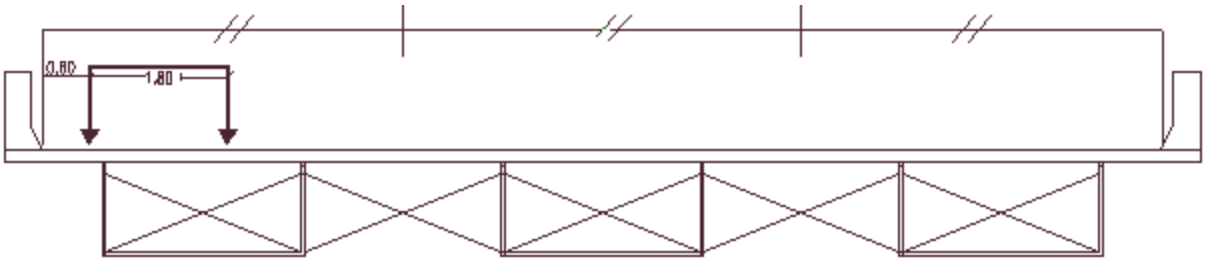

Case (1): Exterior girder-partial load-1

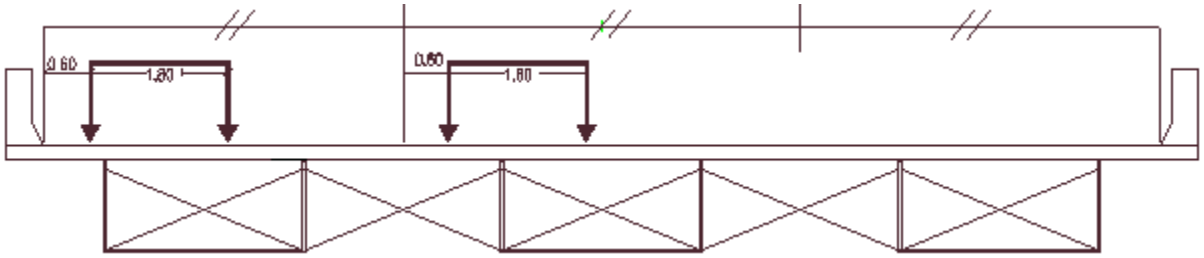

Case (2): Exterior girder-partial load-2

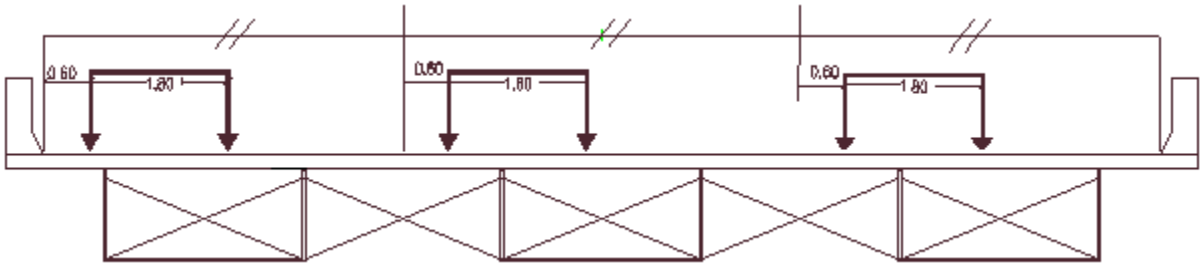

Case (3): Exterior girder-full load

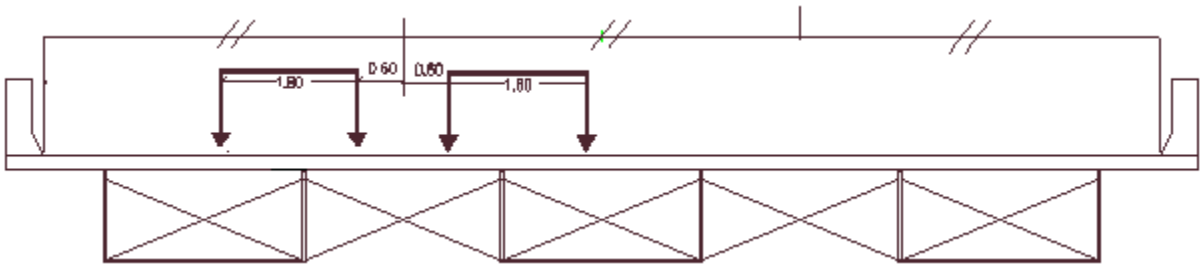

Case (4): Middle girder-partial load

Figure 4.6 Live loading cases for three-lane, three box girders bridges - continue

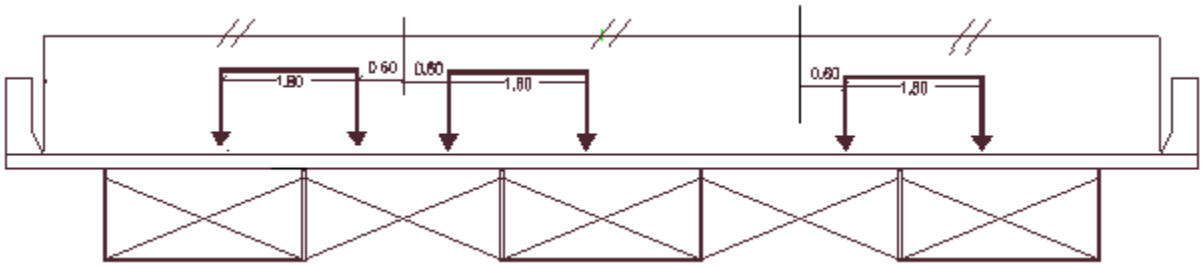

Case (5): Middle girder-full load

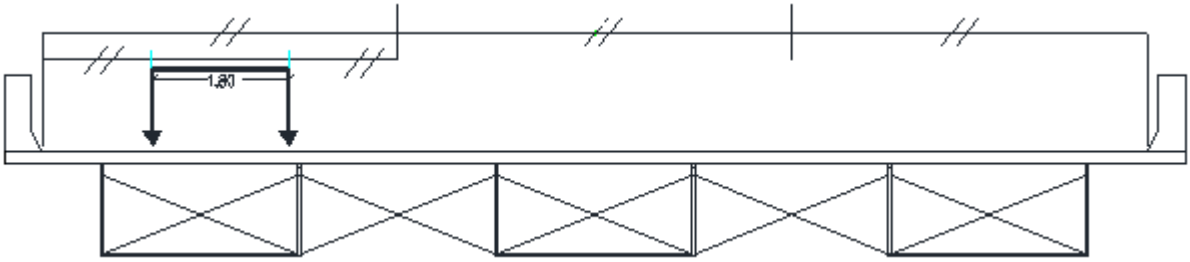

Case (6): Exterior girder-Fatigue case

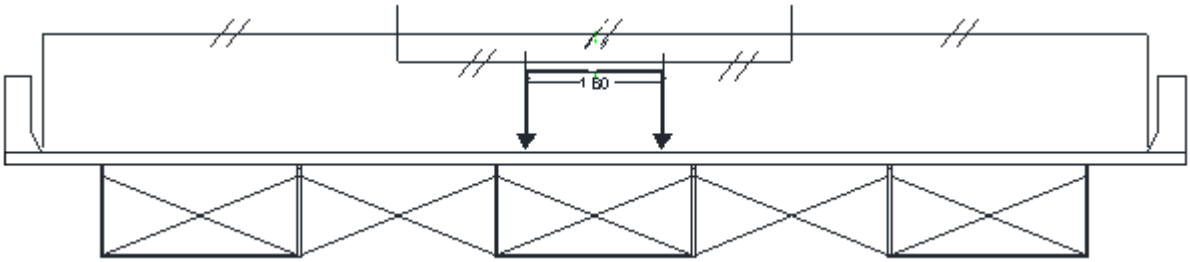

Case (7): Middle girder-Fatigue case

Figure 4.7 Live loading cases for three-lane, three box girder bridges

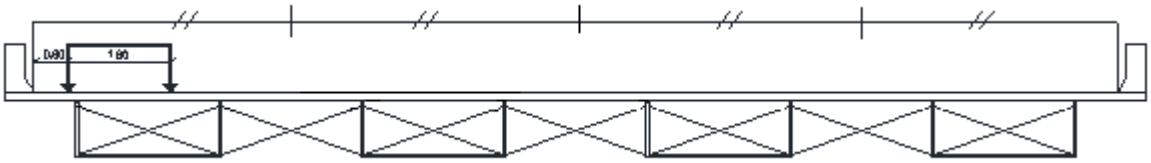

Case (1): Exterior girder-partial load-1

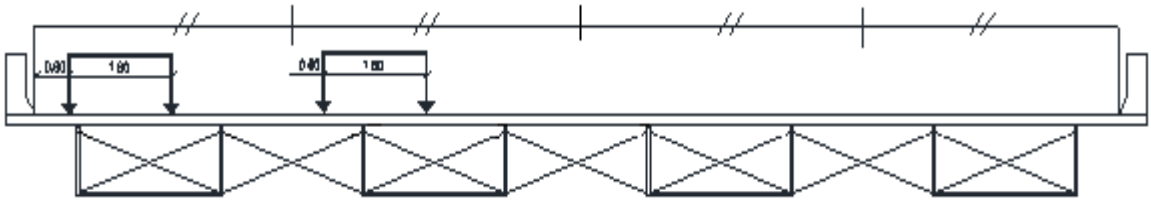

Case (2): Exterior girder-partial load-2

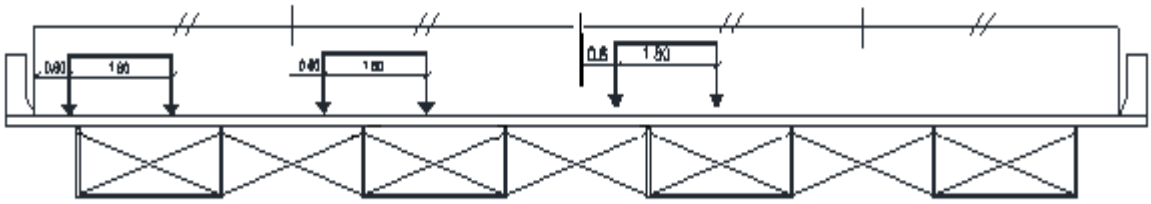

Case (3): Exterior girder-partial load-3

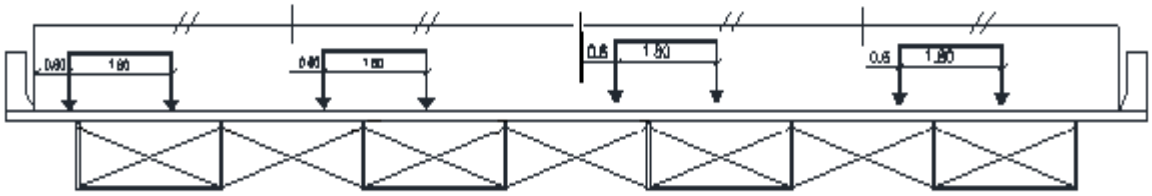

Case (4): Exterior girder-full load

Figure 4.8 Live loading cases for four-lane, four box girder bridges – continue

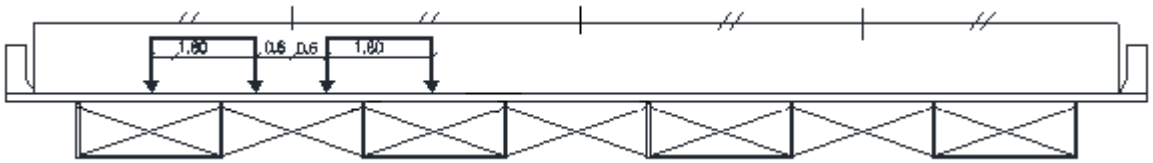

Case (5): Middle girder-partial load-1

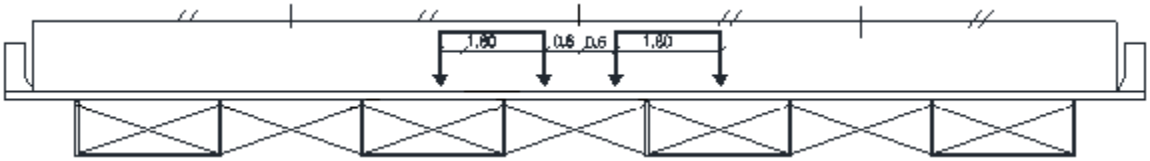

Case (6): Middle girder-partial load-2

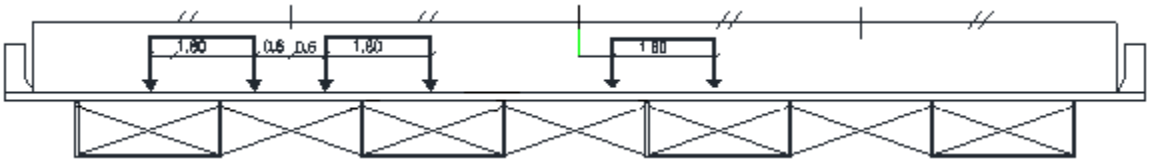

Case (7): Middle girder-partial load-3

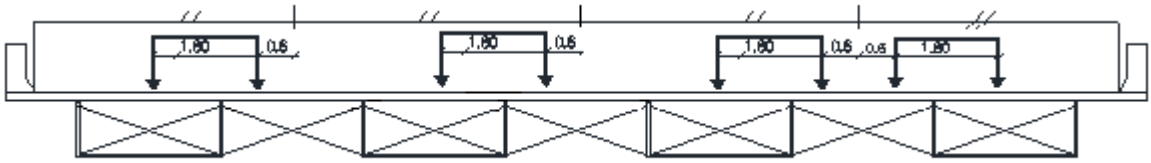

Case (8): Middle girder-full load-1

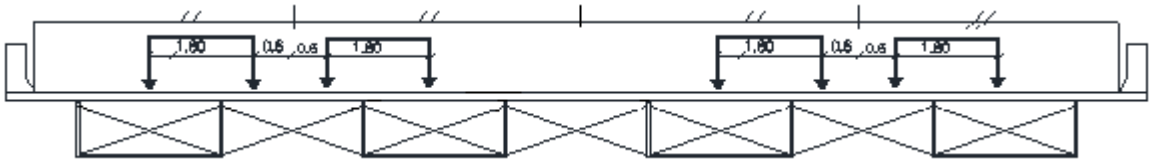

Case (9): Middle girder-full load-2

Figure 4.9 Live loading cases for four-lane, four box girder bridges – continue

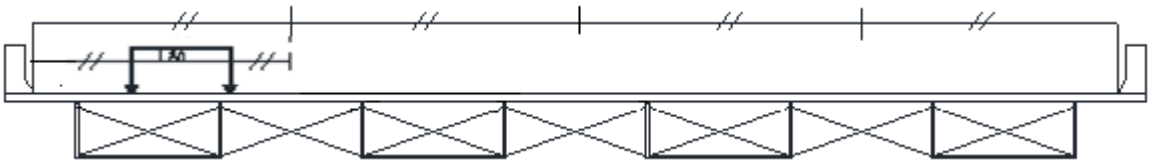

Case (10): Exterior girder-Fatigue case

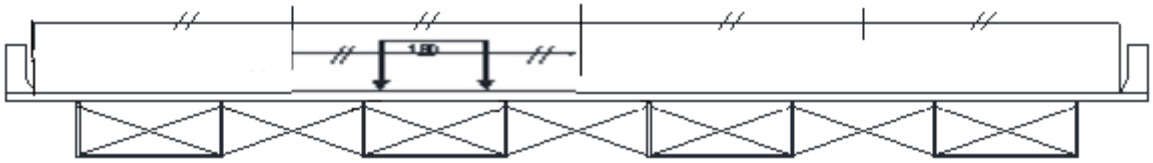

Case (11): Middle girder-Fatigue case-1

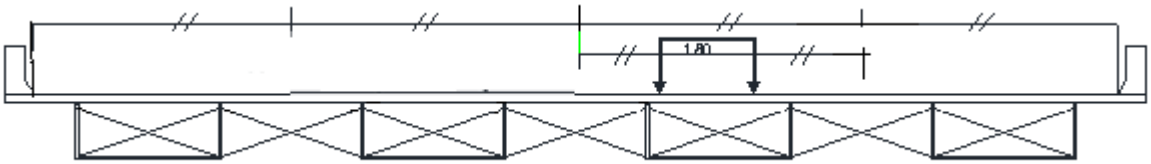

Case (12): Middle girder-Fatigue case-2

Figure 4.10 Live loading cases for four-lane, four box girder bridges

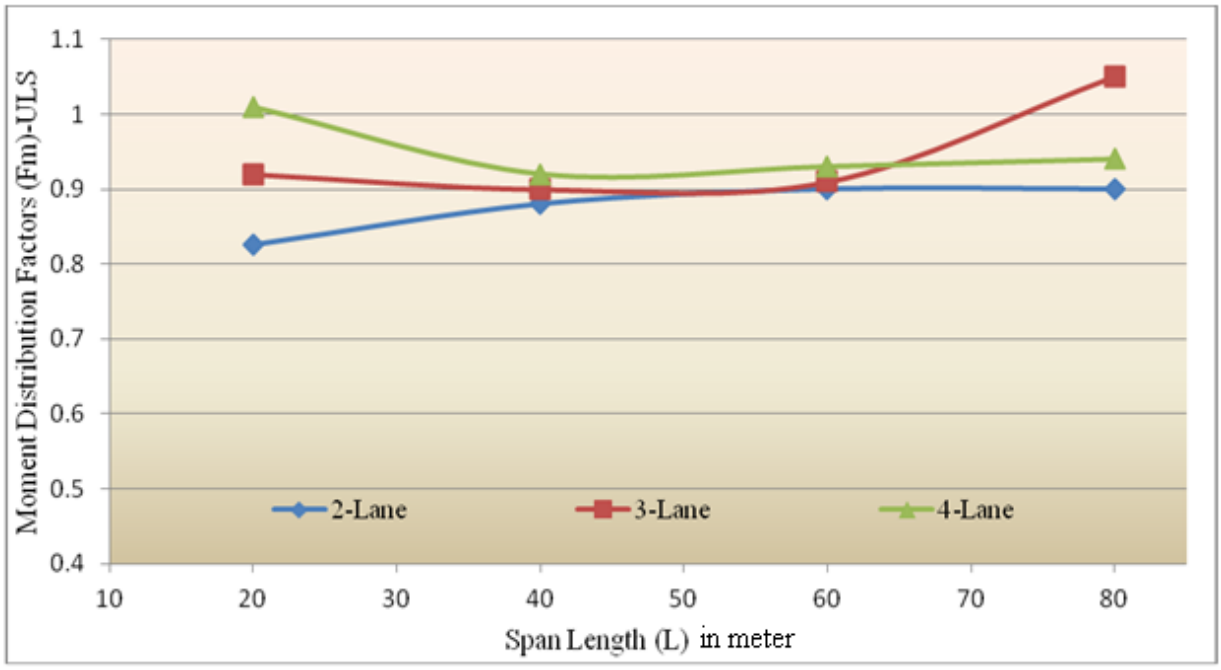

Figure 4.11 Effect of span length on the moment distribution factor for four box girder bridges, due to CHBDC truck loading cases at Ultimate Limit State

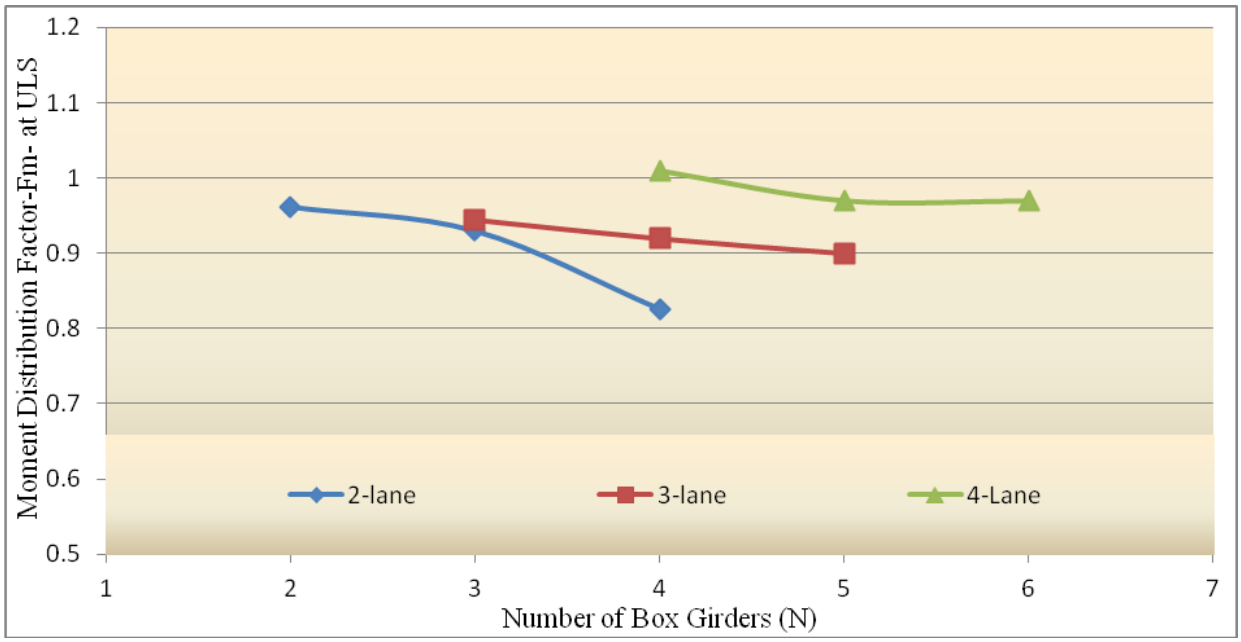

Figure 4.12 Effect of number of box girders of 20-m span bridges on the moment distribution factor due to CHBDC truck loading cases at Ultimate Limit State

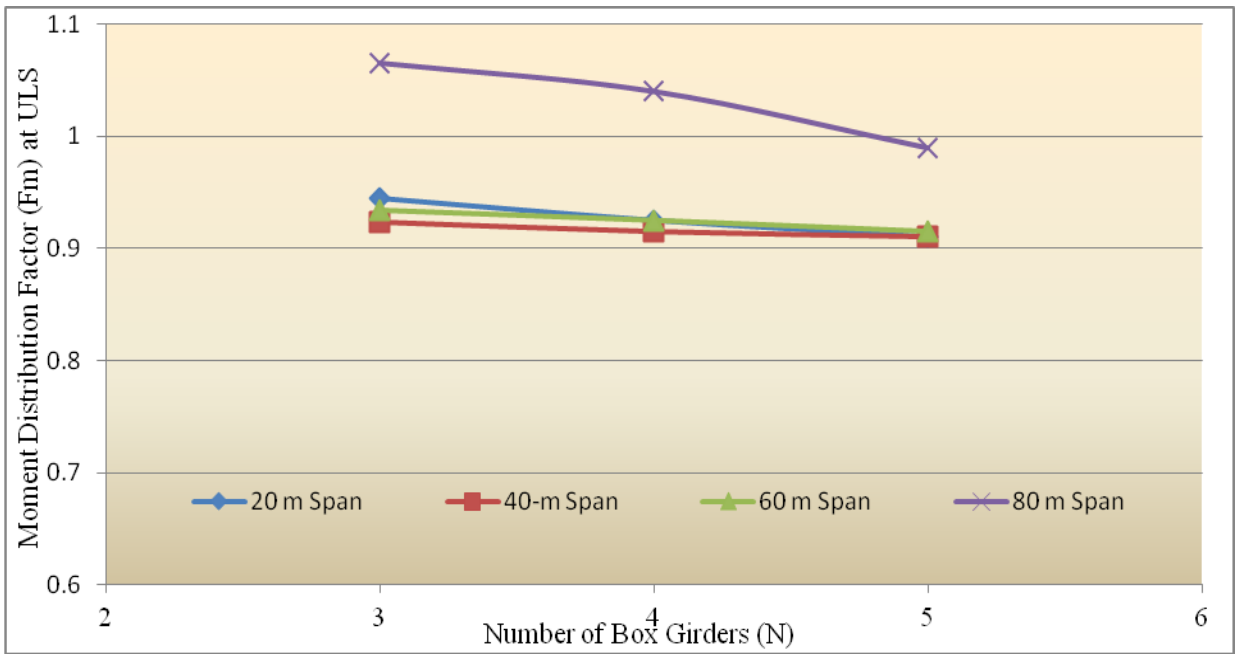

Figure 4.13 Effect of number of box girder on the moment distribution factor due to CHBDC truck loading for three-lane bridges at Ultimate Limit State

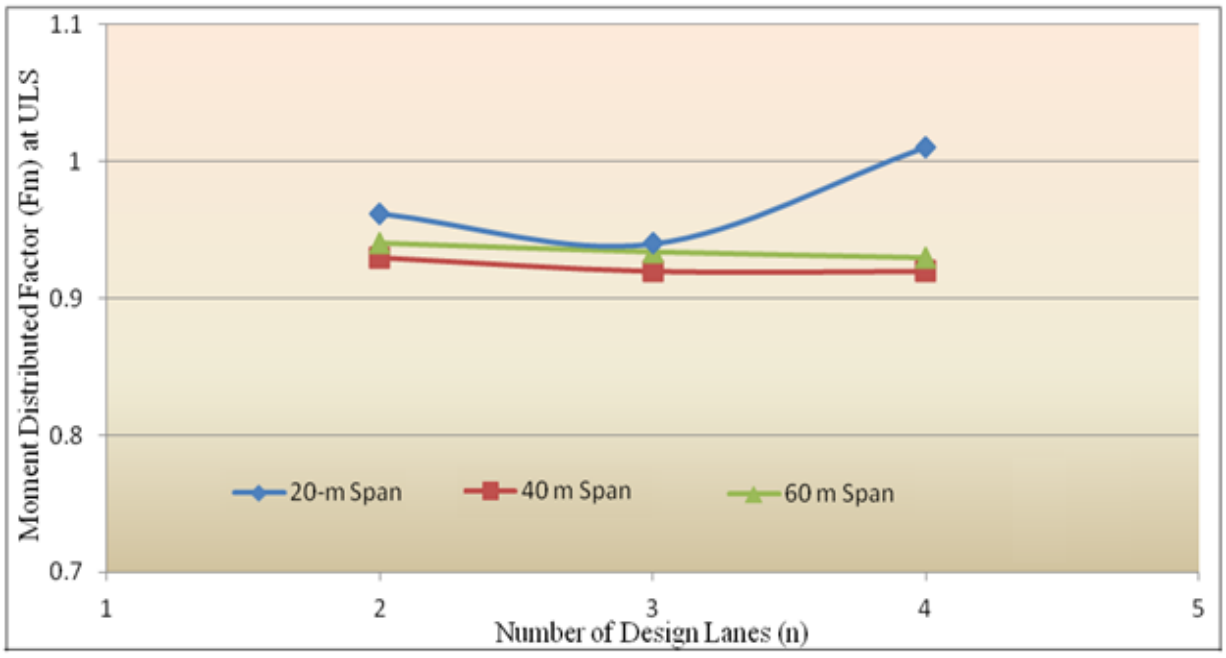

Figure 4.14 Effect of number of design lanes on the moment distribution factor due to CHBDC truck loading cases at Ultimate Limit State

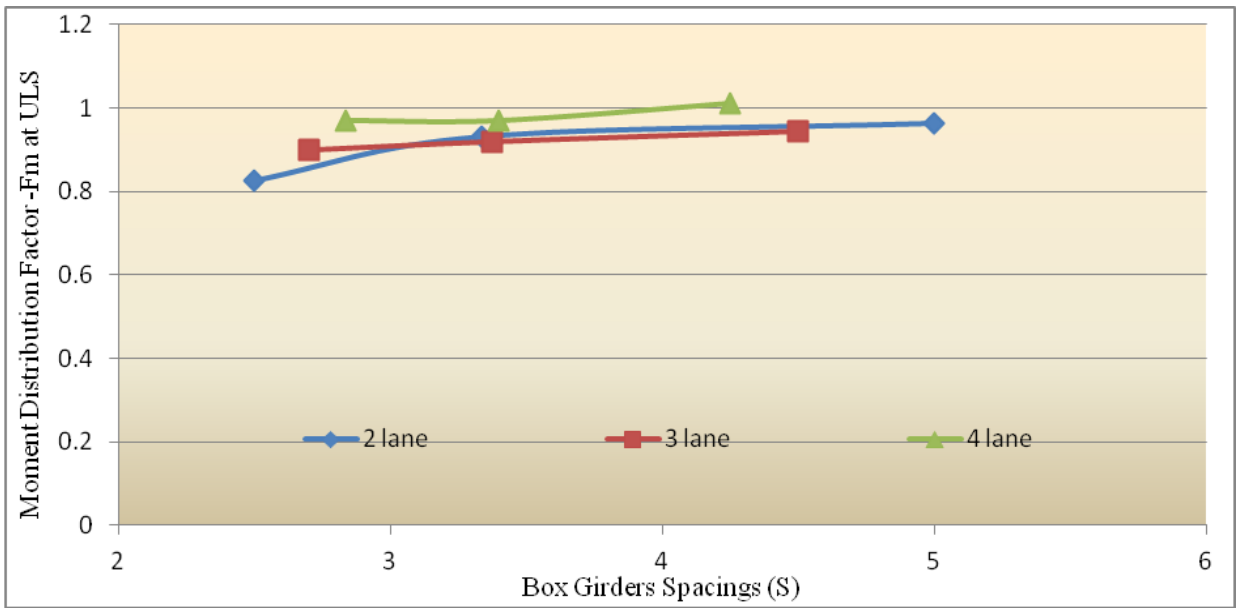

Figure 4.15 Effect of box girder spacing of 20-m span bridges on the moment distribution factor due to CHBDC truck loading cases at Ultimate Limit State

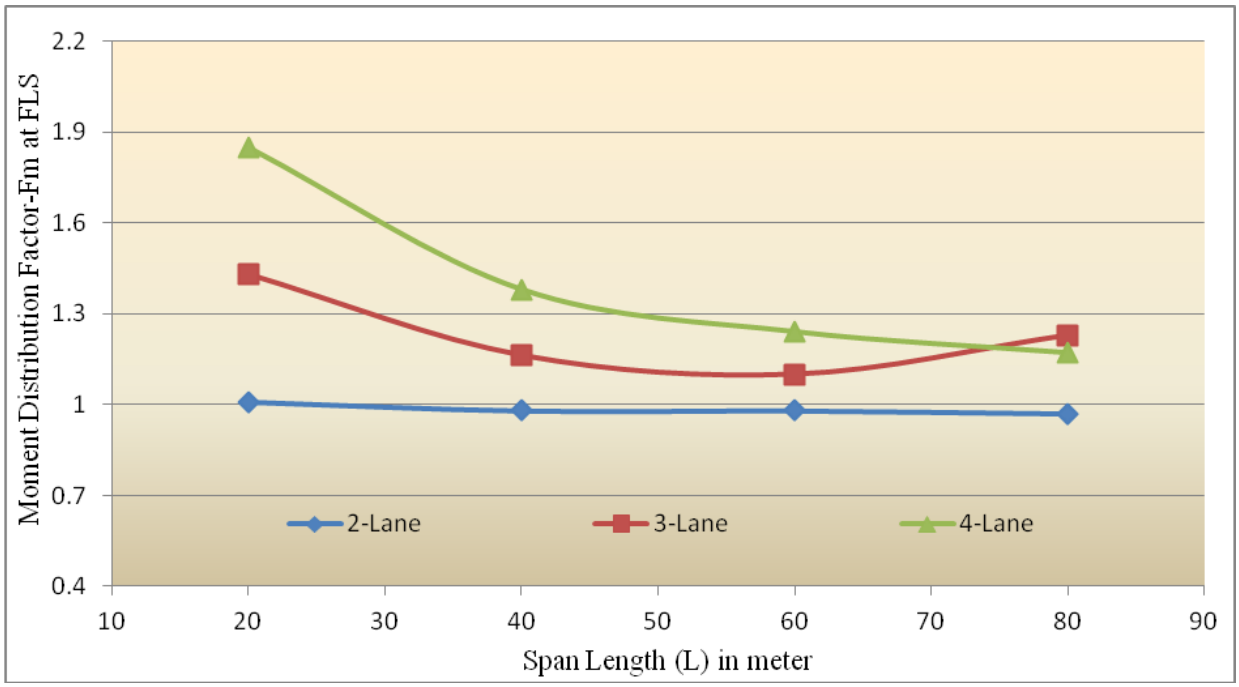

Figure 4.16 Effect of span length on the moment distribution factor for four box girder bridges, due CHBDC truck loading cases at Fatigue Limit State

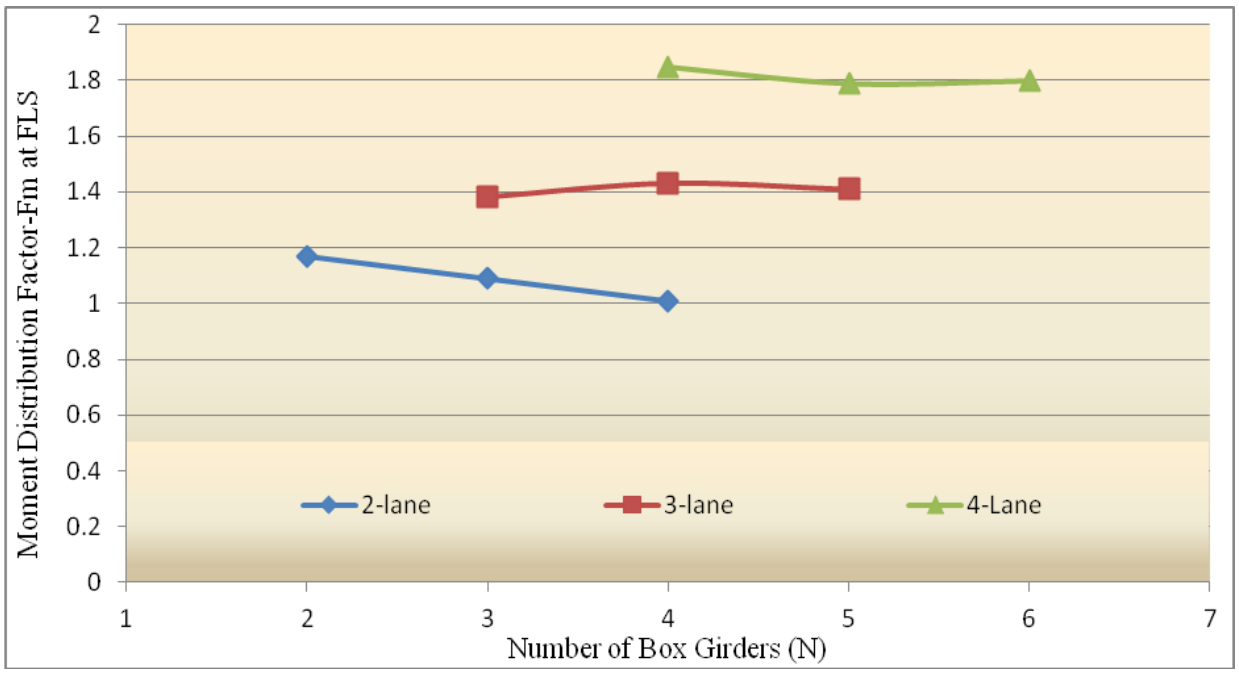

Figure 4.17 Effect of number of box girders of 20-m span bridges on the moment distribution factor due to CHBDC truck loading cases at Fatigue Limit State

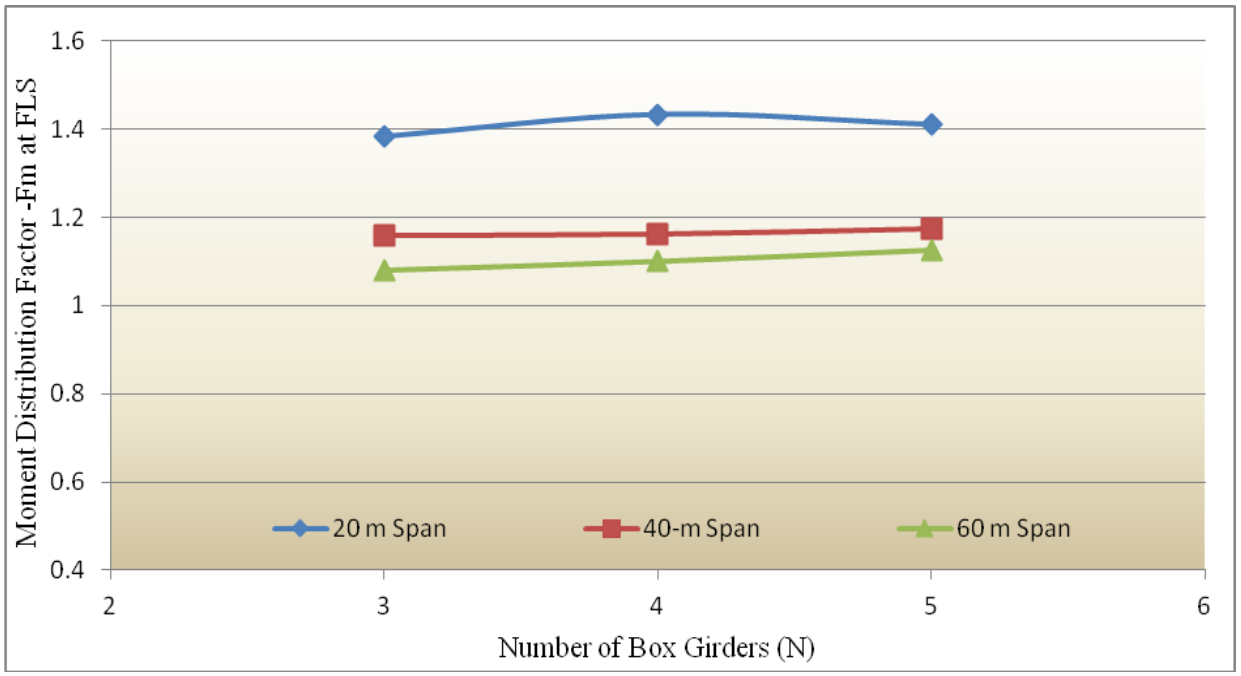

Figure 4.18 - Effect of number of box girders on the moment distribution factor due to CHBDC truck loading cases for three-lane bridges at Fatigue Limit State

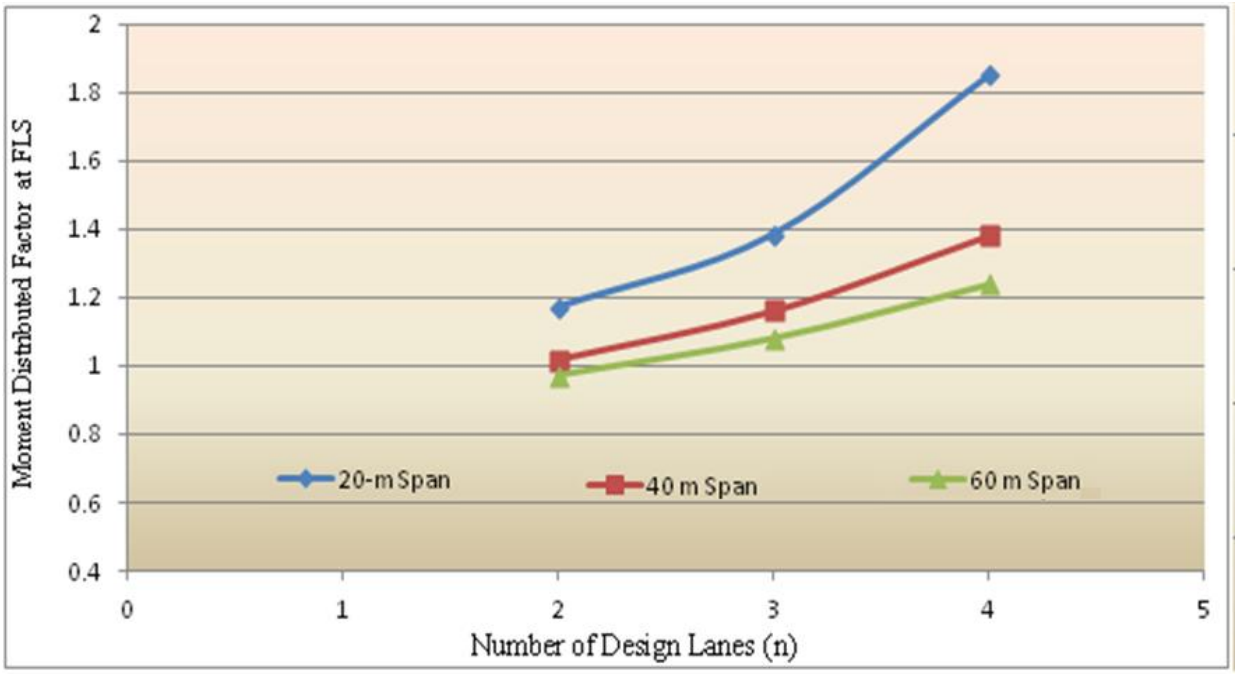

Figure 4.19 Effect of number of design lanes on the moment distribution factor due to CHBDC truck loading cases at Fatigue Limit State

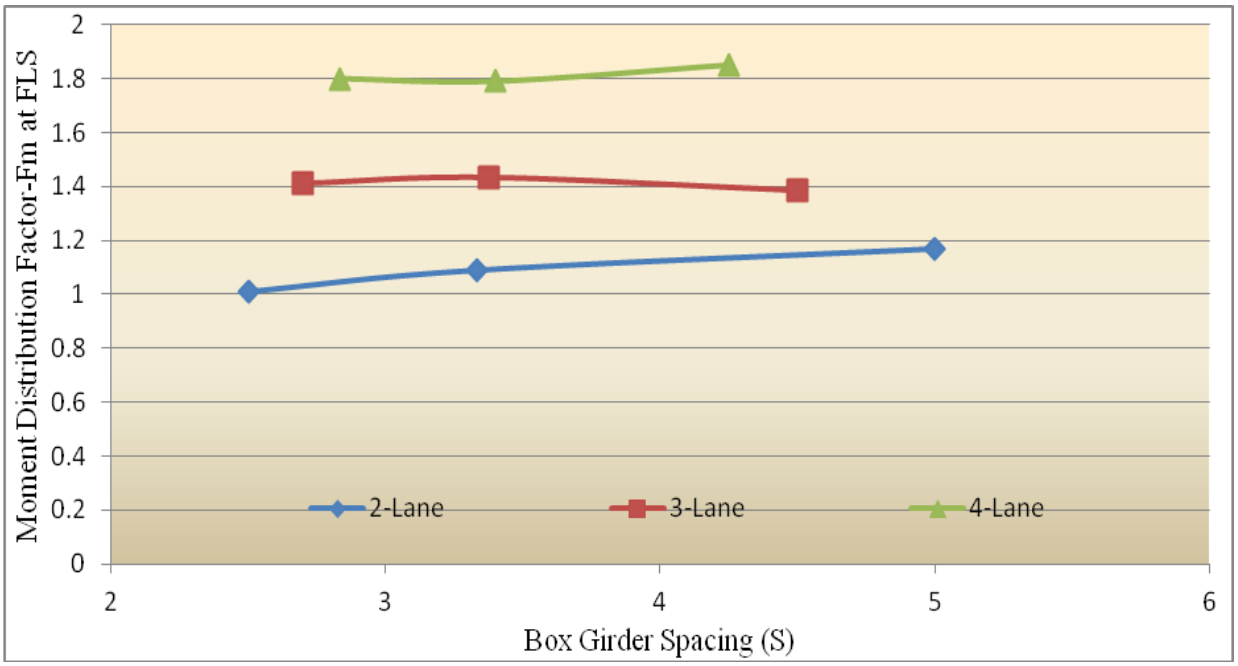

Figure 4.20 Effect of number of box girder spacing of 20-m span bridges on the moment distribution factor due to CHBDC truck loading cases at Fatigue Limit State

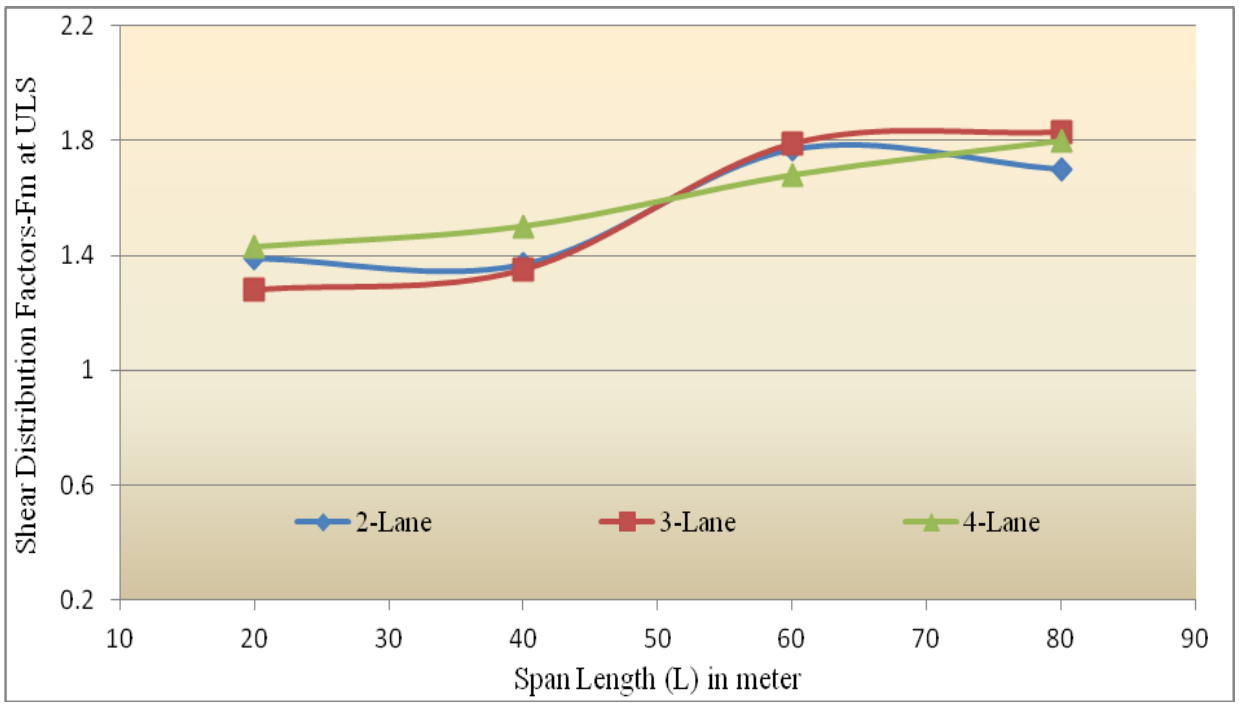

Figure 4.21 Effect of bridge span length on the shear distribution factors for four box girder bridges, due to CHBDC truck loading cases at Ultimate Limit State

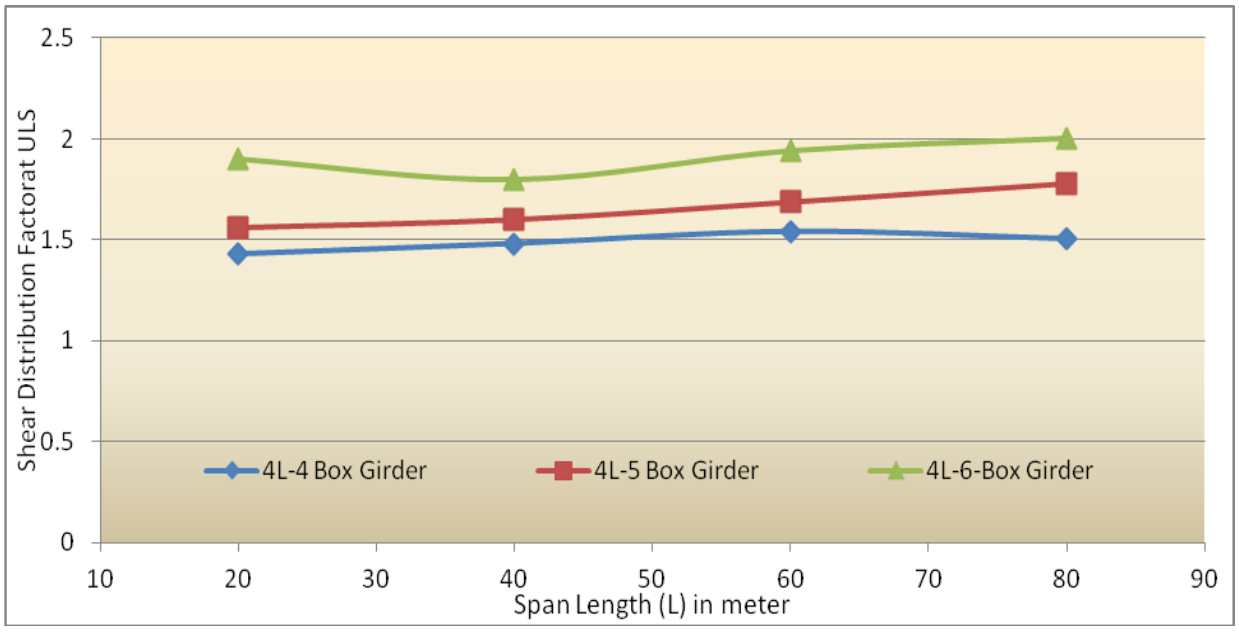

Figure 4.22 Effect of bridge span length on the shear distribution factors due to CHBD truck loading cases at Ultimate Limit State

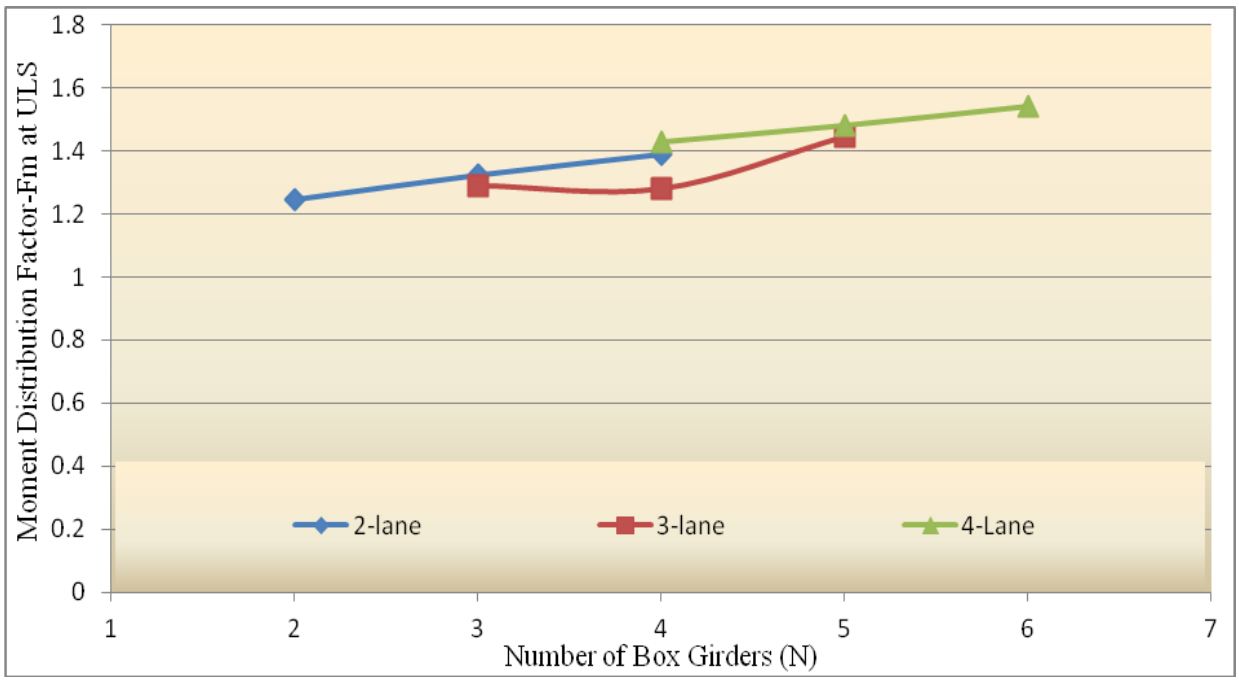

Figure 4.23 Effect of number of box girders of 20-m span bridges on the shear distribution factor due to CHBDC truck loading cases at Ultimate Limit State

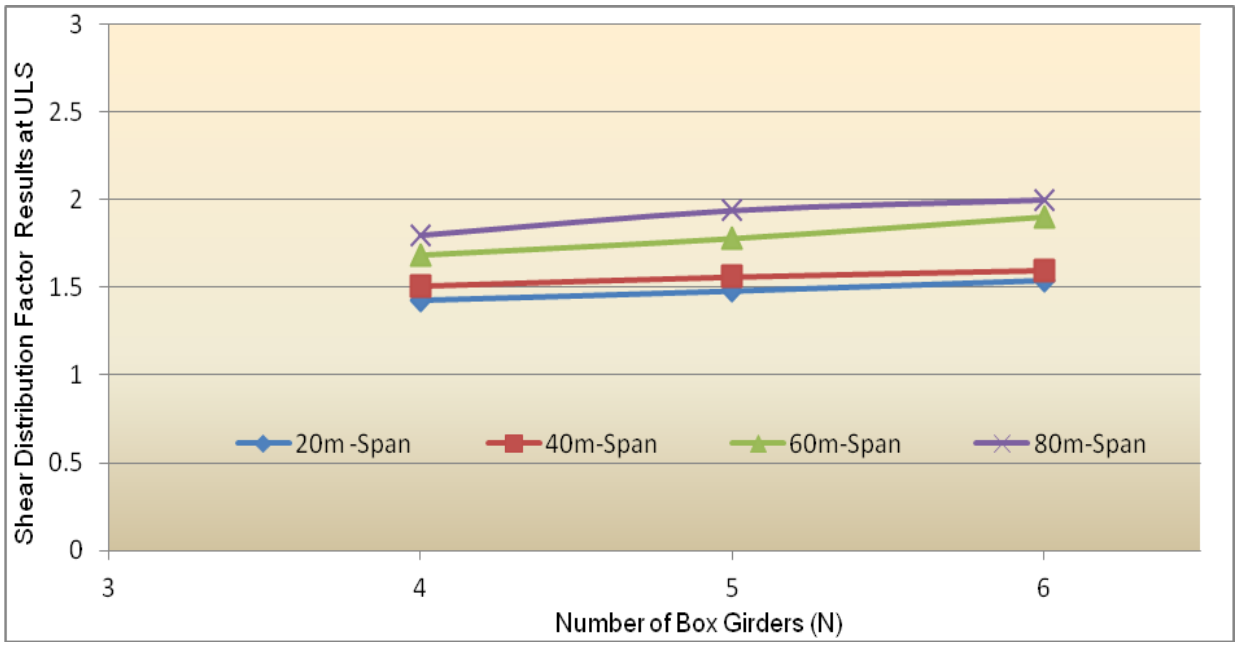

Figure 4.24 Effect of number of box girder of four-lane bridges on the shear distribution factor due to CHBDC truck loading cases at Ultimate Limit State

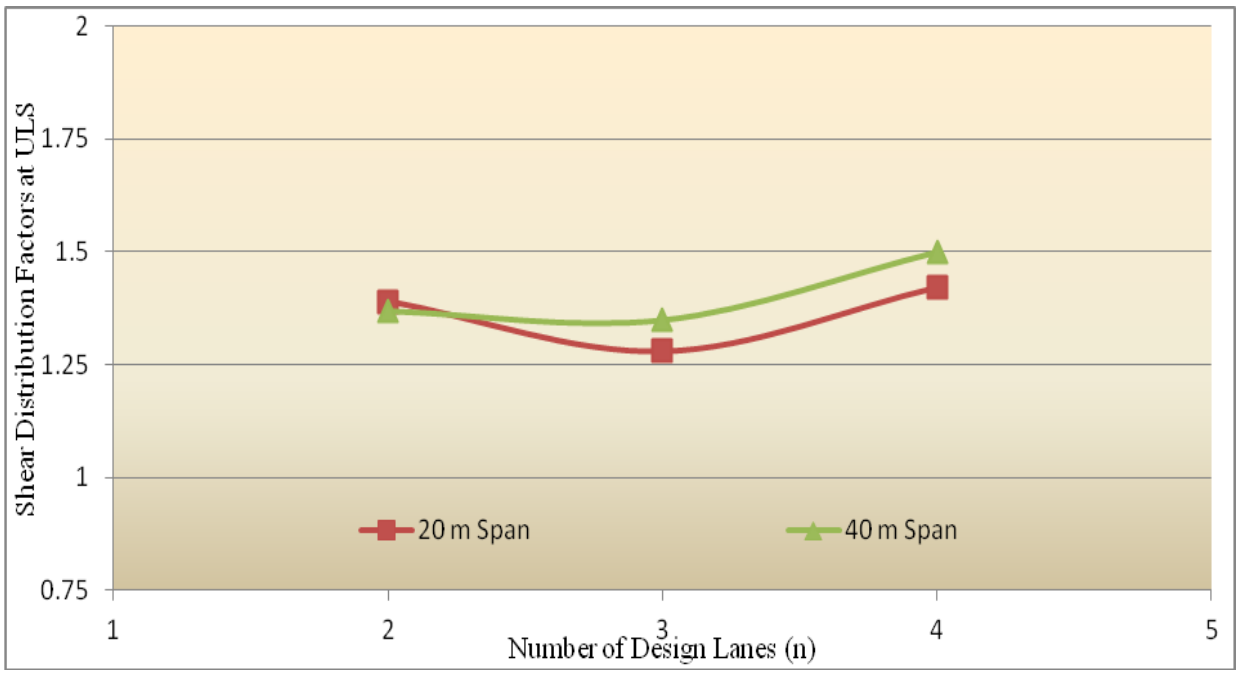

Figure 4.25 Effect of number of design lanes on the shear distribution factor due to CHBDC truck loading cases at Ultimate Limit State

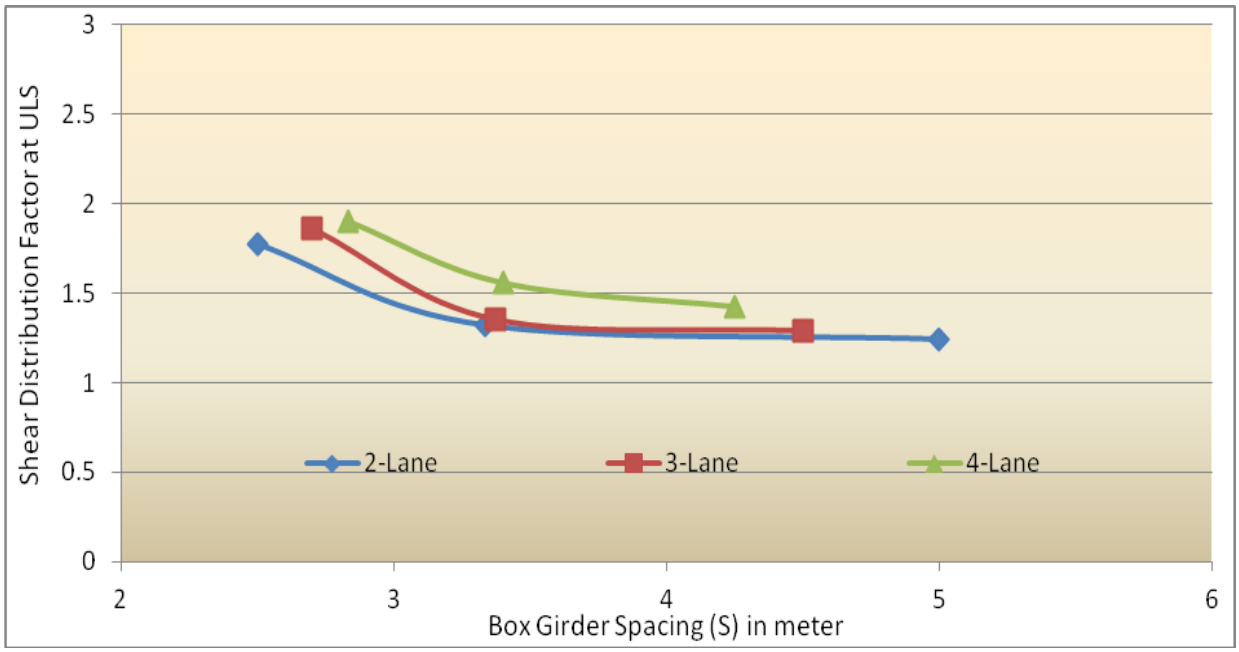

Figure 4.26 Effect of number of box girder spacing of 20-m span bridge on the shear distribution factors due to CHBDC truck loading cases at Ultimate Limit State

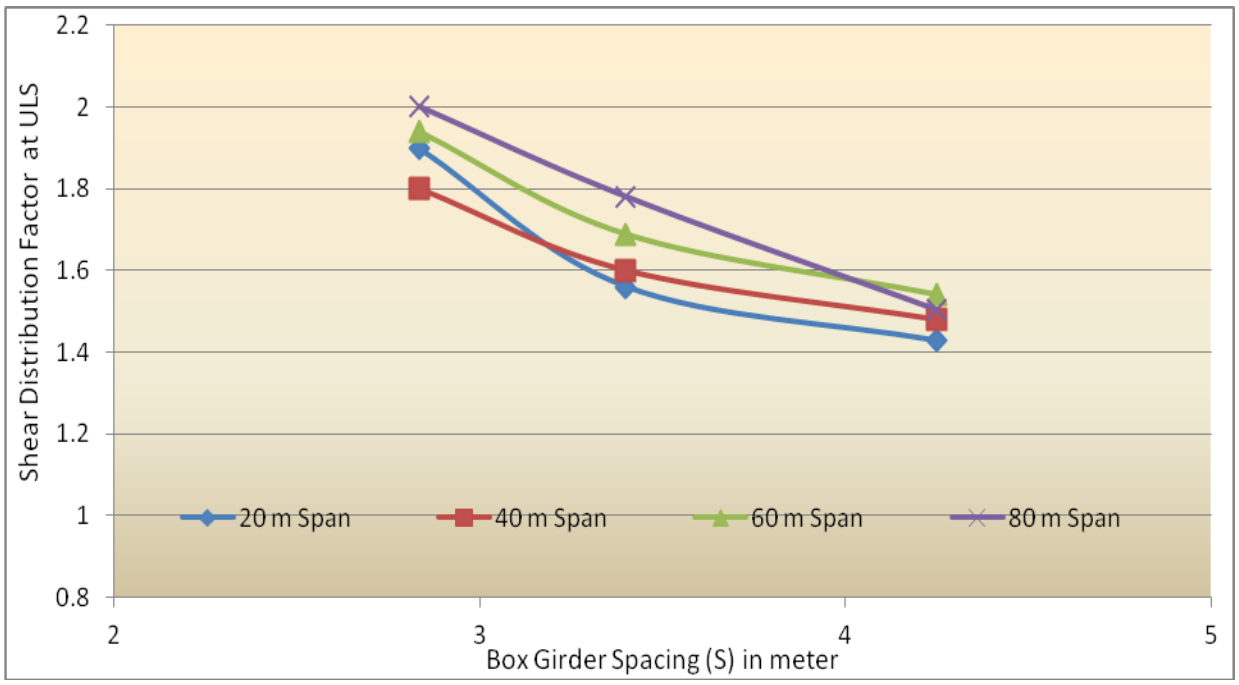

Figure 4.27 Effect of number of box girder spacing of four-lane bridges on the shear distribution factors due to CHBDC truck loading cases at Ultimate Limit State

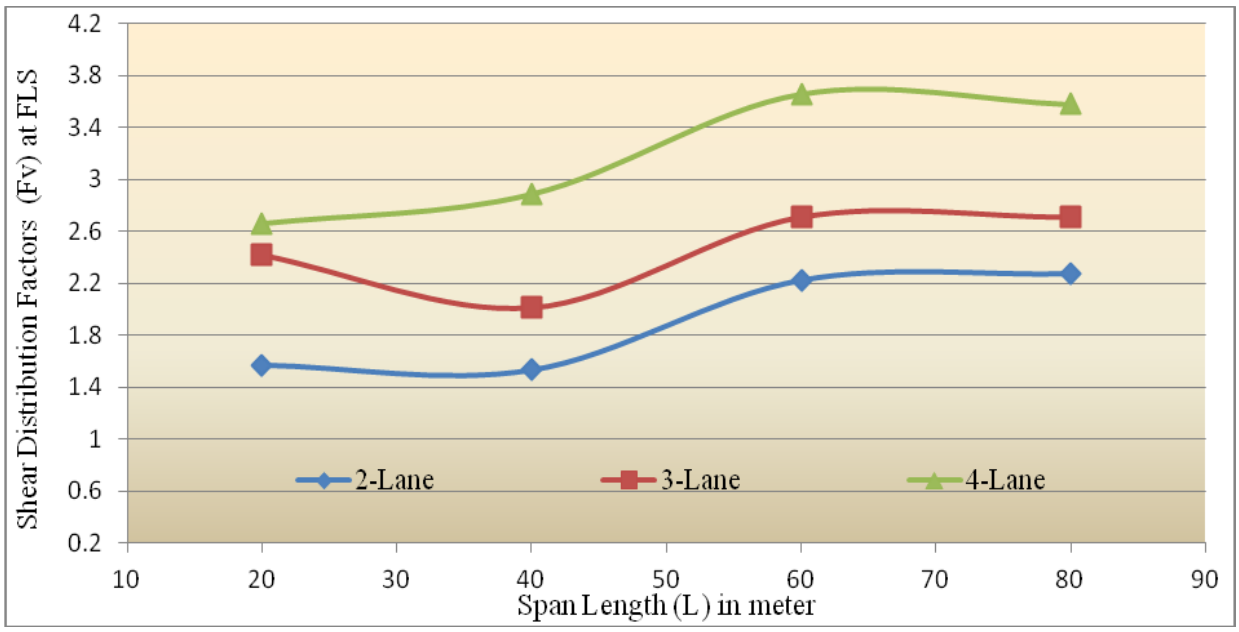

Figure 4.28 Effect of bridge span length on the shear distribution factors for four box girder bridges, due to CHBDC truck loading cases at Fatigue Limit State

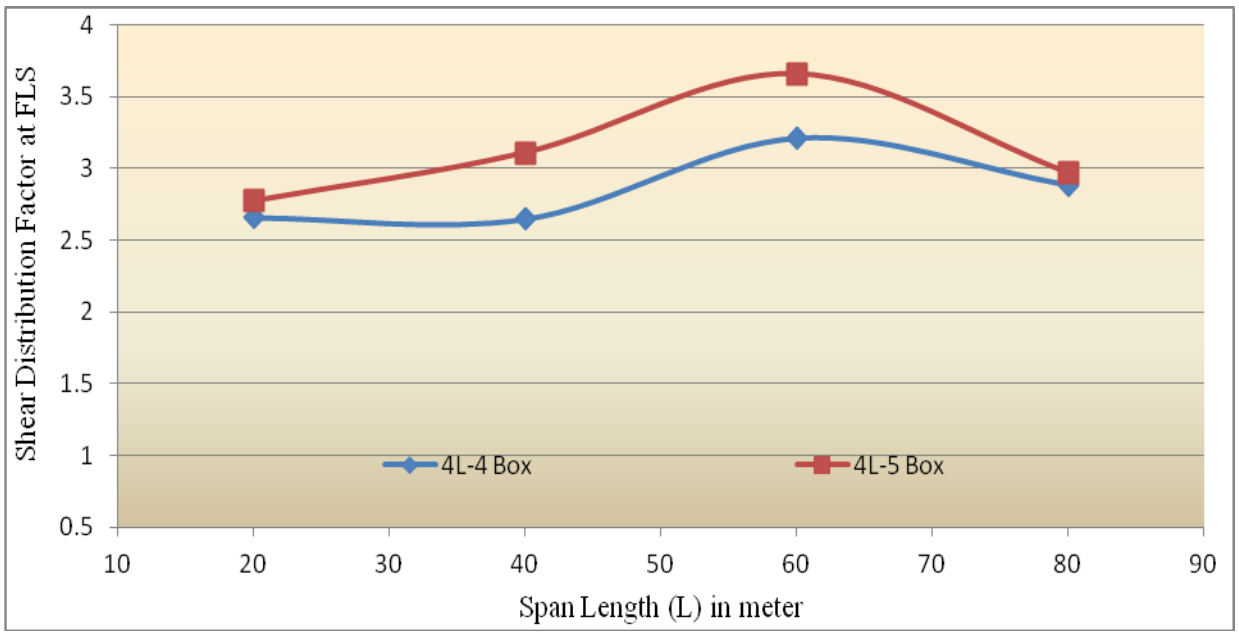

Figure 4.29 Effect of bridge span length on the shear distribution factors due to CHBDC truck loading cases at Fatigue Limit State

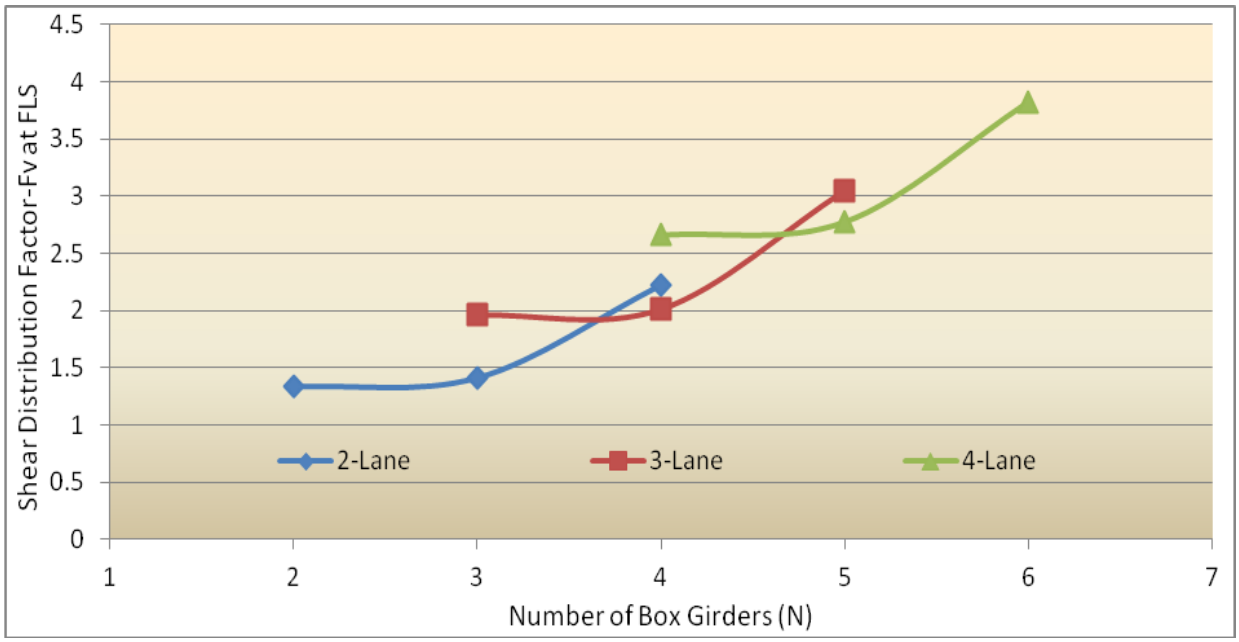

Figure 4.30 Effect of number of box girders of 20-m span bridge on the shear distribution factor due to CHBDC truck loading cases at Fatigue Limit State

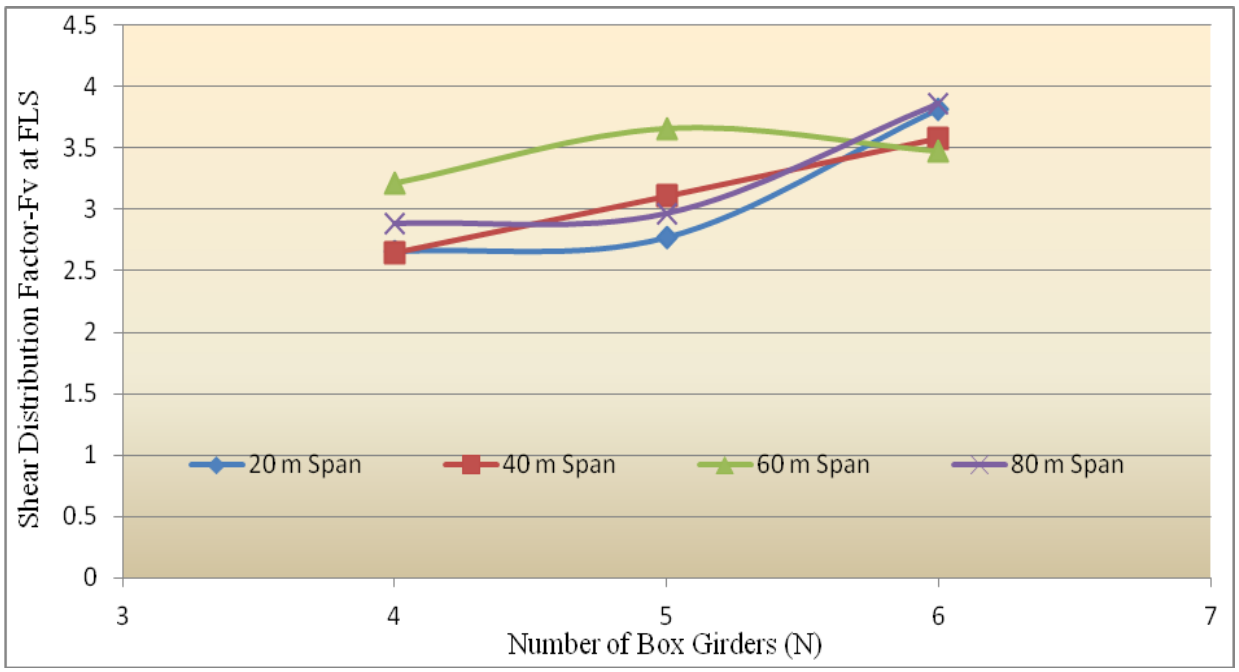

Figure 4.31Effect of number of box girders for four-lane bridges on the shear distribution factor due to CHBDC truck loading cases at Fatigue Limit State

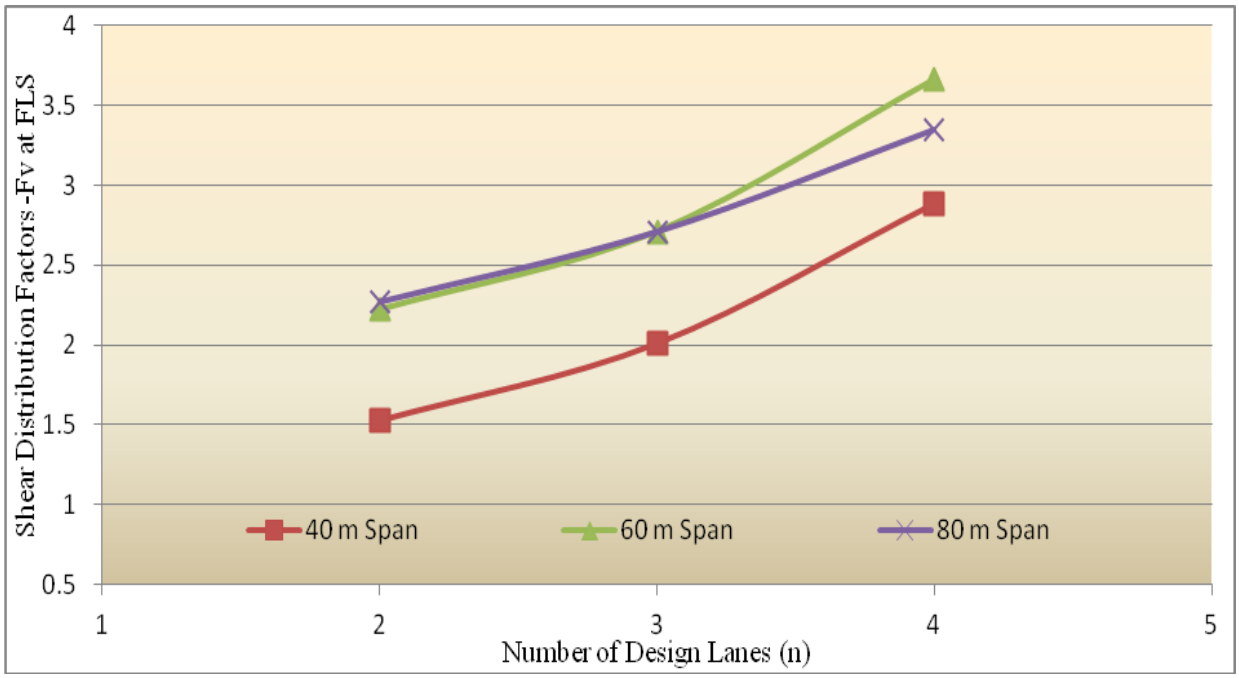

Figure 4.32 Effect of number of design lanes on the shear distribution factor due to CHBDC truck loading cases at Fatigue Limit State

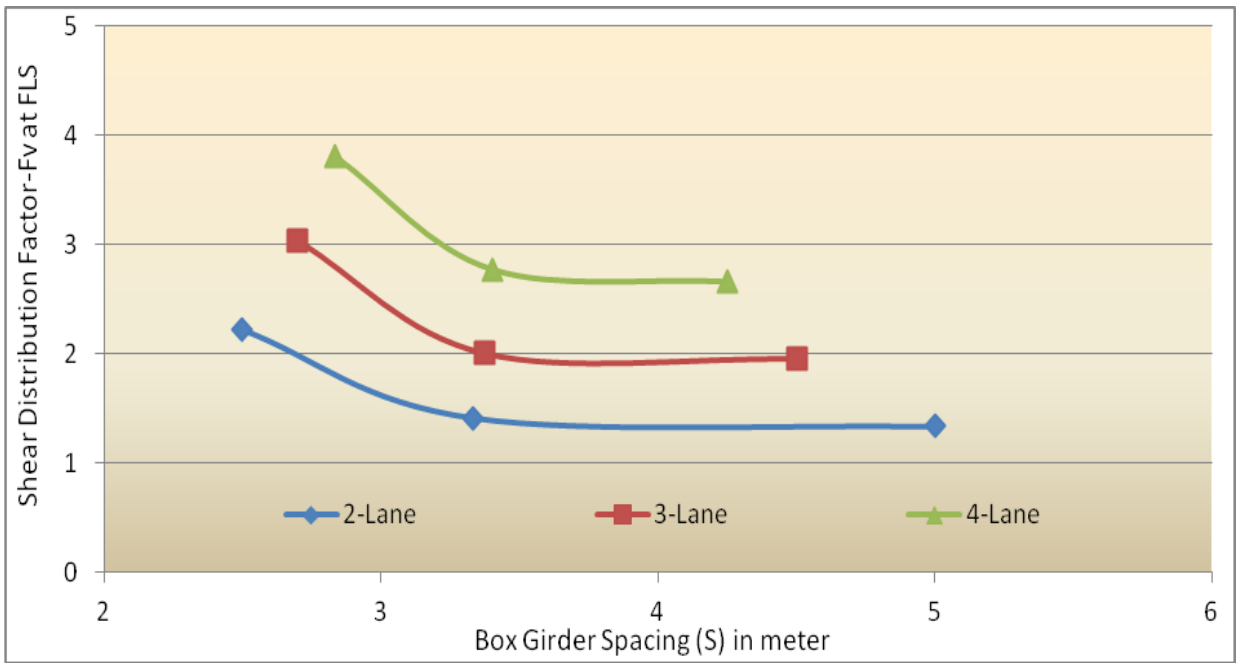

Figure 4.33 Effect of box girder spacing of 20-m span bridges on the shear distribution factor due to CHBDC truck loading cases at Fatigue Limit State

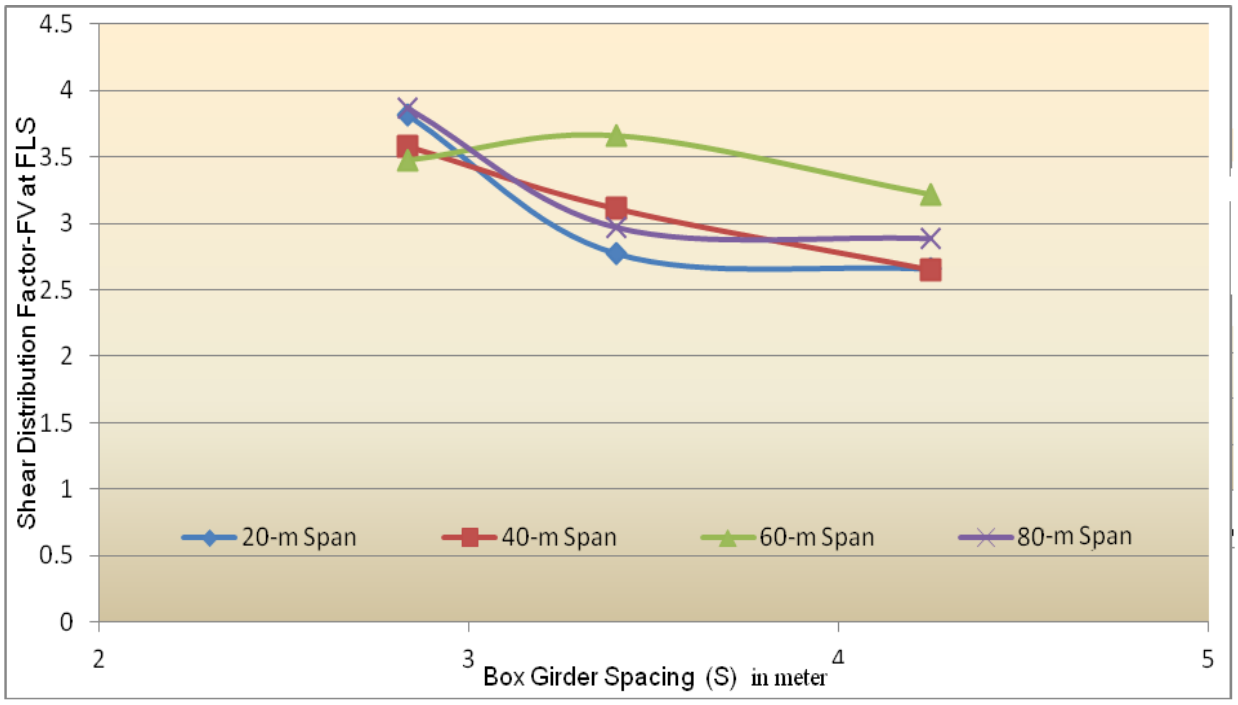

Figure 4.34 Effect of box girder spacing for four-lane bridges on the shear distribution factor due to CHBDC truck loading cases at Fatigue Limit State

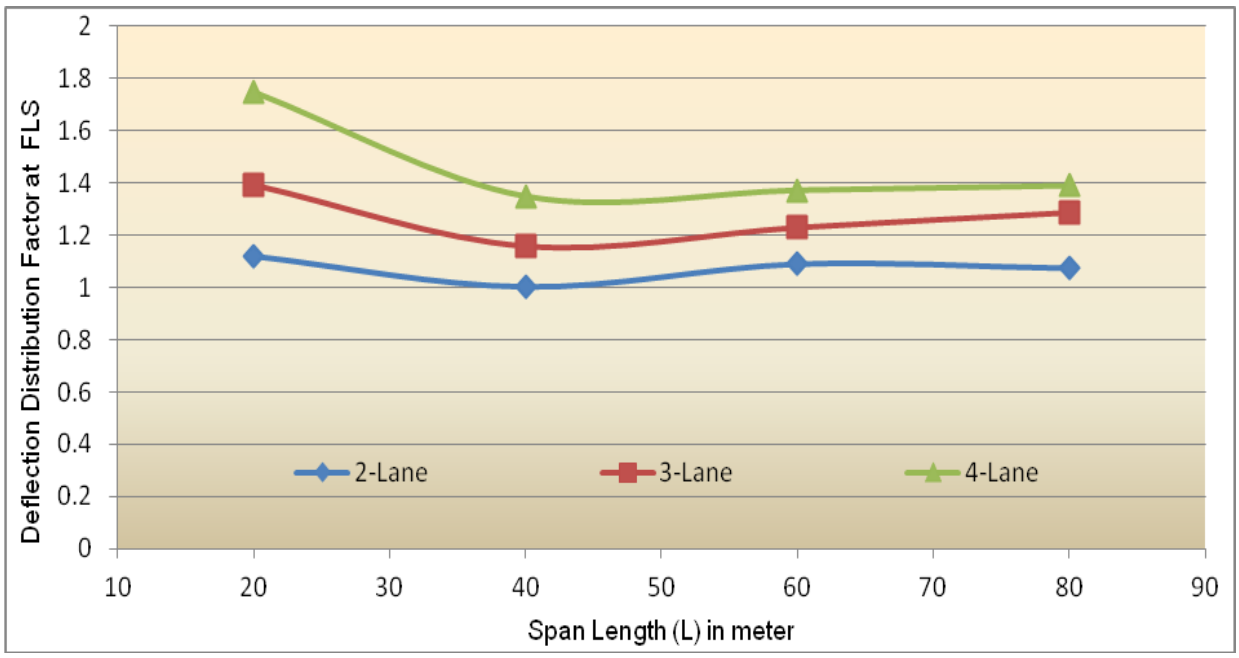

Figure 4.35 Effect of bridge span length on the deflection distribution factor due to CHBDC truck loading cases for four box girder bridges at Fatigue Limit State

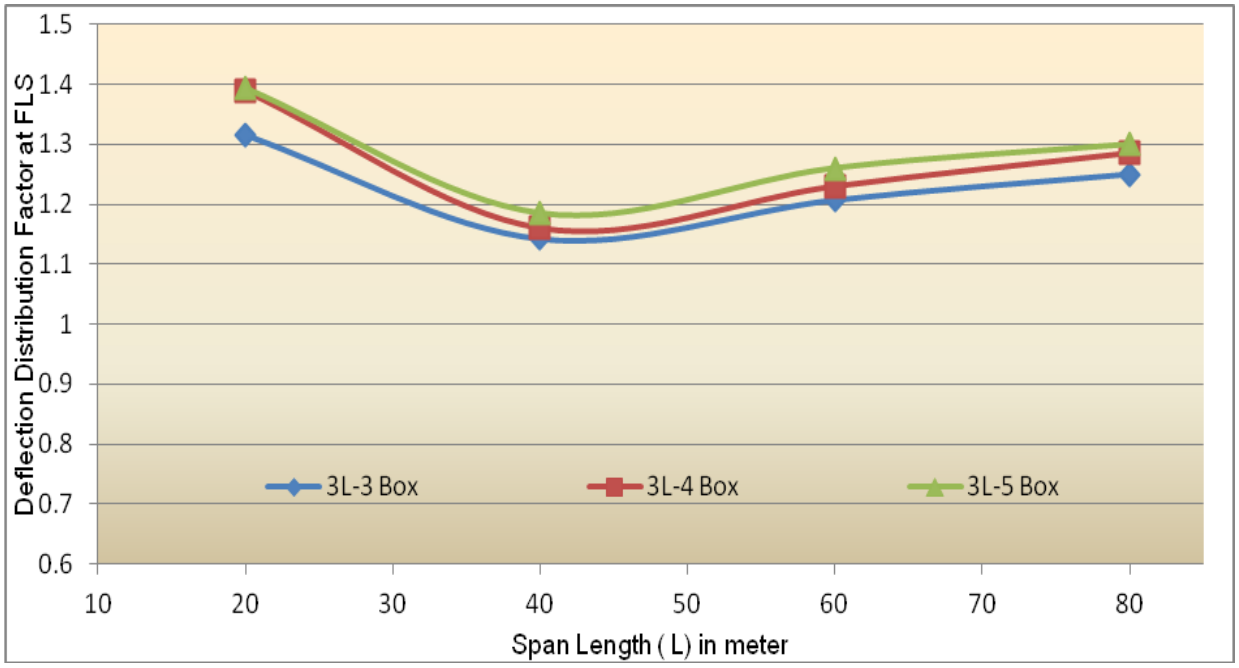

Figure 4.36 Effect of bridges span length on the deflection distribution factor due to CHBDC truck loading cases at Fatigue Limit State

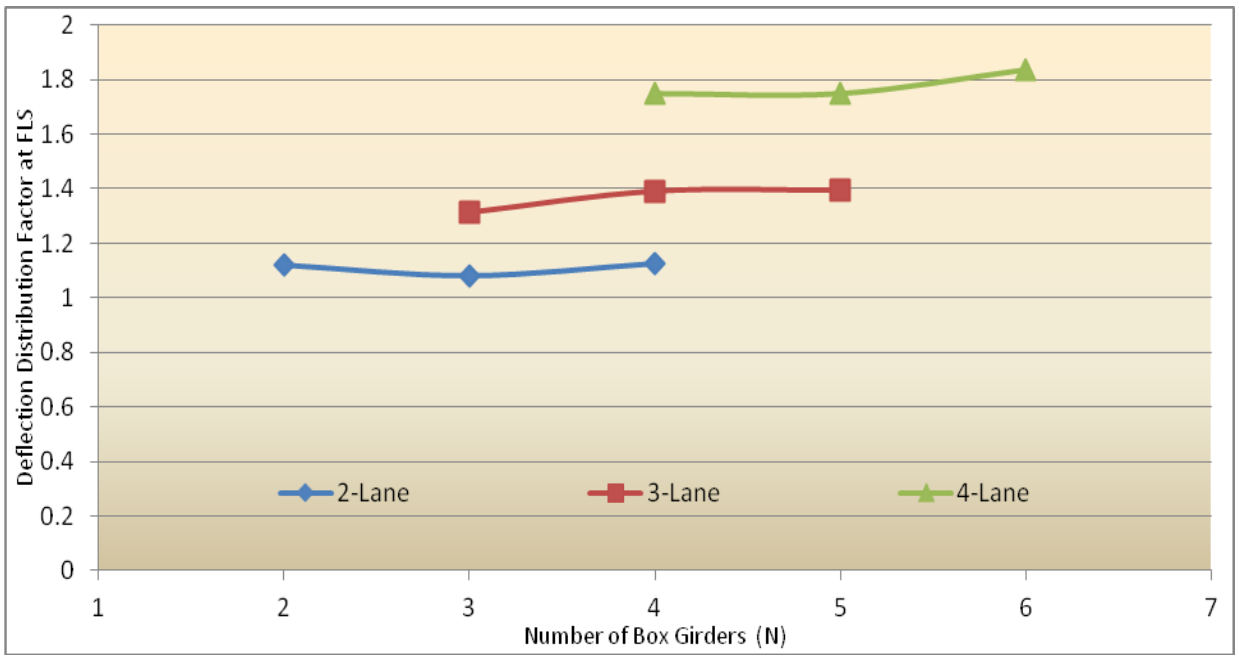

Figure 4.37 Effect of number of box girders on deflection distribution factor due to CHBDC truck loading cases for 20-m span bridges at Fatigue Limit State

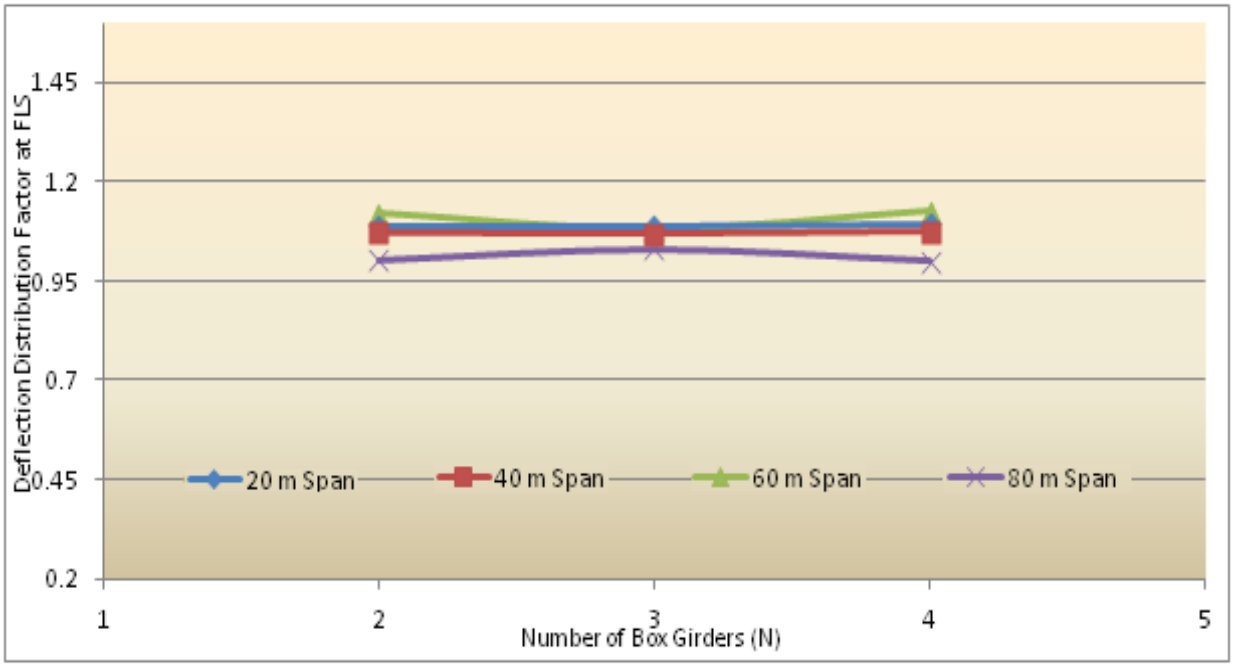

Figure 4.38 Effect of number of box girders on deflection distribution factor due to CHBDC truck loading cases for two-lane bridges at Fatigue Limit State

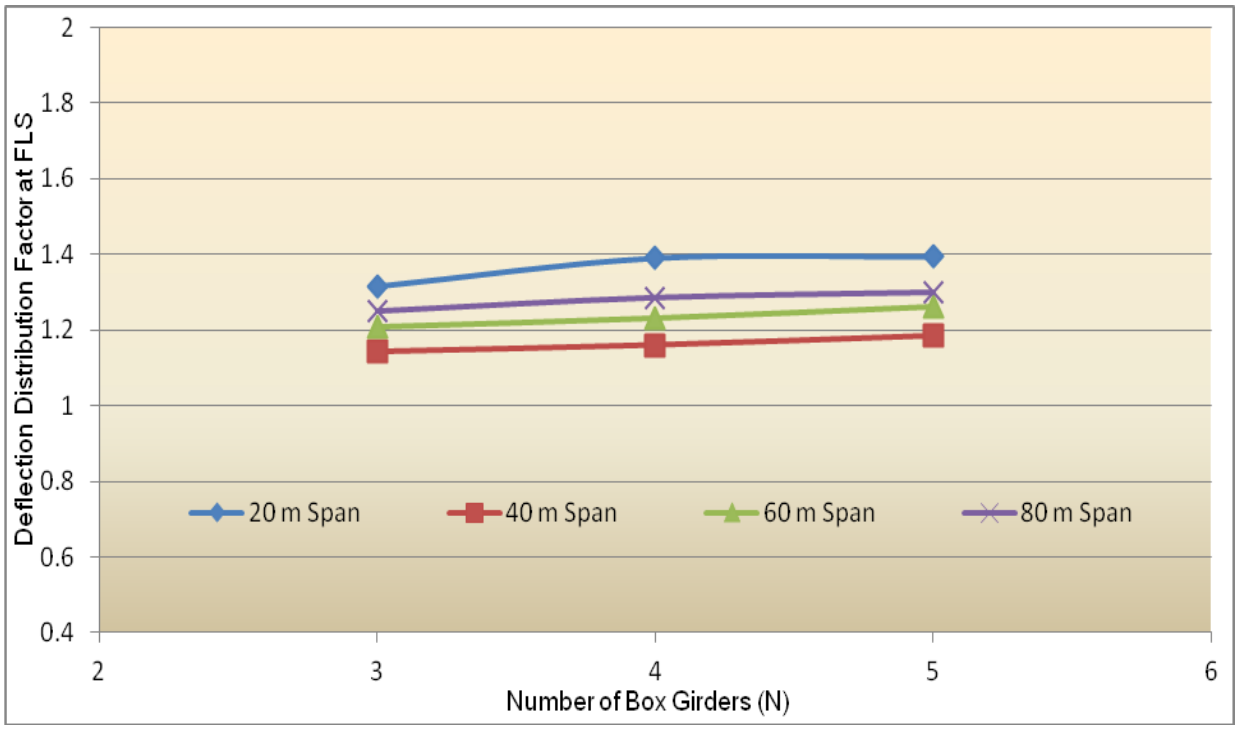

Figure 4.39 Effect of number of box girders on deflection distribution factor due to CHBDC truck loading cases three-lane bridges at Fatigue Limit State

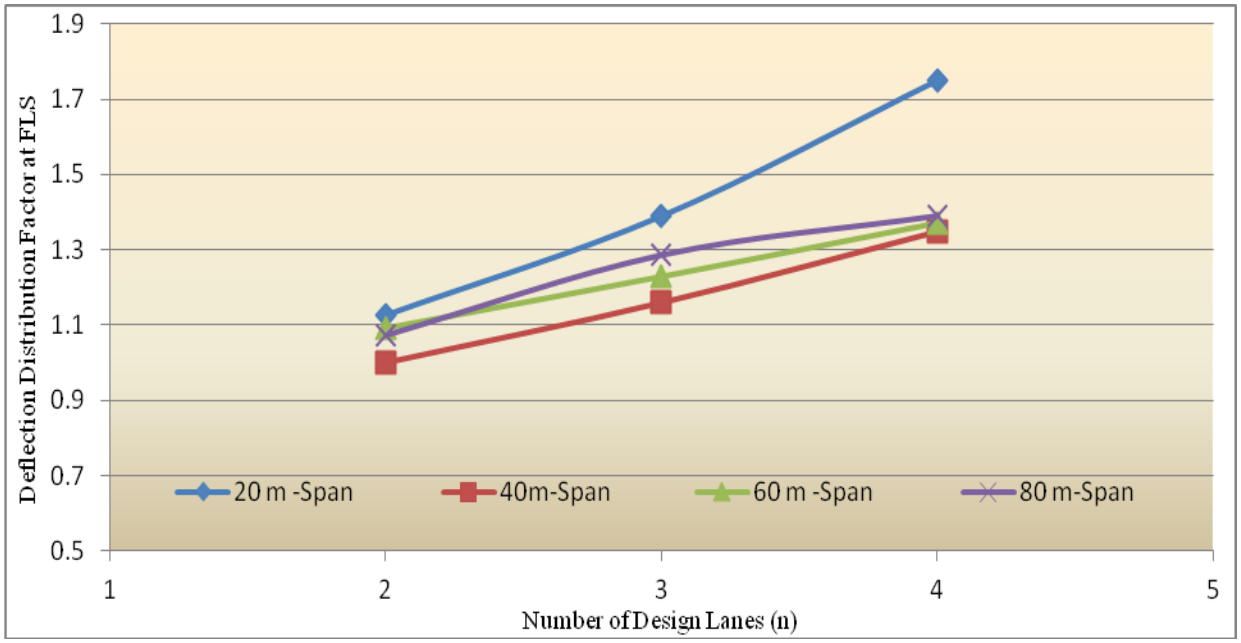

Figure 4.40 Effect of number of design lanes on deflection distribution factor due to CHBDC truck loading cases at Fatigue Limit State

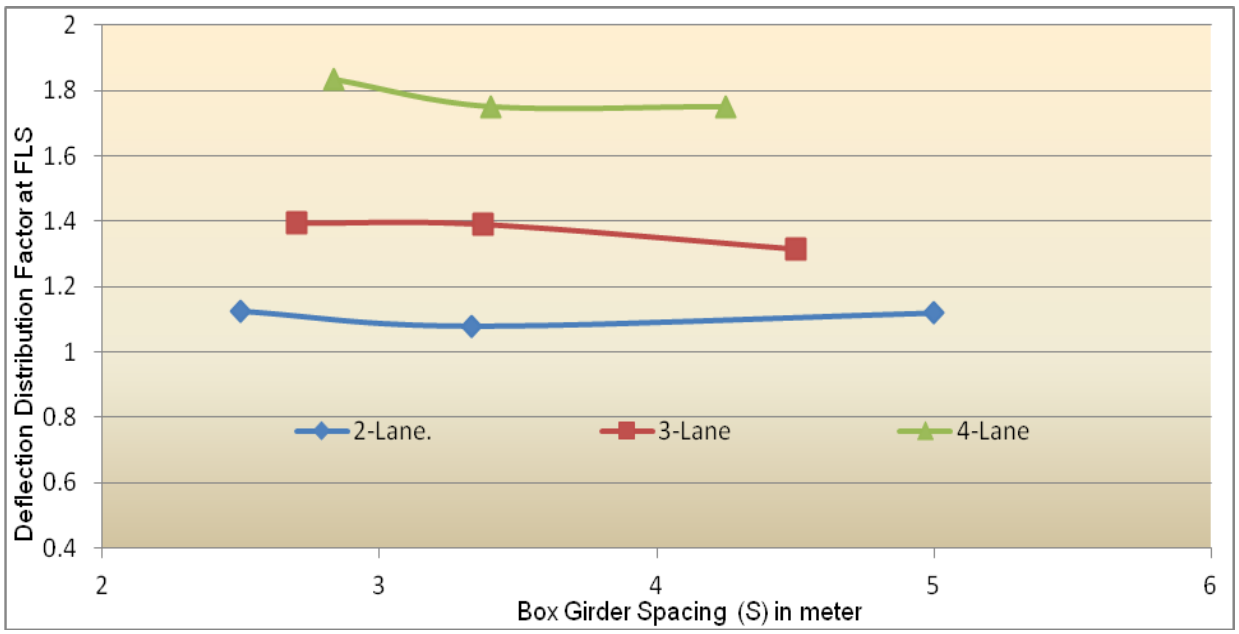

Figure 4.41 Effect of box girder spacing on deflection distribution factor due to CHBDC truck loading cases at Fatigue Limit State

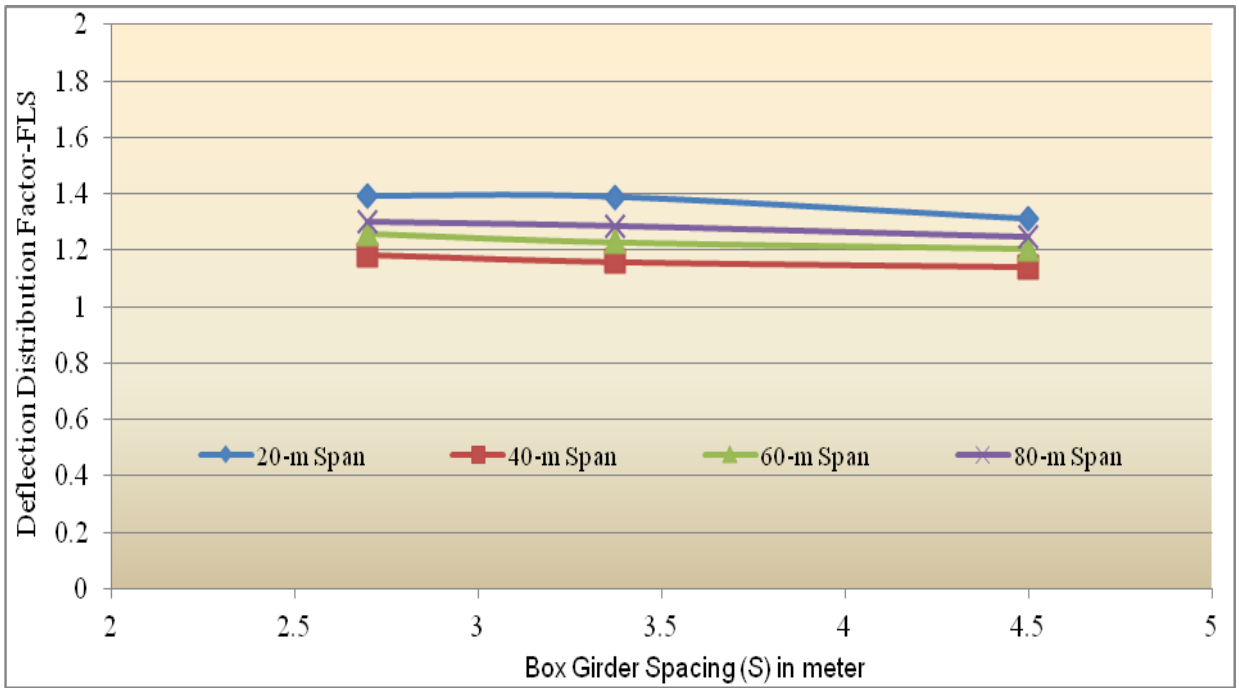

Figure 4.42 Effect of box girder spacing on deflection distribution factor due to CHBDC truck loading cases for three-lane bridges at Fatigue Limit State

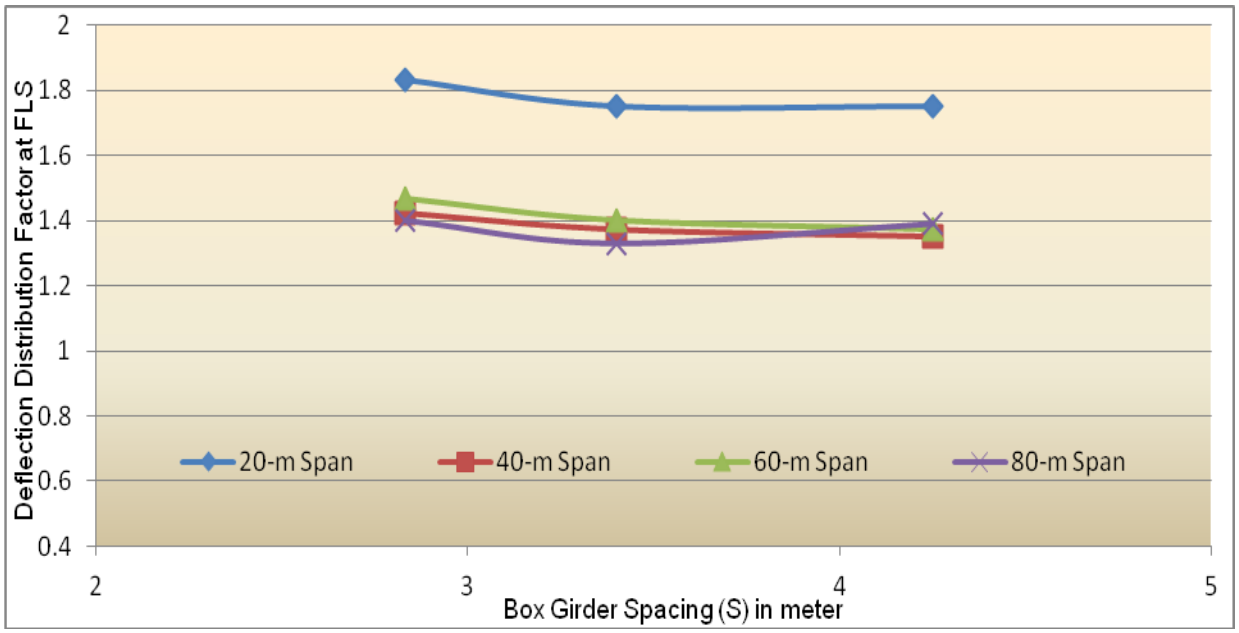

Figure 4.43 Effect of box girders spacing on deflection distribution factor due to CHBDC truck loading cases for four-lane bridges at Fatigue Limit State

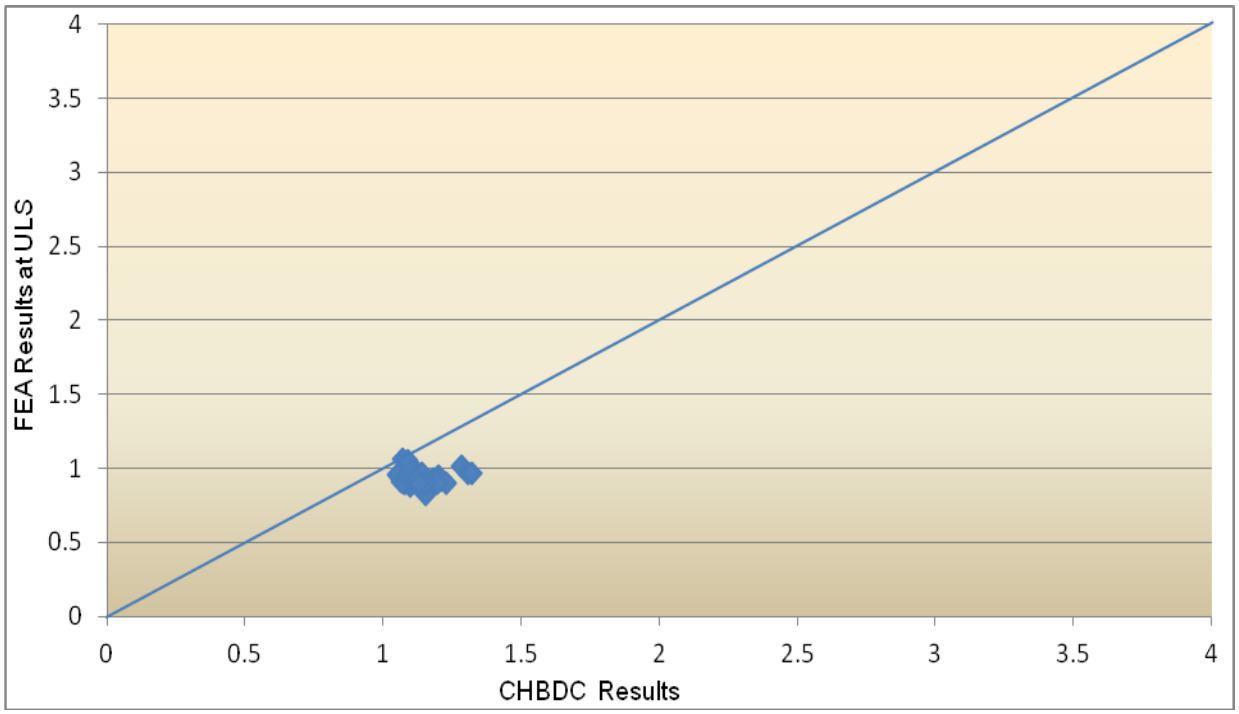

Figure 4.44 Correlation between the moment distribution factor F_m from FEA and CHBDC results at Ultimate Limit State

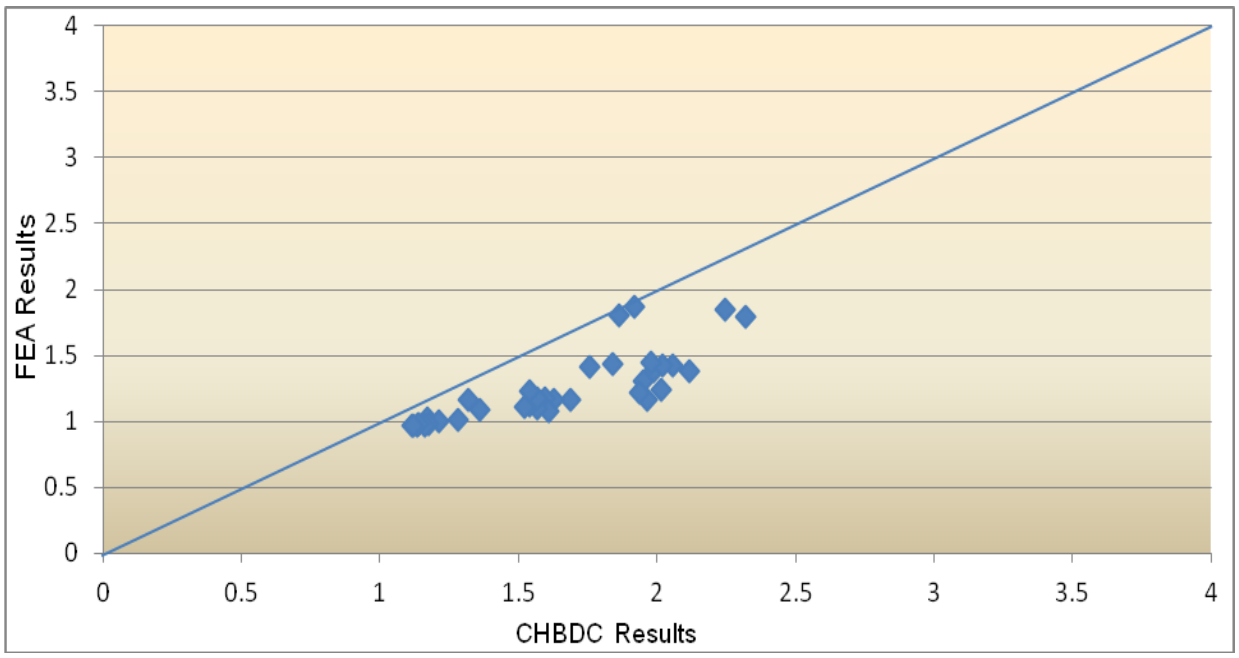

Figure 4.45 Correlation between the moment distribution factor F_m from FEA and CHBDC results at Fatigue Limit State

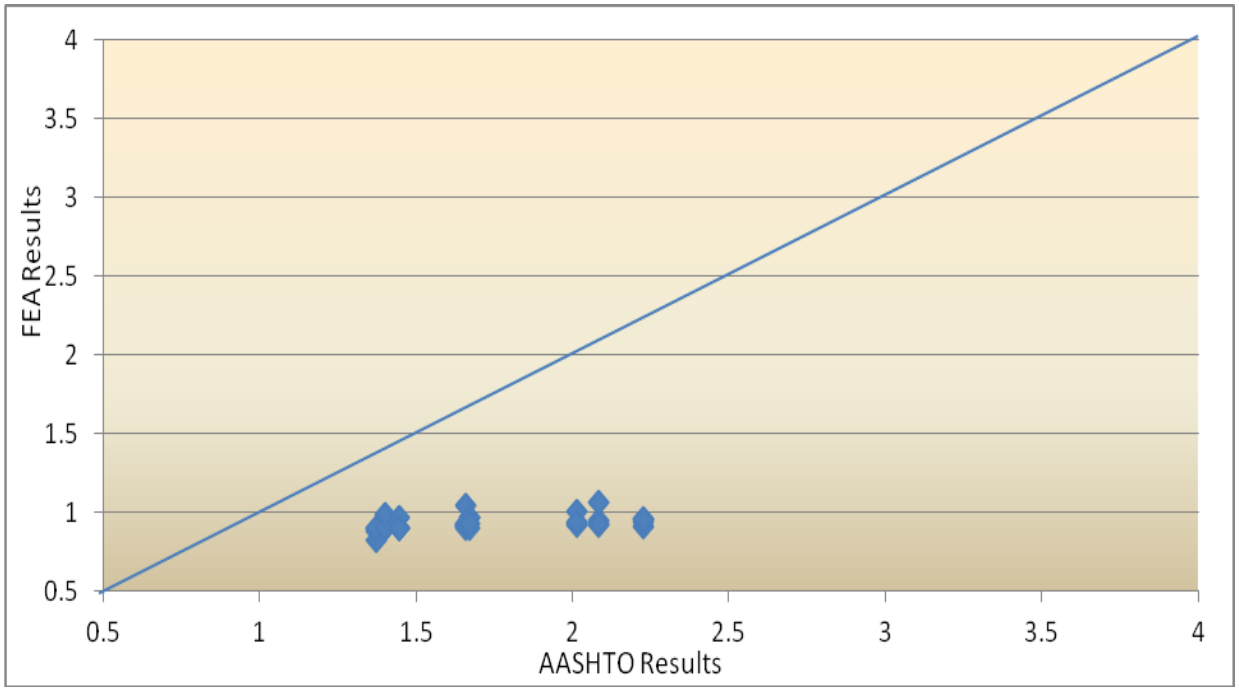

Figure 4.46 Correlation between the moment distribution factor F_m from FEA and AASHTO results at Ultimate Limit State

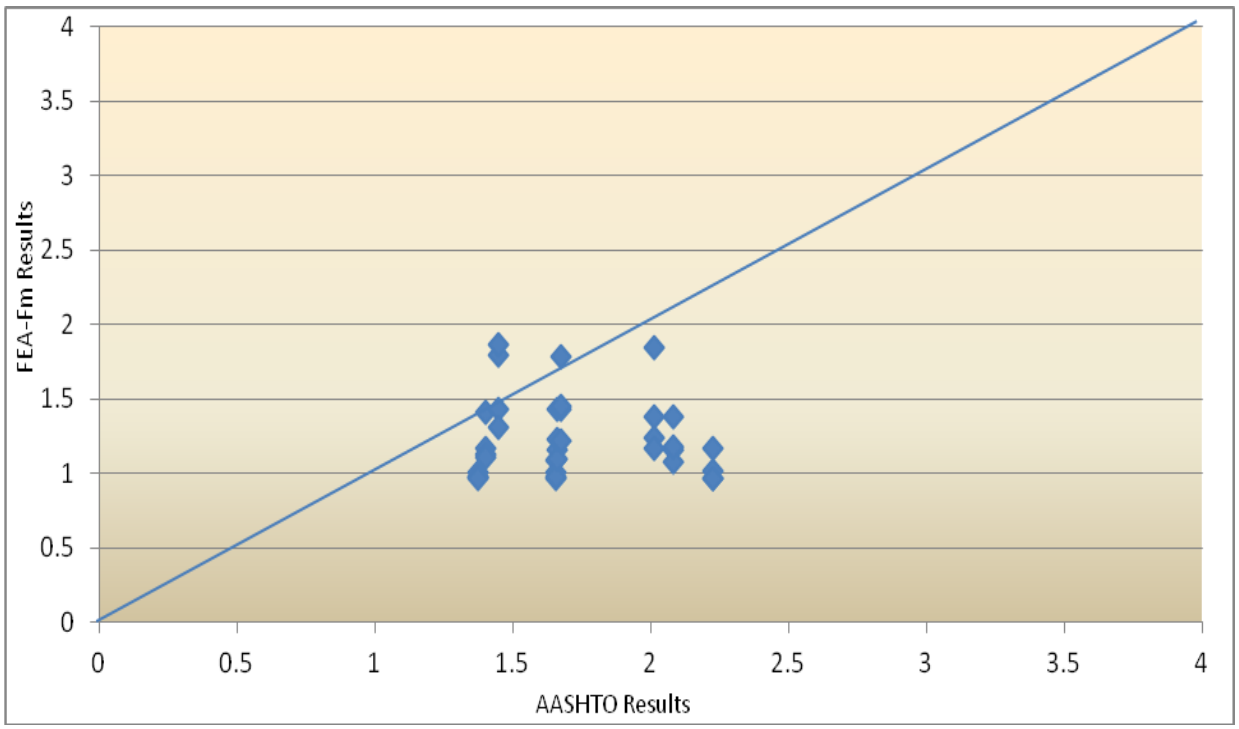

Figure 4.47 Correlation between the moment distribution factor F_m from FEA and AASHTO results at Fatigue Limit State

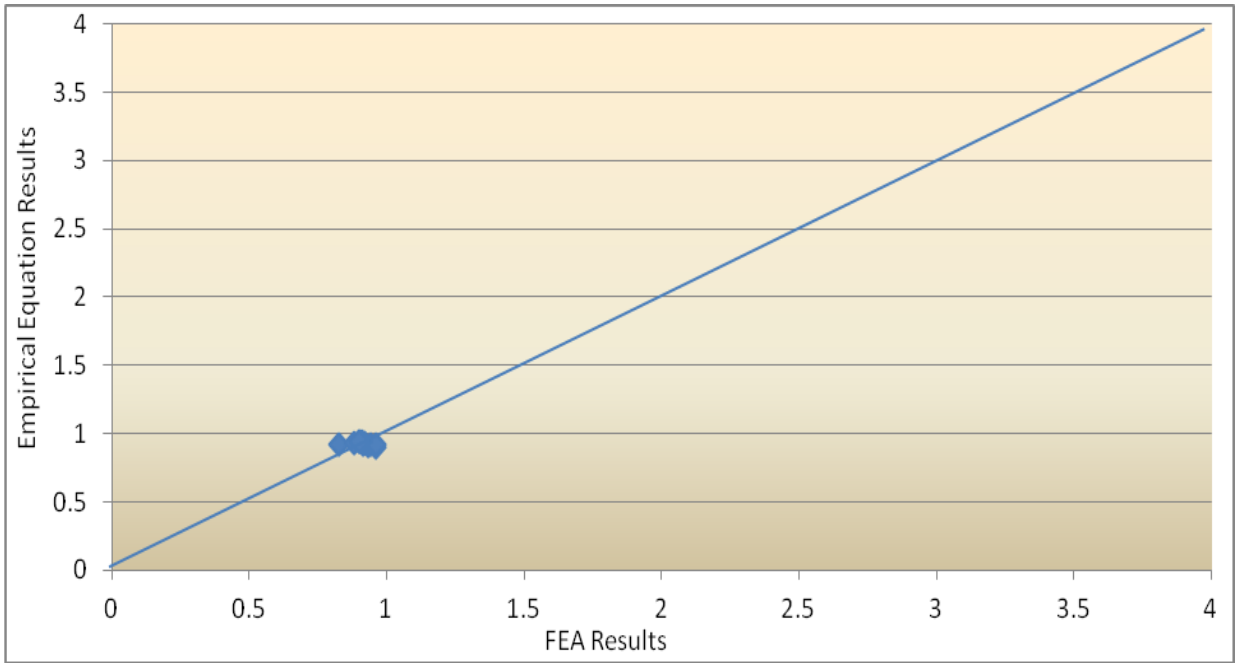

Figure 4.48 Comparison between the moment distribution factor F_m from FEA and empirical equation results for two-lane bridges at Ultimate Limit State

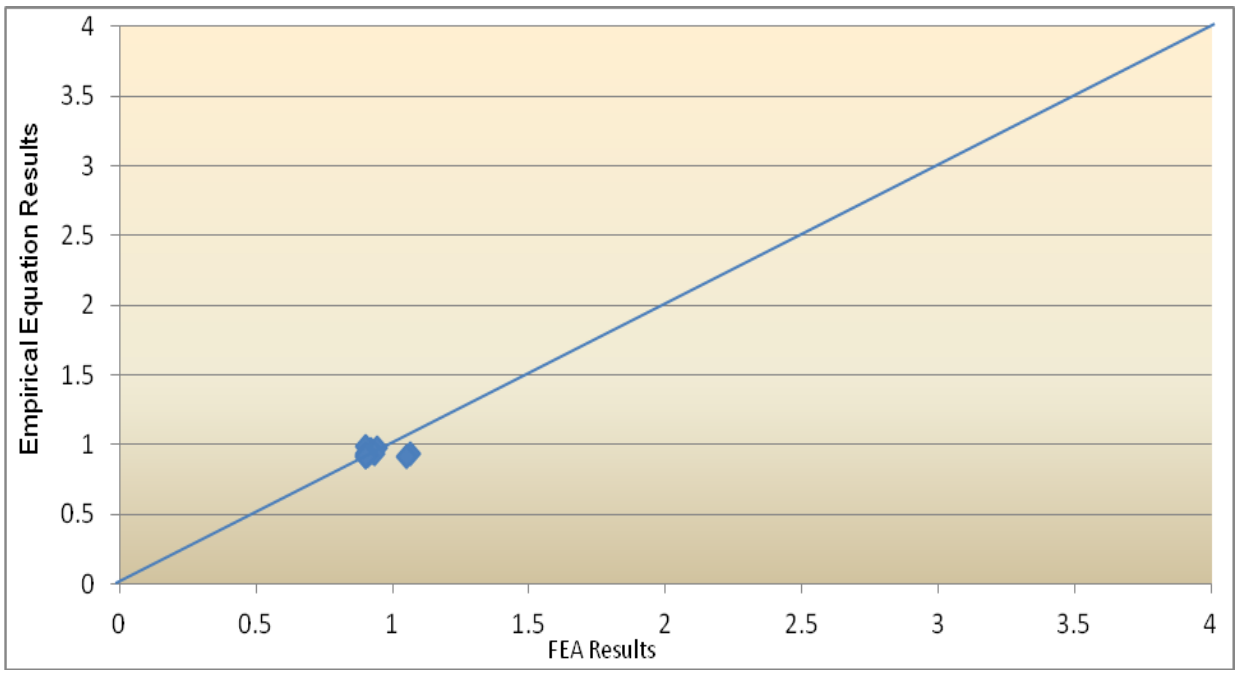

Figure 4.49 Comparison between the moment distribution factor F_m from FEA and empirical equation results for three-lane bridges at Ultimate Limit State

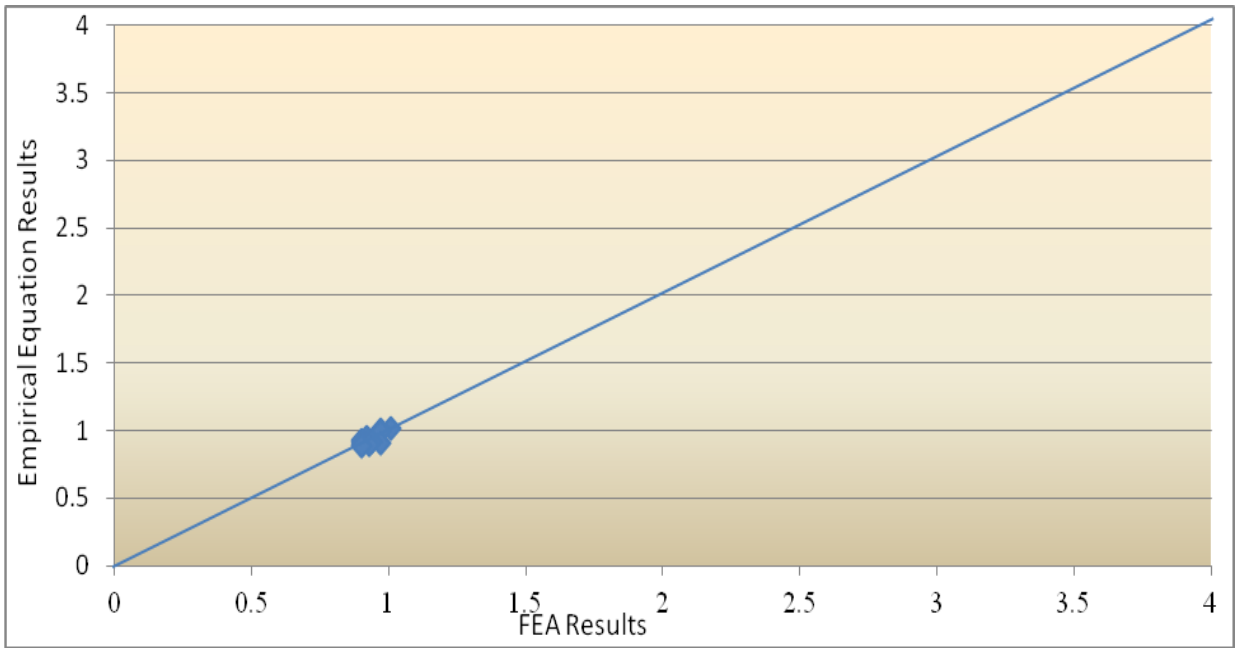

Figure 4.50 Comparison between the moment distribution factor F_m from FEA and empirical equation results for four-lane bridges at Ultimate Limit State

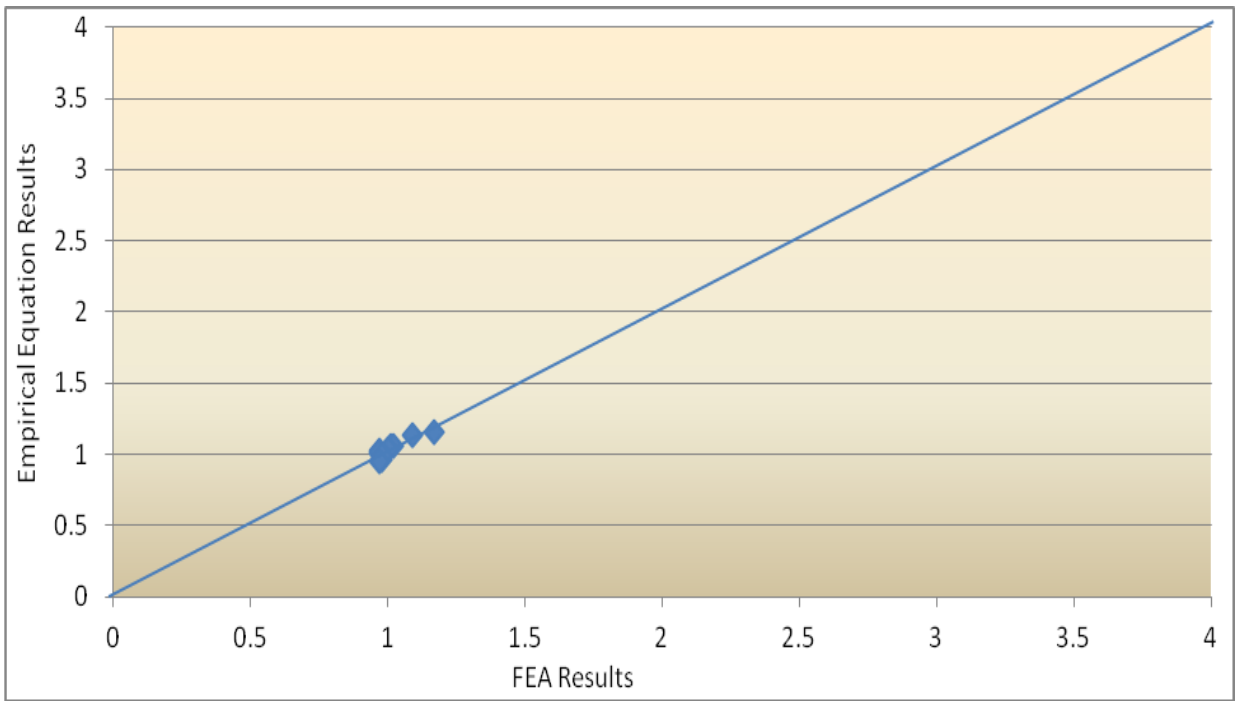

Figure 4.51 Comparison between the moment distribution factor F_m from FEA and empirical equation results for two-lane bridges at Fatigue Limit State

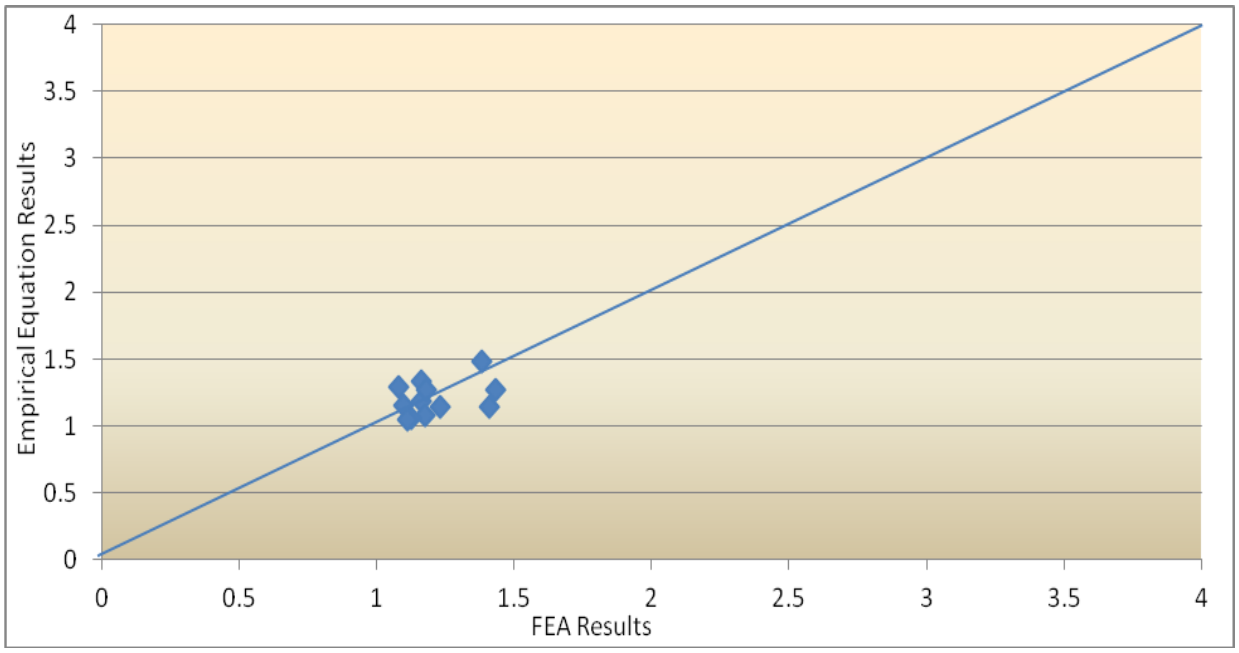

Figure 4.52 Comparison between the moment distribution factor F_m from FEA and empirical equation results for three-lane bridges at Fatigue Limit State

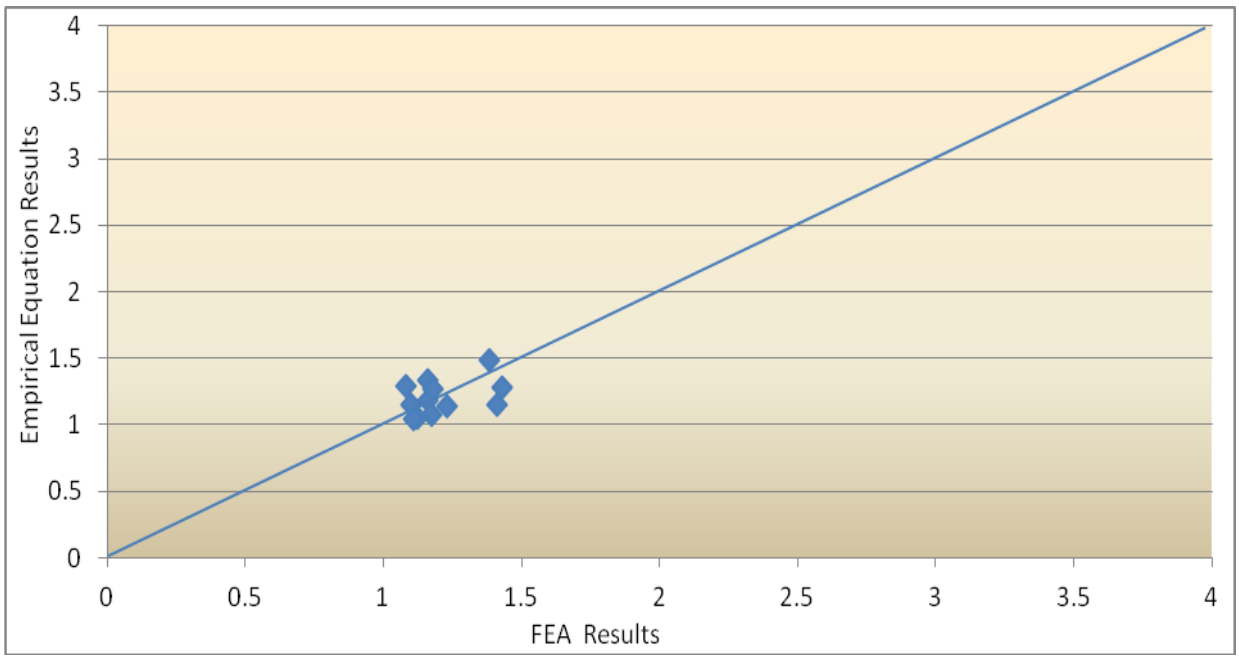

Figure 4.53 Comparison between the moment distribution factor F_m from FEA and empirical equation results for four-lane bridges at Fatigue Limit State

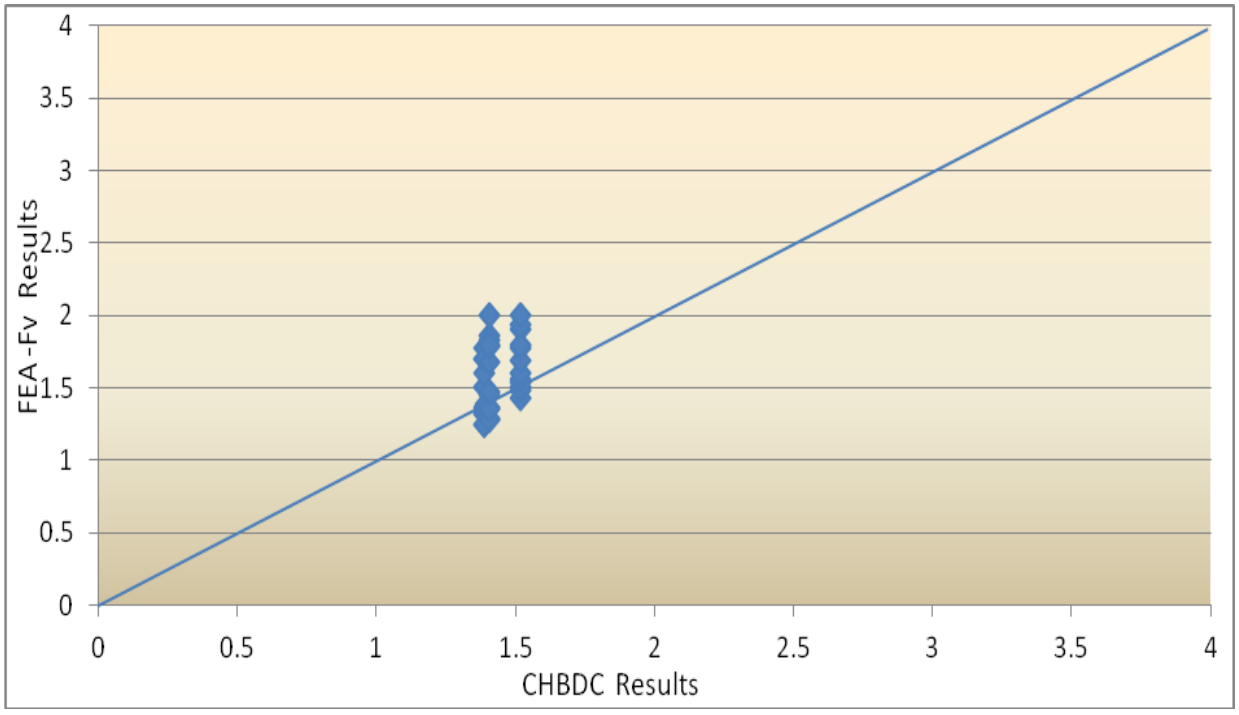

Figure 4.54 Correlation between the shear distribution factor F_v from FEA and CHBDC results at Ultimate Limit State

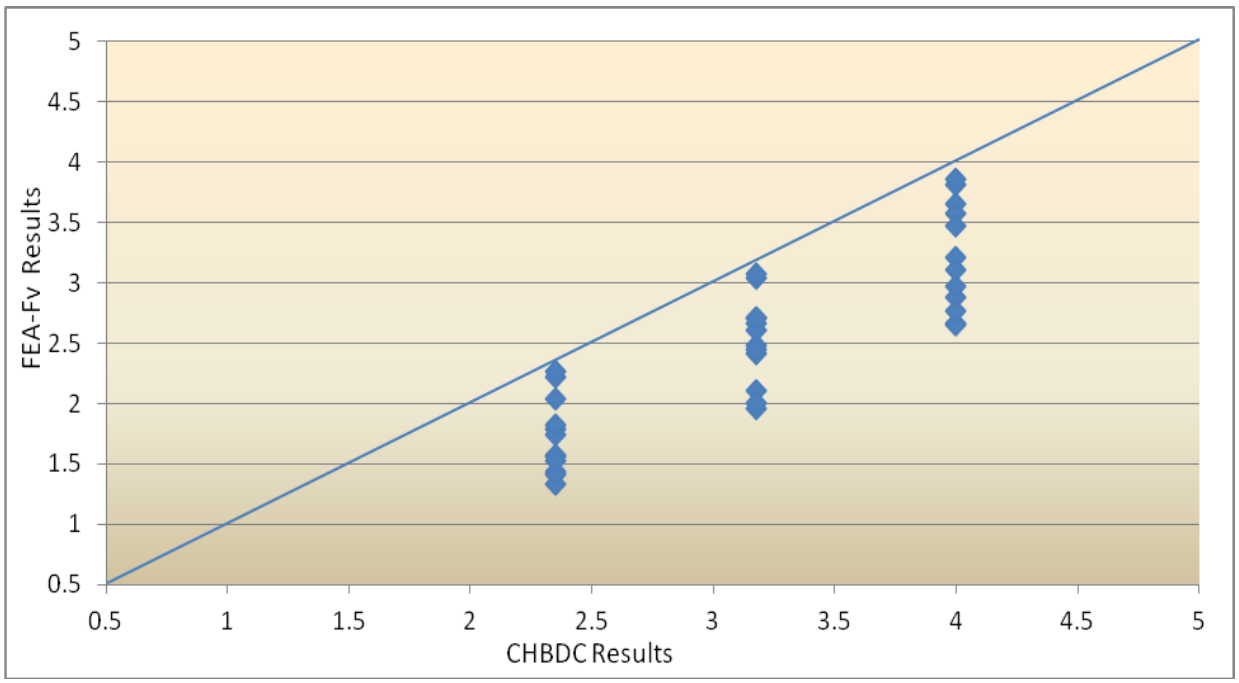

Figure 4.55 Correlation between the shear distribution factor F_v from FEA and CHBDC results at Fatigue Limit State

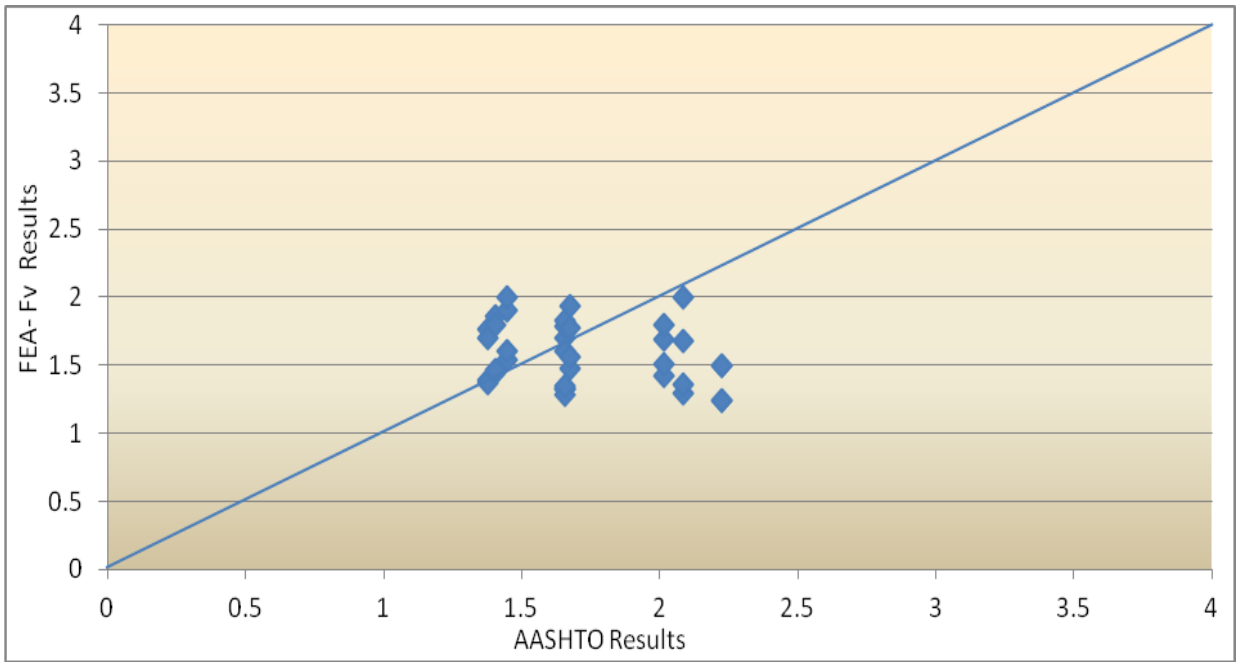

Figure 4.56 Correlation between the shear distribution factor F_v from FEA and AASHTO results at Ultimate Limit State

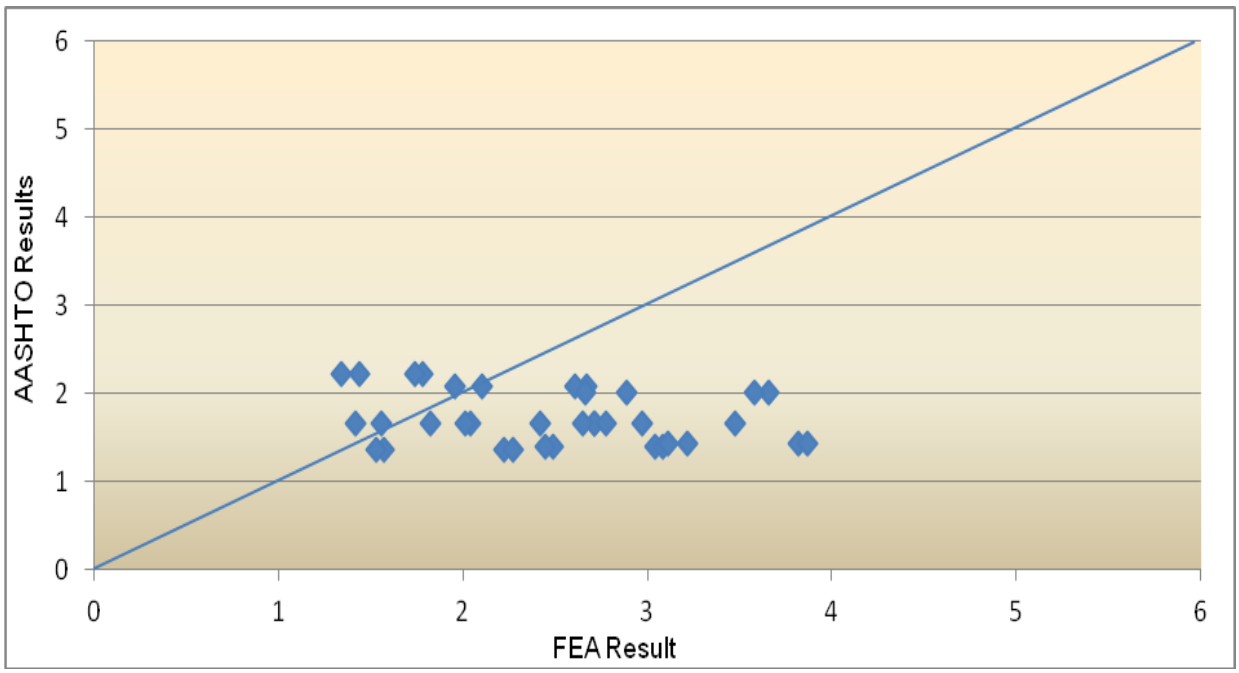

Figure 4.57 Correlation between the shear distribution factors F_v from FEA and AASHTO results at Fatigue Limit State

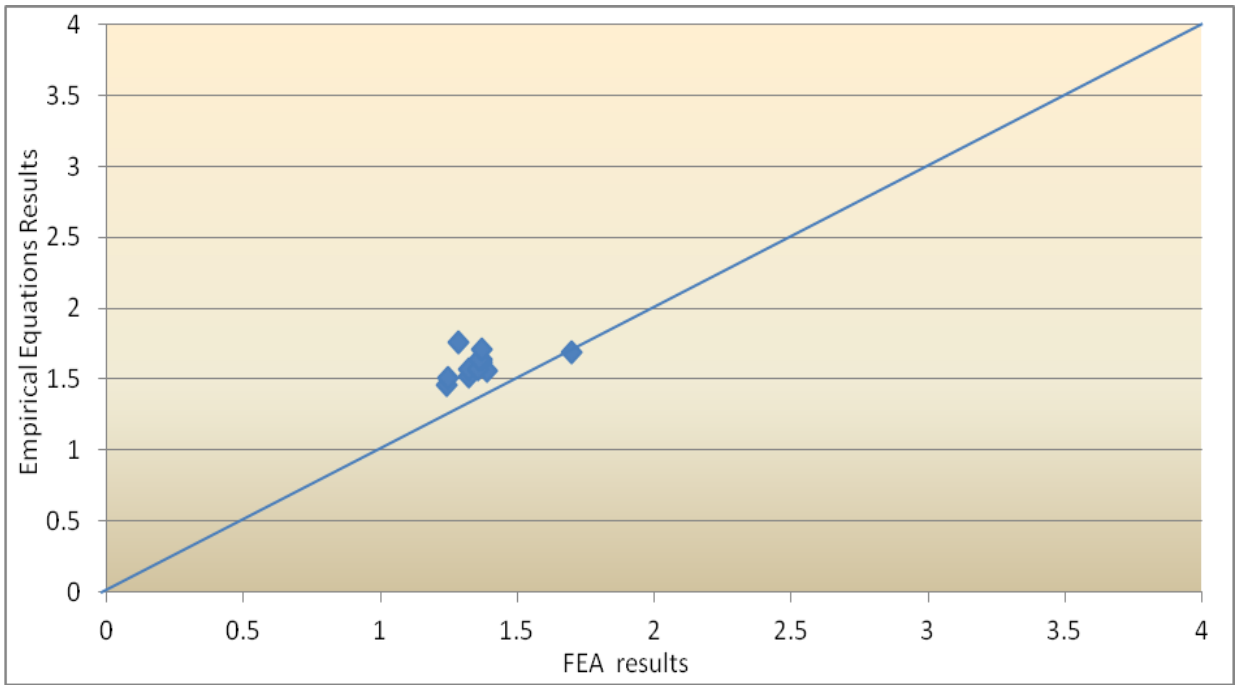

Figure 4.58 Comparison between the shear distribution factor F_v from FEA and empirical equation results for two-lane bridges on which F is a function of L at Ultimate Limit State

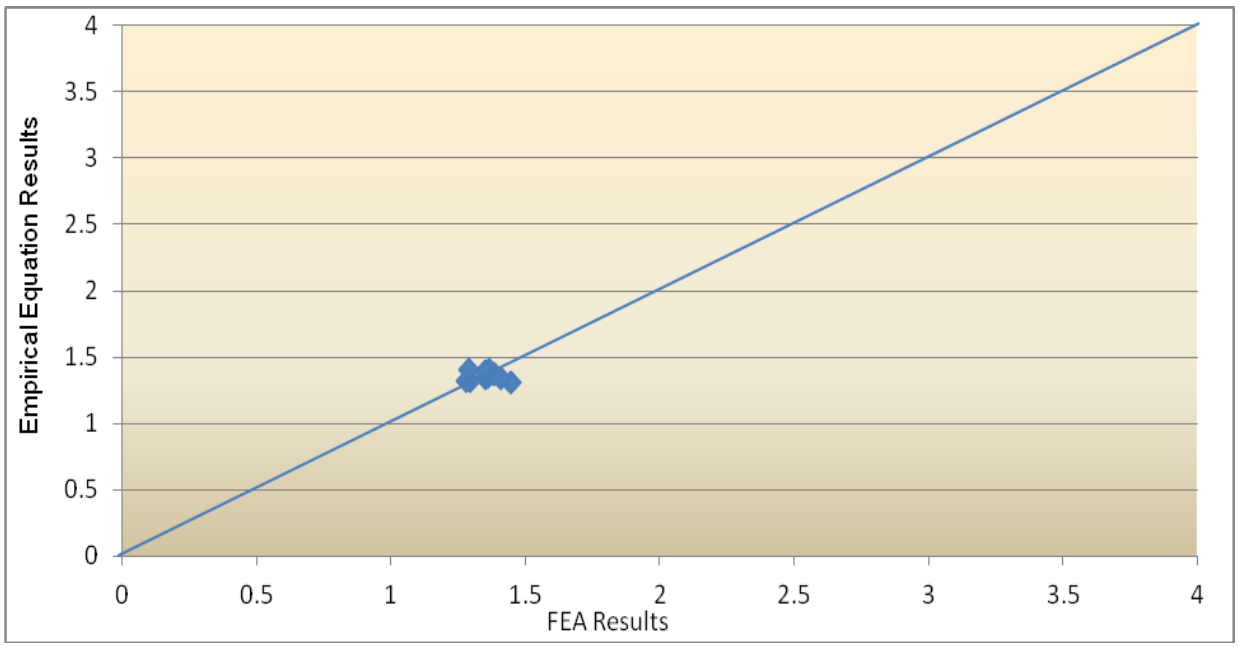

Figure 4.59 Comparison between the shear distribution factor F_v from FEA and empirical equation results for three-lane bridges on which F is a function of L at Ultimate Limit State

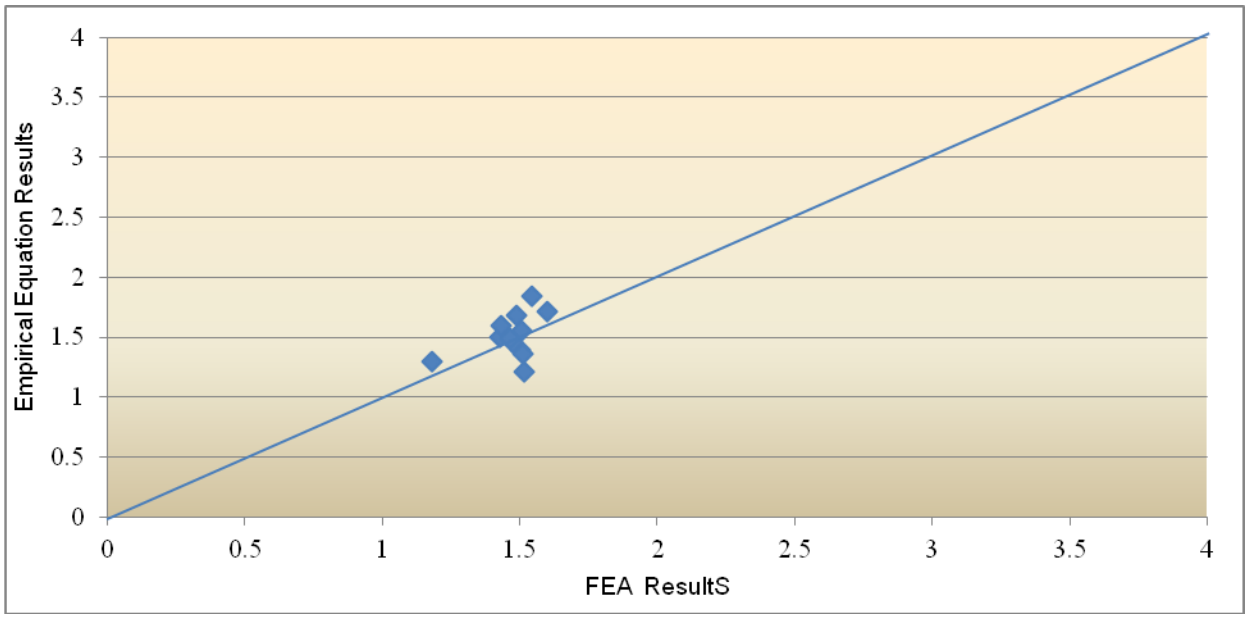

Figure 4.60 Comparison between the shear distribution factors F_v from FEA and empirical equation results for four-lane bridges on which F is a function of L at Ultimate Limit State

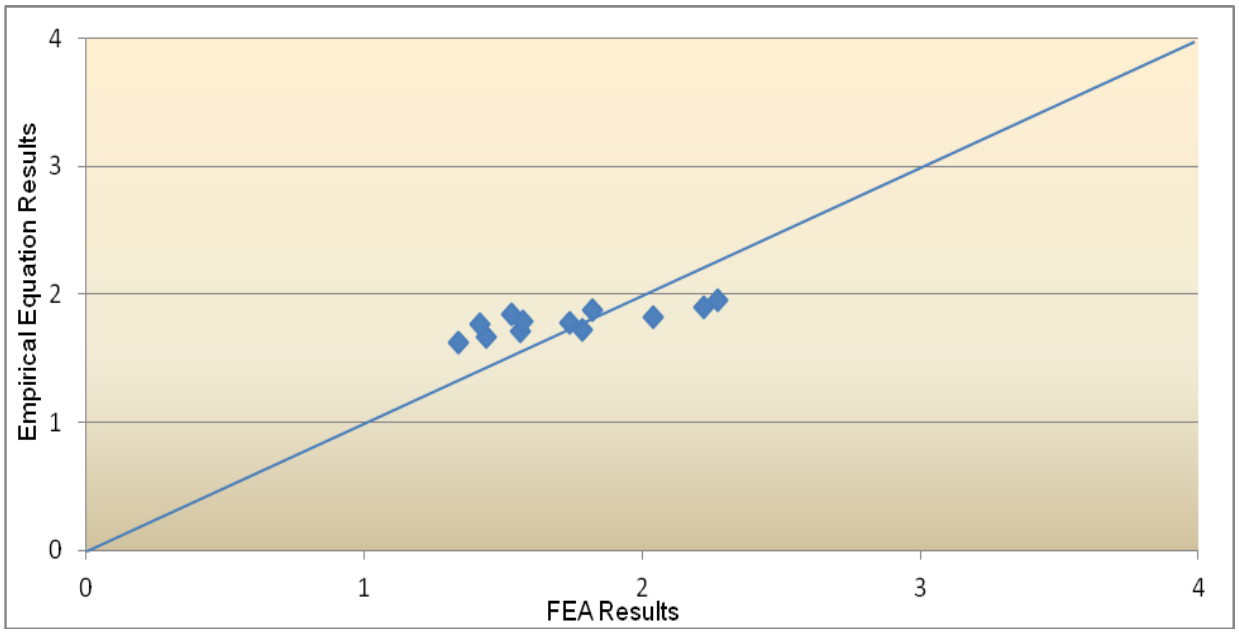

Figure 4.61 Comparison between the shear distribution factor F_v from FEA and empirical equation results for two-lane bridges on which F is a function of L at Fatigue Limit State

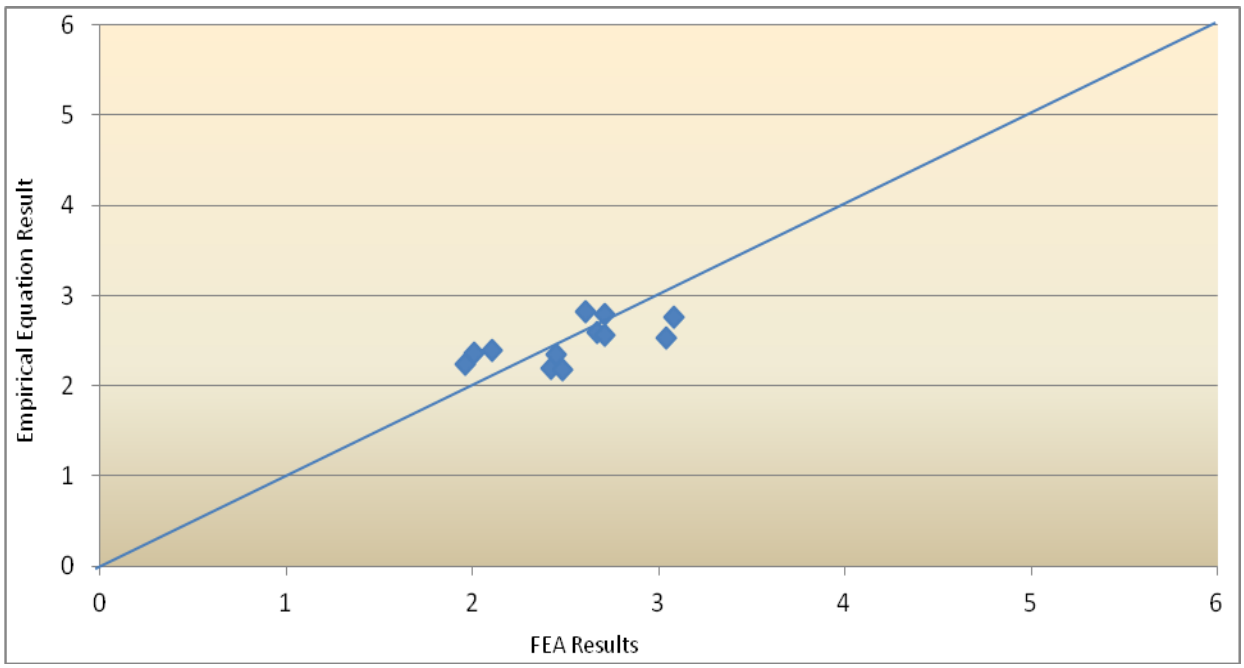

Figure 4.62 Comparison between the shear distribution factor F_v from FEA and empirical equation results for three-lane bridges on which F is a function of L at Fatigue Limit State

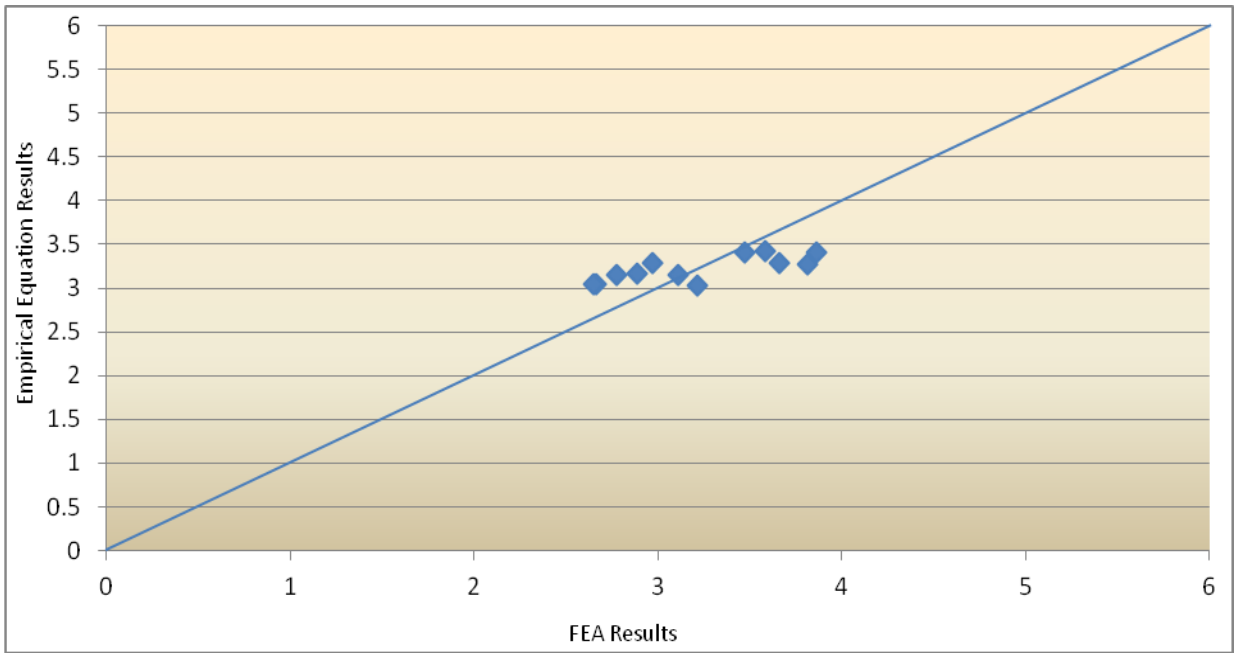

Figure 4.63 Comparison between the shear distribution factor F_v from FEA and empirical equation results for four-lane bridges on which F is a function of L at Fatigue Limit State

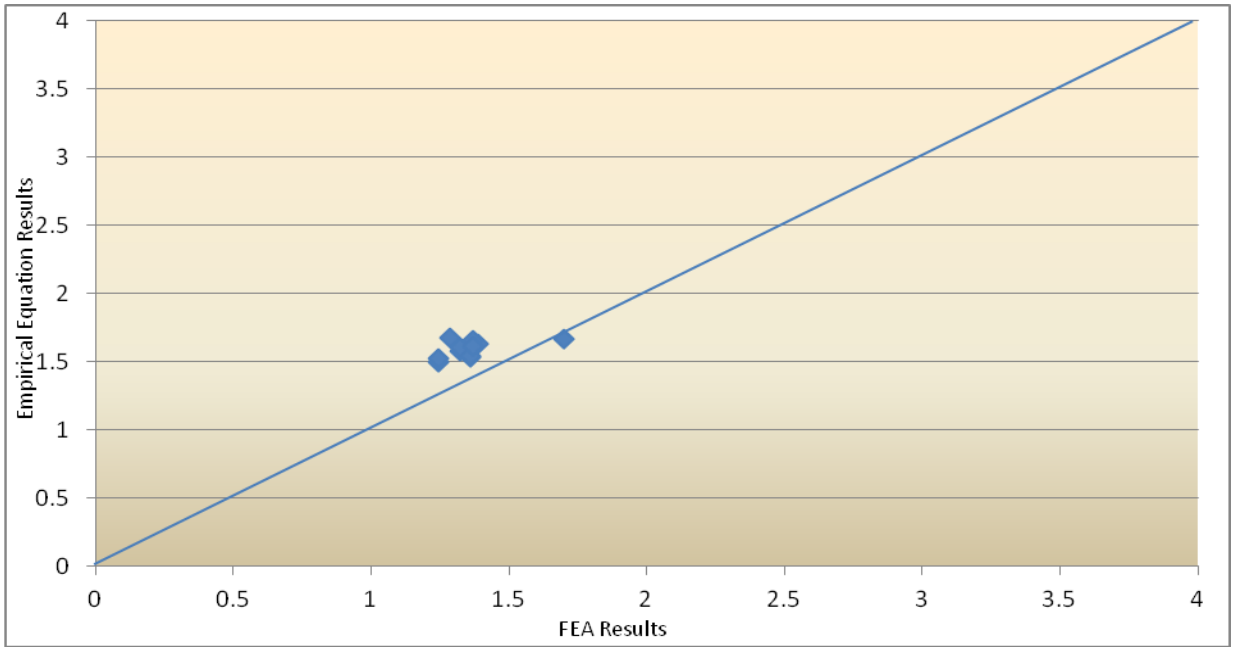

Figure 4.64 Comparison between the shear distribution factor F_v from FEA and empirical equation results for two-lane bridges on which F is a function of $\mathcal{B}$ at Ultimate Limit State

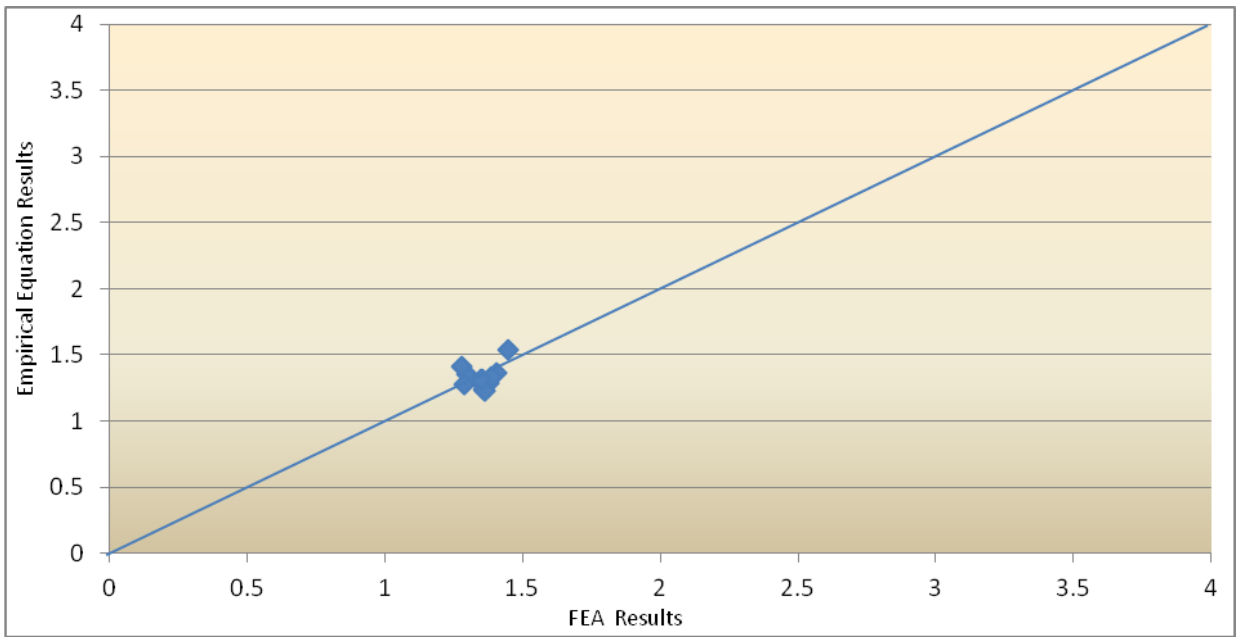

Figure 4.65 Comparison between the shear distribution factors F_v from FEA and empirical equation results for three-lane bridges on which F is a function of $\mathscr{B}$ at Ultimate Limit State

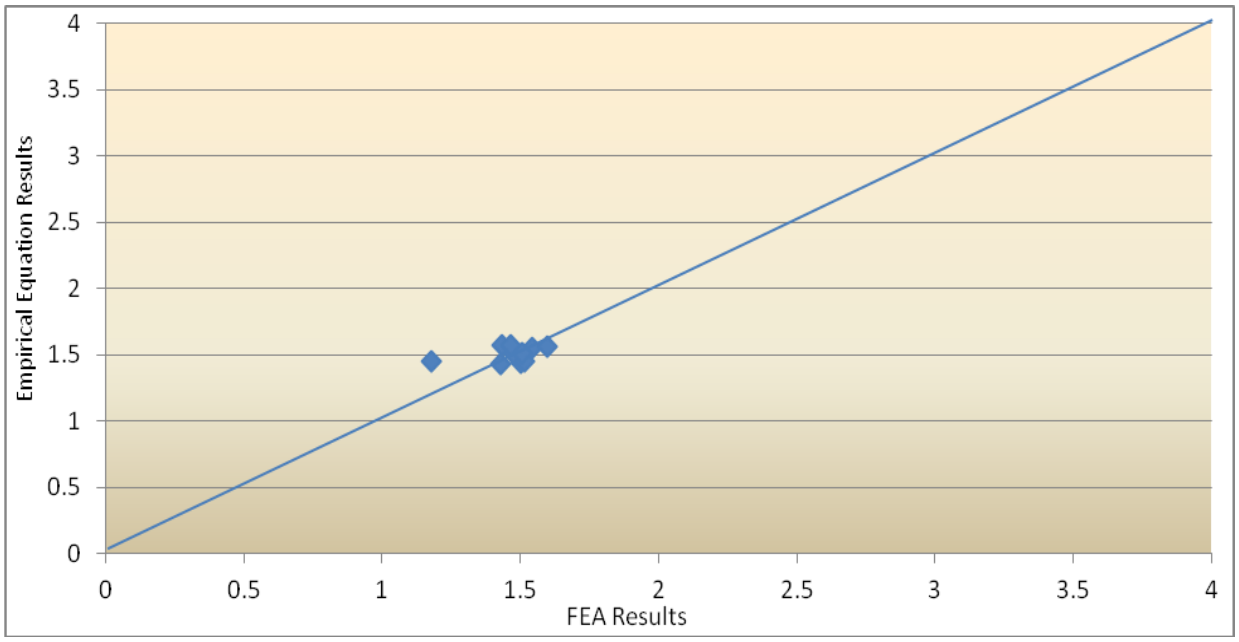

Figure 4.66 Comparison between the shear distribution factor F_v from FEA and empirical equation results for four-lane bridges on which F is a function of $\mathscr{B}$ at Ultimate Limit State

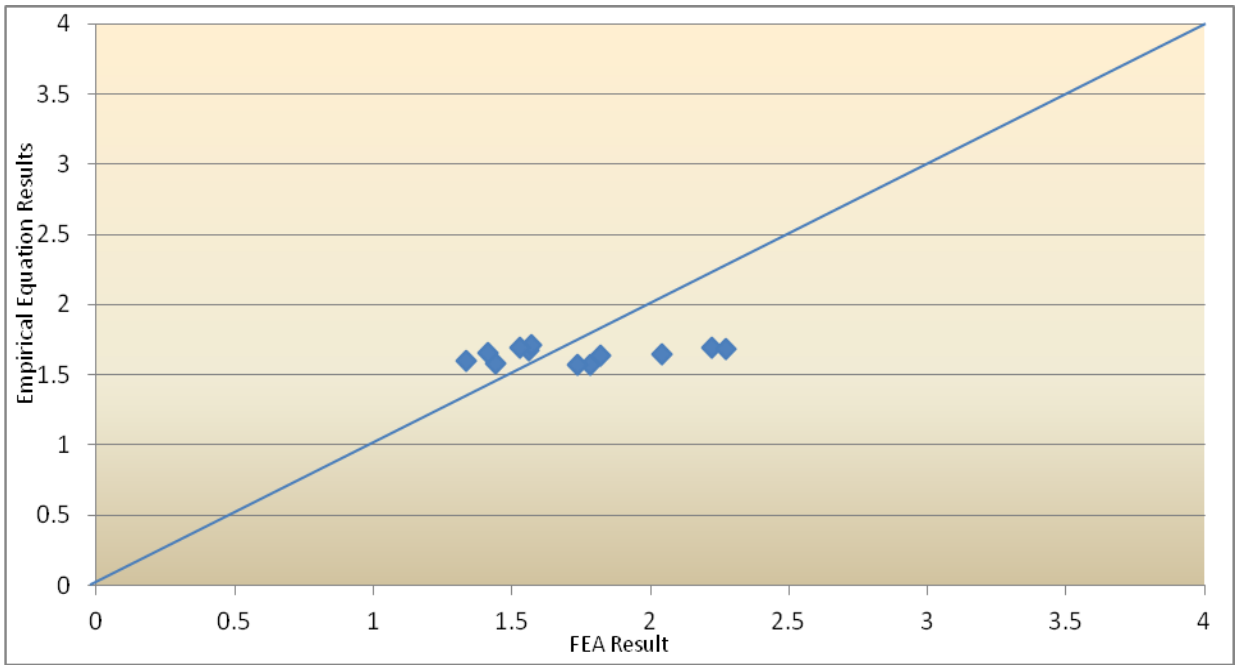

Figure 4.67 Comparison between the shear distribution factor F_v from FEA and empirical equation results for two-lane bridges on which F is a function of $\mathcal{B}$ at Fatigue Limit State

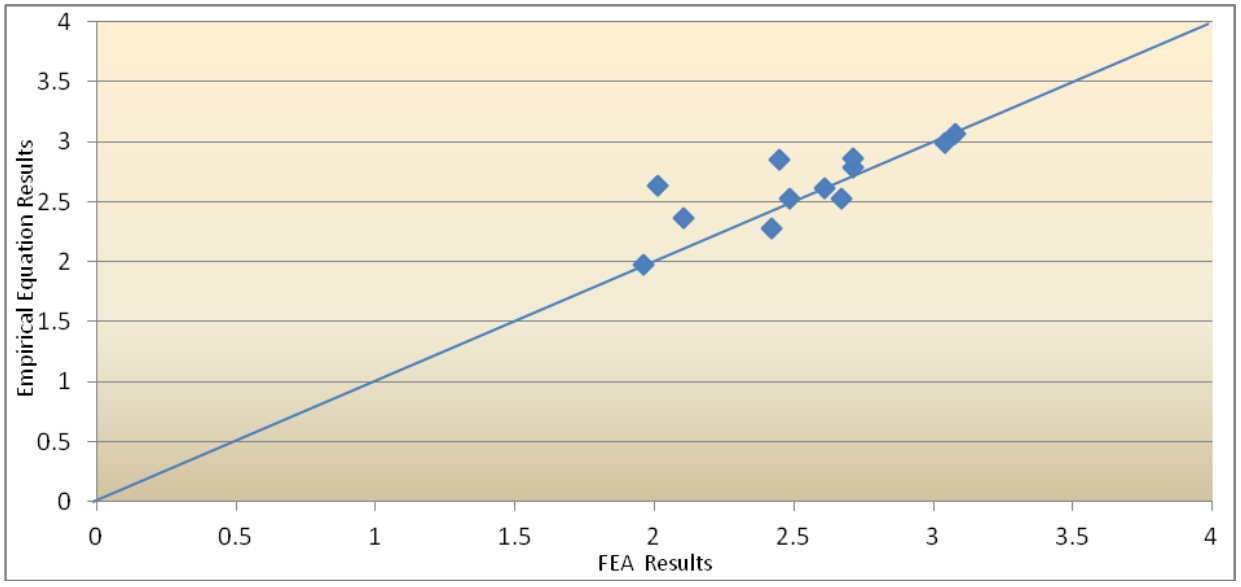

Figure 4.68 Comparison between the shear distribution factor F_v from FEA and empirical equation results for three-lane bridges on which F is a function of $\mathcal{B}$ at Fatigue Limit State

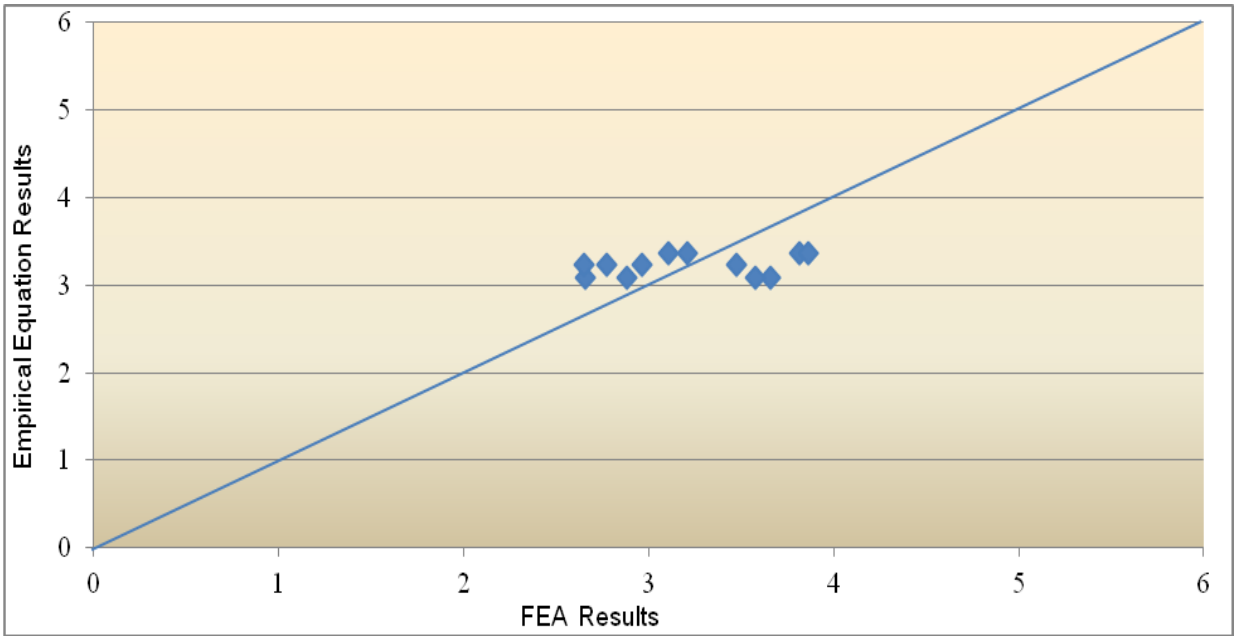

Figure 4.69 Comparison between the shear distribution factor F_v from FEA and empirical equation results for four-lane bridges on which F is a function of $\mathcal{B}$ at Fatigue Limit State

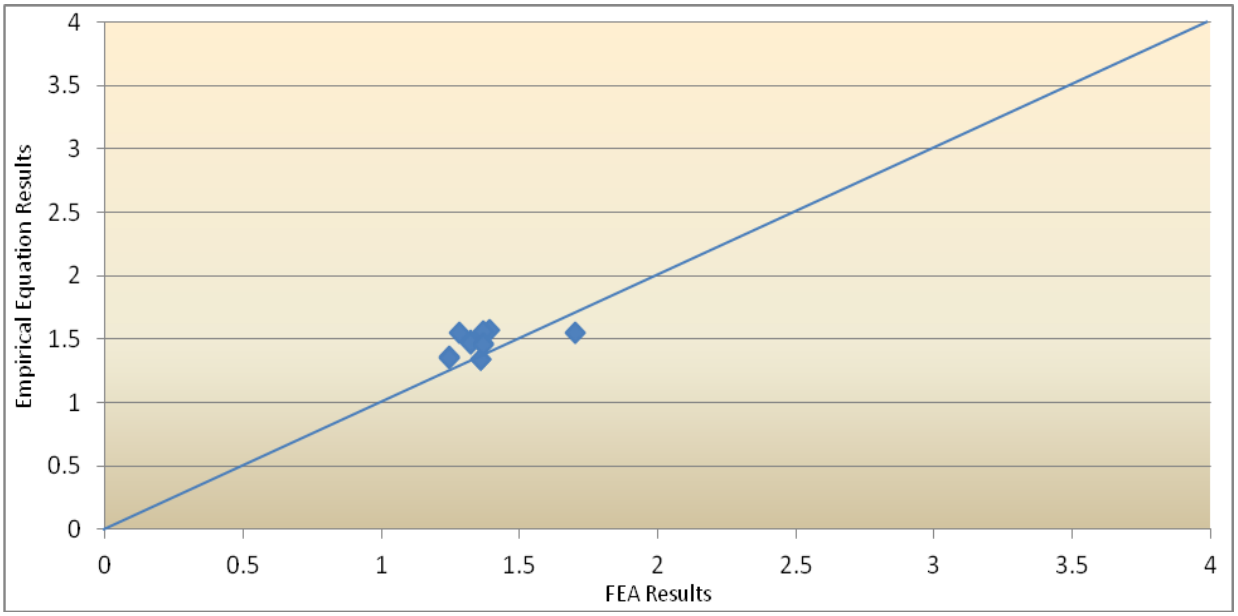

Figure 4.70 Comparison between the shear distribution factor F_v from FEA and empirical equation results for two-lane bridges on which F is a function of box girder spacing at Ultimate Limit State

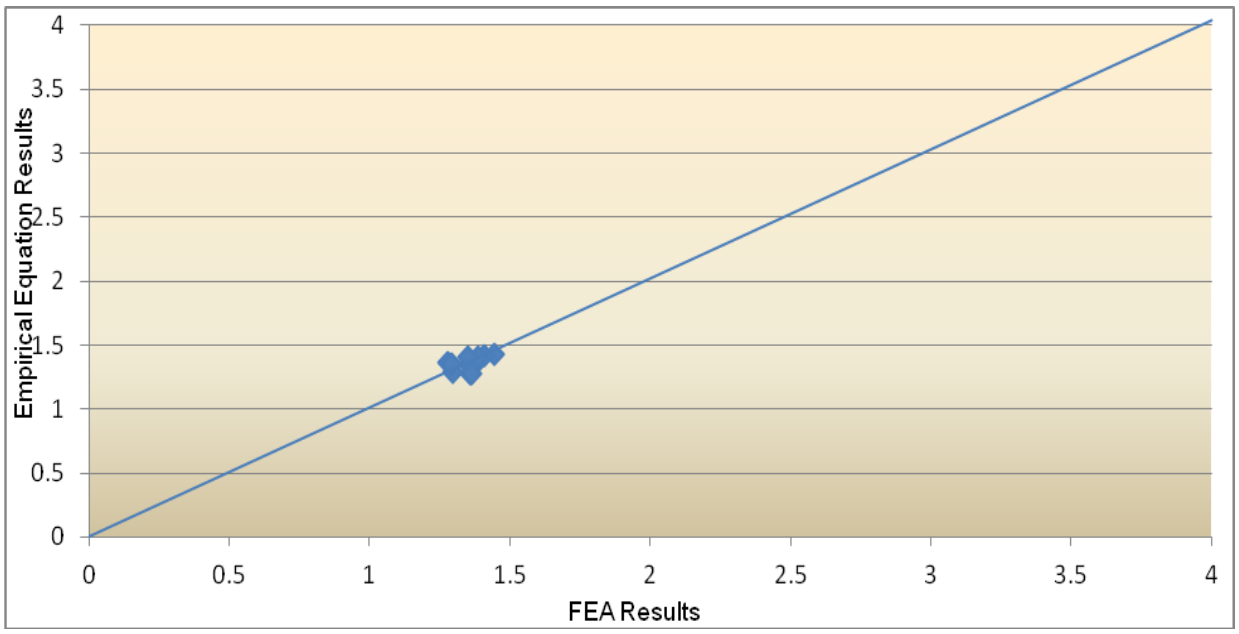

Figure 4.71 Comparison between the shear distribution factor F_v from FEA and Empirical equation results for three-lane bridges on which F is a function of box girder spacing at Ultimate Limit State

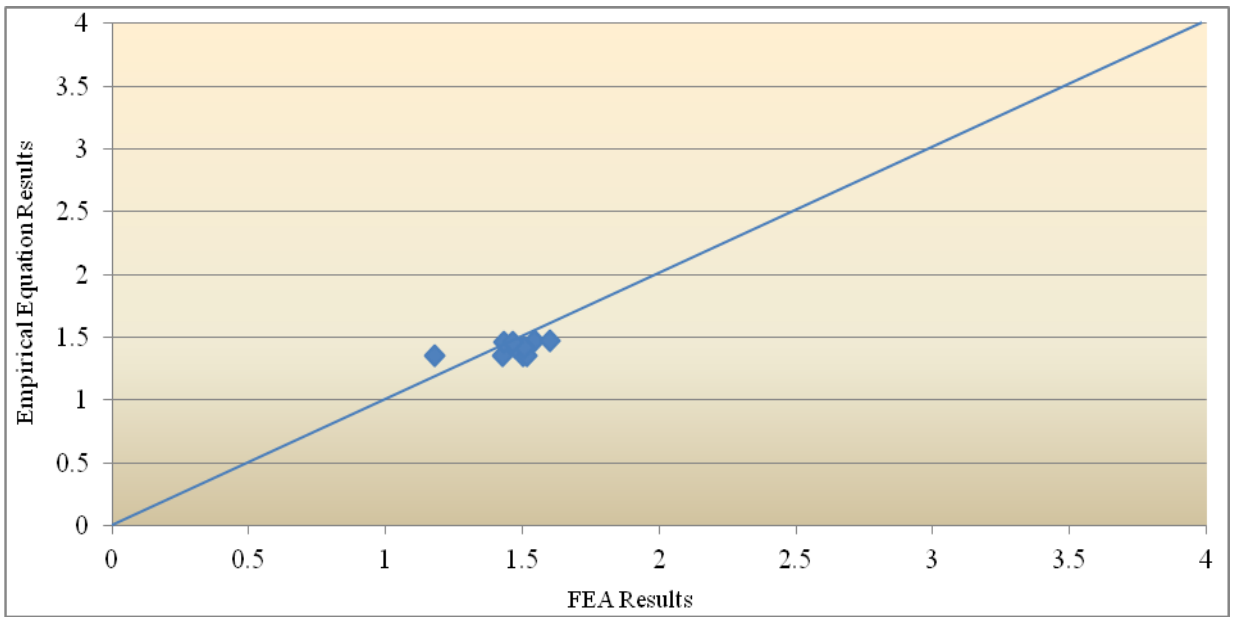

Figure 4.72 Comparison between the shear distribution factor F_v from FEA and empirical equation results for four-lane bridges on which F is a function of box girder spacing at Ultimate Limit State

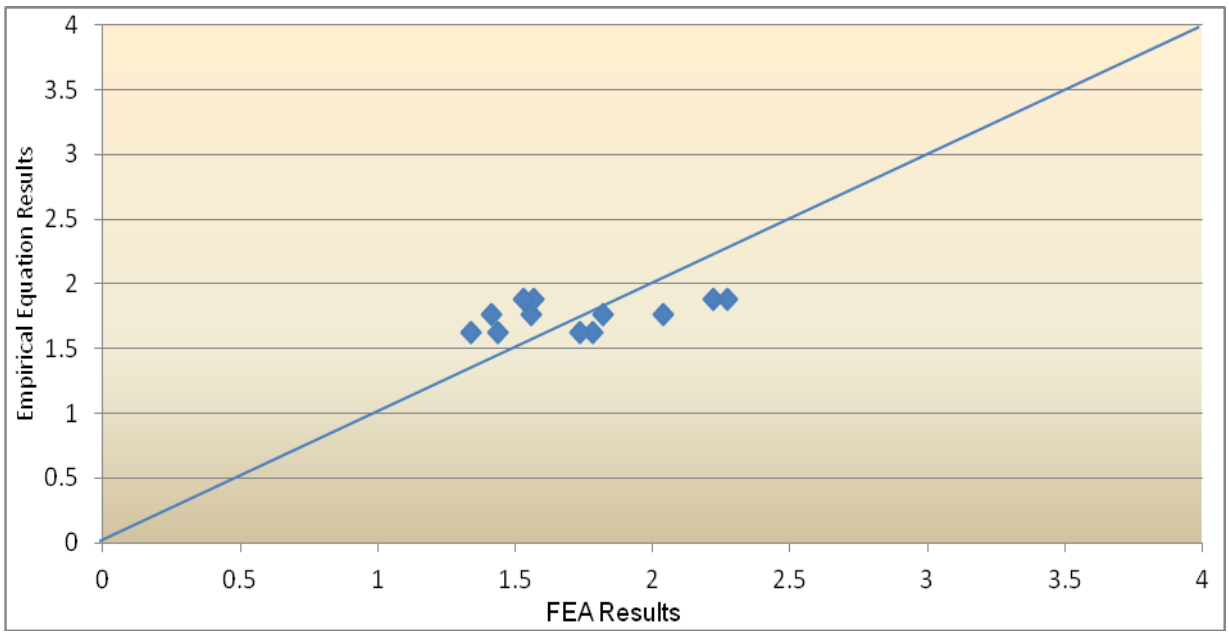

Figure 4.73 Comparison between the shear distribution factor F_v from FEA and empirical equation results for two-lane bridges on which F is a function of box girder spacing at Fatigue Limit State

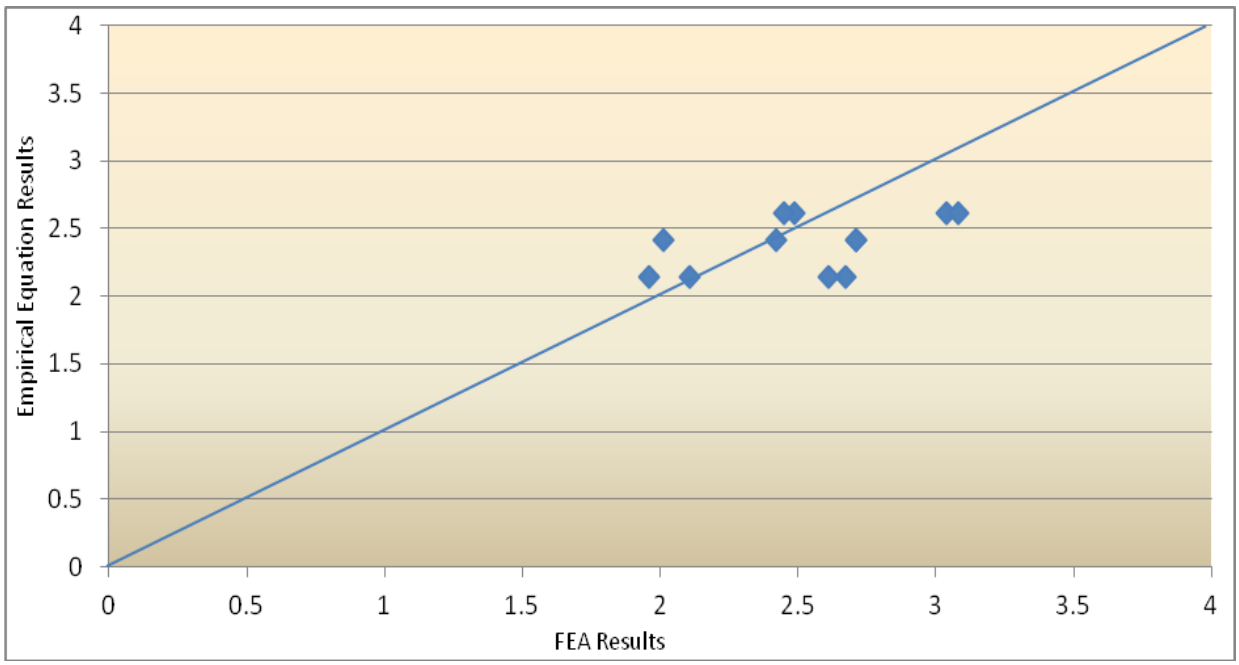

Figure 4.74 Comparison between the shear distribution factor F_v from FEA and empirical equation results for three-lane bridges on which F is a function of box girder spacing at Fatigue Limit State

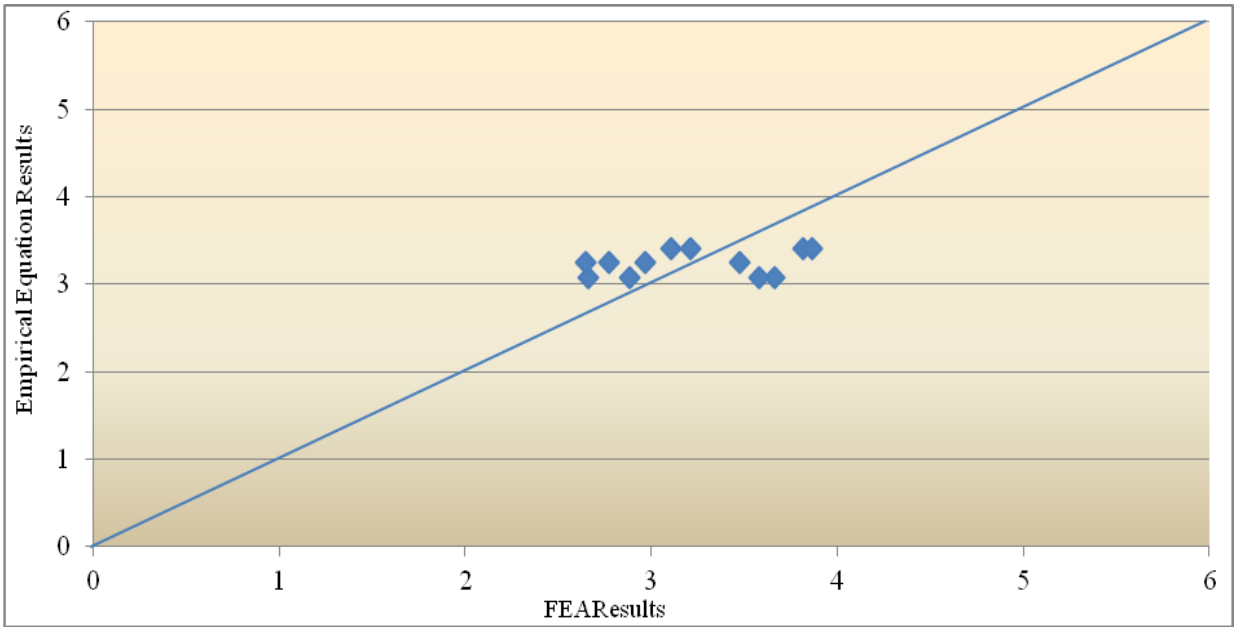

Figure 4.75 Comparison between the shear distribution factor F_v from FEA and empirical equation results for four-lane bridges on which F is a function of box girder spacing at Fatigue Limit State

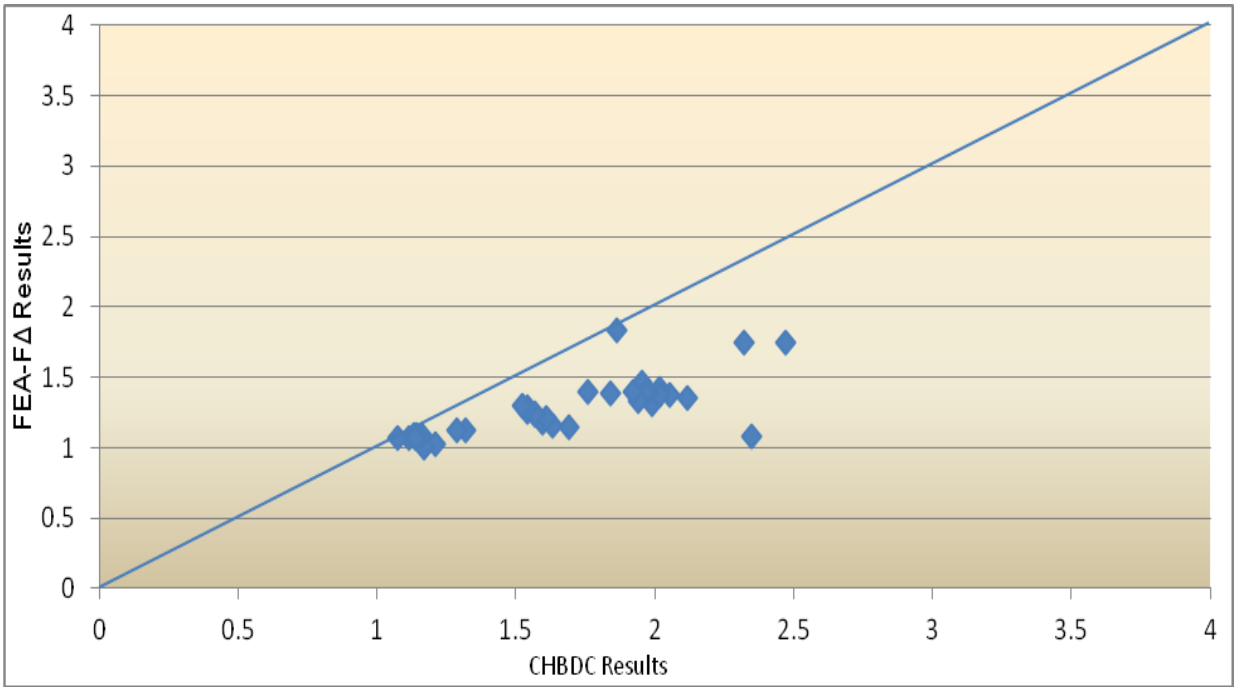

Figure 4.76 Correlation between the deflection distribution factor F_Δ from FEA and CHBDC results at Fatigue Limit State

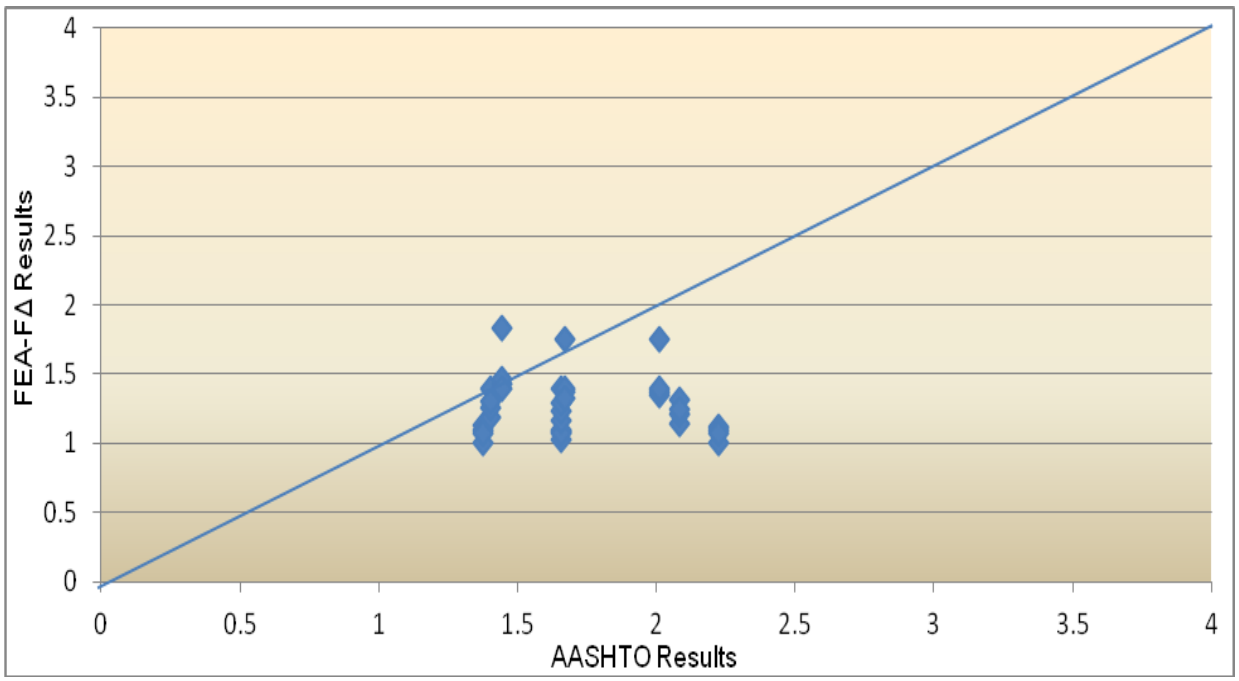

Figure 4.77 Correlation between the deflection distribution factor F_{Δ} from FEA and AASHTO results at Fatigue Limit State

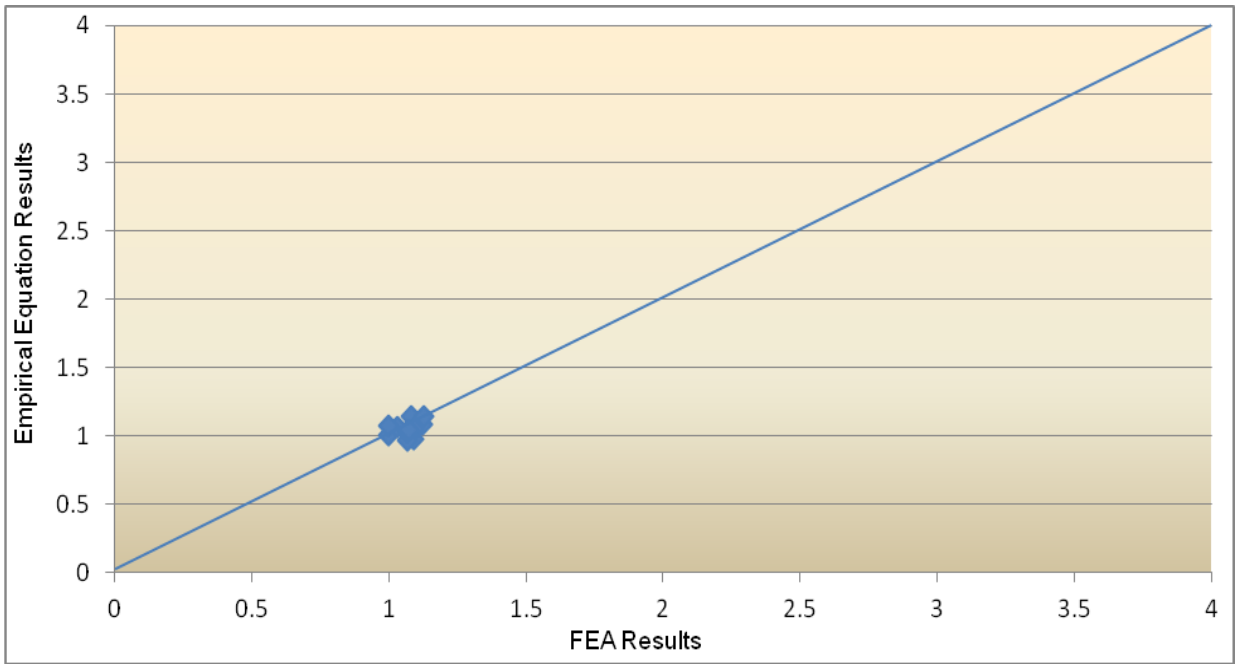

Figure 4.78 Comparison between the deflection distribution factor F_{Δ} from FEA and from empirical equation results for two-lane bridges at Fatigue Limit State

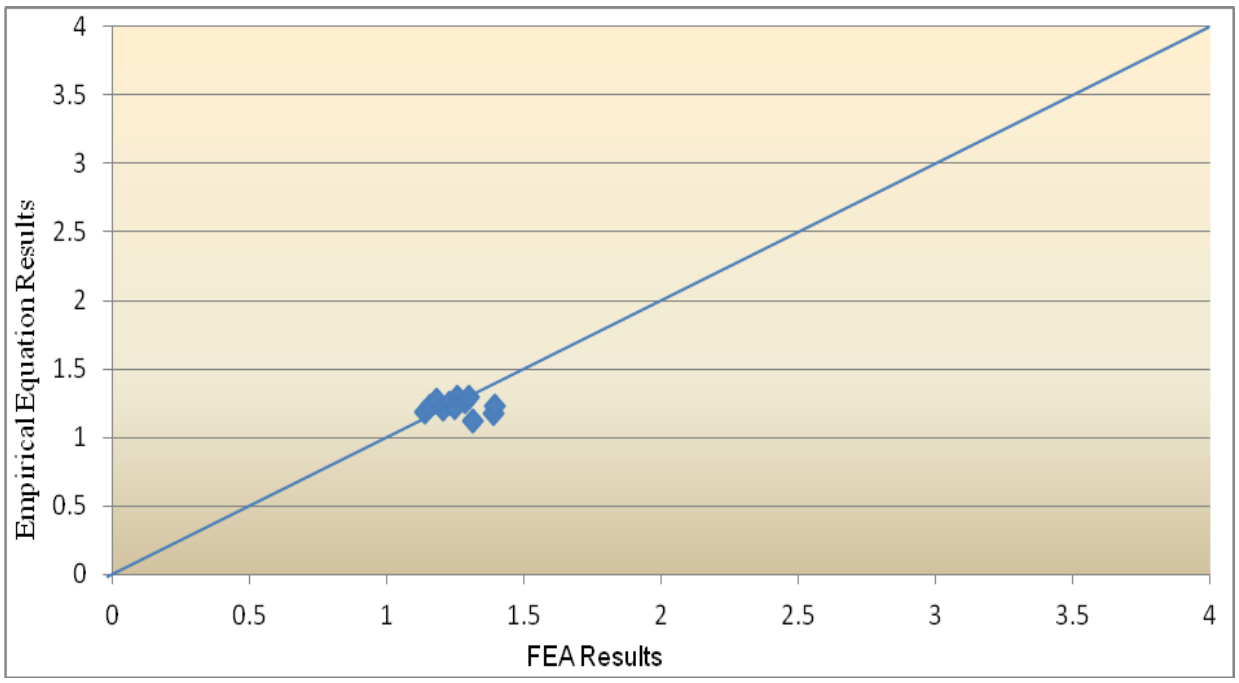

Figure 4.79 Comparison between the deflection distribution factor F_{Δ} from FEA and from empirical equation results for three-lane bridges at Fatigue Limit State

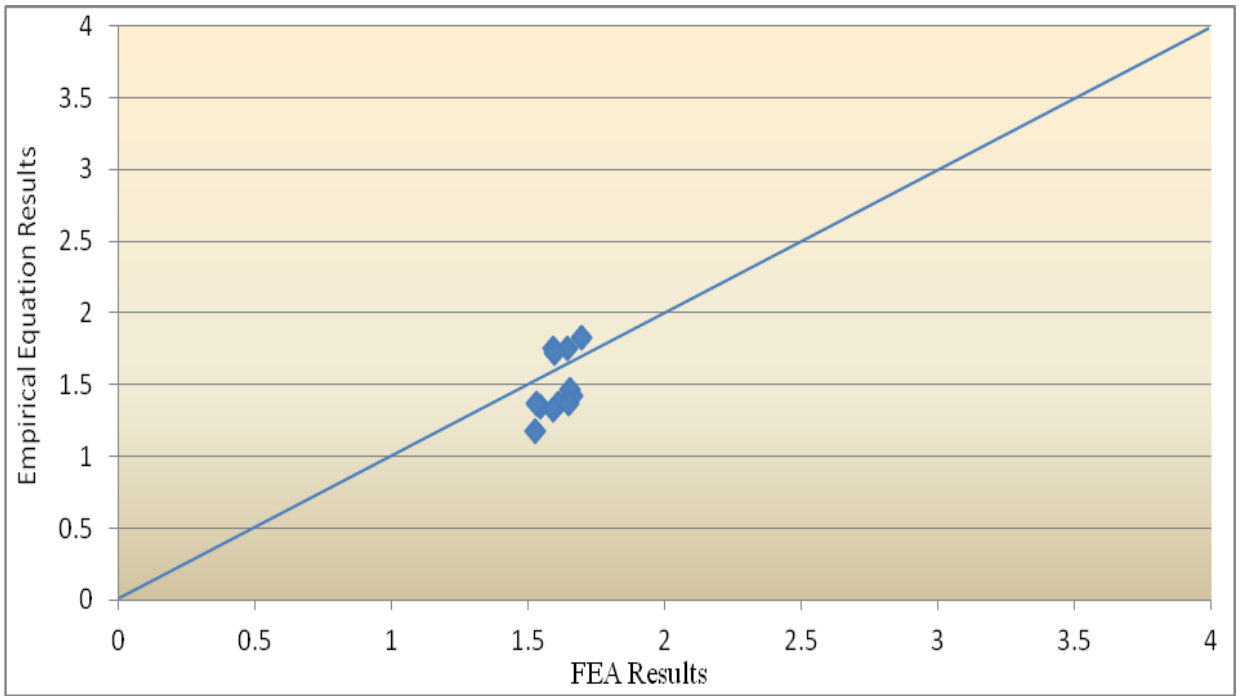

Figure 4.80 Comparison between the deflection distribution factor F_{Δ} from FEA and from empirical equation results for four-lane bridges at Fatigue Limit State

Appendix A.1 Parameters of empirical equation of moment distribution factors at Ultimate Limit State ULS for two-lane bridges

Bridge Type	Loading Case	No of Box Girder	Box Girder Spacing (m)	$\mathcal{B}$	F CHBDC	C_F CHBDC	F_m FEA	F_m CHBDC	Length (m)	RL	$R'L$	F_m Empirical equation	Empirical Equation Variables						Difference %
													a	b	c	d	**e**	m	
2L-2B-20	External Fully	2	5	1.93	7.92	12.139	0.962	1.125	20	0.9	0.9	0.926897	9	0.45	-0.04	14	-1.5	0.1	3.7872
2L-3B-20	External Fully	3	3.334	2.13	7.858	11.721	0.93	1.139	20	0.9	0.9	0.933483	9	0.45	-0.04	14	-1.5	0.1	-0.373
2L-4B-20	middle fully	4	2.5	2.34	7.79	11.305	0.825	1.152	20	0.9	0.9	0.935436	9	0.45	-0.04	14	-1.5	0.1	-11.8058
2L-2B-40	middle fully	2	5	1.13	8.158	13.722	0.913	1.0778	40	0.9	0.9	0.960921	9	0.45	-0.04	14	-1.5	0.1	-4.986
2L-3B-40	External Fully	3	3.334	1.35	8.093	13.287	0.92	1.09	40	0.9	0.9	0.967074	9	0.45	-0.04	14	-1.5	0.1	-4.867
2L-4B-40	External Fully	4	2.5	1.50	8.048	12.98	0.88	1.1	40	0.9	0.9	0.971448	9	0.45	-0.04	14	-1.5	0.1	-9.413
2L-2B-60	middle fully	2	5	0.87	8.237	14.251	0.942	1.062	60	0.9	0.9	0.972732	9	0.45	-0.04	14	-1.5	0.1	-3.159
2L-3B-60	middle fully	3	3.334	1.04	8.185	13.9	0.92	1.07	60	0.9	0.9	0.980855	9	0.45	-0.04	14	-1.5	0.1	-6.204
2L-4B-60	External Fully	4	2.5	1.21	8.134	13.566	0.9	1.08	60	0.9	0.9	0.984392	9	0.45	-0.04	14	-1.5	0.1	-8.573
2L-2B-80	External Fully	2	5	0.73	8.278	14.52	0.96	1.05	80	0.9	0.9	0.978895	9	0.45	-0.04	14	-1.5	0.1	-1.930
2L-3B-80	External Fully	3	3.334	0.90	8.228	14.189	0.911	1.064	80	0.9	0.9	0.987413	9	0.45	-0.04	14	-1.5	0.1	-7.738
2L-4B-80	External Fully	4	2.5	1.06	8.18	13.87	0.9	1.073	80	0.9	0.9	0.991317	9	0.45	-0.04	14	-1.5	0.1	-9.211

Appendix A.2 Parameters of empirical equation of moment distribution factors at Ultimate Limit State ULS for three-lane bridges

Bridge Type	Loading Case	No of Box Girder	Box Girder Spacing (m)	$\mathcal{B}$	F CHBDC	C_F CHBDC	F_m FEA	F_m CHBDC	Length (m)	R_L	R'_L	F_m Empirical equation	Empirical Equation Variables						Difference %
													a	b	c	d	e	m	
3L-3B-20	External Fully	3	4.5	2.662	10.16	10.67	0.94	1.199	20	0.8	0.8	1.021	12.36	-0.38	0.02	15.38	-1.6	-0.1	7.48
3L-4B-20	External Fully	4	3.375	2.875	10.06	10.24	0.92	1.21	20	0.8	0.8	1.022	12.36	-0.38	0.02	15.38	-1.6	-0.1	10.05
3L-5B-20	External Fully	5	2.7	3.86	9.95	9.82	0.9	1.23	20	0.8	0.8	1.052	12.36	-0.38	0.02	15.38	-1.6	-0.1	14.51
3L-3B-40	middle fully	3	4.5	1.594	10.70	12.81	0.92	1.18	40	0.8	0.8	0.986	12.36	-0.38	0.02	15.38	-1.6	-0.1	6.37
3L-4B-40	middle fully	4	3.375	1.781	10.60	12.43	0.9	1.13	40	0.8	0.8	0.987	12.36	-0.38	0.02	15.38	-1.6	-0.1	8.81
3L-5B-40	middle fully	5	2.7	1.963	10.51	12.07	0.9	1.145	40	0.8	0.8	0.988	12.36	-0.38	0.02	15.38	-1.6	-0.1	8.94
3L-3B-60	middle fully	3	4.5	1.23	10.88	13.53	0.93	1.09	60	0.8	0.8	0.975	12.36	-0.38	0.02	15.38	-1.6	-0.1	4.28
3L-4B-60	middle fully	4	3.375	1.407	10.79	13.18	0.91	1.104	60	0.8	0.8	0.975	12.36	-0.38	0.02	15.38	-1.6	-0.1	6.71
3L-5B-60	External Fully	5	2.7	1.57	10.71	12.84	0.9	1.116	60	0.8	0.8	0.976	12.36	-0.38	0.02	15.38	-1.6	-0.1	7.81
3L-3B-80	middle fully	3	4.5	1.04	10.97	13.9	1.06	1.07	80	0.8	0.8	0.970	12.36	-0.38	0.02	15.38	-1.6	-0.1	8.49
3L-4B-80	middle fully	4	3.375	1.21	10.89	13.57	1.05	1.09	80	0.8	0.8	0.969	12.36	-0.38	0.02	15.38	-1.6	-0.1	-8.28
3L-5B-80	External Fully	5	2.7	1.37	10.81	13.24	0.99	1.102	80	0.8	0.8	1.021	12.36	-0.38	0.02	15.38	-1.6	-0.1	3.036

Appendix A.3 Parameters of empirical equation of moment distribution factors at Ultimate Limit State ULS for four-lane bridges

Bridge Type	Loading Case	No of Box Girder	Box Girder Spacing (m)	$\mathcal{B}$	F CHBDC	C_F CHBDC	F_m FEA	F_m CHBDC	Length (m)	R_L	R'_L	F_m Empirical Equation	Empirical Equation Variables						Difference %
													a	b	c	d	e	m	
4L-4B-20	External partial	4	4.25	3.4	12.11	9.198	1.01	1.284	20	0.7	0.7	1.02	14.72	-0.7	0.13	4	8	0.1	-0.942
4L-5B-20	External partial	5	3.4	3.614	11.97	8.771	0.97	1.305	20	0.7	0.7	1	14.72	-0.7	0.13	4	8	0.1	-3.221
4L-6B-20	External partial	6	2.8334	3.8244	11.822	8.3511	0.97	1.32	20	0.7	0.7	1	14.72	-0.7	0.13	4	8	0.1	-2.070
4L-4B -40	middle Loading	4	4.25	2.05	13.064	11.8999	0.92	1.162	40	0.7	0.7	0.95	14.72	-0.7	0.13	4	8	0.1	-3.155
4L-5B -40	External partial	5	3.4	2.226	12.941	11.547	0.9	1.177	40	0.7	0.7	0.93	14.72	-0.7	0.13	4	8	0.1	-3.326
4L-6B -40	Middle full	6	2.8334	2.419	12.8065	11.161	0.9	1.194	40	0.7	0.7	0.92	14.72	-0.7	0.13	4	8	0.1	-1.975
4L-4B -60	Middle full	4	4.25	1.592	13.385	12.815	0.93	1.125	60	0.7	0.7	0.93	14.72	-0.7	0.13	4	8	0.1	0.096
4L-5B -60	Middle full	5	3.4	1.766	13.263	12.467	0.97	1.139	60	0.7	0.7	0.91	14.72	-0.7	0.13	4	8	0.1	6.583
4L-6B -60	Middle full	6	2.8334	1.935	13.145	12.129	0.9	1.153	60	0.7	0.7	0.90	14.72	-0.7	0.13	4	8	0.1	0.432
4L-4B -80	Middle full	4	4.25	1.357	13.549	13.28	0.94	1.107	80	0.7	0.7	0.90	14.72	-0.7	0.13	4	8	0.1	2.288
4L-5B -80	Middle full	5	3.4	1.5224	13.434	12.955	0.93	1.12	80	0.7	0.7	0.92	14.72	-0.7	0.13	4	8	0.1	3.381
4L-6B -80	Middle full	6	2.8334	1.68	13.32	12.63	0.9	1.133	80	0.7	0.7	0.90	14.72	-0.7	0.13	4	8	0.1	1.681

Appendix A.4 Parameters of empirical equation of moment distribution factors at Fatigue Limit State FLS for two-lane bridges

Bridge Type	Loading Case	no of Box Girder	Box Girder Spacing (m)	$\mathcal{B}$	F CHBDC	C_F CHBDC	F_m FEA	F_m CHBDC	Length (m)	R_L	R'_L	F_m Empirical equation	Empirical Equation Variables						Difference %
													a	**b**	**c**	**d**	**e**	**m**	
2L-2B-20	Fatigue load	2	5	1.93	6.762	12.13	1.17	1.31862	20	0.9	0.9	1.156503	8.53	-0.69	0.1	9.51	-1	1.23	1.153
2L-3B-20	Fatigue load	3	3.334	2.139	6.57	11.721	1.09	1.36	20	0.9	0.9	1.137624	8.53	-0.69	0.1	9.51	-1	1.23	-4.369
2L-4B-20	Fatigue load	4	2.5	1.76	6.91	12.478	1.01	1.28	20	0.9	0.9	1.058599	8.53	-0.69	0.1	9.51	-1	1.23	-4.811
2L-2B-40	Fatigue load	2	5	1.1385	7.4753	13.722	1.018	1.17	40	0.9	0.9	1.060103	8.53	-0.69	0.1	9.51	-1	1.23	-4.135
2L-3B-40	Fatigue load	3	3.334	1.356	7.279	13.28	1.004	1.2126	40	0.9	0.9	1.042291	8.53	-0.69	0.1	9.51	-1	1.23	-3.813
2L-4B-40	Fatigue load	4	2.5	1.1306	7.4823	13.7386	0.98	1.175	40	0.9	0.9	0.988277	8.53	-0.69	0.1	9.51	-1	1.23	-0.844
2L-2B-60	Fatigue load	2	5	0.874	7.713	14.251	0.97	1.134	60	0.9	0.9	1.030867	8.53	-0.69	0.1	9.51	-1	1.23	-6.274
2L-3B-60	Fatigue load	3	3.334	1.0489	7.55598	13.902	0.972	1.16	60	0.9	0.9	1.008523	8.53	-0.69	0.1	9.51	-1	1.23	-3.757
2L-4B-60	Fatigue load	4	2.5	0.912	7.6786	14.174	0.98	1.14	60	0.9	0.9	0.965674	8.53	-0.69	0.1	9.51	-1	1.23	1.461
2L-2B-80	Fatigue load	2	5	0.738	7.835	14.522	0.97	1.114	80	0.9	0.9	1.016357	8.53	-0.69	0.1	9.51	-1	1.23	-4.779
2L-3B-80	Fatigue load	3	3.334	0.905	7.685	14.189	0.98	1.139	80	0.9	0.9	0.993327	8.53	-0.69	0.1	9.51	-1	1.23	-1.359
2L-4B-80	Fatigue load	4	2.5	0.7986	7.781	14.4	0.97	1.123	80	0.9	0.9	1.156503	8.53	-0.69	0.1	9.51	-1	1.23	-19.227

Appendix A.5 Parameters of empirical equation of moment distribution factors at Fatigue Limit State FLS for three-lane bridges

Bridge Type	Loading Case	no of Box Girder	Box Girder Spacing (m)	$\mathcal{B}$	F CHBDC	C_F CHBDC	F_m FEA	F_m CHBDC	Length (m)	R_L	R'_L	F_m Empirical equation	Empirical Equation Variables						differences %
													a	b	c	d	e	m	
3L-3B-20	Fatigue load	3	4.5	2.662	6.1039	10.675	1.38	1.99	20	0.8	0.8	1.482484	6.8	-0.45	0.35	21.7	-2.9	0.9	6.643
3L-4B-20	Fatigue load	4	3.375	2.156	6.558	11.6864	1.43	1.84	20	0.8	0.8	1.276355	6.8	-0.45	0.35	21.7	-2.9	0.9	-12.19
3L-5B-20	Fatigue load	5	2.7	1.851	6.83352	12.296	1.41	1.759	20	0.8	0.8	1.147006	6.8	-0.45	0.35	21.7	-2.9	0.9	-22.92
3L-3B-40	Fatigue load	3	4.5	1.594	7.065	12.811	1.16	1.69	40	0.8	0.8	1.339274	6.8	-0.45	0.35	21.7	-2.9	0.9	13.38
3L-4B-40	Fatigue load	4	3.375	1.336	7.297	13.327	1.16	1.63	40	0.8	0.8	1.182938	6.8	-0.45	0.35	21.7	-2.9	0.9	1.68
3L-5B-40	Fatigue load	5	2.7	1.178	7.439	13.643	1.17	1.596	40	0.8	0.8	1.078675	6.8	-0.45	0.35	21.7	-2.9	0.9	-8.83
3L-3B-60	Fatigue load	3	4.5	1.233	7.3898	13.533	1.08	1.609	60	0.8	0.8	1.296235	6.8	-0.45	0.35	21.7	-2.9	0.9	16.68
3L-4B-60	Fatigue load	4	3.375	1.055	7.549	13.88	1.1	1.57	60	0.8	0.8	1.153671	6.8	-0.45	0.35	21.7	-2.9	0.9	4.65
3L-5B-60	Fatigue load	5	2.7	0.945	7.648	14.108	1.12	1.54	60	0.8	0.8	1.056715	6.8	-0.45	0.35	21.7	-2.9	0.9	-6.46
3L-3B-80	Fatigue load	3	4.5	1.048	7.556	13.9	1.18	1.568	80	0.8	0.8	1.275024	6.8	-0.45	0.35	21.7	-2.9	0.9	7.452
3L-4B-80	Fatigue load	4	3.375	0.910	7.6807	14.179	1.23	1.539	80	0.8	0.8	1.138997	6.8	-0.45	0.35	21.7	-2.9	0.9	-7.98
3L-5B-80	Fatigue load	5	2.7	0.826	7.756	14.3467	1.11	1.522	80	0.8	0.8	1.045746	6.8	-0.45	0.35	21.7	-2.9	0.9	-6.14

Appendix A.6 Parameters of empirical equation of moment distribution factors at Fatigue Limit State FLS for four-lane bridges

Bridge Type	Loading Case	no of Box Girder	Box Girder Spacing (m)	$\mathcal{B}$	F CHBDC	C_F CHBDC	F_m FEA	F_m CHBDC	Length (m)	R_L	R'_L	F_m Empirical equation	Empirical Equation Variables						Differences %
													a	b	c	d	e	m	
4L-4B-20	Fatigue load	4	4.25	2.55	6.2	10.899	1.85	2.247	20	0.7	0.7	1.762331	10.0	-1	0.11	18.8	-2.4	0.95	4.738
4L-5B-20	Fatigue load	5	3.4	2.168	6.548	11.663	1.79	2.32	20	0.7	0.7	1.6246	10.0	-1	0.11	18.8	-2.4	0.95	9.238
4L-6B-20	Fatigue load	6	2.83	1.912	6.778	12.1755	1.8	1.862	20	0.7	0.7	1.5349	10.0	-1	0.11	18.8	-2.4	0.95	14.72
4L-4B -40	Fatigue load	4	4.25	1.53	7.1162	12.92	1.38	2.1154	40	0.7	0.7	1.523	10.0	-1	0.11	18.8	-2.4	0.95	-10.408
4L-5B -40	Fatigue load	5	3.4	1.335	7.297	13.328	1.43	2.055	40	0.7	0.7	1.4470	10.0	-1	0.11	18.8	-2.4	0.95	-1.189
4L-6B -40	Fatigue load	6	2.83	1.209	7.411	13.58	1.43	2.019	40	0.7	0.7	1.3947	10.0	-1	0.11	18.8	-2.4	0.95	2.461
4L-4B -60	Fatigue load	4	4.25	1.194	7.425	13.611	1.24	2.015	60	0.7	0.7	1.4555	10.0	-1	0.11	18.8	-2.4	0.95	-17.380
4L-5B -60	Fatigue load	5	3.4	1.059	7.546	13.88	1.45	1.978	60	0.7	0.7	1.3954	10.0	-1	0.11	18.8	-2.4	0.95	3.758
4L-6B -60	Fatigue load	6	2.83	0.967	7.629	14.064	1.31	1.953	60	0.7	0.7	1.3518	10.0	-1	0.11	18.8	-2.4	0.95	-3.194
4L-4B -80	Fatigue load	4	4.25	1.017	7.583	13.964	1.17	1.966	80	0.7	0.7	1.4226	10.0	-1	0.11	18.8	-2.4	0.95	-21.591
4L-5B -80	Fatigue load	5	3.4	0.913	7.677	14.173	1.22	1.939	80	0.7	0.7	1.3696	10.0	-1	0.11	18.8	-2.4	0.95	-12.262
4L-6B -80	Fatigue load	6	2.83	0.841	7.74	14.316	1.43	1.92	80	0.7	0.7	1.3303	10.0	-1	0.11	18.8	-2.4	0.95	6.968

Appendix B.1 Parameters of empirical equation of shear distribution factors at Ultimate Limit State ULS on which F is a function of span length L for two-lane bridges

Bridge Type	Loading Case	no of Box Girder	Box Girder Spacing (m)	$\mathcal{B}$	F CHBDC	Number of Lane	F_v FEA	F_v CHBDC	Length (m)	R_L	R'_L	F_m Empirical equation	Empirical Equation Variables			Difference %
													a	b	c	
2L-2B-20	External fully	2	5	1.93	7.2	2	1.244	1.389	20	0.9	0.9	1.423784	7.8	-0.011	-0.11	12.627
2L-3B-20	External partial	3	3.334	2.139	7.2	2	1.3228	1.389	20	0.9	0.9	1.489022	7.8	-0.011	-0.11	11.163
2L-4B-20	External partial	4	2.5	2.347	7.2	2	1.39	1.39	20	0.9	0.9	1.536588	7.8	-0.011	-0.11	9.539
2L-2B-40	External partial	2	5	1.138	7.2	2	1.245	1.389	40	0.9	0.9	1.466343	7.8	-0.011	-0.11	15.094
2L-3B-40	External partial	3	3.334	1.356	7.2	2	1.322	1.3889	40	0.9	0.9	1.53353	7.8	-0.011	-0.11	13.793
2L-4B-40	External partial	4	2.5	1.505	7.2	2	1.368	1.3889	40	0.9	0.9	1.582518	7.8	-0.011	-0.11	13.555
2L-2B-60	External partial	2	5	0.874	7.2	2	1.358	1.3889	60	0.9	0.9	1.511524	7.8	-0.011	-0.11	10.156
2L-3B-60	Middle fully	3	3.334	1.048	7.2	2	1.37	1.3889	60	0.9	0.9	1.580782	7.8	-0.011	-0.11	13.334
2L-4B-60	External Fully	4	2.5	1.216	7.2	2	1.77	1.3889	60	0.9	0.9	1.63128	7.8	-0.011	-0.11	-4.212
2L-2B-80	External partial g	2	5	0.738	7.2	2	1.36	1.3889	80	0.9	0.9	1.4463	7.8	-0.011	-0.11	12.796
2L-3B-80	External fully	3	3.334	0.905	7.2	2	1.37	1.3889	80	0.9	0.9	1.5065	7.8	-0.011	-0.11	16.004
2L-4B-80	External partial	4	2.5	1.064	7.2	2	1.284	1.3889	80	0.9	0.9	1.5502	7.8	-0.011	-0.11	23.714

Appendix B.2 Parameters of empirical equation of shear distribution factors at Ultimate Limit State ULS on which F is a function of span length L for three-lane bridges

Bridge Type	Loading Case	no of Box Girder	Box Girder Spacing (m)	$\mathcal{B}$	F CHBDC	Number of Lane	F_v FEA	F_v CHBDC	Length (m)	R_L	R'_L	F_m Empirical equation	Empirical Equation Variables			Differences %
													a	b	C	
3L-3B-20	External partial	3	4.5	2.6623	9.6	3	1.2966	1.40625	20	0.8	0.8	1.32	10.3	-0.01	0.01	1.9235
3L-4B-20	Middle fully	4	3.375	2.87567	9.6	3	1.28	1.40625	20	0.8	0.8	1.31	10.3	-0.01	0.01	2.900
3L-5B-20	External partial	5	2.7	3.86	9.6	3	1.446	1.40625	20	0.8	0.8	1.31	10.3	-0.01	0.01	-9.93
3L-3B-40	External partial	3	4.5	1.594	9.6	3	1.36	1.40625	40	0.8	0.8	1.35	10.3	-0.01	0.01	-0.835
3L-4B-40	External partial	4	3.375	1.781	9.6	3	1.3525	1.40625	40	0.8	0.8	1.34	10.3	-0.01	0.01	-0.567
3L-5B-40	External partial	5	2.7	1.96356	9.6	3	1.407	1.40625	40	0.8	0.8	1.34	10.3	-0.01	0.01	-4.854
3L-3B-60	Middle fully	3	4.5	1.2337	9.6	3	1.36	1.40625	60	0.8	0.8	1.38	10.3	-0.01	0.01	1.202
3L-4B-60	External partial	4	3.375	1.40747	9.6	3	1.379	1.40625	60	0.8	0.8	1.37	10.3	-0.01	0.01	-0.466
3L-5B-60	External partial	5	2.7	1.5763	9.6	3	1.386	1.40625	60	0.8	0.8	1.37	10.3	-0.01	0.01	-1.202
3L-3B-80	External partial	3	4.5	1.048	9.6	3	1.365	1.40625	80	0.8	0.8	1.40	10.3	-0.01	0.01	2.883
3L-4B-80	External partial	4	3.375	1.2137	9.6	3	1.29	1.40625	80	0.8	0.8	1.40	10.3	-0.01	0.01	7.955
3L-5B-80	External partial	5	2.7	1.3777	9.6	3	1.35	1.40625	80	0.8	0.8	1.40	10.3	-0.01	0.01	3.458

Appendix B.3 Parameters of empirical equation of shear distribution factors at Ultimate Limit State ULS on which F is a function of span length L for four-lane bridges

Bridge Type	Loading Case	no of Box Girder	Box Girder Spacing (m)	$\mathcal{B}$	F CHBDC	Number of Design Lane	F_v FEA	F_v CHBDC	Length (m)	R_L	R'_L	F_m Empirical equation	Empirical Equation Variables			Difference %
													a	b	C	
4L-4B-20	External partial	4	4.25	3.4	11.2	4	1.428	1.517	20	0.7	0.7	1.4988	21.2	0.09	-0.51	-4.729
4L-5B-20	External partial	5	3.4	3.614	11.2	4	1.488	1.517	20	0.7	0.7	1.6795	21.2	0.09	-0.51	-11.405
4L-6B-20	External partial	6	2.8334	3.8244	11.2	4	1.543	1.517	20	0.7	0.7	1.8432	21.2	0.09	-0.51	-16.29
4L-4B -40	External partial	4	4.25	2.05	11.2	4	1.5038	1.517	40	0.7	0.7	1.3901	21.2	0.09	-0.51	8.178
4L-5B -40	External partial	5	3.4	2.226	11.2	4	1.506	1.517	40	0.7	0.7	1.5576	21.2	0.09	-0.51	-3.316
4L-6B -40	External partial	6	2.8334	2.419	11.2	4	1.6	1.517	40	0.7	0.7	1.7094	21.2	0.09	-0.51	-6.404
4L-4B -60	External partial	4	4.25	1.592	11.2	4	1.18	1.517	60	0.7	0.7	1.2960	21.2	0.09	-0.51	-8.953
4L-5B -60	External partial	5	3.4	1.766	11.2	4	1.476	1.517	60	0.7	0.7	1.4522	21.2	0.09	-0.51	1.635
4L-6B -60	External partial	6	2.8334	1.935	11.2	4	1.434	1.517	60	0.7	0.7	1.5938	21.2	0.09	-0.51	-10.0265
4L-4B -80	External partial	4	4.25	1.357	11.2	4	1.517	1.517	80	0.7	0.7	1.2138	21.2	0.09	-0.51	24.969
4L-5B -80	External partial	5	3.4	1.5224	11.2	4	1.5088	1.517	80	0.7	0.7	1.3602	21.2	0.09	-0.51	10.924
4L-6B -80	External partial	6	2.8334	1.68	11.2	4	1.465	1.517	80	0.7	0.7	1.4927	21.2	0.09	-0.51	-1.861

Appendix B.4 Parameters of empirical equation of shear distribution factors at Fatigue Limit State FLS on which F is a function of span length L for two-lane bridges

Bridge Type	Loading Case	no of Box Girder	Box Girder Spacing (m)	$\mathcal{B}$	F CHBDC	Number of Design Lane	F_v FEA	F_v CHBDC	Length (m)	R_L	R'_L	F_m Empirical equation	Empirical Equation Variables			Difference %
													a	b	c	
2L-2B-20	Fatigue load	2	5	1.93	4.25	2	1.337	2.352	20	0.9	0.9	1.99	7	-0.01	-0.14	17.491
2L-3B-20	Fatigue load	3	3.334	2.139	4.25	2	1.56	2.35	20	0.9	0.9	1.88	7	-0.01	-0.14	9.061
2L-4B-20	Fatigue load	4	2.5	1.76	4.25	2	1.57	2.35	20	0.9	0.9	1.81	7	-0.01	-0.14	12.073
2L-2B-40	Fatigue load	2	5	1.1385	4.25	2	1.439	2.35	40	0.9	0.9	1.90	7	-0.01	-0.14	13.809
2L-3B-40	Fatigue load	3	3.334	1.356	4.25	2	1.415	2.35	40	0.9	0.9	1.81	7	-0.01	-0.14	19.939
2L-4B-40	Fatigue load	4	2.5	1.1306	4.25	2	1.531	2.35	40	0.9	0.9	1.74	7	-0.01	-0.14	16.779
2L-2B-60	Fatigue load	2	5	0.874	4.25	2	1.784	2.35	60	0.9	0.9	1.83	7	-0.01	-0.14	-3.616
2L-3B-60	Fatigue load	3	3.334	1.0489	4.25	2	2.04	2.35	60	0.9	0.9	1.73	7	-0.01	-0.14	-11.924
2L-4B-60	Fatigue load	4	2.5	0.912	4.25	2	2.22	2.35	60	0.9	0.9	1.67	7	-0.01	-0.14	-17.015
2L-2B-80	Fatigue load	2	5	0.738	4.25	2	1.738	2.35	80	0.9	0.9	1.76	7	-0.01	-0.14	2.209
2L-3B-80	Fatigue load	3	3.334	0.905	4.25	2	1.821	2.35	80	0.9	0.9	1.67	7	-0.01	-0.14	3.212
2L-4B-80	Fatigue load	4	2.5	0.7986	4.25	2	2.27	2.35	80	0.9	0.9	1.61	7	-0.01	-0.14	-15.912

Appendix B.5 Parameters of empirical equation of shear distribution factors at Fatigue Limit State FLS on which F is a function of span length L for three-lane bridges

Bridge Type	Loading Case	no of Box Girder	Box Girder Spacing (m)	$\mathcal{B}$	F CHBDC	Number of Design Lane	F_v FEA	F_v CHBDC	Length (m)	R_L	R'_L	F_m Empirical equation	Empirical Equation Variables			Difference %
													a	b	c	
3L-3B-20	Fatigue load	3	4.5	2.662	4.25	3	1.959	3.176	20	0.8	0.8	2.23	6.12	-0.02	0.05	-12.309
3L-4B-20	Fatigue load	4	3.375	2.156	4.25	3	2.419	3.176	20	0.8	0.8	2.20	6.12	-0.02	0.05	9.850
3L-5B-20	Fatigue load	5	2.7	1.851	4.25	3	2.4846	3.176	20	0.8	0.8	2.18	6.12	-0.02	0.05	14.095
3L-3B-40	Fatigue load	3	4.5	1.594	4.25	3	2.1065	3.176	40	0.8	0.8	2.40	6.12	-0.02	0.05	-12.300
3L-4B-40	Fatigue load	4	3.375	1.336	4.25	3	2.01	3.176	40	0.8	0.8	2.37	6.12	-0.02	0.05	-15.106
3L-5B-40	Fatigue load	5	2.7	1.178	4.25	3	2.448	3.176	40	0.8	0.8	2.34	6.12	-0.02	0.05	4.553
3L-3B-60	Fatigue load	3	4.5	1.233	4.25	3	2.67	3.176	60	0.8	0.8	2.60	6.12	-0.02	0.05	2.801
3L-4B-60	Fatigue load	4	3.375	1.055	4.25	3	2.712	3.176	60	0.8	0.8	2.56	6.12	-0.02	0.05	5.931
3L-5B-60	Fatigue load	5	2.7	0.945	4.25	3	3.04	3.176	60	0.8	0.8	2.53	6.12	-0.02	0.05	20.075
3L-3B-80	Fatigue load	3	4.5	1.048	4.25	3	2.61	3.176	80	0.8	0.8	2.83	6.12	-0.02	0.05	-7.678
3L-4B-80	Fatigue load	4	3.375	0.910	4.25	3	2.71	3.176	80	0.8	0.8	2.79	6.12	-0.02	0.05	-2.752
3L-5B-80	Fatigue load	5	2.7	0.826	4.25	3	3.08	3.176	80	0.8	0.8	2.76	6.12	-0.02	0.05	11.764

Appendix B.6 Parameters of empirical equation of shear distribution factors at Fatigue Limit State FLS on which F is a function of span length L for four-lane bridges

Bridge Type	Loading Case	no of Box Girder	Box Girder Spacing (m	$\mathcal{B}$	F CHBDC	Number of Design Lane	F_v FEA	F_v CHBDC	Length (m)	R_L	R'_L	F_m Empirical equation	Empirical Equation Variables			Difference %
													a	b	c	
4L-4B-20	Fatigue load	4	4.25	2.55	4.25	4	2.66	4	20	0.7	0.7	3.05	5.7	-0.01	0.01	-12.739
4L-5B-20	Fatigue	5	3.4	2.168	4.25	4	2.65	4	20	0.7	0.7	3.04	5.7	-0.01	0.01	-12.873
4L-6B-20	Fatigue	6	2.8334	1.912	4.25	4	3.213	4	20	0.7	0.7	3.04	5.7	-0.01	0.01	5.826
4L-4B -40	Fatigue	4	4.25	1.537	4.25	4	2.8863	4	40	0.7	0.7	3.16	5.7	-0.01	0.01	-8.759
4L-5B -40	Fatigue	5	3.4	1.335	4.25	4	2.773	4	40	0.7	0.7	3.15	5.7	-0.01	0.01	-12.145
4L-6B -40	Fatigue	6	2.8334	1.209	4.25	4	3.11	4	40	0.7	0.7	3.15	5.7	-0.01	0.01	-1.290
4L-4B -60	Fatigue	4	4.25	1.194	4.25	4	3.66	4	60	0.7	0.7	3.29	5.7	-0.01	0.01	11.332
4L-5B -60	Fatigue	5	3.4	1.059	4.25	4	2.968	4	60	0.7	0.7	3.28	5.7	-0.01	0.01	-9.515
4L-6B -60	Fatigue	6	2.8334	0.967	4.25	4	3.816	4	60	0.7	0.7	3.27	5.7	-0.01	0.01	16.546
4L-4B -80	Fatigue	4	4.25	1.017	4.25	4	3.58	4	80	0.7	0.7	3.42	5.7	-0.01	0.01	4.628
4L-5B -80	Fatigue	5	3.4	0.913	4.25	4	3.474	4	80	0.7	0.7	3.41	5.7	-0.01	0.01	1.757
4L-6B -80	Fatigue	6	2.8334	0.841	4.25	4	3.864	4	80	0.7	0.7	3.40	5.7	-0.01	0.01	13.384

Appendix B.7 Parameters of empirical equation of shear distribution factors at Ultimate Limit State ULS on which F is a function of $\mathcal{B}$ for two-lane bridges

Bridge Type	Loading Case	no of Box Girder	Box Girder Spacing (m)	$\mathcal{B}$	F CHBDC	Number of Design Lane	F_v FEA	F_v CHBDC	Length (m)	R_L	R'_L	F_m Empirical equation	Empirical Equation Variables			Difference %
													a	b	c	
2L-2B-20	External fully	2	5	1.93	7.2	2	1.244	1.389	20	0.9	0.9	1.5011	7	-0.15	-0.13	-17.132
2L-3B-20	External partial	3	3.334	2.139	7.2	2	1.3228	1.389	20	0.9	0.9	1.5759	7	-0.15	-0.13	-16.065
2L-4B-20	External partial	4	2.5	2.347	7.2	2	1.39	1.39	20	0.9	0.9	1.6287	7	-0.15	-0.13	-14.659
2L-2B-40	External partial	2	5	1.138	7.2	2	1.245	1.389	40	0.9	0.9	1.5260	7	-0.15	-0.13	-18.417
2L-3B-40	External partial	3	3.334	1.3563	7.2	2	1.322	1.3889	40	0.9	0.9	1.6016	7	-0.15	-0.13	-17.461
2L-4B-40	External partial	4	2.5	1.505	7.2	2	1.368	1.3889	40	0.9	0.9	1.6572	7	-0.15	-0.13	-17.453
2L-2B-60	External partial	2	5	0.874	7.2	2	1.358	1.3889	60	0.9	0.9	1.534	7	-0.15	-0.13	-11.504
2L-3B-60	Middle fully	3	3.334	1.0489	7.2	2	1.37	1.3889	60	0.9	0.9	1.611	7	-0.15	-0.13	-15.011
2L-4B-60	External Fully	4	2.5	1.216	7.2	2	1.77	1.3889	60	0.9	0.9	1.6672	7	-0.15	-0.13	1.9649
2L-2B-80	External partial g	2	5	0.738	7.2	2	1.36	1.3889	80	0.9	0.9	1.538	7	-0.15	-0.13	-11.627
2L-3B-80	External fully	3	3.334	0.905	7.2	2	1.37	1.3889	80	0.9	0.9	1.6168	7	-0.15	-0.13	-15.268
2L-4B-80	External partial	4	2.5	1.064	7.2	2	1.284	1.3889	80	0.9	0.9	1.6725	7	-0.15	-0.13	-23.231

Appendix B.8 Parameters of empirical equation of shear distribution factors at Ultimate Limit State ULS on which F is a function of $\mathcal{B}$ for three-lane bridges

Bridge Type	Loading Case	no of Box Girder	Box Girder Spacing (m)	$\mathcal{B}$	F CHBDC	Number of Design Lane	F_v FEA	F_v CHBDC	Length (m)	R_L	R'_L	F_m Empirical equation	Empirical Equation Variables			Difference %
													a	b	c	
3L-3B-20	External partial	3	4.5	2.6623	9.6	3	1.2966	1.406	20	0.8	0.8	1.353011	13	-0.7	-0.1	-4.350
3L-4B-20	Middle fully	4	3.375	2.87567	9.6	3	1.28	1.406	20	0.8	0.8	1.41143	13	-0.7	-0.1	-10.268
3L-5B-20	External partial	5	2.7	3.86	9.6	3	1.446	1.406	20	0.8	0.8	1.539848	13	-0.7	-0.1	-6.490
3L-3B-40	External partial	3	4.5	1.594	9.6	3	1.36	1.406	40	0.8	0.8	1.267874	13	-0.7	-0.1	6.774
3L-4B-40	External partial	4	3.375	1.781	9.6	3	1.3525	1.406	40	0.8	0.8	1.319411	13	-0.7	-0.1	2.446
3L-5B-40	External partial	5	2.7	1.96356	9.6	3	1.407	1.406	40	0.8	0.8	1.364014	13	-0.7	-0.1	3.055
3L-3B-60	Middle fully	3	4.5	1.2337	9.6	3	1.36	1.406	60	0.8	0.8	1.241526	13	-0.7	-0.1	8.711
3L-4B-60	External partial	4	3.375	1.40747	9.6	3	1.379	1.406	60	0.8	0.8	1.290697	13	-0.7	-0.1	6.403
3L-5B-60	External partial	5	2.7	1.5763	9.6	3	1.386	1.406	60	0.8	0.8	1.332933	13	-0.7	-0.1	3.828
3L-3B-80	External partial	3	4.5	1.048	9.6	3	1.365	1.406	80	0.8	0.8	1.228369	13	-0.7	-0.1	10.009
3L-4B-80	External partial	4	3.375	1.2137	9.6	3	1.29	1.406	80	0.8	0.8	1.276288	13	-0.7	-0.1	1.062
3L-5B-80	External partial	5	2.7	1.3777	9.6	3	1.35	1.406	80	0.8	0.8	1.317537	13	-0.7	-0.1	2.404

Appendix B.9 Parameters of empirical equation of shear distribution factors at Ultimate Limit State ULS on which F is a function of $\mathcal{B}$ for four-lane bridges

Bridge Type	Loading Case	no of Box Girder	Box Girder Spacing (m)	$\mathcal{B}$	F CHBDC	Number of Design Lane	F_v FEA	F_v CHBDC	Length (m)	R_L	R'_L	F_m Empirical equation	Empirical Equation Variables			Difference %
													a	b	c	
4L-4B-20	External partial	4	4.25	3.4	11.2	4	1.428	1.517	20	0.7	0.7	1.43	15.3	0.17	-0.2	-0.401
4L-5B-20	External partial	5	3.4	3.614	11.2	4	1.488	1.517	20	0.7	0.7	1.50	15.3	0.17	-0.2	-0.610
4L-6B-20	External partial	6	2.8334	3.8244	11.2	4	1.543	1.517	20	0.7	0.7	1.55	15.3	0.17	-0.2	-0.496
4L-4B -40	External partial	4	4.25	2.05	11.2	4	1.5038	1.517	40	0.7	0.7	1.44	15.3	0.17	-0.2	3.980
4L-5B -40	External partial	5	3.4	2.226	11.2	4	1.506	1.517	40	0.7	0.7	1.51	15.3	0.17	-0.2	-0.299
4L-6B -40	External partial	6	2.8334	2.419	11.2	4	1.6	1.517	40	0.7	0.7	1.56	15.3	0.17	-0.2	2.255
4L-4B -60	External partial	4	4.25	1.592	11.2	4	1.18	1.517	60	0.7	0.7	1.45	15.3	0.17	-0.2	-18.649
4L-5B -60	External partial	5	3.4	1.766	11.2	4	1.476	1.517	60	0.7	0.7	1.51	15.3	0.17	-0.2	-2.574
4L-6B -60	External partial	6	2.8334	1.935	11.2	4	1.434	1.517	60	0.7	0.7	1.57	15.3	0.17	-0.2	-8.639
4L-4B -80	External partial	4	4.25	1.357	11.2	4	1.517	1.517	80	0.7	0.7	1.45	15.3	0.17	-0.2	4.424
4L-5B -80	External partial	5	3.4	1.5224	11.2	4	1.5088	1.517	80	0.7	0.7	1.52	15.3	0.17	-0.2	-0.566
4L-6B -80	External partial	6	2.8334	1.68	11.2	4	1.465	1.517	80	0.7	0.7	1.57	15.3	0.17	-0.2	-6.817

Appendix B.10 Parameters of empirical equation of shear distribution factors at Fatigue Limit State FLS on which F is a function of $\mathcal{B}$ for two-lane bridges

Bridge Type	Loading Case	no of Box Girder	Box Girder Spacing (m)	$\mathcal{B}$	F CHBDC	Number of Design Lane	F_v FEA	F_v CHBDC	Length (m)	R_L	R'_L	F_m Empirical equation	Empirical Equation Variables			Difference %
													a	b	c	
2L-2B-20	Fatigue load	2	5	1.93	4.25	2	1.337	2.352	20	0.9	0.9	1.602604	6.9	-0.11	-0.1	16.573
2L-3B-20	Fatigue load	3	3.334	2.139	4.25	2	1.56	2.35	20	0.9	0.9	1.675011	6.9	-0.11	-0.1	6.866
2L-4B-20	Fatigue load	4	2.5	1.76	4.25	2	1.57	2.35	20	0.9	0.9	1.712839	6.9	-0.11	-0.1	8.339
2L-2B-40	Fatigue load	2	5	1.138	4.25	2	1.439	2.35	40	0.9	0.9	1.582008	6.9	-0.11	-0.1	9.039
2L-3B-40	Fatigue load	3	3.334	1.356	4.25	2	1.415	2.35	40	0.9	0.9	1.653641	6.9	-0.11	-0.1	14.431
2L-4B-40	Fatigue load	4	2.5	1.130	4.25	2	1.531	2.35	40	0.9	0.9	1.695337	6.9	-0.11	-0.1	9.693
2L-2B-60	Fatigue load	2	5	0.874	4.25	2	1.784	2.35	60	0.9	0.9	1.575243	6.9	-0.11	-0.1	-13.2523
2L-3B-60	Fatigue load	3	3.334	1.048	4.25	2	2.04	2.35	60	0.9	0.9	1.645407	6.9	-0.11	-0.1	-23.981
2L-4B-60	Fatigue load	4	2.5	0.912	4.25	2	2.22	2.35	60	0.9	0.9	1.689342	6.9	-0.11	-0.1	-31.412
2L-2B-80	Fatigue load	2	5	0.738	4.25	2	1.738	2.35	80	0.9	0.9	1.571787	6.9	-0.11	-0.1	-10.574
2L-3B-80	Fatigue load	3	3.334	0.905	4.25	2	1.821	2.35	80	0.9	0.9	1.641577	6.9	-0.11	-0.1	-10.929
2L-4B-80	Fatigue load	4	2.5	0.798	4.25	2	2.27	2.35	80	0.9	0.9	1.686248	6.9	-0.11	-0.1	-34.618

Appendix B.11 Parameters of empirical equation of shear distribution factors at Fatigue Limit State FLS on which F is a function of $\mathcal{B}$ for three-lane bridges

Bridge Type	Loading Case	no of Box Girder	Box Girder Spacing (m)	$\mathcal{B}$	F CHBDC	Number of Design Lane	F_v FEA	F_v CHBDC	Length (m)	R_L	R'_L	F_m Empirical equation	Empirical Equation Variables			Difference %
													a	b	c	
3L-3B-20	Fatigue load	3	4.5	2.6623	4.25	3	1.959	3.176	20	0.8	0.8	1.978791	5.2	1.31	-0.22	-1.010
3L-4B-20	Fatigue load	4	3.375	2.1567	4.25	3	2.419	3.176	20	0.8	0.8	2.282059	5.2	1.31	-0.22	5.661
3L-5B-20	Fatigue load	5	2.7	1.8516	4.25	3	2.4846	3.176	20	0.8	0.8	2.522513	5.2	1.31	-0.22	-1.525
3L-3B-40	Fatigue load	3	4.5	1.594	4.25	3	2.1065	3.176	40	0.8	0.8	2.35876	5.2	1.31	-0.22	-11.9753
3L-4B-40	Fatigue load	4	3.375	1.33612	4.25	3	2.01	3.176	40	0.8	0.8	2.63501	5.2	1.31	-0.22	-31.095
3L-5B-40	Fatigue load	5	2.7	1.1781	4.25	3	2.448	3.176	40	0.8	0.8	2.852555	5.2	1.31	-0.22	-16.525
3L-3B-60	Fatigue load	3	4.5	1.2334	4.25	3	2.67	3.176	60	0.8	0.8	2.522241	5.2	1.31	-0.22	5.534
3L-4B-60	Fatigue load	4	3.375	1.0556	4.25	3	2.712	3.176	60	0.8	0.8	2.782108	5.2	1.31	-0.22	-2.585
3L-5B-60	Fatigue load	5	2.7	0.9458	4.25	3	3.04	3.176	60	0.8	0.8	2.987369	5.2	1.31	-0.22	1.731
3L-3B-80	Fatigue load	3	4.5	1.048	4.25	3	2.61	3.176	80	0.8	0.8	2.61544	5.2	1.31	-0.22	-0.208
3L-4B-80	Fatigue load	4	3.375	0.9103	4.25	3	2.71	3.176	80	0.8	0.8	2.864948	5.2	1.31	-0.22	-5.717
3L-5B-80	Fatigue load	5	2.7	0.82664	4.25	3	3.08	3.176	80	0.8	0.8	3.061591	5.2	1.31	-0.22	0.597

Appendix B.12 Parameters of empirical equation of shear distribution factors at Fatigue Limit State FLS on which F is a function of $\mathcal{B}$ for four-lane bridges

Bridge Type	Loading Case	no of Box Girder	Box Girder Spacing (m)	$\mathcal{B}$	F CHBDC	Number of Design Lane	F_v FEA	F_v CHBDC	Length (m)	R_L	R'_L	F_m Empirical equation	Empirical Equation Variables			Difference %
													a	b	c	
4L-4B-20	Fatigue load	4	4.25	2.55	4.25	4	2.66	4	20	0.7	0.7	3.085	7.5	-0.01	-0.22	-13.789
4L-5B-20	Fatigue load	5	3.4	2.1684	4.25	4	2.65	4	20	0.7	0.7	3.239	7.5	-0.01	-0.22	-18.186
4L-6B-20	Fatigue load	6	2.8334	1.9122	4.25	4	3.213	4	20	0.7	0.7	3.370	7.5	-0.01	-0.22	-4.674
4L-4B -40	Fatigue load	4	4.25	1.537	4.25	4	2.886	4	40	0.7	0.7	3.081	7.5	-0.01	-0.22	-6.328
4L-5B -40	Fatigue load	5	3.4	1.3356	4.25	4	2.773	4	40	0.7	0.7	3.235	7.5	-0.01	-0.22	-14.293
4L-6B -40	Fatigue load	6	2.8334	1.209	4.25	4	3.11	4	40	0.7	0.7	3.367	7.5	-0.01	-0.22	-7.643
4L-4B -60	Fatigue load	4	4.25	1.194	4.25	4	3.66	4	60	0.7	0.7	3.079	7.5	-0.01	-0.22	18.83607
4L-5B -60	Fatigue load	5	3.4	1.059	4.25	4	2.968	4	60	0.7	0.7	3.234	7.5	-0.01	-0.22	-8.232
4L-6B -60	Fatigue load	6	2.8334	0.9677	4.25	4	3.816	4	60	0.7	0.7	3.366	7.5	-0.01	-0.22	13.359
4L-4B -80	Fatigue load	4	4.25	1.0179	4.25	4	3.58	4	80	0.7	0.7	3.079	7.5	-0.01	-0.22	16.265
4L-5B -80	Fatigue load	5	3.4	0.913	4.25	4	3.474	4	80	0.7	0.7	3.23	7.5	-0.01	-0.22	7.433
4L-6B -80	Fatigue load	6	2.8334	0.8417	4.25	4	3.864	4	80	0.7	0.7	3.365	7.5	-0.01	-0.22	14.804

Appendix B.13 Parameters of empirical equation of shear distribution factors at Ultimate Limit State ULS on which F is a function of box girder spacing for two-lane bridges

Bridge Type	Loading Case	no of Box Girder	Box Girder Spacing (m)	$\mathcal{B}$	F CHBDC	Number of Design Lane	F_v FEA	F_v CHBDC	Length (m)	R_L	R'_L	F_m Empirical equation	Empirical Equation Variables			Difference %
													a	b	c	
2L-2B-20	External fully	2	5	1.93	7.2	2	1.244	1.389	20	0.9	0.9	1.363675	5.45	-0.07	0.2	8.775
2L-3B-20	External partial	3	3.334	2.139	7.2	2	1.322	1.389	20	0.9	0.9	1.483186	5.45	-0.07	0.2	10.813
2L-4B-20	External partial	4	2.5	2.347	7.2	2	1.39	1.39	20	0.9	0.9	1.575101	5.45	-0.07	0.2	11.751
2L-2B-40	External partial	2	5	1.138	7.2	2	1.245	1.389	40	0.9	0.9	1.349597	5.45	-0.07	0.2	7.750
2L-3B-40	External partial	3	3.334	1.356	7.2	2	1.322	1.3889	40	0.9	0.9	1.468011	5.45	-0.07	0.2	9.946
2L-4B-40	External partial	4	2.5	1.505	7.2	2	1.368	1.3889	40	0.9	0.9	1.557732	5.45	-0.07	0.2	12.180
2L-2B-60	External partial	2	5	0.874	7.2	2	1.358	1.3889	60	0.9	0.9	1.344969	5.45	-0.07	0.2	-0.968
2L-3B-60	Middle fully	3	3.334	1.048	7.2	2	1.37	1.3889	60	0.9	0.9	1.462136	5.45	-0.07	0.2	6.301
2L-4B-60	External Fully	4	2.5	1.216	7.2	2	1.77	1.3889	60	0.9	0.9	1.551858	5.45	-0.07	0.2	-9.546
2L-2B-80	External partial g	2	5	0.738	7.2	2	1.36	1.3889	80	0.9	0.9	1.342597	5.45	-0.07	0.2	-1.296
2L-3B-80	External fully	3	3.334	0.905	7.2	2	1.37	1.3889	80	0.9	0.9	1.459402	5.45	-0.07	0.2	6.125
2L-4B-80	External partial	4	2.5	1.064	7.2	2	1.284	1.3889	80	0.9	0.9	1.548786	5.45	-0.07	0.2	17.096

Appendix B.14 Parameters of empirical equation of shear distribution factors at Ultimate Limit State ULS on which F is a function of box girder spacing for three-lane bridges

Bridge Type	Loading Case	no of Box Girder	Box Girder Spacing (m)	$\mathcal{B}$	F CHBDC	Number of Design Lane	F_v FEA	F_v CHBDC	Length (m)	R_L	R'_L	F_m Empirical equation	Empirical Equation Variables			Difference %
													a	b	C	
3L-3B-20	External partial	3	4.5	2.662	9.6	3	1.2966	1.40625	20	0.8	0.8	1.29	8	-0.05	0.19	0.547
3L-4B-20	Middle fully	4	3.375	2.875	9.6	3	1.28	1.40625	20	0.8	0.8	1.36	8	-0.05	0.19	-6.546
3L-5B-20	External partial	5	2.7	3.86	9.6	3	1.446	1.40625	20	0.8	0.8	1.43	8	-0.05	0.19	0.980
3L-3B-40	External partial	3	4.5	1.594	9.6	3	1.36	1.40625	40	0.8	0.8	1.28	8	-0.05	0.19	5.823
3L-4B-40	External partial	4	3.375	1.781	9.6	3	1.3525	1.40625	40	0.8	0.8	1.35	8	-0.05	0.19	-0.137
3L-5B-40	External partial	5	2.7	1.963	9.6	3	1.407	1.40625	40	0.8	0.8	1.41	8	-0.05	0.19	-0.543
3L-3B-60	Middle fully	3	4.5	1.233	9.6	3	1.36	1.40625	60	0.8	0.8	1.27	8	-0.05	0.19	6.037
3L-4B-60	External partial	4	3.375	1.407	9.6	3	1.379	1.40625	60	0.8	0.8	1.35	8	-0.05	0.19	2.018
3L-5B-60	External partial	5	2.7	1.576	9.6	3	1.386	1.40625	60	0.8	0.8	1.41	8	-0.05	0.19	-1.817
3L-3B-80	External partial	3	4.5	1.048	9.6	3	1.365	1.40625	80	0.8	0.8	1.27	8	-0.05	0.19	6.490
3L-4B-80	External partial	4	3.375	1.213	9.6	3	1.29	1.40625	80	0.8	0.8	1.35	8	-0.05	0.19	-4.61381
3L-5B-80	External partial	5	2.7	1.377	9.6	3	1.35	1.40625	80	0.8	0.8	1.40	8	-0.05	0.19	-4.401

Appendix B.15 Parameters of empirical equation of shear distribution factors at Ultimate Limit State ULS on which F is a function of box girder spacing for four-lane bridges

Bridge Type	Loading Case	no of Box Girder	Box Girder Spacing (m)	$\mathcal{B}$	F CHBDC	Number of Design Lane	F_v FEA	F_v CHBDC	Length (m)	R_L	R'_L	F_m Empirical equation	Empirical Equation Variables			Difference %
													a	b	c	
4L-4B-20	External partial	4	4.25	3.4	11.2	4	1.428	1.517	20	0.7	0.7	1.354653	9.43	-0.01	0.2	5.414
4L-5B-20	External partial	5	3.4	3.614	11.2	4	1.488	1.517	20	0.7	0.7	1.416802	9.43	-0.01	0.2	5.025
4L-6B-20	External partial	6	2.8334	3.8244	11.2	4	1.543	1.517	20	0.7	0.7	1.469775	9.43	-0.01	0.2	4.982
4L-4B -40	External partial	4	4.25	2.05	11.2	4	1.5038	1.517	40	0.7	0.7	1.35271	9.43	-0.01	0.2	11.169
4L-5B -40	External partial	5	3.4	2.226	11.2	4	1.506	1.517	40	0.7	0.7	1.414711	9.43	-0.01	0.2	6.452
4L-6B -40	External partial	6	2.8334	2.419	11.2	4	1.6	1.517	40	0.7	0.7	1.467579	9.43	-0.01	0.2	9.023
4L-4B -60	External partial	4	4.25	1.592	11.2	4	1.18	1.517	60	0.7	0.7	1.352052	9.43	-0.01	0.2	-12.7252
4L-5B -60	External partial	5	3.4	1.766	11.2	4	1.476	1.517	60	0.7	0.7	1.41402	9.43	-0.01	0.2	4.383
4L-6B -60	External partial	6	2.8334	1.935	11.2	4	1.434	1.517	60	0.7	0.7	1.466824	9.43	-0.01	0.2	-2.237
4L-4B -80	External partial	4	4.25	1.357	11.2	4	1.517	1.517	80	0.7	0.7	1.351714	9.43	-0.01	0.2	12.22787
4L-5B -80	External partial	5	3.4	1.5224	11.2	4	1.5088	1.517	80	0.7	0.7	1.413654	9.43	-0.01	0.2	6.730
4L-6B -80	External partial	6	2.8334	1.68	11.2	4	1.465	1.517	80	0.7	0.7	1.466426	9.43	-0.01	0.2	-0.097

Appendix B.16 Parameters of empirical equation of shear distribution factors at Fatigue Limit State FLS on which F is a function of box girder spacing for two-lane bridges

Bridge Type	Loading Case	no of Box Girder	Box Girder Spacing (m)	$\mathcal{B}$	F CHBDC	Number of Design Lane	F_v FEA	F_v CHBDC	Length (m)	R_L	R'_L	F_m Empirical equation	Empirical Equation Variables			Difference %
													a	b	c	
2L-2B-20	Fatigue load	2	5	1.93	4.25	2	1.337	2.352	20	0.9	0.9	1.628998	7.3	-0.035	-0.22	-17.925
2L-3B-20	Fatigue load	3	3.334	2.139	4.25	2	1.56	2.35	20	0.9	0.9	1.768977	7.3	-0.035	-0.22	-11.8134
2L-4B-20	Fatigue load	4	2.5	1.76	4.25	2	1.57	2.35	20	0.9	0.9	1.877653	7.3	-0.035	-0.22	-16.385
2L-2B-40	Fatigue load	2	5	1.1385	4.25	2	1.439	2.35	40	0.9	0.9	1.628998	7.3	-0.035	-0.22	-11.663
2L-3B-40	Fatigue load	3	3.334	1.356	4.25	2	1.415	2.35	40	0.9	0.9	1.768977	7.3	-0.035	-0.22	-20.010
2L-4B-40	Fatigue load	4	2.5	1.1306	4.25	2	1.531	2.35	40	0.9	0.9	1.877653	7.3	-0.035	-0.22	-18.462
2L-2B-60	Fatigue load	2	5	0.874	4.25	2	1.784	2.35	60	0.9	0.9	1.628998	7.3	-0.035	-0.22	9.5151
2L-3B-60	Fatigue load	3	3.334	1.0489	4.25	2	2.04	2.35	60	0.9	0.9	1.768977	7.3	-0.035	-0.22	15.320
2L-4B-60	Fatigue load	4	2.5	0.912	4.25	2	2.22	2.35	60	0.9	0.9	1.877653	7.3	-0.035	-0.22	18.232
2L-2B-80	Fatigue load	2	5	0.738	4.25	2	1.738	2.35	80	0.9	0.9	1.628998	7.3	-0.035	-0.22	6.691
2L-3B-80	Fatigue load	3	3.334	0.905	4.25	2	1.821	2.35	80	0.9	0.9	1.768977	7.3	-0.035	-0.22	2.940
2L-4B-80	Fatigue load	4	2.5	0.7986	4.25	2	2.27	2.35	80	0.9	0.9	1.877653	7.3	-0.035	-0.22	20.8956

Appendix B.17 Parameters of empirical equation of shear distribution factors at Fatigue Limit State FLS on which F is a function of box girder spacing for three-lane bridges

Bridge Type	Loading Case	no of Box Girder	Box Girder Spacing (m)	$\mathcal{B}$	F CHBDC	Number of Design Lane	F_v FEA	F_v CHBDC	Length (m)	R_L	R'_L	F_m Empirical equation	Empirical Equation Variables			Difference %
													a	b	c	
3L-3B-20	Fatigue load	3	4.5	2.6623	4.25	3	1.959	3.176	20	0.8	0.8	2.15	3.8	0.6	-0.03	-8.73581
3L-4B-20	Fatigue load	4	3.375	2.1567	4.25	3	2.419	3.176	20	0.8	0.8	2.41	3.8	0.6	-0.03	0.123548
3L-5B-20	Fatigue load	5	2.7	1.8516	4.25	3	2.4846	3.176	20	0.8	0.8	2.61	3.8	0.6	-0.03	-4.94983
3L-3B-40	Fatigue load	3	4.5	1.594	4.25	3	2.1065	3.176	40	0.8	0.8	2.14	3.8	0.6	-0.03	-1.86421
3L-4B-40	Fatigue load	4	3.375	1.33612	4.25	3	2.01	3.176	40	0.8	0.8	2.41	3.8	0.6	-0.03	-16.8052
3L-5B-40	Fatigue load	5	2.7	1.1781	4.25	3	2.448	3.176	40	0.8	0.8	2.61	3.8	0.6	-0.03	-6.34999
3L-3B-60	Fatigue load	3	4.5	1.2334	4.25	3	2.67	3.176	60	0.8	0.8	2.14	3.8	0.6	-0.03	24.38764
3L-4B-60	Fatigue load	4	3.375	1.0556	4.25	3	2.712	3.176	60	0.8	0.8	2.41	3.8	0.6	-0.03	12.25096
3L-5B-60	Fatigue load	5	2.7	0.9458	4.25	3	3.04	3.176	60	0.8	0.8	2.61	3.8	0.6	-0.03	16.2974
3L-3B-80	Fatigue load	3	4.5	1.048	4.25	3	2.61	3.176	80	0.8	0.8	2.15	3.8	0.6	-0.03	21.59241
3L-4B-80	Fatigue load	4	3.375	0.9103	4.25	3	2.71	3.176	80	0.8	0.8	2.42	3.8	0.6	-0.03	12.16817
3L-5B-80	Fatigue load	5	2.7	0.82664	4.25	3	3.08	3.176	80	0.8	0.8	2.61	3.8	0.6	-0.03	17.82763

Appendix B.18 Parameters of empirical equation of shear distribution factors at Fatigue Limit State FLS on which F is a function of box girder spacing for four-lane bridges

Bridge Type	Loading Case	no of Box Girder	Box Girder Spacing (m)	$\mathcal{B}$	F CHBDC	Number of Design Lane	F_v FEA	F_v CHBDC	Length (m)	R_L	R'_L	F_m Empirical equation	Empirical Equation Variables			Difference %
													a	b	C	
4L-4B-20	Fatigue load	4	4.25	2.55	4.25	4	2.66	4	20	0.7	0.7	3.081605	12	-0.5	-0.42	13.681
4L-5B-20	Fatigue load	5	3.4	2.1684	4.25	4	2.65	4	20	0.7	0.7	3.244734	12	-0.5	-0.42	18.329
4L-6B-20	Fatigue load	6	2.8334	1.9122	4.25	4	3.213	4	20	0.7	0.7	3.409271	12	-0.5	-0.42	5.756
4L-4B -40	Fatigue load	4	4.25	1.537	4.25	4	2.8863	4	40	0.7	0.7	3.081605	12	-0.5	-0.42	6.337
4L-5B -40	Fatigue load	5	3.4	1.3356	4.25	4	2.773	4	40	0.7	0.7	3.244734	12	-0.5	-0.42	14.538
4L-6B -40	Fatigue load	6	2.8334	1.209	4.25	4	3.11	4	40	0.7	0.7	3.409271	12	-0.5	-0.42	8.778
4L-4B -60	Fatigue load	4	4.25	1.194	4.25	4	3.66	4	60	0.7	0.7	3.081605	12	-0.5	-0.42	-18.7693
4L-5B -60	Fatigue load	5	3.4	1.059	4.25	4	2.968	4	60	0.7	0.7	3.244734	12	-0.5	-0.42	8.528
4L-6B -60	Fatigue load	6	2.8334	0.9677	4.25	4	3.816	4	60	0.7	0.7	3.409271	12	-0.5	-0.42	-11.930
4L-4B -80	Fatigue load	4	4.25	1.0179	4.25	4	3.58	4	80	0.7	0.7	3.081605	12	-0.5	-0.42	-16.173
4L-5B -80	Fatigue load	5	3.4	0.913	4.25	4	3.474	4	80	0.7	0.7	3.244734	12	-0.5	-0.42	-7.065
4L-6B -80	Fatigue load	6	2.8334	0.8417	4.25	4	3.864	4	80	0.7	0.7	3.409271	12	-0.5	-0.42	-13.338

Appendix C.1 Parameters of empirical equation of deflection distribution factors at Fatigue Limit State FLS for two-lane bridges

Bridge Type	Loading Case	no of Box Girde	Box Girder Spacing (m)	$\mathcal{B}$	F CHBDC	CF CHBDC	F_Δ FEA	F_Δ CHBDC	Length (m)	R_L	R'_L	F_m Empirical equation	Empirical Equation Variables						Difference %
													a	b	c	d	e	m	
2L-2B-20	Fatigue load	2	5	1.93	6.762	12.13	1.121	1.318	20	0.9	0.9	1.08	10.2	-0.7	-0.1	9.51	-1	1.2	3.648
2L-3B-20	Fatigue load	3	3.334	2.139	6.57	11.721	1.08	2.35	20	0.9	0.9	1.15	10.2	-0.7	-0.1	9.51	-1	1.2	-6.308
2L-4B-20	Fatigue load	4	2.5	1.76	6.91	12.478	1.127	1.285	20	0.9	0.9	1.4	10.2	-0.7	-0.1	9.51	-1	1.2	-1.050
2L-2B-40	Fatigue load	2	5	1.138	7.4753	13.722	1.001	1.17	40	0.9	0.9	1	10.2	-0.7	-0.1	9.51	-1	1.2	-0.103
2L-3B-40	Fatigue load	3	3.334	1.356	7.279	13.28	1.03	1.212	40	0.9	0.9	1.06	10.2	-0.7	-0.1	9.51	-1	1.2	-3.427
2L-4B-40	Fatigue load	4	2.5	1.130	7.4823	13.7386	1	1.17	40	0.9	0.9	1.07	10.2	-0.7	-0.1	9.51	-1	1.2	-7.349
2L-2B-60	Fatigue load	2	5	0.874	7.713	14.251	1.09	1.134	60	0.9	0.9	0.98	10.2	-0.7	-0.1	9.51	-1	1.2	10.241
2L-3B-60	Fatigue load	3	3.334	1.048	7.55598	13.902	1.09	1.16	60	0.9	0.9	1.03	10.2	-0.7	-0.1	9.51	-1	1.2	5.004
2L-4B-60	Fatigue load	4	2.5	0.912	7.6786	14.174	1.093	1.14	60	0.9	0.9	1.05	10.2	-0.7	-0.1	9.51	-1	1.2	3.731
2L-2B-80	Fatigue load	2	5	0.738	7.835	14.522	1.07	1.114	80	0.9	0.9	.97	10.2	-0.7	-0.1	9.51	-1	1.2	9.681
2L-3B-80	Fatigue load	3	3.334	0.905	7.685	14.189	1.068	1.139	80	0.9	0.9	1.02	10.2	-0.7	-0.1	9.51	-1	1.2	4.313
2L-4B-80	Fatigue load	4	2.5	0.798	7.781	14.4	1.073	1.073	80	0.9	0.9	1.04	10.2	-0.7	-0.1	9.51	-1	1.2	2.940

Appendix C.2 Parameters of empirical equation of deflection distribution factors at Fatigue Limit State FLS for three-lane bridges

Bridge Type	Loading Case	no of Box Girder	Box Girder Spacing (m)	$\mathcal{B}$	F CHBDC	CF CHBDC	F_Δ FEA	F_Δ CHBDC	Length (m)	R_L	R'_L	F_m Empirical equation	Empirical Equation Variables						Difference %
													a	b	c	d	e	m	
3L-3B-20	Fatigue load	3	4.5	2.6623	6.1039	10.675	1.314	1.99	20	0.8	0.8	1.12	10	0.81	-0.1	21.7	-2.8	0.9	14.959
3L-4B-20	Fatigue load	4	3.375	2.1567	6.558	11.686	1.390	1.84	20	0.8	0.8	1.18	10	0.81	-0.1	21.7	-2.8	0.9	15.122
3L-5B-20	Fatigue load	5	2.7	1.8516	6.83352	12.296	1.393	1.759	20	0.8	0.8	1.22	10	0.81	-0.1	21.7	-2.8	0.9	12.054
3L-3B-40	Fatigue load	3	4.5	1.594	7.065	12.811	1.142	1.69	40	0.8	0.8	1.18	10	0.81	-0.1	21.7	-2.8	0.9	-3.390
3L-4B-40	Fatigue load	4	3.375	1.3361	7.297	13.327	1.159	1.63	40	0.8	0.8	1.23	10	0.81	-0.1	21.7	-2.8	0.9	-6.331
3L-5B-40	Fatigue load	5	2.7	1.1781	7.439	13.643	1.184	1.596	40	0.8	0.8	1.27	10	0.81	-0.1	21.7	-2.8	0.9	-7.451
3L-3B-60	Fatigue load	3	4.5	1.2334	7.3898	13.533	1.207	1.609	60	0.8	0.8	1.20	10	0.81	-0.1	21.7	-2.8	0.9	0.132
3L-4B-60	Fatigue load	4	3.375	1.0556	7.549	13.88	1.23	1.57	60	0.8	0.8	1.25	10	0.81	-0.1	21.7	-2.8	0.9	-1.897
3L-5B-60	Fatigue load	5	2.7	0.9458	7.648	14.108	1.26	1.54	60	0.8	0.8	1.29	10	0.81	-0.1	21.7	-2.8	0.9	-2.371
3L-3B-80	Fatigue load	3	4.5	1.048	7.556	13.9	1.25	1.568	80	0.8	0.8	1.21	10	0.81	-0.1	21.7	-2.8	0.9	2.532
3L-4B-80	Fatigue load	4	3.375	0.9103	7.6807	14.179	1.286	1.539	80	0.8	0.8	1.26	10	0.81	-0.1	21.7	-2.8	0.9	1.706
3L-5B-80	Fatigue load	5	2.7	0.8266	7.756	14.346	1.208	1.522	80	0.8	0.8	1.3	10	0.81	-0.1	21.7	-2.8	0.9	0.076

Appendix C.3 Parameters of empirical equation of deflection distribution factors at Fatigue Limit State FLS for four-lane bridges

Bridge Type	Loading Case	no of Box Girder	Box Girder Spacing (m)	$\mathcal{B}$	F CHBDC	CF CHBDC	F_Δ FEA	F_Δ CHBDC	Length (m)	R_L	R'_L	F_m Empirical equation	Empirical Equation Variables						Difference %
													a	b	c	d	e	M	
4L-4B-20	Fatigue load	4	4.25	2.55	6.2	10.899	1.75	2.47	20	0.7	0.7	1.483579	13	-0.19	-0.14	18.8	-2.4	0.95	15.224
4L-5B-20	Fatigue load	5	3.4	2.1684	6.548	11.663	1.75	2.32	20	0.7	0.7	1.511441	13	-0.19	-0.14	18.8	-2.4	0.95	13.631
4L-6B-20	Fatigue load	6	2.8334	1.912	6.778	12.1755	1.83	1.862	20	0.7	0.7	1.537546	13	-0.19	-0.14	18.8	-2.4	0.95	16.164
4L-4B -40	Fatigue load	4	4.25	1.537	7.1162	12.92	1.34	2.115	40	0.7	0.7	1.43497	13	-0.19	-0.14	18.8	-2.4	0.95	-6.3728
4L-5B -40	Fatigue load	5	3.4	1.335	7.297	13.328	1.37	2.055	40	0.7	0.7	1.470856	13	-0.19	-0.14	18.8	-2.4	0.95	-7.205
4L-6B -40	Fatigue load	6	2.8334	1.209	7.411	13.58	1.42	2.019	40	0.7	0.7	1.502749	13	-0.19	-0.14	18.8	-2.4	0.95	-5.530
4L-4B -60	Fatigue load	4	4.25	1.194	7.425	13.611	1.37	2.015	60	0.7	0.7	1.4191	13	-0.19	-0.14	18.8	-2.4	0.95	-3.432
4L-5B -60	Fatigue load	5	3.4	1.059	7.546	13.88	1.72	1.978	60	0.7	0.7	1.457769	13	-0.19	-0.14	18.8	-2.4	0.95	15.442
4L-6B -60	Fatigue load	6	2.8334	0.967	7.629	14.064	1.46	1.953	60	0.7	0.7	1.491104	13	-0.19	-0.14	18.8	-2.4	0.95	-1.643
4L-4B -80	Fatigue load	4	4.25	1.017	7.583	13.964	1.17	1.966	80	0.7	0.7	1.411063	13	-0.19	-0.14	18.8	-2.4	0.95	-19.784
4L-5B -80	Fatigue load	5	3.4	0.913	7.677	14.173	1.33	1.939	80	0.7	0.7	1.450937	13	-0.19	-0.14	18.8	-2.4	0.95	-9.093
4L-6B -80	Fatigue load	6	2.8334	0.841	7.74	14.316	1.37	1.92	80	0.7	0.7	1.485081	13	-0.19	-0.14	18.8	-2.4	0.95	-8.400

Appendix D.1 Finite-element Analysis, CHBDC and AASHTO-LRFD results at Ultimate Limit State for two-lane bridges

Bridge Type	Loading Case	no of Box Girder	Box Girder Spacing (m)	$\mathcal{B}$	F CHBDC-F_m	CF CHBDC F_m	F_m FEA	F_m CHBDC	Length (m)	F_v FEA	F_v CHBDC	AASHTO-LRFD
2L-2B-20	Fully Loading	2	5	1.93	7.92	12.139	0.962	1.125	20	1.244	1.389	2.225
2L-3B-20	Fully Loading	3	3.334	2.139	7.858	11.7213	0.93	1.139	20	1.3228	1.389	1.658
2L-4B-20	Fully Loading	4	2.5	2.347	7.79	11.305	0.825	1.152	20	1.39	1.39	1.375
2L-2B-40	Fully Loading	2	5	1.138	8.158	13.722	0.913	1.0778	40	1.245	1.389	2.225
2L-3B-40	Fully Loading	3	3.334	1.3563	8.093	13.287	0.92	1.09	40	1.322	1.3889	1.658
2L-4B-40	Fully Loading	4	2.5	1.505	8.048	12.98	0.88	1.1	40	1.368	1.3889	1.375
2L-2B-60	Fully Loading	2	5	0.874	8.2377	14.2518	0.942	1.062	60	1.358	1.3889	2.225
2L-3B-60	Fully Loading	3	3.334	1.0489	8.185	13.9	0.92	1.07	60	1.37	1.3889	1.658
2L-4B-60	Fully Loading	4	2.5	1.216	8.134	13.566	0.9	1.08	60	1.77	1.3889	1.375
2L-2B-80	Fully Loading	2	5	0.738	8.278	14.52	0.96	1.05	80	1.36	1.3889	2.225
2L-3B-80	Fully Loading	3	3.334	0.905	8.228	14.189	0.911	1.064	80	1.37	1.3889	1.658
2L-4B-80	Fully Loading	4	2.5	1.064	8.18	13.87	0.9	1.073	80	1.284	1.3889	1.375

Appendix D.2 Finite-element Analysis, CHBDC and AASHTO –LRFD results at Ultimate Limit State for three-lane bridges

Bridge Type	Loading Case	no of Box Girder	Box Girder Spacing (m)	$\mathcal{B}$	F CHBDC F_m	CF CHBDC F_m	F_m FEA	F_m CHBDC	Length (m)	Fv FEA	Fv CHBDC	AASHTO-LRFD
3L-3B-20	Fully Loading	3	4.5	2.6623	10.168	10.675	0.945	1.199	20	1.29	1.40625	2.0833
3L-4B-20	Fully Loading	4	3.375	2.8756	10.062	10.248	0.92	1.21	20	1.28	1.40625	1.6583
3L-5B-20	Fully Loading	5	2.7	3.86	9.9569	9.827	0.9	1.23	20	1.446	1.40625	1.403
3L-3B-40	Fully Loading	3	4.5	1.594	10.702	12.811	0.924	1.18	40	1.36	1.40625	2.0833
3L-4B-40	Fully Loading	4	3.375	1.781	10.6092	12.43	0.9	1.13	40	1.3525	1.40625	1.6583
3L-5B-40	Fully Loading	5	2.7	1.9635	10.518	12.072	0.9	1.145	40	1.47	1.40625	1.403
3L-3B-60	Fully Loading	3	4.5	1.2337	10.88	13.532	0.934	1.09	60	1.68	1.40625	2.0833
3L-4B-60	Fully Loading	4	3.375	1.4074	10.796	13.18	0.91	1.104	60	1.79	1.40625	1.6583
3L-5B-60	Fully Loading	5	2.7	1.5763	10.711	12.847	0.9	1.116	60	1.86	1.40625	1.403
3L-3B-80	Fully Loading	3	4.5	1.048	10.97	13.9	1.065	1.07	80	2	1.40625	2.0833
3L-4B-80	Fully Loading	4	3.375	1.2137	10.893	13.57	1.05	1.09	80	1.83	1.40625	1.6583
3L-5B-80	Fully Loading	5	2.7	1.3777	10.8111	13.244	0.99	1.102	80	1.8	1.40625	1.403

Appendix D.3 Finite-element Analysis, CHBDC Results and AASHTO –LRFD results at Ultimate Limit State for four-lane bridges

Bridge Type	Loading Case	no of Box Girder	Box Girder Spacing (m)	$\mathcal{B}$	F CHBDC F_m	CF CHBDC F_m	F_m FEA	F_m CHBDC	Length (m)	Fv FEA	Fv CHBDC	AASHTO-LRFD
4L-4B-20	Fully Loading	4	4.25	3.4	12.11	9.198	1.01	1.284	20	1.428	1.517	2.0125
4L-5B-20	Fully Loading	5	3.4	3.614	11.97	8.771	0.97	1.305	20	1.48	1.517	1.6725
4L-6B-20	Fully Loading	6	2.8334	3.8244	11.822	8.3511	0.97	1.32	20	1.54	1.517	1.44583
4L-4B -40	Fully Loading	4	4.25	2.05	13.064	11.8999	0.92	1.162	40	1.5038	1.517	2.0125
4L-5B -40	Fully Loading	5	3.4	2.226	12.941	11.547	0.9	1.177	40	1.56	1.517	1.6725
4L-6B -40	Fully Loading	6	2.8334	2.419	12.8065	11.161	0.9	1.194	40	1.6	1.517	1.44583
4L-4B -60	Fully Loading	4	4.25	1.592	13.385	12.815	0.93	1.125	60	1.688	1.517	2.0125
4L-5B -60	Fully Loading	5	3.4	1.766	13.263	12.467	0.97	1.139	60	1.78	1.517	1.6725
4L-6B -60	Fully Loading	6	2.8334	1.935	13.145	12.129	0.9	1.153	60	1.9	1.517	1.44583
4L-4B -80	Fully Loading	4	4.25	1.357	13.549	13.28	0.94	1.107	80	1.8	1.517	2.0125
4L-5B -80	Fully Loading	5	3.4	1.5224	13.434	12.955	0.93	1.12	80	1.94	1.517	1.6725
4L-6B -80	Fully Loading	6	2.8334	1.68	13.32	12.63	0.9	1.133	80	2	1.517	1.44583

Appendix D.4 Finite-element Analysis, CHBDC Results and AASHTO –LRFD results at Fatigue Limit State for two-lane bridges

Bridge Type	Loading Case	no of Box Girder	Box Girder Spacing (m)	$\mathcal{B}$	F CHBDC F_m	CF CHBDC F_m	F_m FEA	F_m CHBDC	Length (m)	Fv FEA	Fv CHBDC	AASHTO-LRFD
2L-2B-20	Fatigue load	2	5	1.93	6.762	12.13	1.17	1.31862	20	1.337	2.352	2.225
2L-3B-20	Fatigue load	3	3.334	2.139	6.57	11.721	1.09	1.36	20	1.56	2.35	1.658
2L-4B-20	Fatigue load	4	2.5	1.76	6.91	12.478	1.01	1.28	20	1.57	2.35	1.375
2L-2B-40	Fatigue load	2	5	1.138	7.4753	13.722	1.018	1.17	40	1.439	2.35	2.225
2L-3B-40	Fatigue load	3	3.334	1.356	7.279	13.28	1.004	1.2126	40	1.415	2.35	1.658
2L-4B-40	Fatigue load	4	2.5	1.130	7.4823	13.7386	0.98	1.175	40	1.531	2.35	1.375
2L-2B-60	Fatigue load	2	5	0.874	7.713	14.251	0.97	1.134	60	1.784	2.35	2.225
2L-3B-60	Fatigue load	3	3.334	1.048	7.55598	13.902	0.972	1.16	60	2.04	2.35	1.658
2L-4B-60	Fatigue load	4	2.5	0.912	7.6786	14.174	0.98	1.14	60	2.22	2.35	1.375
2L-2B-80	Fatigue load	2	5	0.738	7.835	14.522	0.97	1.114	80	1.738	2.35	2.225
2L-3B-80	Fatigue load	3	3.334	0.905	7.685	14.189	0.98	1.139	80	1.821	2.35	1.658
2L-4B-80	Fatigue load	4	2.5	0.798	7.781	14.4	0.97	1.123	80	2.27	2.35	1.375

Appendix D.5 Finite-element Analysis, CHBDC Results and AASHTO-LRFD Results at Fatigue Limit State three-lane bridges

Bridge Type	Loading Case	no of Box Girder	Box Girder Spacing (m)	$\mathcal{B}$	F CHBDC F_m	CF CHBDC F_m	F_m FEA	F_m CHBDC	Length (m)	Fv FEA	Fv CHBDC	AASHTO-LRFD
3L-3B-20	Fatigue load	3	4.5	2.6623	6.1039	10.675	1.384	1.99	20	1.959	3.176	2.0833
3L-4B-20	Fatigue load	4	3.375	2.1567	6.558	11.6864	1.432	1.84	20	2.419	3.176	1.6583
3L-5B-20	Fatigue load	5	2.7	1.8516	6.83352	12.296	1.41	1.759	20	2.4846	3.176	1.403
3L-3B-40	Fatigue load	3	4.5	1.594	7.065	12.811	1.16	1.69	40	2.1065	3.176	2.0833
3L-4B-40	Fatigue load	4	3.375	1.3361	7.297	13.327	1.163	1.63	40	2.01	3.176	1.6583
3L-5B-40	Fatigue load	5	2.7	1.1781	7.439	13.643	1.174	1.596	40	2.448	3.176	1.403
3L-3B-60	Fatigue load	3	4.5	1.2334	7.3898	13.533	1.08	1.609	60	2.67	3.176	2.0833
3L-4B-60	Fatigue load	4	3.375	1.0556	7.549	13.88	1.1	1.57	60	2.712	3.176	1.6583
3L-5B-60	Fatigue load	5	2.7	0.9458	7.648	14.108	1.125	1.54	60	3.04	3.176	1.403
3L-3B-80	Fatigue load	3	4.5	1.048	7.556	13.9	1.18	1.568	80	2.61	3.176	2.0833
3L-4B-80	Fatigue load	4	3.375	0.9103	7.6807	14.179	1.23	1.539	80	2.71	3.176	1.6583
3L-5B-80	Fatigue load	5	2.7	0.8266	7.756	14.3467	1.11	1.522	80	3.08	3.176	1.403

Appendix D.6 Finite-element Analysis, CHBDC Results and AASHTO-LRFD Results at Fatigue Limit State for four- lane bridges lane bridges

Bridge Type	Loading Case	no of Box Girder	Box Girder Spacing (m)	$\mathcal{B}$	F CHBDC F_m	CF CHBDC F_m	F_m FEA	F_m CHBDC	Length (m)	Fv FEA	Fv CHBDC	AASHTO-LRFD
4L-4B-20	Fatigue load	4	4.25	2.55	6.2	10.899	1.85	2.247	20	2.66	4	2.0125
4L-5B-20	Fatigue load	5	3.4	2.168	6.548	11.663	1.79	2.32	20	2.65	4	1.6725
4L-6B-20	Fatigue load	6	2.8334	1.912	6.778	12.1755	1.8	1.862	20	3.213	4	1.44583
4L-4B -40	Fatigue load	4	4.25	1.537	7.1162	12.92	1.38	2.1154	40	2.8863	4	2.0125
4L-5B -40	Fatigue load	5	3.4	1.335	7.297	13.328	1.43	2.055	40	2.773	4	1.6725
4L-6B -40	Fatigue load	6	2.8334	1.209	7.411	13.58	1.43	2.019	40	3.11	4	1.44583
4L-4B -60	Fatigue load	4	4.25	1.194	7.425	13.611	1.24	2.015	60	3.66	4	2.0125
4L-5B -60	Fatigue load	5	3.4	1.059	7.546	13.88	1.45	1.978	60	2.968	4	1.6725
4L-6B -60	Fatigue load	6	2.8334	0.967	7.629	14.064	1.31	1.953	60	3.816	4	1.44583
4L-4B -80	Fatigue load	4	4.25	1.017	7.583	13.964	1.17	1.966	80	3.58	4	2.0125
4L-5B -80	Fatigue load	5	3.4	0.913	7.677	14.173	1.22	1.939	80	3.474	4	1.6725
4L-6B -80	Fatigue load	6	2.8334	0.841	7.74	14.316	1.43	1.92	80	3.864	4	1.44583

REFERENCES

Abdel-Mohti, A., & Pekcan, G. (2008). Seismic response of skewed RC box girder bridges. *Earthquake Engineering and Engineering Vibration, 7*(4), 415-426.

Abdullah, M. A., & Abdul-Razzak, A. (1990). Finite strip analysis of prestressed box girder. *Computers and Structures, 36*(5), 817-822.

American Association of State Highway and Transportation Officials, AASHTO. (1996). Standard Specifications for Highway Bridges. Washington, D.C.

American Association of State Highway and Transportation Officials, AASHTO. (1996b). AASHTO LRFD Bridge Design Specifications, 2nd Ed. (1998) with 1999, 2000, and 2001 and 5th Ed 2010 interim revisions. Washington, D.C.

American Association for State Highway and Transportation Officials, AASHTO. (2004). Guide Specification for Horizontally Curved Highway Bridges. Washington, D.C.

Androus, A. (2003). Experimental and theoretical studies of composite multiple-box girders bridges. M.Sc. thesis, Department of Civil Engineering, Ryerson University, Ontario, Canada.

Arizumi, Y., Hamada, S., & Oshiro, T. (1985). *Static behavior of curved composite box girders*. In (pp. 212-215). Tokyo, Japan: Japan Society of Civil Engineers.

Arizumi, Y., Oshiro, T., & Hamada, S. (1982). Finite strip analysis of curved composite girders with incomplete interaction. *Computers and Structures, 15*(6), 603-612.

Batla, F. A., Reisnour, P. H., & Pathak, D. (1984). Finite-element program for analysis of folded-plate bridge superstructures. Transportation Research Record, *Second Bridge Engineering Conference, 1,* 21-27. Minneapolis, MN, USA.

Bazant, Z. P., & El Nimeiri, M. (1974). Stiffness method for curved box girders at initial stress. *ASCE Journal of the Structural Division, 100*(10), 2071-2090.

Boswell, L. F., & Zhang, S. H. (1984). Effect of distortion in thin-walled box –spine beams. *International Journal of Solids and Structures, 20*(9-10), 845-862.

Canadian Standard Association, "Canadian Highway Bridge Design Codes". CHBDC. (2010). Etobicoke, Ontario, Canada.

Chan, M. Y. T., Cheung, M. S., Beauchamp, J. C., & Hachem, H. M. (1990). Thermal stresses in composite box girder bridges. In B. Bakht, R. A. Dorton & L. G. Jaeger (Ed.). *Third*

International conference on Short and Medium Span Bridges, (pp. 355-366). Toronto, Ontario, Canada.

Cheung, M. S., Akhras, G., & Li, W. (1994). Combined boundary element/finite strip analysis of bridges. Journal of Structural Engineering New York, N.Y., 120(3), 716-727.

Cheung, M. S., Bakht, B., & Jaeger, L. G. (1982). Analysis of box girder bridges by grillage and orthotropic plate methods. *Canadian Journal of Civil Engineering, 9*(4), 595-601.

Cheung, M. S., & Chan, M. Y. T. (1978). Finite strip evaluation of effective flange width of bridge girders. *Canadian Journal of Civil Engineering, 5*(2), 174-185.

Cheung, M. S., Cheung, Y. K., & Ghali, A. (1970). Analysis of slab and girder bridges by the finite strip method. *Building Sciences, 5*(2), 95-104.

Cheung, M. S., & Li, W. (1989). Analysis of continuous, haunched box girder bridges by finite strips. *Journal of Structural Engineering New York, N.Y., 115*(5), 1076-1087.

Cheung, M. S., Li, W., & Jaeger, L. G. (1990). Improved finite strip method for nonlinear analysis of long-span cable-stayed bridges. *Canadian Journal of Civil Engineering, 17*(1), 87-93.

Cheung, Y. K. (1969). Analysis of cylindrical orthotropic curved bridge decks. *International Association Bridge Structure Engineering, 29*, 41-52.

Cheung, Y. L. (1985). Finite strip analysis of slab and box girder bridges. *Hong Kong Engineer, 13*(6), 31-41.

Culham, G. A., & Ghali, A. (1977). Distribution of wheel loads on bridge girders. *Canadian Journal of Civil Engineering, 4*(1), 57-65.

DeFries-Skene, A., & Scordelis, A. C. (1964). Direct stiffness solution for folded plates. *ASCE Proceedings- Journal of the Structural Division, 90* (ST4, Part 1), 15-47.

Ebeido, T., & Kennedy, J. B. (1995). Shear distribution in simply supported skew composite bridges. *Canadian Journal of Civil Engineering, 22*(6), 1143-1154.

El-Tawil, S. & Okeil, A. M. (2002). Behaviour and design of composed box girder bridges. Final report submitted to Florida Department of Transportation, University of Central Florida, Orlando, Florida. p. 90.

Evans, H. R., & Rockey, K. C. (1974). Method of analysis for box girders based on the ordinary folded plate theory. *International Centre of Mechanical Sciences*.

Evans, H. R., & Rockey, K. C. (1975). Method of analysis for box girders based on the ordinary folded plates theory. *Bulletin of the International Association for Shell and Spatial Structures, 16*(59), 3-13.

Evans, H. R., & Shanmugam, N. E. (1984). Simplified analysis for cellular structures. *Journal of Structural Engineering, 110*(3), 531-543.

Fam, A., & Turkstra, C. (1975). A finite-element scheme for box bridge analysis. *Computers and Structures, 5*(2-3), 179-186.

Foinquinos, R., Kuzmanovic, B., & Vargas, L. M. (1997). Influence of diaphragms on live load distribution in straight multiple steel box girder bridges. *Proceedings of the 1997 15th Structures Congress, Part 2 (of 2),* April 13, 1997- April 16, *1*, 89-93. Portland, OR, USA.

Fountain, R. S., & Mattock, A. H. (1968). Composite steel-concrete multi-box girder bridges. *Pro. Can. Struct. Eng. Conf., Canadian Steel Industries Construction Council*, 19-30. Toronto, Ontario, Canada.

Furuya, H., & Lu, J. (1999). Combining multilayer neural network and genetic algorithms for structural optimization. Collection of Technical Papers – *Proceedings of the 1999 AIAA/ASME/ASCE/AHS/ASC Structures, Structural Dynamics and Materials Conference, 3*, 1891-1899. St. Louis, MO, USA.

Galuta, E. M., & Cheung, M. S. (1995). Combined boundary element and finite-element analysis of composite box girder bridges. *Computers and Structures, 57*(3), 427-437.

Ghali, A., Cheung, M. S., Dilger, W. H., & Chan, M. Y. T. (1981). Longitudinal stress over supports of concrete box girder bridges. *Canadian Journal of Civil Engineering, 8*(2), 155-164.

Guilford, A. A., & VanHorn, D. A. (1967). Lateral distribution of vehicular loads in prestressed concrete box-beam bridge, Berwick Bridge. *Lehigh University, Department of Civil Engineering*, 104.

Hambly, E. C., & Pennells, E. (1975). Grillage analysis applied to cellular bridge decks. *Structural Engineer, 53*(7), 267-274.

Hassan, W. (2005). Shear distribution in curved composite multiple-box girder bridges. M.Sc. thesis, Department of Civil Engineering, Ryerson University, Ontario, Canada.

Hays Jr., C. O. (1984). Evaluating bridge overloads using the finite-element method. *Official Proceedings - International Bridge Conference.* 232-238. Pittsburgh, PA, USA.

Heins, C. P., & Kuo, J. T. C. (1975). Ultimate live load distribution factor for bridges. ASCE *Journal of the Structural Division, 101*(7), 1481-1496.

Helba, A., & Kennedy, J. B. (1995). Skew composite bridges - analyses for Ultimate load. *Canadian Journal of Civil Engineering, 22*(6), 1092-1103.

Hrennikoff, A. (1941). Solution of problems of elasticity by framework method. *American Society of Mechanical Engineers -- Transactions -- Journal of Applied Mechanics, 8*(4), -169--175.

Hrennikoff, A. (1969). Precision of finite-element method in plane stress. *International Association of Bridge Structural Engineering, 29*, 125-137.

Imbsen, R. A., Liu, W. D., Schamber, R. A., & Nutt, R. V. (1987). Strength evaluation of existing reinforced concrete bridges. *National Cooperative Highway Research Program Report.*

Iranmanesh, A., & Kaveh, A. (1999). Structural optimization by gradient-based neural networks. *International Journal for Numerical Methods in Engineering, 46*(2), 297-311.

Ishac, I. I., & Graves Smith, T. R. (1985). Approximations for moments in box girders. *Journal of Structural Engineering New York, N.Y., 111*(11), 2333-2342.

Jan, R., & Bhat, J. A. (2010). Evaluation of load distribution factors for curved box girder bridges. *International Journal of Earth Sciences and Engineering, 3*(4), 710-719.

Jenkins, W. M. (1993). An enhanced genetic algorithm for structural design optimization. *Neural Networks and Combinational Optimization in Civil and Structural Engineering,* 109-126.

Jenkins, W. M. (1995). Neural network-based approximations for structural analysis. *Developments in Neural Networks and Evolutionary Computing for Civil and Structural Engineering*, 25-35.

Jenkins, W. M. (1996). A neural network trained by genetic algorithm. *Advances in Computational Structures Technology*, 77-84.

Jenkins, W. M. (2006). Neural network weight training by mutation. *Computers & Structures, 84*(31-32), 2107-2112.

Johnston, S. B., & Mattock, A. H. (1967). Lateral distribution of load in composite box girder bridges. *National Research Council Highway Research Board, Highway Research Record,* (167), 25-33.

Kaveh, A., & Iranmanesh, A. (1998). Comparative study of backpropagation and improved counterpropagation neural nets in structural analysis and optimization. *International Journal of Space Structures, 13*(4), 177-185.

Kermani, B., & Waldron, P. (1993). Analysis of continuous box girder bridges including the effects of distortion. *Computers and Structures, 47*(3), 427-440.

Khalafalla, I. E., & Sennah, K. (2010). CHBDC curvature limitations for reinforced concrete slab-on-girder bridges. *Annual Conference of the Canadian Society for Civil Engineering 2010, CSCE 2010, June 9, 2010 - June 12, 1* 774-783.

Kim, H., & Jeong, Y. (2009). Steel–concrete composite bridge deck slab with profiled sheeting. *Journal of Constructional Steel Research, 65*(8-9), 1751-1762.

Kostem, C. N. (1984). Finite-element analysis of highway bridges. *Official Proceedings-International Bridge Conference,* 239-246. Pittsburgh, PA, USA.

Li, Z., Shi, Z., & Ososanya, E. T. (1996). Evaluation of bridge conditions using artificial neural networks. *Proceedings of SOUTHEASTCON '96,* April 11, 1996-April 14, 366-369. Tampa, FL, USA.

Logan, D. A. (2002). *A first course in the finite-element method* (3rd ed.). Ontario, Canada: Ministry of Transportation Ontario, MTO.

Mabsout, M. E., Tarhini, K. M., Frederick, G. R., & Kesserwan, A. (1998). Effect of continuity on wheel load distribution in steel girder bridges. *Journal of Bridge Engineering, 3*(3), 103-110.

Mabsout, M. E., Tarhini, K. M., Frederick, G. R., & Kesserwan, A. (1999). Effect of multilanes on wheel load distribution in steel girder bridges. *Journal of Bridge Engineering, 4*(2), 99-106.

Mabsout, M. E., Tarhini, K. M., Frederick, G. R., & Kobrosly, M. (1997). Influence of sidewalks and railings on wheel load distribution in steel girder bridges. *Journal of Bridge Engineering, 2*(3), 88-96.

Maisel, B. I. (1985). Analysis of concrete box beams using small computer capacity. *Canadian Journal of Civil Engineering, 12*(2), 265-278.

Mavaddat, S., & Mirza, M. S. (1989). Computer analysis of thin-walled concrete box beams. *Canadian Journal of Civil Engineering, 16*(6), 902-909.

Mikkola, M. J., & Paavola, J. (1980). Finite-element analysis of box girders. ASCE *Journal of the Structural Division, 106*(6), 1343-1357.

Miller, R., Shahrooz, B., Baseheart, T. M., Long, E., Jones, J., Knarr, R., & Spraque, R. (1998). Testing of high-performance concrete single-span box girder. *Transportation Research Record,* (1624), 118-124.

Moffatt, K. R., & Dowling, P. J. (1975). Shear lag in steel box girder bridges. *Structural Engineer, 53*(10), 439-448.

Newmark, N. M., Siess, C. P., & Peckham, W. M. (1948). *Studies of slab and beam highway bridges.* Urbana, IL, United States: University of Illinois.

Nour, S. I. (2000). Load distribution in curved composite concrete deck-steel multiple box girder bridges. *2000 Annual Conference - Canadian Society for Civil Engineering, June 7, 2000 - June 10,* 208.

Ontario Ministry of Transportation and Communication. (1992). *Ontario highway bridge design code, OHBDC*. Third Edition, Downsview, Ontario, Canada.

Owens, G. W., Dowling, P. J., & Hargreaves, A. C. (1982). Experimental behaviour of a composite bifurcated box girder bridge. *International Conference on Short and Medium Span Bridges, 1,* 357-374.

Phuvoravan, K., Chung, W., Liu, J., & Sotelino, E. D. (2004). Simplified live load distribution factor equation for steel girder bridges. *Transportation Research Record,* (1892) 88-97.

Puckett, J. A., Huo, X. S., Patrick, M. D., Jablin, M. C., Mertz, D., & Peavy, M. D. (2005). Simplified live load distribution factor equations for bridge design. *Transportation Research Board - 6th International Bridge Engineering Conference: Reliability, Security, and Sustainability in Bridge Engineering,* July 17, 2005 - July 20, 67-78. Boston, MA, USA.

Rafiq, M. Y., Bugmann, G., & Easterbrook, D. J. (1999). Guidelines for designing neural networks for civil engineering applications. *Artificial Intelligence Applications in Civil and Structural Engineering,* 109-115.

Razaqpur, A. G., & Esfandiari, A. (2006). Redistribution of longitudinal moments in straight, continuous concrete slab - steel girder composite bridges. *Canadian Journal of Civil Engineering, 33*(4), 471-488.

Razaqpur, A. G., & Li, H. (1997). Analysis of curved multicell box girder assemblages. *Structural Engineering and Mechanics, 5*(1), 33-49.

Richmond, B. (1966). Twisting of thin-walled box girders. *Institution of Civil Engineers-Proceedings,* April 1966, *33*, 659-675.

Richmond, B. (1969). Trapezoidal boxes with continuous diaphragms. *Institution of Civil Engineers-Proceedings,* August 1, 1969, *43*, 641-650.

Roll, F., & Aneja, I. (1966). Model tests of box-beam highway bridges with cantilevered deck slabs. *ASCE Transportation Engineering Conference,* Oct 17, 1966- Oct 21, 395 [33p].

Samaan, M. (2004). Dynamic and static analyses of continuous curved composite multiple-box girder bridges. Ph.D. Dissertation Faculty of Graduate Studies and Research University of Windsor, Windsor, Ontario, Canada.

Samaan, M., Kennedy, J. B., & Sennah, K. (2007). Impact factors for curved continuous composite multiple-box girder bridges. *Journal of Bridge Engineering, 12*(1), 80-88.

Samaan, M., Sennah, K., & Kennedy, J. B. (2002). Distribution of wheel loads on continuous steel spread-box girder bridges. *Journal of Bridge Engineering, 7*(3), 175-183.

Samaan, M., Sennah, K., & Kennedy, J. B. (2002). Positioning of bearings for curved continuous spread-box girder bridges. *Canadian Journal of Civil Engineering, 29*(5), 641-652.

Samaan, M., Sennah, K., & Kennedy, J. B. (2003). Vibration of simply-supported multiple-box girder bridges. *Canadian Society for Civil Engineering - 31st Annual Conference: 2003 Building our Civilization,* June 4, 2003- June 7, 2003, 1266-1272. Moncton, NB, Canada.

Sargious, M. A. (1970). Principal stresses at the intermediate support of prestressed concrete continuous beams. *Journal of American Concrete Institution, 67*(10), 828-36.

Sargious, M. A., Dilger, W. H., & Hawk, H. (1979). Box girder bridge diaphragms with openings. ASCE *Journal of the Structural Division, 105*(1), 53-65.

Scordelis, A. C. (1984). Berkeley computer programs for the analysis of concrete box girder bridges. *Analysis and Design of Bridges (Proceedings of the NATO Advanced Study Institute) conference,* (74) 119-189. Izmir, Turk.

Scordelis, A. C. (1984). Computer analysis of reinforced and prestressed concrete box girder bridges. *Proceedings of the International Conference on Computer-Aided Analysis and Design of Concrete Structures,* 997-1011. Split, Yugosl.

Scordelis, A. C. (1984). Computer models for nonlinear analysis of reinforced and prestressed concrete structures. *Prestressed Concrete Institute-Journal, 29*(6), 116-135.

Scordelis, A. C., & Gerasimenko, P. V. (1966). Strength of reinforced concrete folded plate models. *American Society of Civil Engineers Proceedings, Journal of the Structural Division, 92*(ST1), 351-363.

Scordelis, A. C., Samarzich, W., & Pirtz, D. (1960). Load distribution on prestressed concrete slab bridge. *Prestressed Concrete Institute - Journal, 5*(2), 18-33.

Sennah, K. M., & Kennedy, J. B. (1997). Free-vibration response of simply-supported composite concrete deck-steel multi-cell bridges. *Part 4 (of 7), may 27, 1997 - may 30, ,4* 11-20.

Sennah, K. M., & Kennedy, J. B. (2001). State-of-the-art in design of curved box girder bridges. *Journal of Bridge Engineering, 6*(3), 159-167.

Sennah, K., Kennedy, J. B., & Nour, S. (2003). Design for shear in curved composite multiple steel box girder bridges. *Journal of Bridge Engineering, 8*(3), 144-152.

Shahawy, M., & Huang, D. (2001). Analytical and field investigation of lateral load distribution in concrete slab-on-girder bridges. ACI Structural Journal, 98(4), 590-599.

Sisodiya, R. G., Cheung, Y. K., & Ghali, A. (1972). New finite-elements with application to box girder bridges. *Proceedings of the Institution of Civil Engineers (London).Part 1 - Design & Construction*, x.

Sitaram, P., Swartz, S., & Channakeshava, C. (1994). Nonlinear analysis of a reinforced concrete folded plate structure. *Proceedings of the IASS-ASCE International Symposium 1994, April 24, 1994 - April 28,* 857-866.

Srinivas, V., & Ramanjaneyulu, K. (2006). Application of artificial neural networks for design responses of bridge decks. *Journal of the Institution of Engineers (India): Civil Engineering Division, 86,* 151-158.

Sudou, H., & Sugihara, N. (2004). Development of composite slab "hit slab" for the bridge. *Hitachi Zosen Technical Review, 65*(2), 22-5.

Suksawang, N., & Nassif, H. H. (2007). Development of live load distribution factor equation for girder bridges. *Transportation Research Record,* (2028), 9-18.

Tarhini, K. M. (1995). Experimental evaluation of wheel load distribution on steel I-girder bridges. *Part 1 (of 2), may 21, 1995 - may 24,1* 593-596.

Tarhini, K. M., & Frederick, G. R. (1992). Wheel load distribution in I-girder highway bridges. *Journal of Structural Engineering New York, N.Y., 118*(5), 1285-1294.

Tarhini, K. M., Mabsout, M., Harajli, M., & Tayar, C. (1995). Finite-element modeling techniques of steel girder bridges. *Proceedings of the 2nd Congress on Computing in Civil Engineering. Part 1 (of 2)*, June 5, 1995- June 8, *1*, 773-780. Atlanta, GA, USA.

Tene, Y., Epstein, M., & Sheinman, I. (1975). Dynamics of curved beams involving shear deformation. *International Journal of Solids and Structures, 11*(7-8), 827-840.

Vasseghi, A., Nateghi, F., & Haghi, M. P. (2008). Effect of link slab on seismic response of two span straight and skew bridges. *International Journal of Engineering, Transactions B: Applications, 21*(3), 257-266.

Vlasov, V. Z. (1949). *Computation of thin-walled prismatic shells*. Washington, DC, United States: National Advisory Committee for Aeronautics (NACA), Technical Memorandums, (1234), 51.

Wassef, J. (2004). Simplified design method of curved concrete slab-on-steel I-girder bridges. M.A.Sc. thesis, Civil Engineering Dept., Ryerson University, Toronto, Ont., Canada.

Yousif, Z. G., & Hindi, R. A. (2006). AASHTO-LRFD live load distribution: Limitations and applicability. *3rd International Conference on Bridge Maintenance, Safety and Management - Bridge Maintenance, Safety, Management, Life-Cycle Performance and Cost, July 16, 2006 - July 19*, 655-656.

Yousif, Z., & Hindi, R. (2007). AASHTO-LRFD live load distribution for beam-and-slab bridges: Limitations and applicability. *Journal of Bridge Engineering, 12*(6), 765-773.

Yuki, T., Shimada, T., & Hikami, Y. (1973). Studies on finite-element method for structural analysis-large deformation structure analysis program for suspension bridge and plane frame. *Ishikawajima-Harima Giho/IHI Engineering Review, 6*(2), 24-29.

Zhang, J., Ye, J., & Wang, C. (2008). Dynamic bayesian estimation of displacement parameters of continuous thin walled straight box with segregating slab based on CG method. *Jisuan Lixue Xuebao/Chinese Journal of Computational Mechanics, 25*(4), 574-580.

Zhang, X., Sennah, K., & Kennedy, J. B. (2003). Evaluation of impact factors for composite concrete-steel cellular straight bridges. *Engineering Structures, 25*(3), 313-321.

Zhang, Y., & Luo, R. (2012). Patch loading and improved measures of incremental launching of steel box girder. *Journal of Constructional Steel Research, 68*(1), 11-19.

Zhang, Y., Wang, L., & Li, Q. (2010). One-dimensional finite-element method and its application for the analysis of shear lag effect in box girders. *Tumu Gongcheng Xuebao/China Civil Engineering Journal, 43*(8), 44-50.

Zureick, A., & Naqib, R. (1999). Horizontally curved steel I-girders state-of-the-art analysis methods. *Journal of Bridge Engineering, 4*(1), 38-47.